Prenatal Diagnosis of Orofacial Malformations

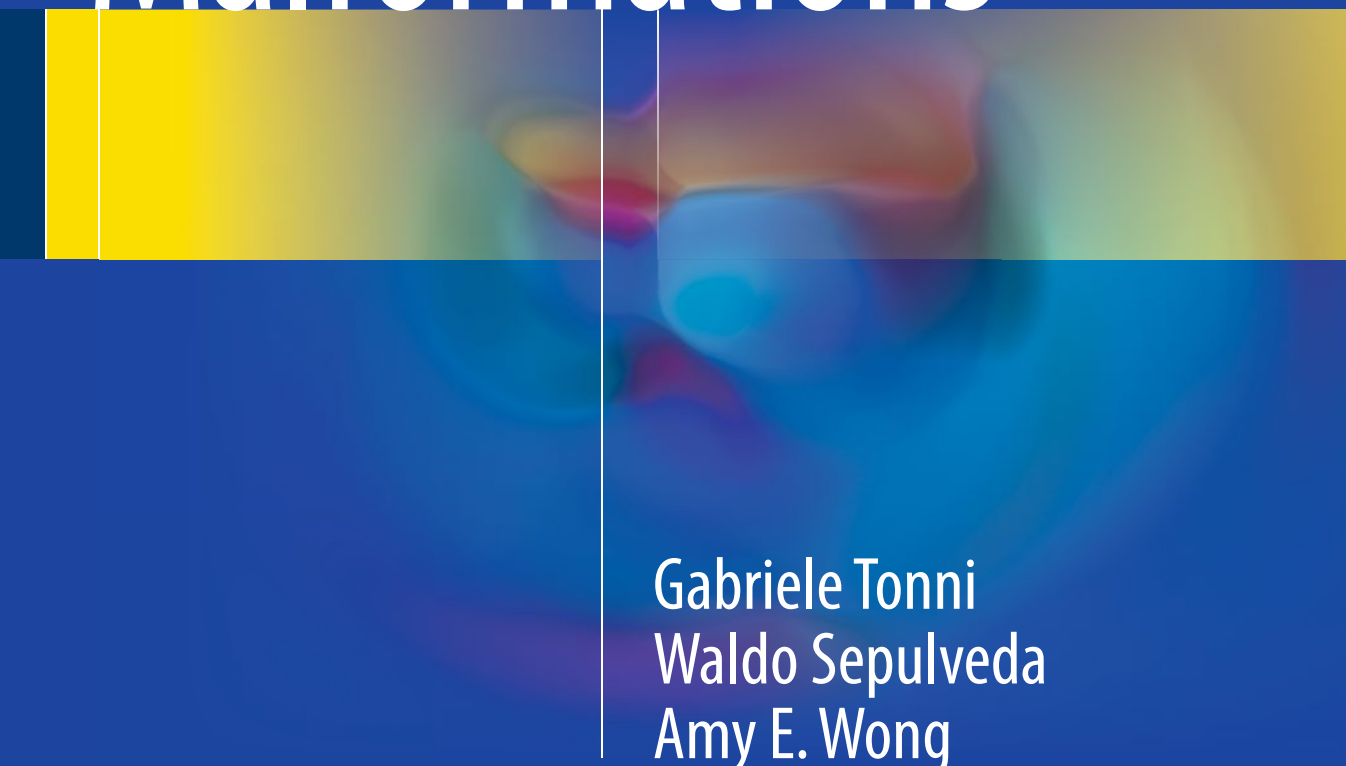

Gabriele Tonni
Waldo Sepulveda
Amy E. Wong
Editors

Springer

Prenatal Diagnosis of Orofacial Malformations

Gabriele Tonni • Waldo Sepulveda
Amy E. Wong
Editors

Prenatal Diagnosis of Orofacial Malformations

Springer

Editors
Gabriele Tonni
Department of Obstetrics and Gynecology
Prenatal Diagnostic Service
Guastalla Civil Hospital
AUSL Reggio Emilia
Reggio Emilia
Italy

Amy E. Wong
Department of Maternal-Fetal Medicine
Palo Alto Medical Foundation
Mountain View
California
USA

Waldo Sepulveda
Maternal-Fetal Diagnostic Center
Fetalmed
Santiago
Chile

ISBN 978-3-319-32514-9 ISBN 978-3-319-32516-3 (eBook)
DOI 10.1007/978-3-319-32516-3

Library of Congress Control Number: 2017933706

Printed on acid-free paper

This Springer imprint is published by Springer Nature
The registered company is Springer International Publishing AG
The registered company address is: Gewerbestrasse 11, 6330 Cham, Switzerland

“This book is dedicated to my families. To my beloved father Romano, a rare example of honesty, and a light in the complexity of life. Thanks to my wife Ramona for her patience, support, understanding, and selflessness that made it possible to pursue my editorial passion. To my loved daughters Silvia and Sara, who are at the beginning of their professions and to whom I encourage to proceed with passion and ethics. This Book is also dedicated to the memory of Prof. J.A. Low, who introduced me to research methodology in perinatal life and to Prof. K. Nicolaides. I am also greatly indebt to my Teachers Prof. Merialdi and Prof. Ferrari who trained me as Specialist in Obstetrics & Gynecology at Parma School of Medicine and to modern “ultrasound advancements” that have enabled me to progress into the fascinating journey of prenatal diagnosis”.

Gabriele Tonni

“To my family, the cornerstone of my life: my beautiful wife Monica, for your endless support and love; my son Rafael, for your charisma, brilliant mind, and always been yourself; my “one and only daughter” Pia, for your beauty, loveliness, and charm; my son Francisco, for your strength, courage, and determination in pursuing your goals; and my parents, Waldo and Eliana, for paving the path with love and wisdom. To my mentors in obstetric ultrasound and fetal medicine, Roberto Romero, Nicholas M. Fisk, and Kypros Nicolaides, for your continuous teaching and example in clinical and academic life.”

Waldo Sepulveda

“For Waldo, to whom I am indebted for sparking my interest in fetal medicine, launching my career in this rewarding field, and continuing to inspire me with your boundless passion and dedication to lifelong learning and advancement of the area of prenatal diagnosis.”

Amy E. Wong

Foreword

El universo (que otros llaman la Biblioteca)…
Jorge Luis Borges: *La Biblioteca de Babel, 1941*

Books, books, books, and more books…

In this phantasmagoric and troubled era of Web 2.0, the difficult nights of the traditional publishers are crossed by the same fundamental question: "Will there be a public out there for this or that hardcover edition?"

The answer is not an easy one. The Web abounds with information, images, and videos; furthermore, these often come for free. And it goes without saying that the traditional format of the medical book is challenged by multimedia products.

But the publishers know that a market exists for good products. The quality and veracity of information retrieved from the Web even by sophisticated search engines are variable and often quite scarce. The potential for multimedia products is great, but honestly, they tend to be difficult to consult and usually time demanding.

A well-structured book with selected contributions by qualified authors, complemented by informative and high-quality images, remains a great asset to everyday practice. Easy to reach on the shelf of your office, rapid to leaf through.

Is there a need for a book on the prenatal diagnosis of craniofacial anomalies?

Of course there is. And a great one too.

This is a new field. Until a few years ago, a facial malformation diagnosed *in utero* was a rare event. Scanning the fetal face was not recommended in everyday practice. It was considered technically infeasible, out of reach for the majority of practitioners. I still remember the overwhelming skepticism of the reviewers when I sent—not too many years ago—one paper on this subject.

The situation has much changed. Virtually all national and international guidelines now recommend the visualization of the fetal face in standard sonographic examinations of low-risk patients. This new standard has created a sometimes unrealistic expectation from the public. And fetal sonologists now have to face the big jump that modern medicine is imposing more and more frequently upon practitioners: from nothing to everything.

Unfortunately, facial malformations are not only among the most frequent of all anomalies, but they may also pose significant conundrums to the diagnosis, prognosis, and management of a condition.

Due to these relevant problems, there is certainly a major need for a standard textbook on the subject written by the leading scientific authorities that covers all possible technical and clinical aspects of the issue.

This is precisely the book you are holding now in your hands. If you are working in the field of fetal sonography, or in the parallel field of postnatal management of craniofacial anomalies, I am afraid you cannot do without it.

Gianluigi Pilu
Department of Obstetrics and Gynecology
University of Bologna, Bologna, Italy

Preface

Diagnosis is not the end, but the beginning of practice
Martin H. Fischer (1879–1962)

It was in the year 1987 that the book entitled *Prenatal Diagnosis of Congenital Anomalies* by Romero, Pilu, Jeanty, Ghidini, and Hobbins was launched. Since that time and over many years, the book has represented a milestone for all physicians involved in the difficult task of prenatal diagnosis, which was based mainly on conventional cytogenetic and two-dimensional ultrasound. During the late 1990s, the development of three-dimensional (3D) ultrasound has brought sonographers and researchers a novel diagnostic *armamentarium* that could potentially improve fetal imaging. At the same time, technology has facilitated communication and collaboration among physicians to help them develop their knowledge and technical competence. Impressive 3D ultrasound advancement has ensued, and sonographers can now manage important applications that allow the operator to reconstruct anatomical details from 3D volume data or investigate the fetal heart in 3D real time using spatiotemporal image correlation. In addition, the 3D volume data can be resliced and displayed on the screen in a manner that resembles that of computed tomography scan or magnetic resonance imaging. Surface details have been also recently enhanced by the development of lighting techniques that enable visualization of the fetus in a realistic and almost "virtual" manner. Sophisticated applications allow the fetus to be reconstructed in detail and printed on polymerase resin to create a 3D virtual physical model of congenital anomalies.

Structural abnormalities involving the face represent the second most common type of congenital anomaly. Similar to congenital heart defects, abnormalities of the face can be considered major structural malformations, as the vast majority of cases require postnatal surgery. In addition, one cannot forget to mention the social and psychological impact for parents and their relatives when a baby is delivered with a facial malformation. Fortunately, a dramatic improvement in reconstructive surgery has occurred in recent years that has significantly improved the quality of life of affected children.

We hope that readers of this book *Prenatal Diagnosis of Orofacial Malformations* will not only find it to be an up-to-date and valuable tool in their profession, but also share in our amazement of the progress that has been made in the area of prenatal diagnosis. To accomplish this task, we were fortunate to count on a team of experts to whom we are extremely grateful for

accepting our invitation to participate in this book and for their novel contributions to this area. Special thanks to Pilar Martinez-Ten, Daniela Prayer, David Chitayat, Edward Araujo Júnior, Gustavo Malinger, and Neil Sebire, world-renowned clinical investigators in their respective areas of prenatal diagnosis. We are also appreciative of those who provided case reports on unusual and rare syndromes. Lastly, we are indebted to Alessandra Born and Springer for transforming this idea into reality.

Reggio Emilia, Italy — Gabriele Tonni
Santiago, Chile — Waldo Sepulveda
Palo Alto, California, USA — Amy E. Wong

Contents

Contributors

Inbal Dona Amar Ultrasound Unit, Department of Obstetrics and Gynecology, Assaf Harofeh Medical Center, Zerifin, Israel

Israel Sackler School of Medicine, Tel Aviv University, Tel Aviv, Israel

Edwards Araujo Júnior Department of Obstetrics, Paulista School of Medicine – Sao Paulo Federal University of Sao Paulo (EPM-UNIFESP), Sao Paulo, Brazil

Susan Blaser Department of Diagnostic Imaging, Division of Paediatric Neuroradiology; Department of Pediatrics, Division of Paediatric Neuroradiology, The Hospital for Sick Children, University of Toronto, Toronto, ON, Canada

Maria Paola Bonasoni Pathology Service, IRCCS Arcispedale "Santa Maria Nuova", Reggio Emilia, Italy

David Chitayat Department of Obstetrics and Gynecology, The Prenatal Diagnosis and Medical Genetics Program, Mount Sinai Hospital, and Division of Clinical and Metabolic Genetics, Department of Pediatrics, The Hospital for Sick Children, University of Toronto, Toronto, ON, Canada

Rebecca Cohn Ultrasound Unit, Department of Obstetrics and Gynecology, Assaf Harofeh Medical Center, Zerifin, Israel

Sackler School of Medicine, Tel Aviv University, Tel Aviv, Israel

Alejandra Colubriale Diagnus – Prenatal Diagnosis and Teaching Center, Cordoba, Argentina

Marco di Maurizio Diagnostic Imaging, University Hospital Meyer, Florence, Italy

Adriana Echegaray Diagnus – Prenatal Diagnosis and Teaching Center, Cordoba, Argentina

Lydia Masako Ferreira Division of Plastic Surgery, Federal University of Sao Paulo/UNIFESP, Sao Paulo, Brazil

Roberta Granese Department of Obstetrics and Gynecology, Azienda Ospedaliera Universitaria di Messina, G. Martino, Messina, Italy

Gianpaolo Grisolia Prenatal Diagnostic Service, Department of Obstetrics & Gynecology, "Carlo Poma" Hospital, Mantua, Italy

Gerlinde M. Gruber Department of Systematic Anatomy, Center for Anatomy and Cell Biology, Medical University of Vienna, Vienna, Austria

J. Ciaran Hutchinson Department of Paediatric Pathology, Great Ormond Street Hospital for Children, London, UK

Arie Koifman Institute of Human Genetics, Prenatal Genetic Diagnosis Service, Soroka University Medical Center, Ben-Gurion University of the Negev, Beer-Sheva, Israel

Mario Lituania Periconceptional and Prenatal Diagnostic Service, IRCCS Galliera Hospital, Genoa, Italy

Gustavo Malinger OB-GYN Ultrasound Unit, Department of Obstetrics and Gynecology, Lis Maternity Hospital, Tel Aviv Medical Center, Tel Aviv, Israel

Pilar Martinez-Ten Delta – Ultrasound Diagnostic Center in Obstetrics and Gynecology, Madrid, Spain

Ron Maymon Ultrasound Unit, Department of Obstetrics and Gynecology, Assaf Harofeh Medical Center, Zerifin, IsraelSackler School of Medicine, Tel Aviv University, Tel Aviv, Israel

Yaakov Melcer Ultrasound Unit, Department of Obstetrics and Gynecology, Assaf Harofeh Medical Center, Zerifin, Israel

Sackler School of Medicine, Tel Aviv University, Tel Aviv, Israel

Gláucia Aparecida Menezes Department of Gynecology and Obstetrics, Federal University of Latin American Integration (UNILA), Foz do Iguacu, PR, Brazil

Alice Munari Pediatric Radiology and Neuroradiology Department, Children's Hospital "V. Buzzi", Milan, Italy

Fabio Xerfan Nahas Division of Plastic Surgery, Federal University of Sao Paulo/UNIFESP, Sao Paulo, Brazil

Marcello Napolitano Pediatric Radiology and Neuroradiology Department, Children's Hospital "V. Buzzi", Milan, Italy

Jose H. Ochoa Diagnus – Prenatal Diagnosis and Teaching Center, and Department of Fetal Diagnosis, Cordoba University Hospital, Cordoba, Argentina

Marcella Palmisano Department of Obstetrics and Gynecology, Prenatal Diagnostic Service, AUSL Reggio Emilia, Guastalla Civil Hospital, Reggio Emilia, Brazil

Jurandir Piassi Passos Department of Obstetrics and Gynecology, Paulista School of Medicine – Sao Paulo Federal University of Sao Paulo (EPM-UNIFESP), Sao Paulo, Brazil

Elisabetta Pelo Medical Genetics, High-Risk Obstetrics and Pediatrics Department, University Hospital Careggi, Florence, Italy

Daniela Prayer Division of Neuroradiology and Musculoskeletal Radiology, Department of Radiology, Medical University of Vienna, Vienna, Austria

Anna Ravelli Pediatric Radiology and Neuroradiology Department, Children's Hospital "V. Buzzi", Milan, Italy

Lucia Rosignoli Prenatal Diagnostic Unit, University Hospital Meyer, Florence, Italy

Natasha Sallum Division of Plastic Surgery, Federal University of São Paulo/UNIFESP, Sao Paulo, Brazil

Eduardo Félix Martins Santana Department of Obstetrics, Paulista School of Medicine – Sao Paulo Federal University of Sao Paulo (EPM-UNIFESP), Sao Paulo, Brazil

Neil J. Sebire Department of Paediatric Pathology, Great Ormond Street Hospital for Children, London, UK

Francisco Sepulveda Division of Neuroradiology, Department of Radiology, UNC Hospital, University of North Carolina at Chapel Hill, Chapel Hill, NC, USA

Anna Venegoni Pediatric Radiology and Neuroradiology Department, Children's Hospital "V. Buzzi", Milan, Italy

Rolando P. Vildoza Diagnus – Prenatal Diagnosis and Teaching Center, and Department of Fetal Diagnosis, Cordoba University Hospital, Cordoba, Argentina

Heron Werner Department of Radiology, Clínica de Diagnóstico por Imagem (CDPI), Rio de Janeiro, RJ, Brazil

Part I

Prenatal Diagnosis of Orofacial Malformations

1 Orofacial Clefts in the Fetus: What We Know and What We Should Know

Gabriele Tonni, Waldo Sepulveda, and Amy E. Wong

1.1 Introduction

During embryogenesis, the development of the lips and palate begins at an early stage; the lips develop by week 4 postfertilization age, the primary palate fuses between 4 and 6 weeks, and the secondary palate is formed between 8 and 12 weeks. Cleft lip (CL) is the result of failure of the maxillary process to fuse with the medial nasal prominence, while a cleft in the secondary palate is the result of failure of the palatine process to elevate or grow [1]. Cleft palate (CP) originates at the uvula, causing uvula bifida, and progresses along the midline involving the soft palate or both the soft palate and the hard palate; in contrast, a cleft lip and cleft palate (CLP) starts at the lip and continues posteriorly involving the alveolar ridge, the hard palate, and the soft palate [2].

G. Tonni, MD, PhD (✉)
Department of Obstetrics and Gynecology, Prenatal Diagnostic Service, Guastalla Civil Hospital, AUSL Reggio Emilia, Reggio Emilia, Italy
e-mail: Tonni.Gabriele@ausl.re.it

W. Sepulveda, MD
Maternal-Fetal Diagnostic Center, Fetalmed, Santiago, Chile

A.E. Wong, MD
Department of Maternal-Fetal Medicine, Palo Alto Medical Foundation, Mountain View, California, USA

1.2 Epidemiology and Incidence

Cleft lip with or without cleft palate (CL/CLP) may occur as a result of a number of causes. Cigarette smoking during pregnancy has been documented to be associated with an increased chance of having a child with CL/CLP [3], although no consistent evidence between orofacial clefts with maternal exposure to ambient air pollutants can be documented [4].

Nonsyndromic cleft lip and cleft palate (NSCL/P) occurs with no positive family history in the vast majority of cases, although NSCL/P may be commonly found in cousins [5].

The prevalence of CL/CLP varies by ethnicity. In a large survey over 7.5 million births, the overall prevalence of CL/CLP was 9.92 per 10,000 (3.28 per 10,000 for CL and 6.64 per 10,000 for CL/CLP, respectively). Of these, 77% of CL/CLP were isolated, 16% had associated malformations, and 7.3% occurred as part of recognized syndromes [6]. The National Birth Defects Prevention Study (NBDPS), a large database used to identify genetic and environmental risk factors for birth defects, reported the prevalence of NSCL/CLP to be 0.3/1,000 live births for CL, 0.5/1,000 live births for CL/CLP, and 0.4/1,000 live births for CP. Cleft involvement was predominantly unilateral in cases of CL and CL/CLP, with left-sided cleft as the most frequent type observed. Orofacial clefts were isolated in 80% of cases and 25% had Pierre Robin sequence [7]. In Nova Scotia, the overall prevalence of orofacial clefts was 2.1 in 1,000 live

G. Tonni, W. Sepulveda, and A.E. Wong (eds.), *Prenatal Diagnosis of Orofacial Malformations*,
DOI 10.1007/978-3-319-32516-3_1

births and, although no cases of isolated CP were detected prenatally, there was a trend towards an improvement in detection of CL/CLP over the years (from 14% during 1992–1996 to 30% during 1997–2002). Of cases of orofacial clefting in this study, 34% were associated with additional fetal structural malformations and 9.8% were associated with chromosomal abnormalities [8]. When considering the prevalence of orofacial clefts among the Asian population, the Chinese Birth Defects Monitoring Network reported prevalence rates of 14.2 per 10,000 live births for NSCL/P and 2.4 per 10,000 live births for syndromic CL/CLP, for an overall prevalence of orofacial clefting of 16.6 per 10,000 live births. In addition, this study showed that CL/CLP varied by gender, urban–rural classification, and geographic location when compared to cleft palate, particularly for nonsyndromic cases [9]. These findings were also confirmed by the study of Johnson et al. [10].

1.3 Genetics of Orofacial Clefts

NSCL/P has a multifactorial etiology that includes both genetic and environmental factors. In a European genome-wide association study, susceptibility loci for NSCL/P have been identified on chromosomes 8q24, 10q25, and 17q22. In addition, the IRF6 (interferon regulatory factor 6) gene has been demonstrated to be a genetic risk factor for NSCL/P, particularly in northern Europe [11–14]. Moreover, MSX1 (muscle segment homeobox) and TGFB3 (transforming growth factor beta-3) genes may be involved in the pathogenesis of clefting. In a non-Caucasian population, TGFA (transforming growth factor alpha) has shown to play less of a role than it does in Caucasians in cases of NSCL/P [15,16]. Different orofacial cleft (OFC) loci have been mapped on chromosome 6p24 (OFC1), 2p13 (OFC2), 19q13.2 (OFC3), and 4q (OFC4). OFC5-8 are identified by mutations in the MSX1, IRF6, PVRL1 (poliovirus receptor-like 1 or nectin-1, responsible for cleft lip/palate-ectodermal syndrome and Tessier cleft palate type 7), and TP73L (tumor protein) genes, respectively. OFC9 maps to 13q33.1-q34, whereas OFC10 is secondary to mutation haploinsufficiency of the SUMO1 (small ubiquitin-like modifier 1) gene located on 2q33.1.

In addition, MTHFR, TGF-beta3, and RAR alpha play a role in cleft development, and the TBX22 gene located on Xp21.1 is responsible for cleft palate with ankyloglossia and is involved in cases of isolated CP [17].

1.4 Associated Fetal Malformations

Orofacial clefts can be associated with other structural fetal malformations, chromosomal abnormalities (orofacial clefts are seen in 40.7% of trisomy 13 cases and 6.9% of trisomy 18 cases) [18], or genetic syndromes. The incidence of associated structural abnormalities is reported to vary with the type of cleft: 9.8% in cases of unilateral CL/CLP, 25% in cases of bilateral CL/CLP, and 100% of cases of midline CL/CLP [19–22]. When CL/CLP occurs in isolation, there does not appear to be an increased risk of chromosomal abnormalities in fetuses [23]; for example, Gilham et al. [24] reported no karyotype abnormalities in over 200 cases of isolated unilateral or bilateral CL/CLP. However, in a series by Chmait et al. [25], 22% of cases of CL/CLP that were presumed to be isolated prenatally were found to have an additional anomaly after delivery, which must be taken into account when counseling parents regarding the utility of invasive amniocentesis and neonatal prognosis.

Orofacial clefts are also associated with first-trimester findings, occurring in 19.5 per 1,000 live births with an enlarged nuchal translucency (NT). The relative risk of an isolated or non-isolated cleft in a fetus with enlarged NT is 8 and 53, respectively [26].

1.5 Accuracy of 2D and 3D Ultrasound in the Prenatal Detection of CL/P: First Versus Second Trimester of Pregnancy

The accuracy of detecting orofacial clefts has changed dramatically over the past 20 years with the trend toward improved detection in recent years. It should be kept in mind that CL is associated with CP in approximately 80% of cases [27]. In a French study, the detection rates increased

from approximately 5% in the early 1980s to over 26% in the late 1990s [28], while in Norway, the detection rate was as high as 58% in the late 1990s to 2004 [21]. In Western Australia, the detection rate for CL/CLP was reported to be 22.2% from 1996–2003, with no detection prior to 15 weeks of gestation [29]. The detection rate was almost similar in cases of unilateral CL/P (40.6%) and bilateral (44.4%); although the detection rate for isolated CL was 33.3%, no cases of isolated CP were diagnosed by prenatal ultrasound. Bister et al. [30] reported antenatal ultrasound to have a higher detection rate of specifically CL/CLP of 93%, although the sensitivity of ultrasound for the detection of all types of orofacial clefts, including isolated CL and isolated CLP, was only 65%. However, sensitivity was 100% with no cases of false positives.

1.6 The Role of 2D Ultrasound

The prenatal detection rate of isolated CP when only 2D ultrasound is used is typically very poor, ranging from 0 to 1.4% [21,22,24,31,32]. For example, the Eurofetus group reported the sensitivity of 2D ultrasound to diagnose orofacial clefts at routine scan to be 25%, 22% for CL/CLP, and 1.4% for isolated CP [32] depending on the experience and training of the examiner. Brohnstein et al. [33] diagnosed CL/CLP in only 0.07% of cases using transvaginal ultrasound between 12 and 16 weeks of gestation with a false-negative rate of 8%, while Jones reported a higher detection rate (14–25%) of CL/CLP [34]. According to Maarse et al. [35], the diagnostic accuracy of second-trimester transabdominal 2D ultrasound at detecting orofacial clefts in low- and high-risk populations ranged from 9–100% for CL/CLP, 0–22% for CP only, and 0–73% for all types of orofacial clefts. In contrast, 3D ultrasound in high-risk women resulted in a detection rate of 100% for CL, 86–90% for CL/CLP, and 0–89% for CP only.

1.7 The Role of 3D Ultrasound

Although facial clefting of the fetus can be prenatally diagnosed by 2D ultrasound, the introduction of 3D ultrasound together with the development of new software applications has led to new insights into the prenatal ultrasound study of the fetal palate. There is now a growing body of evidence that 3D ultrasound may enhance the prenatal visualization of the fetal face and hence the detection of orofacial clefting, especially if 3D ultrasound is performed as a targeted examination in cases of suspected clefting after 2D ultrasound. The best time frame for ultrasound-based screening is 18–23 weeks of gestation [1].

For this purpose, several techniques have been developed such as the "flipped-face" view [36], the "reverse-face" view [37], the Faure technique and "angle insonation" [38], the "oblique-face" view [39], and the "retronasal triangle (RNT)" view [40]. The RNT view was specifically developed to analyze the primary palate during the first-trimester scan.

Martinez-Ten et al. [36] have reported that the "oblique-face" view appears to be the best method when the secondary palate is involved; this view correctly identified involvement of the hard palate in 100% of cases, compared to the 71% detection rate of the "reverse-face" view and 86% detection rate of the "flipped-face" view. Shadowing from the surrounding bony structures and the fetal tongue may limit the study of the degree of extension of the cleft to the posterior palate [41]. The diagnosis of CL/CLP may be improved by the use of 3D ultrasound in surface mode [42–45]. Campbell and Lees [46] have demonstrated that 3D ultrasound using the "reverse-face" view may enhance sensitivity by examining the fetal face initially in the frontal plane and subsequently rotating 180° on the vertical axis to examine the secondary palate. 3D ultrasound may be clinically useful in the visualization and reconstruction of the fetal primary and secondary palate, especially in cases in which 2D ultrasound is limited by acoustic shadowing [1,36,47]. When 2D ultrasound is complemented by 3D applications, compared with 2D ultrasound alone, the prenatal diagnosis of CP is improved from 22 to 89% [47].

1.8 The Role and Value of Ultrasound-Targeted MRI (Magnetic Resonance Imaging)

Ultrasound-targeted fetal magnetic resonance imaging (MRI) may be a useful integrated diagnostic tool for ultrasonographically suspected CL/CLP [41,48–50]. MRI can evaluate the

anterior six tooth buds and the horseshoe-shaped curve bony structure of the tooth-bearing alveolar ridge better than ultrasound [51]. While the sagittal plane is useful in the study of the hard and soft palates, the coronal plane remains the best plane for diagnosis of abnormalities of the nose and lips [52].

Isolated clefts of both the soft and hard palate are more easily detected by real-time MRI [53]; a positive predictive value of 96% and negative predictive value of 80% have been reported [54]. Using T2-weighted half-Fourier acquisition single-shot turbo spin echo (HASTE) sequence using sagittal, coronal, and axial planes, Wang et al. [55] reported that 91% of cleft palates were correctly detected. In a study by Mailáth-Pokorny et al. [56], fetal MRI successfully visualized a cleft in the primary and secondary palates in 100% of cases, especially in the axial and coronal planes. MRI is less dependent on examiner expertise, maternal habitus with increased body mass index, severe oligohydramnios, and unfavorable fetal position than ultrasound.

Conclusions

1. Orofacial clefts are one of the most common congenital anomalies, with a variable prevalence ranging between 1:500 and 1:1,000 live births.
2. The number of infants with clefts in a population can vary according to maternal age, maternal race/ethnicity, genetic predisposition, socioeconomic factors, and environmental factors during intrauterine life, such as smoking and alcohol.
3. At least 15% of fetuses with CL/CLP have other associated anomalies, such as structural malformations, chromosomal abnormalities, and/or genetic syndromes.
4. CL/CLP can be diagnosed at the time of first-trimester screening, as diagnostic criteria have now been established especially for 3D ultrasound.
5. 2D ultrasound evaluation of the face and upper lip should become an integrated part of the of second-trimester scan.
6. 3D/4D ultrasound can provide, in expert hands, additional information to the study of the secondary and soft palate.
7. Advanced 3D/4D ultrasound techniques have been developed, which are particularly useful to study the hard and soft palates in the axial plane.
8. Other techniques such as the "equals sign" are clinically useful in detecting a cleft involving the secondary and/or the soft palate.
9. The use of color-Doppler ultrasound may aid prenatal diagnosis by demonstrating a bidirectional flow between the oral and nasal cavities.
10. Once a CL/CLP is prenatally diagnosed, accuracy should be exerted to ascertain that CL/CLP is an isolated finding. A thorough maxillofacial scan as well as a fetal echocardiography and neurosonography should be carried out.
11. Genetic studies (karyotype and arrays), should be offered, especially if the cleft lip is median or bilateral, with or without cleft palate.
12. Fetal MRI, where possible, should be arranged and integrated with ultrasound in the diagnostic workup, as it may improve the antenatal diagnosis of clefts, especially those cases of isolated clefts and those involving the secondary palate.

References

1. Tonni G, Centini G, Rosignoli L. Prenatal screening for fetal face and clefting in a prospective study on low-risk population: Can 3- and 4-dimensional ultrasound enhance visualization and detection rate? Oral Surg Oral Med Oral Pathol Oral Radiol Endod. 2005;100:420–6.
2. Wilhelm L, Borgers H. The 'equals sign': a novel marker in the diagnosis of fetal isolated cleft palate. Ultrasound Obstet Gynecol. 2010;36:439–44.
3. Xuan Z, Zhongpeng Y, Yanjun G, Jiaqi D, Yuchi Z, Bing S, Chenghao L. Maternal active smoking and risk of oral clefts: a meta-analysis. Oral Surg Oral Med Oral Pathol Oral Radiol. 2016;122:680–90.

4. Marshall EG, Harris G, Wartenberg D. Oral cleft defects and maternal exposure to ambient air pollutants in New Jersey. Birth Defects Res A Clin Mol Teratol. 2010;88:205–1.
5. Martelli DR, Bonan PR, Soares MC, Paranaíba LR, Martelli-Júnior H. Analysis of familial incidence of non-syndromic cleft lip and palate in a Brazilian population. Med Oral Patol Oral Cir Bucal. 2010;15(6):e898–901.
6. Mastroiacovo P, Maraschini A, Leoncini E, Mossey P, Bower C, Castilla EE, Feldkamp ML, et al. Prevalence at birth of cleft lip with or without cleft palate: data from the International Perinatal Database of Typical Oral Clefts (IPDTOC). Cleft Palate Craniofac J. 2011;48:66–81.
7. Genisca AE, Frías JL, Broussard CS, Honein MA, Lammer EJ, Moore CA, Shaw GM, National Birth Defects Prevention Study. Orofacial clefts in the National Birth Defects Prevention Study, 1997–2004. Am J Med Genet A. 2009;149A:1149–58.
8. Russell KA, Allen VM, MacDonald ME, Smith K, Dodds L. A population-based evaluation of antenatal diagnosis of orofacial clefts. Cleft Palate Craniofac J. 2008;45:148–53.
9. Dai L, Zhu J, Mao M, Li Y, Deng Y, Wang Y, Liang J, et al. Time trends in oral clefts in Chinese newborns: data from the Chinese National Birth Defects Monitoring Network. Birth Defects Res A Clin Mol Teratol. 2010;88:41–7.
10. Johnson CY, Honein MA, Hobbs CA, Rasmussen SA. National Birth Defects Prevention Study. Prenatal diagnosis of orofacial clefts, National Birth Defects Prevention Study, 1998–2004. Prenat Diagn. 2009;29:833–9.
11. Mangold E, Reutter H, Birnbaum S, Walier M, Mattheisen M, Henschke H, Lauster C, et al. A Genome-wide linkage scan of nonsyndromic orofacial clefting in 91 families of central European origin. Am J Med Genet A. 2009;149A:2680–94.
12. Rojas-Martinez A, Reutter H, Chacon-Camacho O, Leon-Cachon RB, Munoz-Jimenez SG, Nowak S, Becker J, et al. Genetic risk factors for nonsyndromic cleft lip with or without cleft palate in a Mesoamerican population: evidence for IRF6 and variants at 8q24 and 10q25. Birth Defects Res A Clin Mol Teratol. 2010;88:535–7.
13. Ghassibé M, Bayet B, Revencu N, Verellen-Dumoulin C, Gillerot Y, Vanwijck R, Vikkula M. Interferon regulatory factor-6: a gene predisposing to isolated cleft lip with or without cleft palate in the Belgian population. Eur J Hum Genet. 2005;13:1239–42.
14. Jugessur A, Rahimov F, Lie RT, Wilcox AJ, Gjessing HK, Nilsen RM, Nguyen TT, et al. Genetic variants in IRF6 and the risk of facial clefts: single-marker and haplotype-based analyses in a population-based case–control study of facial clefts in Norway. Genet Epidemiol. 2008;32:413–24.
15. Lidral AC, Murray JC, Buetow KH, Basart AM, Schearer H, Shiang R, Naval A, et al. Studies of the candidate genes TGFB2, MSX1, TGFA, and TGFB3 in the etiology of cleft lip and palate in the Philippines. Cleft Palate Craniofac J. 1997;34:1–6.
16. Lidral AC, Romitti PA, Basart AM, Doetschman T, Leysens NJ, Daack-Hirsch S, Semina EV, et al. Association of MSX1 and TGFB3 with nonsyndromic clefting in humans. Am J Hum Genet. 1998;63:557–68.
17. Carinci F, Scapoli L, Palmieri A, Zollino I, Pezzetti F. Human genetic factors in nonsyndromic cleft lip and palate: an update. Int J Pediatr Otorhinolaryngol. 2007;71:1509–19.
18. Snijders RJ, Sebire NJ, Psara N, Souka A, Nicolaides KH. Prevalence of fetal facial cleft at different stages of pregnancy. Ultrasound Obstet Gynecol. 1995;6:327–9.
19. Demircioglu M, Kangesu I, Ismail A, Lake E, Hughes J, Wright S, Sommerland BC. Increasing accuracy of antenatal ultrasound diagnosis of cleft lip with or without cleft palate, in cases referred to the North Thames London Region. Ultrasound Obstet Gynecol. 2008;31:647–51.
20. Stoll C, Alembik Y, Dott B, Roth MP. Associated malformations in cases with oral clefts. Cleft Palate Craniofac J. 2000;37:41–7.
21. Offerdal K, Jebens N, Syvertsen T, Blaas HG, Johansen OJ, Eik-Nes SH. Prenatal ultrasound detection of facial clefts: a prospective study of 49,314 deliveries in a non-selected population in Norway. Ultrasound Obstet Gynecol. 2008;31:639–46.
22. Beriaghi S, Myers SL, Jensen SA, Kaimal S, Chan CM, Schaefer GB. Cleft lip and palate: association with other congenital malformations. J Clin Pediatr Dent. 2009;33:207–10.
23. Perrotin F, de Poncheville LM, Marret H, Paillet C, Lansac J, Body G. Chromosomal defects and associated malformations in fetal cleft lip with or without cleft palate. Eur J Obstet Gynecol Reprod Biol. 2001;99:19–24.
24. Gillham JC, Anand S, Bullen PJ. Antenatal detection of cleft lip with or without cleft palate: incidence of associated chromosomal and structural anomalies. Ultrasound Obstet Gynecol. 2009;34:410–5.
25. Chmait R, Pretorius D, Moore T, Hull A, James G, Nelson T, Jones M. Prenatal detection of associated anomalies in fetuses diagnosed with cleft lip with or without cleft palate in utero. Ultrasound Obstet Gynecol. 2006;27:173–6.
26. Timmerman E, Pajkrt E, Maas SM, Bilardo CM. Enlarged nuchal translucency in chromosomally normal fetuses: strong association with orofacial clefts. Ultrasound Obstet Gynecol. 2010;36:427–32.
27. Nemana LJ, Marazita ML, Melnick M. Genetic analysis of cleft lip with or without cleft palate in Madras, India. Am J Med Genet. 1992;42:5–9.
28. Stoll C, Dott B, Alembik Y, Roth MP. Evaluation of prenatal diagnosis of cleft lip/palate by foetal ultra sonographic examination. Am Genet. 2000;43:11–4.

29. Hanikeri M, Savundra J, Gillet D, Walters M, McBain W. Antenatal transabdominal ultrasound detection of cleft lip and palate in Western Australia from 1996 to 2003. Cleft Palate Craniofac J. 2006;43:61–6.
30. Bister D, Set P, Cash C, Coleman N, Fanshawe T. Incidence of facial clefts in Cambridge, United Kingdom. Eur J Orthod. 2011;33:372–6.
31. Cash C, Set P, Coleman N. The accuracy of antenatal ultrasound in the detection of facial clefts in a low-risk screening population. Ultrasound Obstet Gynecol. 2001;18:432–6.
32. Grandjean H, Larroque D, Levi S. Sensitivity of routine ultrasound screening of pregnancies in the Eurofetus database. The Eurofetus Team. Ann N Y Acad Sci. 1998;847:118–24.
33. Bronshtein M, Blumenfeld I, Kohn J, Blumenfeld Z. Detection of cleft lip by early second-trimester transvaginal sonography. Obstet Gynecol. 1994;84:73–6.
34. Jones MC. Prenatal diagnosis of cleft lip and palate: detection rates, accuracy of ultrasonography, associated anomalies, and strategies for counseling. Cleft Palate Craniofac J. 2002;39:169–73.
35. Maarse W, Bergé SJ, Pistorius L, van Barneveld T, Kon M, Breugem C, Mink van der Molen AB. Diagnostic accuracy of transabdominal ultrasound in detecting prenatal cleft lip and palate: a systematic review. Ultrasound Obstet Gynecol. 2010;35:495–502.
36. Martínez-Ten P, Perez-Pedregosa J, Santacruz B, Adiego B, Barron E, Sepulveda W. Three-dimensional ultrasound diagnosis of cleft palate: 'reverse face', 'flipped face' or 'oblique face'-which method is best? Ultrasound Obstet Gynecol. 2009;33:399–406.
37. Campbell S, Lees C, Moscoso G, Halls P. Ultrasound antenatal diagnosis of cleft palate by a new technique: the 3D 'reverse face' view. Ultrasound Obstet Gynecol. 2005;25:12–8.
38. Faure JM, Captier G, Bäumler M, Boulot P. Sonographic assessment of normal fetal palate using three-dimensional imaging: a new technique. Ultrasound Obstet Gynecol. 2007;29:159–65.
39. Pilu G, Segata M. A novel technique for visualization of the normal and cleft fetal secondary palate: angled insonation and three-dimensional ultrasound. Ultrasound Obstet Gynecol. 2007;29:166–9.
40. Sepulveda W, Wong AE, Martínez-Ten P, Perez-Pedregosa J. Retronasal triangle: a sonographic landmark for the screening of cleft palate in the first trimester. Ultrasound Obstet Gynecol. 2010;35:7–13.
41. Ghi T, Tani G, Savelli L, Gandolfi Colleoni G, Pilu G, Bovicelli L. Prenatal imaging of facial clefts by magnetic resonance imaging with emphasis on the posterior palate. Prenat Diagn. 2003;23:970–5.
42. Lee W, Kirk JS, Shaheen KW, Hodges AN, Comstock CH. Fetal cleft lip and palate detection by three-dimensional ultrasonography. Ultrasound Obstet Gynecol. 2000;16:299–301.
43. Johnson DD, Pretorius DM, Budorick NE, Jones NE, Jones MC, Lou KV, James GM, et al. Fetal lip and primary palate; three-dimensional ultrasound. Radiology. 2000;217:236–9.
44. Shipp TD, Mullikan JB, Bromley B, Benacerraf B. Three-dimensional prenatal diagnosis of frontonasal malformation and unilateral cleft lip/palate. Ultrasound Obstet Gynecol. 2002;20:290–3.
45. Chamait R, Pretorius D, Jones M, Hull A, James G, Nelson T, Moore T. Prenatal evaluation of facial clefts with two dimensional and adjunctive three dimensional ultrasonography: a prospective trial. Am J Obstet Gynecol. 2002;187:946–9.
46. Campbell S, Lees C. The three-dimensional reverse face (3D RF) view for the diagnosis of cleft palate. Ultrasound Obstet Gynecol. 2003;22:552–4.
47. Wang LM, Leung KY, Tang M. Prenatal evaluation of facial clefts by three-dimensional extended imaging. Prenat Diagn. 2007;27:722–9.
48. Smith AS, Estroff JA, Barnewolt CE, Mulliken JB, Levine D. Prenatal diagnosis of cleft lip and cleft palate using MRI. AJR. 2004;183:229–35.
49. Kazan-Tannus JF, Levine D, McKenzie C, Lim KH, Cohen B, Farrar N, Busse FR, et al. Real-time magnetic resonance imaging aids prenatal diagnosis of isolated cleft palate. J Ultrasound Med. 2005;24:1533–40.
50. Robson CD, Barnewolt CE. MR imaging of the fetal head and neck anomalies. Neuroimaging Clin N Am. 2004;14:273–91.
51. Babcook CJ. The fetal face and neck. In: Callen PW, editor. Ultrasound in obstetrics and gynecology. Philadelphia: WB Saunders; 2000. p. 307–30.
52. Tonni G, Lituania M. A novel 3-dimensional sonographic technique in the study of the fetal hard and soft palates omni view algorithm. J Ultrasound Med. 2012;31:313–8.
53. Benacerraf BR, Sadow PM, Barnewolt CE, Estroff JA, Benson C. Cleft of the secondary palate without cleft lip diagnosed with three-dimensional ultrasound and magnetic resonance imaging in a fetus with Fryns' syndrome. Ultrasound Obstet Gynecol. 2006;27:566–70.
54. Descamps MJ, Golding SJ, Sibley J, McIntyre A, Alvey C, Goodacre T. MRI for definitive in utero diagnosis of cleft palate: a useful adjunct to antenatal care? Cleft Palate Craniofac J. 2010;47:578–85.
55. Wang G, Shan R, Zhao L, Zhu X, Zhang X. Fetal cleft lip with and without cleft palate: comparison between MR imaging and US for prenatal diagnosis. Eur J Radiol. 2011;79:437–42.
56. Mailáth-Pokorny M, Worda C, Krampl-Bettelheim E, Watzinger F, Brugger PC, Prayer D. What does magnetic resonance imaging add to the prenatal ultrasound diagnosis of facial clefts? Ultrasound Obstet Gynecol. 2010;36:445–51.

The Genetics of Facial Cleft

2

Arie Koifman, Susan Blaser, and David Chitayat

2.1 Introduction

Cleft lip ± cleft palate (CL/P) and cleft palate (CP) are the most common congenital craniofacial abnormalities with an estimated prevalence of 1:690 in the United States [1]. Both conditions can be divided into syndromic (associated with other abnormalities) and non-syndromic (isolated) with about 70 % of the cases with CL/P and 50 % of the cases with CP being non-syndromic [2]. In the United States, the prevalence of isolated cleft lip (CL) is 1:3226 live births, of isolated cleft lip and palate (CL + CP) 1:1786, and of isolated CP 1:1695 live births [1]. While the prevalence of CP is the same in different countries and ethnic backgrounds, the incidence of CL/P differs according to the race, ethnic background, environmental exposures, socioeconomic status, and geographical origin. Thus, in the United States the prevalence of isolated CL/P is lowest among blacks and highest among American Indians. The incidence of CL/P is also high among the First Nations population in British Columbia, Canada [1/300] [3]. Furthermore, while CP is more common in females, CL/P is more common in males.

A. Koifman, MD
Institute of Human Genetics, Prenatal genetic diagnosis service, Soroka University Medical Center, Ben-Gurion University of the Negev, Beer-Sheva, Israel

S. Blaser, MD
Professor of Medical Imaging (Neuroradiology), Department of Diagnostic Imaging, Division of Paediatric Neuroradiology; Department of Pediatrics, Division of Paediatric Neuroradiology, The Hospital for Sick Children, University of Toronto, Toronto, ON, Canada

D. Chitayat, MD, FABMG, FACMG, FCCMG, FRCPC (✉)
Department of Obstetrics and Gynecology, The Prenatal Diagnosis and Medical Genetics Program, Mount Sinai Hospital, University of Toronto, The Ontario Power Generation Building, 700 University Avenue, Room 3-709, Toronto, ON M5G 1Z5, Canada

Division of Clinical and Metabolic Genetics, Department of Pediatrics, The Hospital for Sick Children, University of Toronto, Toronto, ON, Canada
e-mail: dchitayat@mtsinai.on.ca

2.2 Embryology

2.2.1 Development of the Face

Five mesenchymal processes are formed during embryogenesis (2 mandibular, 2 maxillary, and 1 frontonasal), and two nasal pits develop in the ventrolateral aspects of the frontonasal prominences, thereby forming two lateral and medial nasal prominences. Complex growth and fusion of these structures forms the face. Key points in facial development include growth of the mandibular prominences to form a single mandible

G. Tonni, W. Sepulveda, and A.E. Wong (eds.), *Prenatal Diagnosis of Orofacial Malformations*,
DOI 10.1007/978-3-319-32516-3_2

Fig. 2.1 Drawing in an anterior oblique view of the late fetal face showing the contributions of the various facial processes. *Green* indicates the frontonasal process; *yellow*, the lateral nasal processes; *purple*, the medial nasal processes; *orange*, the maxillary processes; and *blue*, the mandibular processes (Courtesy of Som and Naidich, *AJNR*, 2014 [4])

and growth of the maxillary prominences toward the midline, fusing with the lateral nasal prominences. A deep groove called the nasolacrimal groove forms between the maxillary and lateral nasal prominences on either side of the developing nose (Fig. 2.1). Most of the groove is obliterated with fusion of the maxillary and lateral nasal prominences, but a small portion of the groove persists and forms the nasolacrimal duct and lacrimal sac. Continued growth of the maxillary prominences combined with regression of the frontonasal prominence eventually develop into the midline of the nose and philtrum of the upper lip. Disruption of the development of any of the facial prominences can result in a variety of facial anomalies, such as cleft lip (failure of the maxillary and medial nasal prominences to fuse), oblique facial cleft (unilateral or bilateral failure of the maxillary, medial and lateral nasal prominences to fuse), horizontal lateral cleft (incomplete lateral merging of the maxillary and mandibular processes), median cleft lip (incomplete fusion of the medial nasal prominences), and frontonasal dysplasia (hyperplasia of the inferior frontonasal prominence which prevents fusion of the medial nasal prominences) [4].

Each of the clefts, apart from the midline clefts, can be unilateral or bilateral, and the cleft lip can be with or without CP with the left side being more frequently affected than the right.

Cleft palate, on the other hand, is the result of incomplete fusión of the palatal shelves and can involve the primary palate, the secondary palate, or both, and can be unilateral or bilateral. In some cases, almost the entire hard and soft palate are missing (Fig. 2.2).

2.3 Non-syndromic Cleft Lip/ Cleft Palate and Cleft Palate

Non-syndromic CL/P and CP have a multifactorial mode of inheritance. In this mode of inheritance, the defect is due to interaction between multiple genes, each having a small additive effect with environmental factors; when the combination of both components reaches a threshold, it results in the abnormality which can be of variable severity (Fig. 2.3). Of the genes involved, some have a major effect such as sonic hedgehog [5], transforming growth factor alpha and beta 3 [6, 7], and IRF6 [8], and some have small additive contributions such as polymorphisms for genes coding for enzymes in the folic acid metabolism pathway [9]. Of the environmental factors, most are not known but some have a major teratogenic effect when exposed during the first trimester of pregnancy. The most important teratogens associated with CL/P and CP are antiseizure medications (phenytoin, sodium valproate, and topiramate) [10] and folic acid antagonists such as methotrexate [11]. Other exposures suspected to be associated with CL/P and CP are cigarette smoking [12], folic acid deficiency [13], and exposure to corticosteroids [14].

As in other multifactorial conditions, the recurrence risk for isolated CL/P depends on the

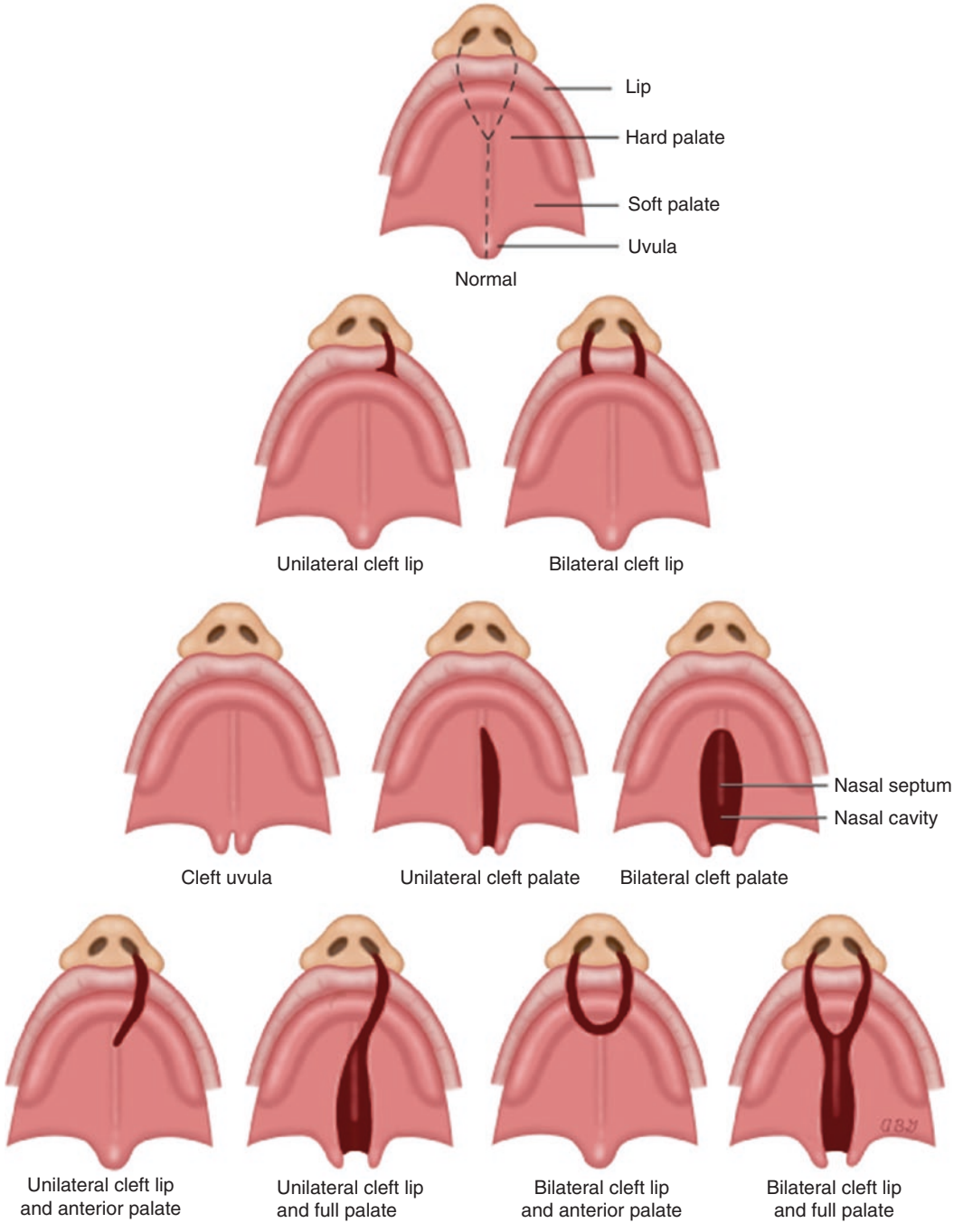

Fig. 2.2 Types of cleft lip ± palate

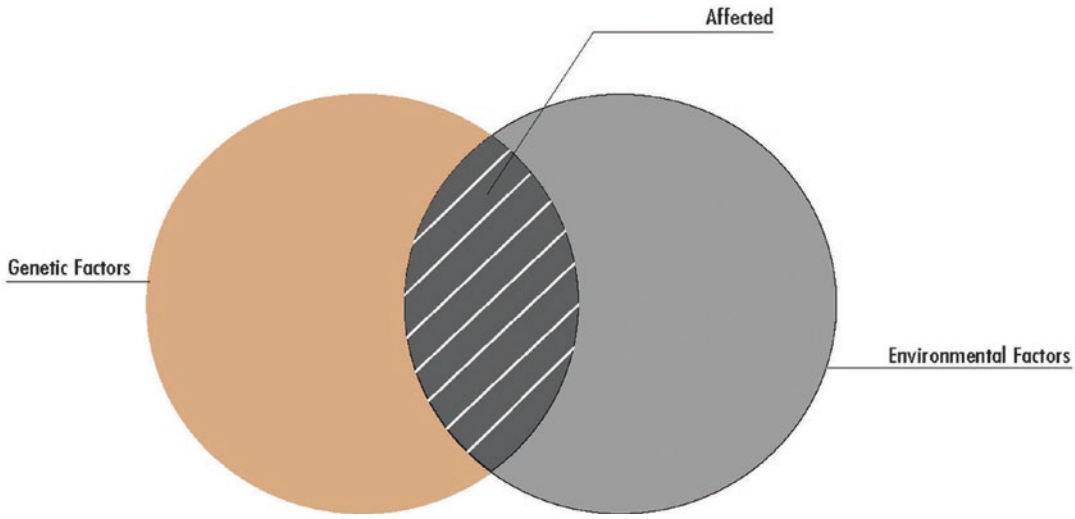

Fig. 2.3 Multifactorial mode of inheritance. Interaction between genes and environment (Courtesy of Greenwood Genetic Center)

Table 2.1 Recurrence risk of oral clefts in percent [15]

Relative	CL	CL/P	CP
Sib	2.5	3.9	3.3
Half sib	1.0	0.5	1.0
Parent	2.5	2.5	2.1
Offspring	3.5	4.1	4.2
Niece/nephew	0.9	0.8	1.1
Aunt/uncle	0.6	1.1	0.6
First cousin	0.3	0.5	0.4

severity of the defect, the number of family members affected, gender (in CL/P, affected females have a higher recurrence risk), and ethnic background (American Indian/First Nations > Asian > Caucasian > African) (Table 2.1).

The recurrence risk of isolated CP does not seem to be influenced by the ethnic background but is higher when a male is the proband.

2.4 Syndromic Cleft Lip/Palate and Cleft Palate

2.4.1 Chromosomal Abnormalities

- *Trisomy 13*: This is also called Patau syndrome and has an incidence of about 1:16,000 newborns. In 80 % of the cases, the chromosome count is 47 and these cases are associated with maternal age. However, 20 % of the cases are due to translocation involving chromosome number 13, and some of these cases are inherited from a parent who carries a chromosome rearrangement involving chromosome number 13, usually as a Robertsonian translocation. The condition is associated with severe intellectual disability, facial dysmorphism, scalp defects, CL/P (occasionally midline) or CP, anophthalmia/microphthalmia, brain and cardiac abnormalities, genital malformations, and postaxial polydactyly. Only 5–10 % of the cases this condition live past their first year [16].
- *Trisomy 18*: This is also called Edwards syndrome and has incidence of 1: 5,000 newborns. About 85 % of the cases recognized during pregnancy do not survive to term, and the chance of having a child with this condition increases with maternal age. Full trisomy 18 always occurs *de novo* and is associated with intrauterine growth restriction (IUGR) and low birth weight, severe intellectual disability, characteristic facial features, CL/P or CP, cardiac abnormalities, clenched fists with overlapping fingers, rocker-bottom feet, and prominent heels. Many individuals with trisomy 18 die in the first month of life, and only 5–10 % of the newborns live past their first year [16].

2.4.2 Microdeletion/ Microduplication Syndromes

- *4p deletion*: This is also known as Wolf-Hirschhorn syndrome and is associated with delayed growth and development, characteristic facial features ("Greek warrior helmet"), microcephaly, CL/P or CP, iris and/or optic nerve coloboma and other eye defects, scoliosis and kyphosis, club feet, and occasional cardiac and genital malformations. The prevalence of Wolf-Hirschhorn syndrome is estimated to be 1 in 50,000 births [17].
- *22q11.2 deletion syndrome*: This is also known as velo-cardio-facial syndrome, DiGeorge syndrome, or Shprintzen syndrome, and is associated with a large interstitial deletion of 22q11.2. At least 30 genes have been mapped to the region, but most phenotypes of the syndrome are believed to be the haploinsufficiency of the gene TBX1. The condition is associated with short stature (1/3 of cases), CL/P or CP, conductive hearing loss usually secondary to the cleft palate, velopharyngeal incompetence, bulbous/square nose, narrow palpebral fissures, micro-/retrognathia, cardiac abnormalities, cellular immunodeficiency, and hyperparathyroidism (usually transient). Moderate or severe learning problems are present in ~20%, and 10% have psychiatric disorders (schizophrenia and/or bipolar disorder).
- *1q43-q44 deletion*: This condition is characterized by prenatal and postnatal growth restriction, intellectual disability (moderate to severe), characteristic facial features including microcephaly, prominent forehead, short nose with a broad nasal tip, and CP. Agenesis of the corpus callosum and other brain abnormalities are common [18].
- *3q29 microdeletion syndrome*: The condition is associated with variable phenotypes despite an almost identical deletion size. Common clinical findings include mild to moderate mental retardation, autism, gait ataxia and only slightly dysmorphic facial features including microcephaly, a narrow face, short philtrum, high nasal bridge, CP or CL/P, horseshoe kidney, hypospadias and ligamentous laxity [19].

2.5 Mendelian Syndromes Associated with Cleft Lip/ Palate

2.5.1 Autosomal Dominant (AD)

- *van der Woude syndrome*: This syndrome has an incidence of 1:35,000–1:100,000 and is caused by mutations in the interferon regulatory factor 6 (*IRF6*). It is characterized by lower lip pits (80%), hypodontia, missing teeth, CL/P or CP, and cleft uvula. The average IQ of individuals with van der Woude syndrome is similar to that of the general population. Missense mutations in the same gene cause multiple pterygium syndrome [20].
- *Stickler syndrome*: This AD disorder is characterized by Robin sequence, flat facies, myopia, retinal detachment and cataracts, spondyloepiphyseal dysplasia and CP and/or CL/P. Other findings include hearing loss (both sensorineural and conductive), hyperextensible joints, and talipes equinovarus. Gene mutations known to be associated with this condition occur in *COL2A1, COL11A1, COL11A2, COL9A1*, and *COL9A2*, which cause Stickler syndrome types I through V, respectively. These genes are involved in the production of three types of collagen: type II, type IX, and type XI. Stickler syndrome types I, II, and III are inherited in an autosomal dominant pattern, and types IV and V have an autosomal recessive mode of inheritance [21].
- *Treacher Collins syndrome*: This condition is caused by mutations in the *TCOF1* (78–93%) and in the *POLR1D* and *POLR1C* genes. The dysmorphic features, although variable, are distinctive and consist of mandibular/malar hypoplasia, CP with or without cleft lip, hypoplastic zygomatic bone, lower eyelid coloboma, partial to total absence of the lower eyelashes, abnormal auricles/external ear canal, unilateral or bilateral choanal stenosis or atresia, and conductive deafness usually caused by malformation of the ossicles and hypoplasia of the middle ear cavities. Inner ear structures are usually normal. The incidence is about 1:50,000 [22].

- *Ectrodactyly-ectodermal dysplasia-clefting syndrome (EEC) or ankyloblepharon-ectodermal defects-cleft lip/palate (AEC) syndrome*: This condition is associated with CL/P (in about 2/3 of cases), maxillary and malar hypoplasia, short philtrum, ankyloblepharon, labyrinthine dysplasia and distal limb defects including syndactyly, camptodactyly, and ectrodactyly (in up to 85% of cases). Ectodermal dysplasia includes sparse wiry hair, skin erosions, nail changes, dental changes, decreased sweating, and hypoplastic nipples. Partial anodontia and microdontia are common. Genitourinary anomalies are present in about half of the cases and include megaureter, duplicated collecting system, vesicoureteral reflux, ureterocele, bladder diverticula, and renal agenesis/dysplasia. The condition is caused by mutations in *TP63* which is also known to be associated with Hay-Wells syndrome [23].

2.5.2 Autosomal Recessive (AR)

- *Smith-Lemli-Opitz syndrome* (*SLO*): This condition is caused by mutations in the *DHCR7* gene affecting the cholesterol biosynthesis and resulting in low plasma cholesterol level and elevated concentrations of 7-dehydrocholesterol. Clinical features include facial dysmorphism, CL/P, short stature, microcephaly, micrognathia, polydactyly, syndactyly, genitourinary abnormalities (hypospadias, cryptorchidism, micropenis, hypoplastic scrotum, bifid scrotum, microurethra, ureteropelvic junction obstruction, hydronephrosis, renal cystic dysplasia, renal duplication, renal agenesis), and cardiac malformations [24].
- *Fryns syndrome*: This condition is characterized by coarse facies with ocular hypertelorism, broad and flat nose and nasal bridge, long philtrum, large mouth, micrognathia, poorly formed ears, CL/CP or CP, diaphragmatic defects (diaphragmatic hernia, eventration, hypoplasia, or agenesis), distal digital hypoplasia, and eye abnormalities including cloudy corneas and/or microphthalmia, renal dysplasia/cortical cysts, and brain, genital, and cardiac abnormalities. Most cases die within the neonatal period. The gene has not been delineated [25].

2.5.3 X-Linked

- *Opitz G/BBB syndrome*: This syndrome consists of facial abnormalities including prominent forehead, hypertelorism, broad and flat nasal bridge with anteverted nostrils, and CL/P. Other findings include bifid uvula, cleft tongue, omega-shaped epiglottis, tracheomalacia, brain abnormalities including agenesis/hypoplasia of the corpus callosum, and genital abnormalities. Mild to moderate intellectual disability is detected in 2/3 of the patients. The condition is known to be associated with mutations in the *MID1* gene although an AD form of the condition has been reported [26].
- *Oral-facial-digital syndrome type 1 (OFD)*: This is a primary ciliary abnormality characterized by oral abnormalities including lobed tongue with hamartomas or lipomas, CL/P or CP, and/or median cleft or pseudocleft upper lip, accessory gingival frenulae, dental abnormalities and digital abnormalities including brachydactyly, preaxial or postaxial polydactyly, syndactyly of varying degrees, and clinodactyly of the fifth finger on the hands as well as duplicated hallux and facial abnormalities including hypertelorism, telecanthus, hypoplasia of the alae nasi, and micrognathia [27]. Renal cysts other abnormalities include renal cysts and brain involvement such as intracerebral cysts, agenesis of the corpus callosum, and Dandy-Walker malformation. Developmental delay is found in as many as 50% of the patients with OFD1, and almost all affected individuals are female with the condition being mainly lethal in males.

2.5.4 Facial Clefts

Facial cleft is a term used to describe all clefts apart from CL/P and CP. These defects can affect both skin/soft tissue and bone. Facial clefts are extremely rare and in most cases are associated

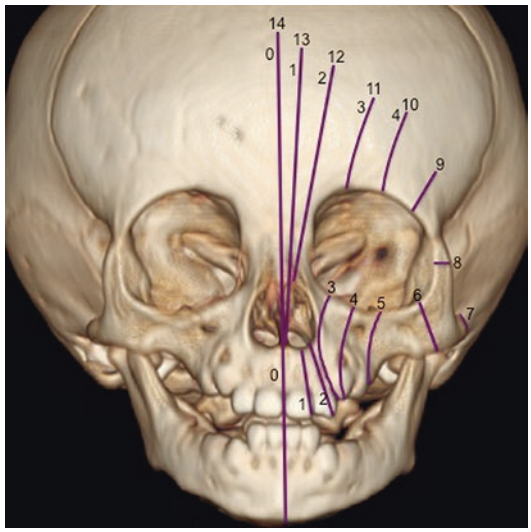

Fig. 2.4 Tessier lines of vertical clefting

with other craniofacial abnormalities. The etiology, apart from the cases associated with amniotic band, is not known and almost all are sporadic/not inherited.

In 1976 Paul Tessier [28] (Fig. 2.4) published a classification on facial clefts based on the anatomical position of the clefts. The different types of Tessier clefts are numbered 0–14. These 15 different types of clefts can be put into four groups, based on their position: midline clefts, paramedian clefts, orbital clefts, and lateral clefts. The Tessier classification describes the level of clefting in both the soft tissue and bone since the two may be different.

2.5.5 Midline Clefts

According to Tessier classification, the midline clefts (numbers 0 and 14) are vertical; Tessier number 0 bisects the maxilla and the nose, and Tessier number 14 bisects the nose and frontal bone.

2.5.6 Oblique Clefts

These consist of paramedian and orbital clefts. The paramedian clefts are numbers 1, 2, 12, and 13, and although they are quite similar to the midline clefts, they are further away from the midline of the face. The orbital clefts are Tessier numbers 3, 4, 5, 9, 10, and 11 and involve the orbit. Tessier numbers 3, 4, and 5 are through the maxilla and the orbital floor, and Tessier numbers 9, 10, and 11 are between the upper side of the orbit and the forehead or the temple of the head. Tessier number 11 is an extension of number 3, number 10 is an extension of number 4, and number 9 is an extension of number 5.

2.5.7 Lateral Clefts

These consist of Tessier numbers 6, 7, and 8 and result in congenital macrostomia. The condition is rare and caused by failure of fusion of the maxillary and mandibular processes of the first branchial arch. Tessier number 7 is positioned on the line between the corner of the mouth and the ear. Tessier number 8 runs from the outer corner of the eye toward the ear. The combination of a Tessier number 6-7-8 is seen in Treacher Collins syndrome, Tessier number 7 is found in relation to hemifacial microsomia, and number 8 is found in Goldenhar syndrome. The severity of the clefts varies; most are unilateral and do not extend beyond the anterior border of the masseter.

2.6 Summary and Recommendations

CL/P and CP are the most common craniofacial abnormalities identified in the newborn. About 70 % of the cases of CL/P and 50 % of the cases of CP are non-syndromic, and thus a medical geneticist should be consulted on all cases. Non-syndromic isolated CL/P is more common than non-syndromic isolated CP alone, and the prevalence of CL/P varies with gender, race/ethnicity, and geographic location.

When detected pre- or postnatally, a referral to the orofacial/cleft lip and palate team should be initiated as well as referral to a medical geneticist, and the following should be included in the assessment:

Obtain pregnancy history: Information regarding maternal diseases, maternal exposures, prenatal screening and testing, and fetal ultrasound findings.

Obtain family history: A three-generation pedigree of both parents.

Perform detailed physical examination: A detailed and systematic physical examination of the patient is mandatory looking for abnormalities that can distinguish between syndromic and non-syndromic conditions and can help make the diagnosis. A detailed examination of the orofacial region is of utmost importance.

2.7 Investigation

In cases with apparently non-syndromic CL/P and CP, microarray analysis is recommended. In syndromic cases, if a specific condition is suspected, mutation analysis should be performed. If the diagnosis is not known, whole exome/genome sequencing should be considered.

Depending on the finding on physical examination and the suspected diagnosis, further investigation may be needed including:

1. Cardiac assessment/echocardiography
2. Eye examination
3. Abdominal/renal ultrasound
4. Brain ultrasound/MRI
5. Skeletal survey

References

1. Mai CT, Cassell CH, Meyer RE, Isenburg J, Canfield MA, Rickard R, Olney RS, Stallings EB, Beck M, Hashm SS, et al. Birth defects data from population-based birth defects surveillance programs in the United States, 2007 to 2011: highlighting orofacial clefts. Birth Defects Res A Clin Mol Teratol. 2014;100:895–904.
2. Shi M, Wehby GL, Murray JC. Review on genetic variants and maternal smoking in the etiology of oral clefts and other birth defects. Birth Defects Res C Embryo Today Rev. 2008;84:16–29.
3. Lowry RB, Johnson CY, Gagnon F, Little J. Segregation analysis of cleft lip with or without cleft palate in the First Nations (Amerindian) people of British Columbia and review of isolated cleft palate etiologies. Birth Defects Res A Clin Mol Teratol. 2009;85:568–73.
4. Som PM, Naidich TP. Illustrated review of the embryology and development of the facial region, part 2: late development of the fetal face and changes in the face from the newborn to adulthood. AJNR Am J Neuroradiol. 2014;35:10–8.
5. Young DL, Schneider RA, Hu D, Helms JA. Genetic and teratogenic approaches to craniofacial development. Crit Rev Oral Biol Med. 2000;11:304–17.
6. Lu XC, Yu W, Tao Y, Zhao PL, Li K, Tang LJ, Zheng JY, Li L. Contribution of transforming growth factor α polymorphisms to nonsyndromic orofacial clefts: a HuGE review and meta-analysis. Am J Epidemiol. 2014;179:267–81.
7. Lidra AC, Romitti PA, Basart AM, Doetschman T, Leysens NJ, Daack-Hirsch S, Semina EV, Johnson LR, Machida J, Burds A, et al. Association of MSX1 and TGFB3 with nonsyndromic clefting in humans. Am J Hum Genet. 1998;63:557–68.
8. Blanton SH, Cortez A, Stal S, Mulliken JB, Finnell RH, Hecht JT. Variation in IRF6 contributes to nonsyndromic cleft lip and palate. Am J Med Genet A. 2005;37A:259–62.
9. van Rooij IALM, Swinkels DW, Blom HJ, Merkus HMWM, Steegers-Theunissen RPM. Vitamin and homocysteine status of mothers and infants and the risk of nonsyndromic orofacial clefts. Am J Obstet Gynecol. 2003;189:1155–60.
10. Hunt S, Russel A, Smithson WH, Parsons L, Robertson I, Waddell R, Irwin B, Morrison PJ, Morrow J, Craig J, et al. Topiramate in pregnancy: preliminary experience from the UK Epilepsy and Pregnancy Register. Neurology. 2008;71:272–6.
11. Hyoun SC, Običan SG, Scialli AR. Teratogen update: methotrexate. Birth Defects Res A Clin Mol Teratol. 2012;94:187–207.
12. Shaw GM, Wasserman CR, Lammer EJ, O'Malley CD, Murray JC, Basart AM, Tolarova MM. Orofacial clefts, parental cigarette smoking, and transforming growth factor-alpha gene variants. Am J Hum Genet. 1996;58:551–61.
13. Butali A, Little J, Chevrier C, Cordier S, Steegers-Theunissen R, Jugessur A, Oladugba B, Mossey PA. Folic acid supplementation use and the MTHFR C677T polymorphism in orofacial clefts etiology: an individual participant data pooled-analysis. Birth Defects Res A Clin Mol Teratol. 2013;97:509–14.
14. Fraser FC, Sajoo A. Teratogenic potential of corticosteroids in humans. Teratology. 1995;51:45–6.
15. Grosen D, Chevrier C, Skytthe A, Bille C, Mølsted K, Sivertsen A, Murray JC, Christensen K. A cohort study of recurrence patterns among more than 54,000 relatives of oral cleft cases in Denmark: support for the multifactorial threshold model of inheritance. J Med Genet. 2010;47:162–8.
16. Rasmussen SA, Wong LYC, Yang Q, May KM, Friedman JM. Population-based analyses of mortality in trisomy 13 and trisomy 18. Pediatrics. 2003;111:777–84.

17. Zollino M, Murdolo M, Marang G, Pecile V, Galasso C, Mazzanti L, Neri G. On the nosology and pathogenesis of Wolf-Hirschhorn syndrome: genotype-phenotype correlation analysis of 80 patients and literature review. Am J Med Genet C Semin Med Genet. 2008;148C:257–69.
18. De Vries BB, Knight SJ, Homfray T, Smithson SF, Flint J, Winter RM. Submicroscopic subtelomeric 1qter deletions: a recognisable phenotype? J Med Genet. 2001;38:175–8.
19. Digilio MC, Bernardini L, Mingarell R, Capolino R, Capalbo A, Giuffrida MG, Versacci P, Novelli A, Dallapiccola B. 3q29 Microdeletion: a mental retardation disorder unassociated with a recognizable phenotype in two mother-daughter pairs. Am J Med Genet A. 2009;149A:1777–81.
20. Kondo S, Schutte BC, Richardson RJ, Bjork BC, Knight AS, Watanabe Y, Howard E, de Lima RLF, Daack-Hirsch S, Sander A, et al. Mutations in IRF6 cause Van der Woude and popliteal pterygium syndromes. Nat Genet. 2002;32:285–9.
21. Pagon RA, Adam MP, Ardinger HH, Bird TD, Dolan CR, Fong CT, Smith RJ, Stephens K, Robin NH, Moran RT, et al. Stickler syndrome. Seattle: University of Washington, Seattle; 1993.
22. Saka D, Trainor PA. Treacher Collins syndrome: unmasking the role of Tcof1/treacle. Int J Biochem Cell Biol. 2009;41:1229–32.
23. Cole P, Hatef DA, Kaufman Y, Magruder A, Bree A, Friedman E, Sindwani R, Hollier LH. Facial clefting and oroauditory pathway manifestations in ankyloblepharon-ectodermal defects-cleft lip/palate (AEC) syndrome. Am J Med Genet A. 2009;149A:1910–5.
24. Nowaczyk MJM, Irons MB. Smith-Lemli-Opitz syndrome: phenotype, natural history, and epidemiology. Am J Med Genet C Semin Med Genet. 2012;160C:250–62.
25. Arora K, Thukral A, Das RR, Gupta N, Kabra M, Agarwal R. Fryns syndrome: a lethal birth defect with variable phenotypic expressions in siblings. Indian J Pediatr. 2014;81:614–6.
26. Hu CH, Liu YF, Yu JS, Ng YY, Chen SJ, Su PH, Chen JY. A MID1 gene mutation in a patient with Opitz G/BBB syndrome that altered the 3D structure of SPRY domain. Am J Med Genet A. 2012;158A:726–31.
27. Bisschoff IJ, Zeschnigk C, Horn D, Wellek B, Rieß A, Wessels M, Willems P, Jensen P, Busche A, Bekkebraten J, et al. Novel mutations including deletions of the entire OFD1 gene in 30 families with type 1 orofaciodigital syndrome: a study of the extensive clinical variability. Hum Mutat. 2013;34:237–47.
28. Tessier P. Anatomical classification facial, craniofacial and latero-facial clefts. J Maxillofac Surg. 1976;4:69–92.

Evaluation of the Fetal Face in the First Trimester

3

Waldo Sepulveda, Amy E. Wong,
Pilar Martinez-Ten, and Gabriele Tonni

3.1 Introduction

Evaluation of the fetal face during the first trimester of pregnancy is a relatively new area of research in Fetal Medicine. The first attempts to examine the fetal face in early pregnancy were performed using transvaginal or transabdominal embryofetoscopy in the early 1990s [1–3]. Although this invasive technique allowed the early diagnosis of facial abnormalities in several high-risk cases [4, 5], the high rate of miscarriage made this approach unacceptable for diagnostic and therapeutic purposes in ongoing pregnancies [6]. Currently, the use of this technique is confined to confirm ultrasound diagnosis before first-trimester termination of pregnancy [7].

Ultrasound has been the primary diagnostic tool for prenatal examination of the fetal face for more than 30 years. The prenatal ultrasound diagnosis of cleft lip and palate (CLP) was first reported in 1981 [8], the ultrasound technique for examining the fetal upper lip to improve the detection of CLP was first described in 1983 [9], and detailed ultrasound features of the fetal face in second- and third-trimester fetuses were fully described in the mid-1980s [10, 11]. Nevertheless, the 2003 American Institute of Ultrasound in Medicine (AIUM) Practice Guideline for the performance of an antepartum obstetric ultrasound examination, developed in collaboration with the American College of Radiology (ACR) and the American College of Obstetricians and Gynecologists (ACOG), did not include examination of the fetal face as part of the standard ultrasound examination [12]. Currently, however, prenatal evaluation of the fetal face is an integral part of the routine second-trimester ultrasound examination as recommended by the AIUM, ACR, ACOG, Society of Radiologists in Ultrasound (SRU), and International Society of Ultrasound in Obstetrics and Gynecology (ISUOG) [13–15]. Although in these guidelines it is implicit that evaluation of the fetal face should include an attempt to visualize the upper lip for possible cleft lip anomaly, only the ISUOG guideline specifically states that this should include a focused visualization of the upper lip and, if technically possible, the profile, orbits, nose, and nostrils [14].

W. Sepulveda, MD (✉)
Fetalmed – Maternal-Fetal Diagnostic Center, Estoril 50, Room 515, Las Condes, Santiago 7591047, Chile
e-mail: waldosepulveda@fetalmed.cl

A.E. Wong, MD
Department of Maternal-Fetal Medicine, Palo Alto Medical Foundation, Mountain View, CA, USA

P. Martinez-Ten, MD
Delta – Ultrasound Diagnostic Center in Obstetrics and Gynecology, Madrid, Spain

G. Tonni, MD, PhD
Department of Obstetrics and Gynecology, Prenatal Diagnostic Service, Guastalla Civil Hospital, AUSL Reggio Emilia, Reggio Emilia, Italy

G. Tonni, W. Sepulveda, and A.E. Wong (eds.), *Prenatal Diagnosis of Orofacial Malformations*,
DOI 10.1007/978-3-319-32516-3_3

A primary goal of a focused examination of the fetal face at any given gestational age is the prenatal detection of orofacial clefts or other facial dysmorphisms that may suggest the presence of an underlying genetic or chromosomal disorder. Therefore, a thorough ultrasound examination should focus on ruling out several conditions, mainly CLP, absence or hypoplasia of the nasal bones, micrognathia, and hypertelorism or hypotelorism among others [16, 17]. In particular, the prenatal diagnosis of CLP is usually made during the second or third trimester, at which time examination of the coronal plane of the fetal face shows a defect involving the upper lip and, at the axial view at the level of the alveolus, a gap in the upper lip and alveolar ridge [18–21]. In cases of bilateral cleft lip, the premaxilla is often dislodged anteriorly; this protruding mass can be detected by ultrasound in the midsagittal view of the fetal face as a paranasal echogenic mass, the "premaxillary protrusion" sign [22]. In cases of central clefts, however, the entire premaxillary area is missing and the cleft extends posteriorly affecting the secondary palate, resulting in a flat profile due to severe hypoplasia of the midface. These latter cases are often associated with lethal aneuploidies [23].

During the early development of high-resolution ultrasound, detection of facial abnormalities in the first trimester was reported only in a handful of cases, most of them detected incidentally or in a high-risk population undergoing an early scan because of a history of a previously affected infant or fetus [24–28]. The relatively recent widespread incorporation of the first-trimester ultrasound screening for aneuploidy between 11 and 13 weeks of gestation [29–31] has made it possible to detect structural anomalies in the general population in early pregnancy [32–39]. Nevertheless, focused examination of the fetal face has been rarely included in the first-trimester ultrasound scanning protocol even though one of the main criteria for the correct measurement of the nuchal translucency (NT) thickness and assessment of the nasal bone is the mandatory visualization of the fetal profile in the true midsagittal view of the face [30, 31]. Indeed, the 2013 ISUOG Practice Guidelines for performance of the first-trimester fetal ultrasound scan suggested that the fetal face is an optional structure to examine and failure to examine the face should not prompt further examination earlier than the second-trimester anatomy scan [40].

On the other hand, evaluation of the face in the first trimester has been suggested to increase the detection rate of fetuses with aneuploidy, particularly those with trisomy 21. Indeed, ultrasound markers for aneuploidy involving the face, such as visualization of the nasal bone [41] and measurement of the frontomaxillary facial angle [42], have been incorporated into the first-trimester ultrasound protocol with variable detection rates. Of note, despite the strong impact of the previously mentioned ultrasound markers in the first-trimester detection of aneuploid fetuses, which has led to the early diagnosis of trisomy 21 in numerous cases, the evaluation of the fetal profile did not improve the detection of CLP despite the similar incidence of these two conditions in the general population.

In this chapter, we will discuss the main first-trimester ultrasound features of the normal and abnormal fetal face. Ultrasound examination of the fetal face using both the sagittal and coronal views, as well as the role of three-dimensional (3D) ultrasound in the assessment of the normal lip and palate and in the diagnosis of orofacial clefts and other common facial malformations that are potentially diagnosable at the first-trimester ultrasound scan at 11-13 weeks of gestation, will be emphasized. As clefts of the soft palate are not currently possible to detect in the first trimester, this particular topic will not be covered in this chapter.

3.2 Normal Ultrasound Anatomy of the Fetal Face in the First Trimester

The fetal face can be readily identified and examined during the first-trimester ultrasound scan at 11–13 weeks of gestation using two-dimensional (2D) high-resolution real-time ultrasound (Fig. 3.1). This examination is facilitated by the clear contrast between the amniotic fluid and the facial outline, unless the fetus is in a persistent prone or lateral position. If a proper midsagittal plane is obtained and adequate magnification is

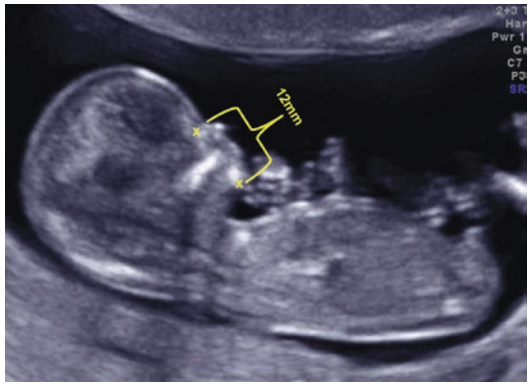

Fig. 3.1 Sagittal two-dimensional ultrasound view in a 13-week fetus. The fetal profile is clearly depicted despite the small size of the fetal face; calipers denote the nasion-to-chin distance, which in this case was 12 mm

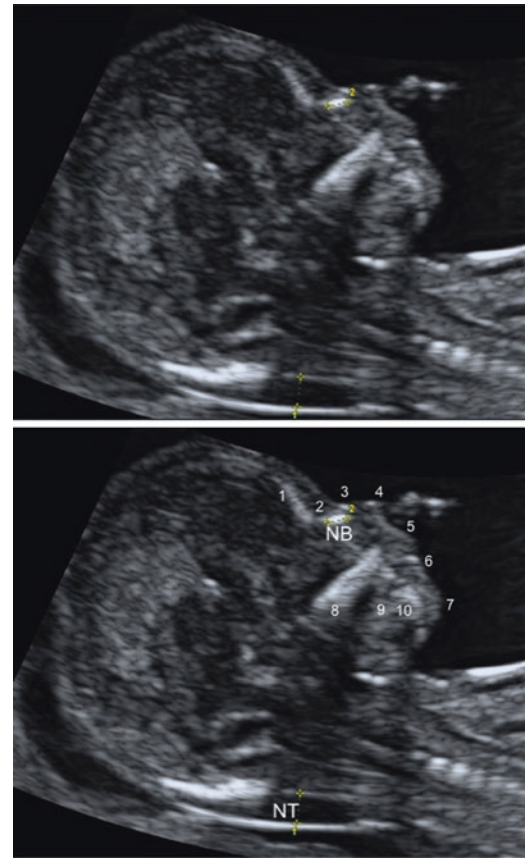

Fig. 3.2 Sagittal view of the fetal head used for first-trimester aneuploidy screening purposes to measure the nuchal translucency (NT) thickness and assess the nasal bone (NB). The facial structures that are clearly visualized at this gestational age are: *1* frontal bone, *2* prefrontal and prenasal subcutaneous tissue, *3* nasal skin, *4* tip of the nose, *5* upper lip, *6* lower lip, *7* chin, 8 palate, *9* oral cavity and tongue, *10* mandibular bone

used, the entire profile can be examined (Fig. 3.2). In this plane, several anatomic landmarks including the forehead, prefrontal and prenasal subcutaneous soft tissue, nasal bone, upper and lower lips, and chin can be identified and evaluated using adequate ultrasound settings. On deeper planes, the primary and secondary palates are always identified and appear together as a single thick, rectangular echogenic line almost perpendicular to the profile. The anterior portion of the mandible is also seen in this view as a small echogenic square in the lower aspect of the profile. The tongue can be seen within the oral cavity, particularly when swallowing movements are present. The nose and nasal bone are important structures of the midface with which most sonographers performing first-trimester ultrasound aneuploidy screening are familiar. The three characteristic echogenic lines, including the tip of the nose, the skin line, and the nasal bones, should always be identified for a proper assessment of the midface [30, 31].

In the coronal plane (Fig. 3.3), the two frontal bones are visualized in the upper aspect of the face, which at this gestational age appear clearly separated in the midline by the metopic suture. In a slightly more caudal view, the eyeballs can be identified as predominantly anechoic, paired structures within the orbits. Within each eyeball, the lens is seen as a small, anechoic round structure surrounded by an echogenic rim. In the midface, the maxilla is the most prominent structure, which is seen as an echogenic, triangular-shaped structure forming the "retronasal triangle" (RNT) corresponding to the alveolar ridge at the base and the frontal processes of the maxilla laterally (Fig. 3.4) [43]. At the top of the RNT, the nasal bones can be easily seen [44, 45]. In the lower part of the face, the right and left mandibular bones are seen, normally displaying a gap between them (the "mandibular gap") [46]. In between the maxilla and mandible, the mouth is seen as a predominantly anechoic, oval-shaped area. In contrast to the straightforward visualization of the echogenic alveolar ridge, the upper lip is difficult to image in the coronal plane of the face.

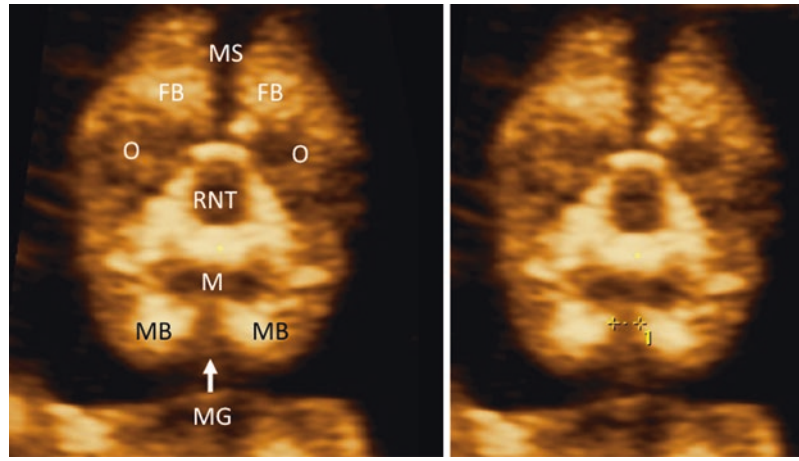

Fig. 3.3 *Left panel*, coronal view of the fetal face in the first trimester. The facial structures that are clearly visualized at this gestational age are *MS* metopic suture, *FB* frontal bone, *O* orbit, *RNT* retronasal triangle (alveolar ridge and frontal processes of the maxilla with the nasal bones on the top, see also Fig. 3.4), *M* mouth, *MB* mandibular bone, *MG* mandibular gap. *Right panel*, calipers delineating the mandibular gap

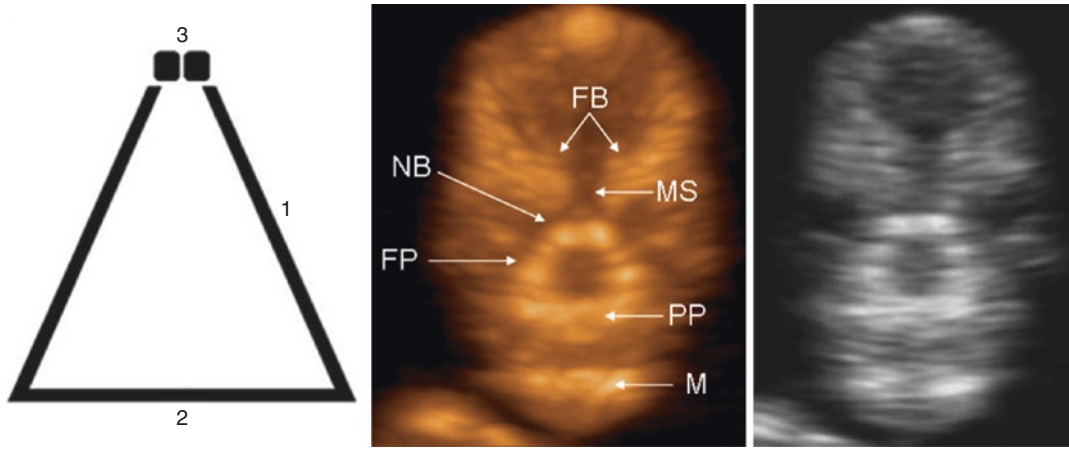

Fig. 3.4 Retronasal triangle. *Left panel*, drawing of the retronasal triangle. *1* frontal process of the maxilla, *2* alveolar ridge (primary palate), *3* nasal bones. *Middle and right panels*, coronal ultrasound view of the face in a first trimester fetus. *FB* frontal bones, *MS* metopic suture, *NB* nasal bones, *FP* frontal process of the maxilla, *PP* primary palate, *M* mandibular bone

A detailed study evaluating which fetal anatomic structures can be identified in the first trimester was undertaken in 1144 singleton pregnancies undergoing first-trimester screening ultrasound in a dedicated Fetal Medicine Center [47]. Visualization rates of the fetal face, aiming to identify the orbits, lens, and profile according to the fetal crown-rump length, were 98.3, 99.5, 99.0, and 100 % for fetuses with crown-rump lengths of 45–54, 55–64, 65–74, and 75–82 mm, respectively. The overall visualization rate of the fetal face was 99.2 % (1135 of 1144 fetuses). In another study involving 300 first-trimester pregnancies with complete pregnancy follow-up, the fetal face was seen in 95 % of cases [48]. These data suggest that properly trained sonographers can confidently visualize the fetal face and hence perform a basic examination of this area during the first-trimester ultrasound scan.

In order to define the normal first-trimester facial structure, normative data have been reported including measurement of the nasal bone [49–52], prenasal thickness [53], maxillary and mandibular bone length [54–56], premaxillary thickness [57], frontomaxillary facial angle [42], and frontal space [58, 59]. These measurements, although potentially useful for the detection of several anomalies affecting the fetal face

in the first trimester, seem to have limited value for screening in the general population and should be restricted either to those cases in which an anomaly is suspected or for research purposes.

The use of 3D ultrasound in the evaluation of the fetal anatomy has been an important contribution to clinical practice. In the particular case of first-trimester fetuses, this technique can provide detailed, high-definition views of the fetal facial anatomy in all possible angles, especially when high-quality volume datasets are obtained with transvaginal probes and analyzed offline. Display of the three orthogonal planes or, alternatively, multiple parallel views using multiplanar mode facilitates the identification of all the facial structures, particularly the frontal bones, orbits, primary and secondary palates, and mandible. Surface-rendering mode is another extremely useful technique to display the upper lip and metopic suture to rule out facial malformations. Surface-rendering views can also be enhanced with the use of HDLive™ technology, which allows lightening and shadowing of certain areas of the anatomy to generate more realistic images of the fetal face [60].

3.3 Retronasal Triangle View

Due to its potential utility in determining the normal facial anatomy in the first trimester, the RNT is discussed separately in this section. The RNT corresponds to the triangular-shaped, echogenic lines seen in the coronal plane of the midface that represents the maxillary bone (Figs. 3.3 and 3.4). The maxilla is formed by the alveolar ridge (the anterior part of the primary palate situated in the caudal aspect of the midface) and two bony prolongations, the frontal processes of the maxilla, which join in the midline superiorly at the level of the nasal bones below the metopic suture. In the first trimester, the coronal view of the maxilla displays an echogenic triangle that can be easily visualized just posterior to the nose, hence the term "retronasal triangle" used to describe this landmark [43]. First-trimester ultrasound screening studies have demonstrated that the visualization rate of the RNT during the scan is very high, ranging from 98 to 100 % [43, 61, 62].

There are two techniques to visualize the RNT with transabdominal ultrasound. The first is to identify the midsagittal plane of the fetal head to image the fetal profile. Then, the transducer is rotated 90° and a sweep to the lower part of the face is performed until the RNT is visualized. The other technique is to first visualize the axial view of the fetal brain at the level of the choroid plexuses ("butterfly" sign) [63] and then to sweep the transducer downward in the same angle until the midface is identified. Once the RNT is visualized, a short sweep should be done to assess the nasal bones and the primary palate. The latter technique is the one recommended by the authors because it has the advantage of being able to evaluate more structures, therefore improving the early detection of other anomalies. Indeed, in this sweep, it is possible to visualize both eyes, including the orbits, eyeballs, and lenses just above the RNT. At the top of the triangle, one or both nasal bones can be easily identified, which can be an alternative technique for the assessment of the nasal bone in the first-trimester screening of aneuploidy [44, 45]. In a more inferior plane, the mandibular bones can also be identified, and this view can be used for the screening of micrognathia by assessing the "mandibular gap," which corresponds to the separation between the two mandibular bones posterior to the chin [46]. In addition, we have noted that by extending the sweep caudally, it is also feasible to identify the clavicles and the upper extremities, which can also be helpful for confirming the presence of the clavicles and the two hands to rule our upper limb reduction defects (unpublished observations).

3.4 3D Ultrasound Evaluation of the Fetal Face in the First Trimester

3D ultrasound is an important tool for the evaluation of the fetal face in the first trimester. Using both multiplanar and surface-rendering

modes, almost all anatomical structures of the fetal face can be identified and examined using offline analysis of the acquired 3D volume datasets. As the acquired 3D volume can be reformatted in any given angle and depth, any desired plane can be obtained. This possibility has enormous advantages over the 2D ultrasound technique, as the 3D volume can be stored and analyzed offline as many times as required without loss of resolution. In addition, 3D datasets can also be sent for remote specialist consultation. Nevertheless, although 3D ultrasound has been extensively used to examine the face in normal and abnormal second- or third-trimester fetuses, its use in the first trimester has intrinsic limitations because the soft tissue at this gestational age is more difficult to delineate and the skeletal bony structures are still hypomineralized. In addition, 3D acquisition should be obtained at optimal planes, with high-resolution equipment and, ideally, using the transvaginal approach. Additional sources of suboptimal imaging are technical factors such as early gestational age, poor fetal position, and maternal habitus or previous abdominal surgery if the transabdominal route is used. If possible, the transvaginal route should be offered to the patient and attempted every time high-quality 3D datasets are required, especially in cases of suspected fetal anomalies.

There are two 3D algorithms that can be used to examine the fetal face in the first trimester. The first is the multiplanar mode, which is extremely useful to examine simultaneously all three orthogonal planes or obtain any desired view of the facial structures (Fig. 3.5). This is the technique of choice to obtain the exact sagittal, coronal, or axial plane if needed for analysis. In addition, it provides a useful tool for avoiding misinterpretation or artifacts in the early evaluation of the fetal face. Several technological modifications of the multiplanar mode have been developed, including the OmniView™ software, which displays up to three simultaneous views in any plane (Fig. 3.6), and the ObliqueView™ software, which displays either a single orthogonal plane or multiple parallel planes of different thickness by drawing a line in any plane of the screen (Figs. 3.7 and 3.8). Visualization of the fetal palate using a commercially available algorithm (Volume NT™), which automatically obtains the true midsagittal plane of the fetal head, has proven to be extremely useful in the first trimester [64]. When the sagittal plane is obtained and combined with the ObliqueView™ utility, the axial view of the secondary palate can be easily obtained since the palate at this gestational age is flat and void of acoustic shadowing. The technique consists of obtaining a midsagittal view of the face by sweeping the mechanical 3D probe for a side-to-side acquisition. The 3D volume is then displayed in the ObliqueView™ mode and a line is drawn through the palate. The orthogonal plane showing the palate is immediately displayed in the dual screen (Fig. 3.9). The advantage of this technique is its simplicity; however, it requires the dedicated software for analysis.

The second algorithm is surface-rendering 3D ultrasound, which can provide high-definition views of the entire surface of the face (Fig. 3.10). This can also be enhanced with the use of HDLive™ algorithm, which can offer improved, vivid views of the facial structures in the first trimester (Fig. 3.11). With the adjunct use of the "magic cut" tool, more realistic views of the face in both the coronal and sagittal planes can also be obtained.

3.5 First-Trimester 2D/3D Ultrasound in Selected Facial Malformations

3.5.1 Cleft Lip and Palate

CLP is a relatively frequent and clinically significant congenital malformation and a prominent feature of both chromosomal abnormalities (particularly trisomy 13 and trisomy 18) and other genetic and nongenetic craniofacial syndromes. Therefore, special effort should be made

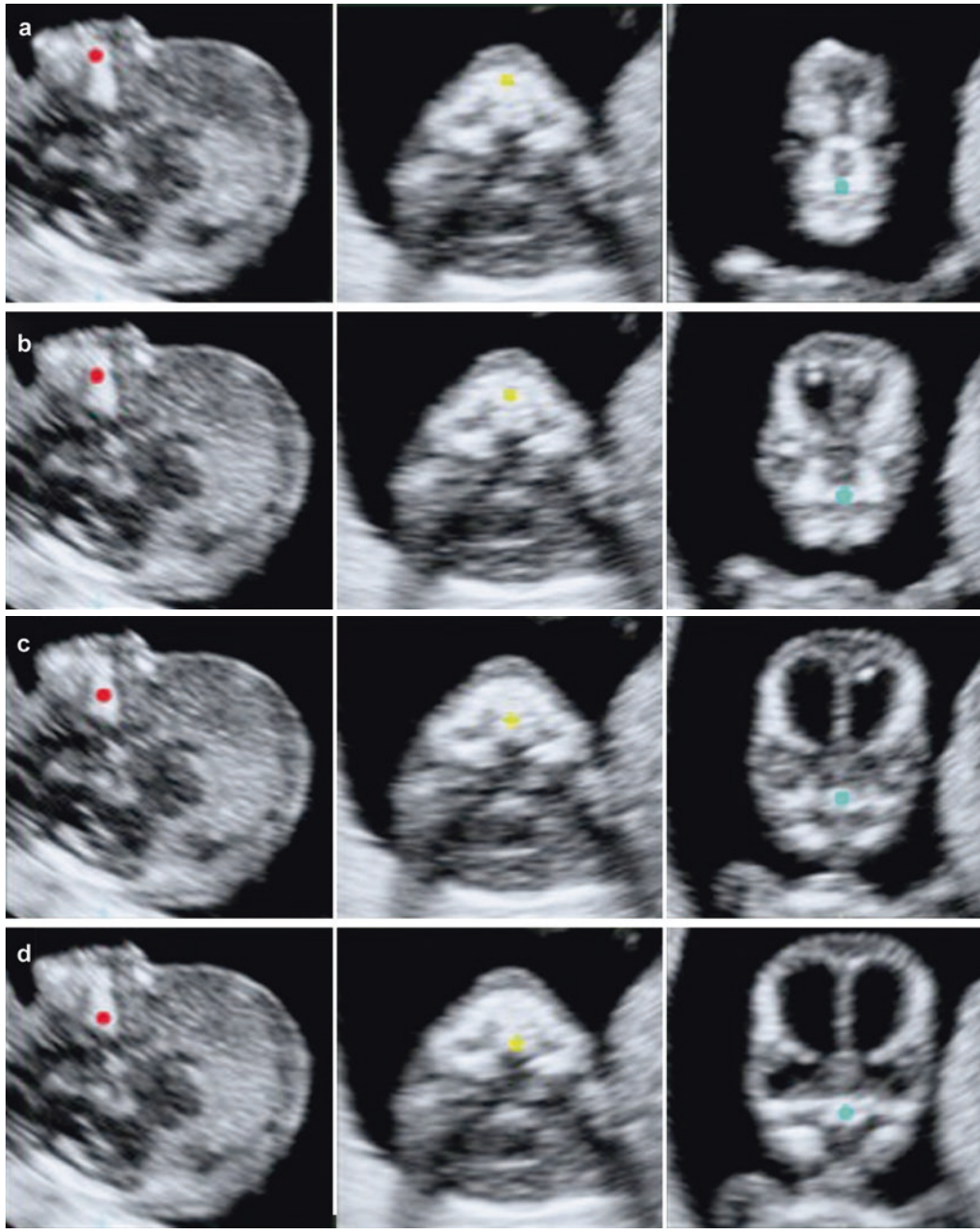

Fig. 3.5 Three-dimensional multiplanar views of the orofacial structures in the first trimester show the three orthogonal planes (*left*, sagittal plane; *middle*, axial plane; *right*, coronal plane). Navigation through the volume allows the simultaneous visualization of different structures of the fetal face in the three planes. The dots represent the intersection of all three orthogonal planes

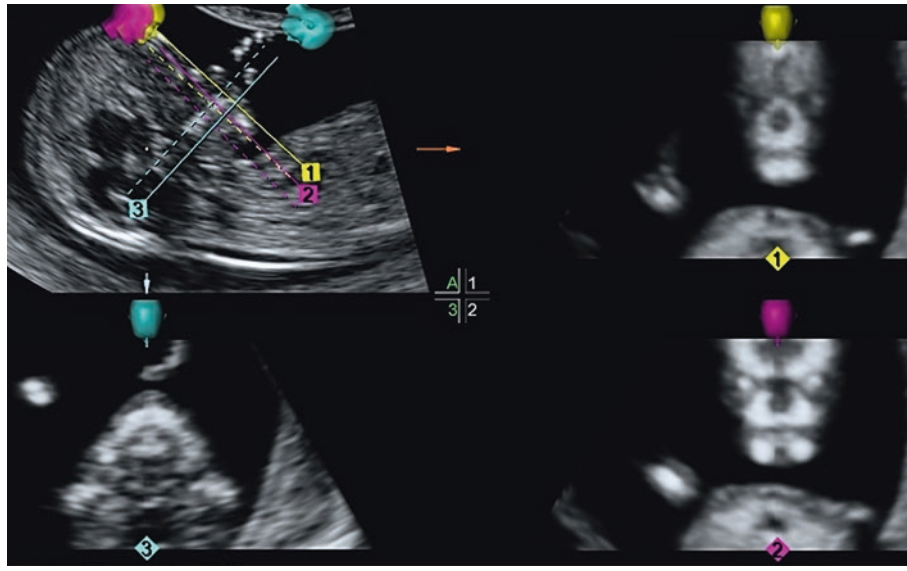

Fig. 3.6 OmniView™ software. Using a reference plane (in this case, the sagital plane), the operator can manually draw up to three observational lines, which generates the corresponding orthogonal planes that are simultaneously displayed in the other panels

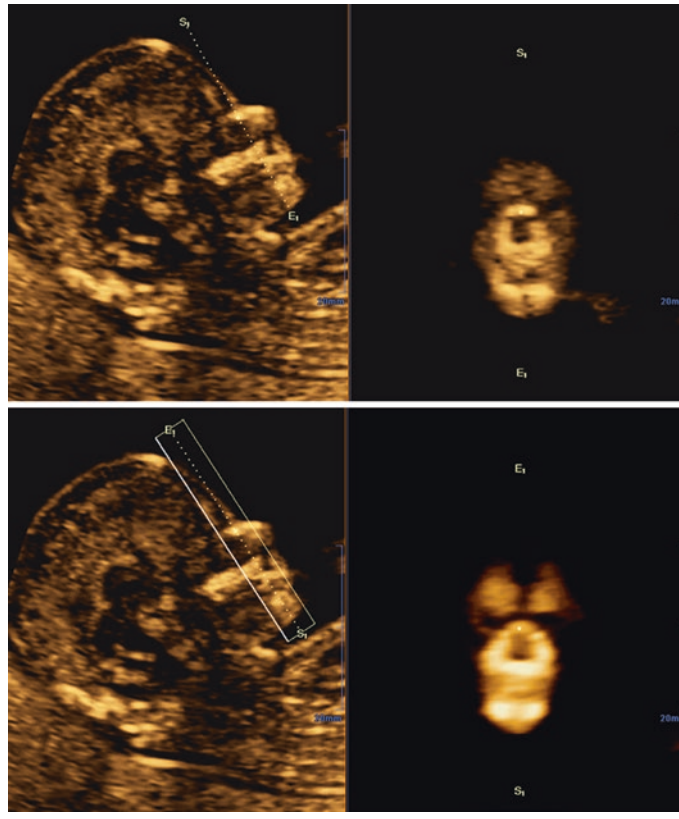

Fig. 3.7 ObliqueView™ software. *Upper panel*, simultaneous visualization of the orthogonal view is obtained by drawing a line through the reference plane. *Lower panel*, a thick slide can be used to enhance the visualization of the bony structures of the face

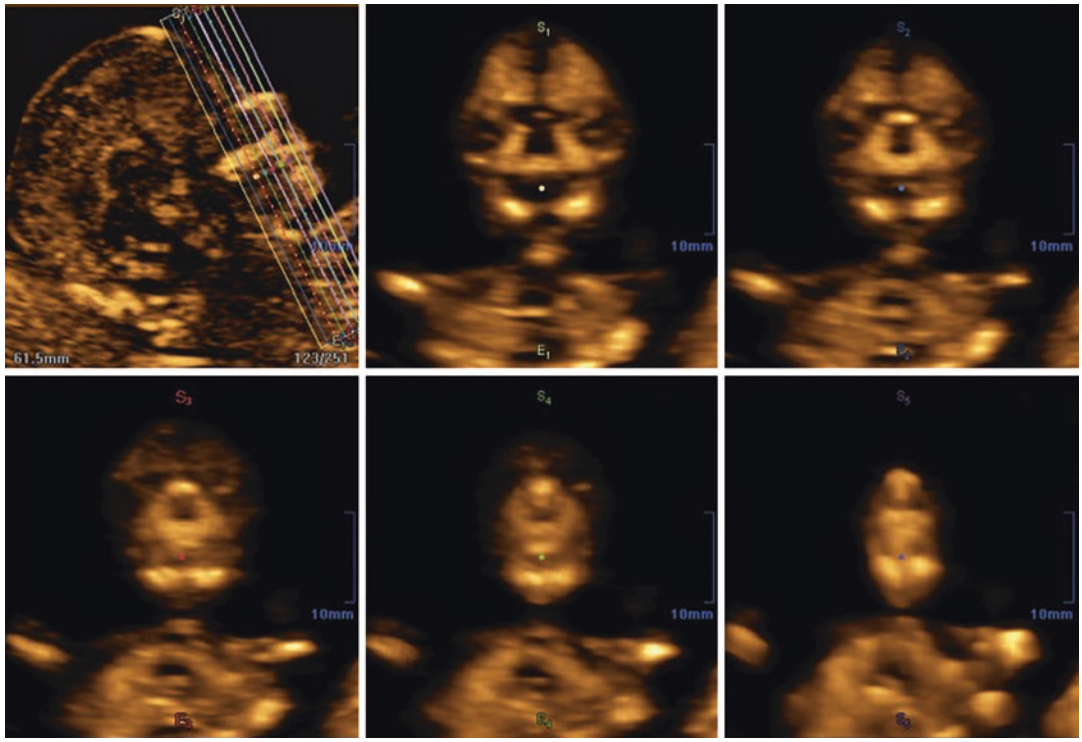

Fig. 3.8 ObliqueView™ software. Simultaneous multiparallel orthogonal views are generated by drawing a line in the reference plane

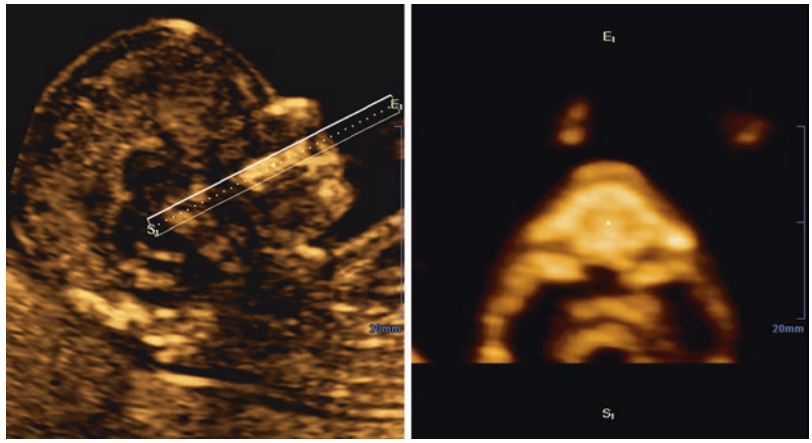

Fig. 3.9 Application of the VolumeNT™ algorithm, which automatically displays the midsagittal plane of the head, in conjuction with the ObliqueView™ software generates the axial plane to assess the secondary palate in the first trimester. Note that at this gestational age, the palate is flat and there is no acoustic shadowing from surrounding bony structures

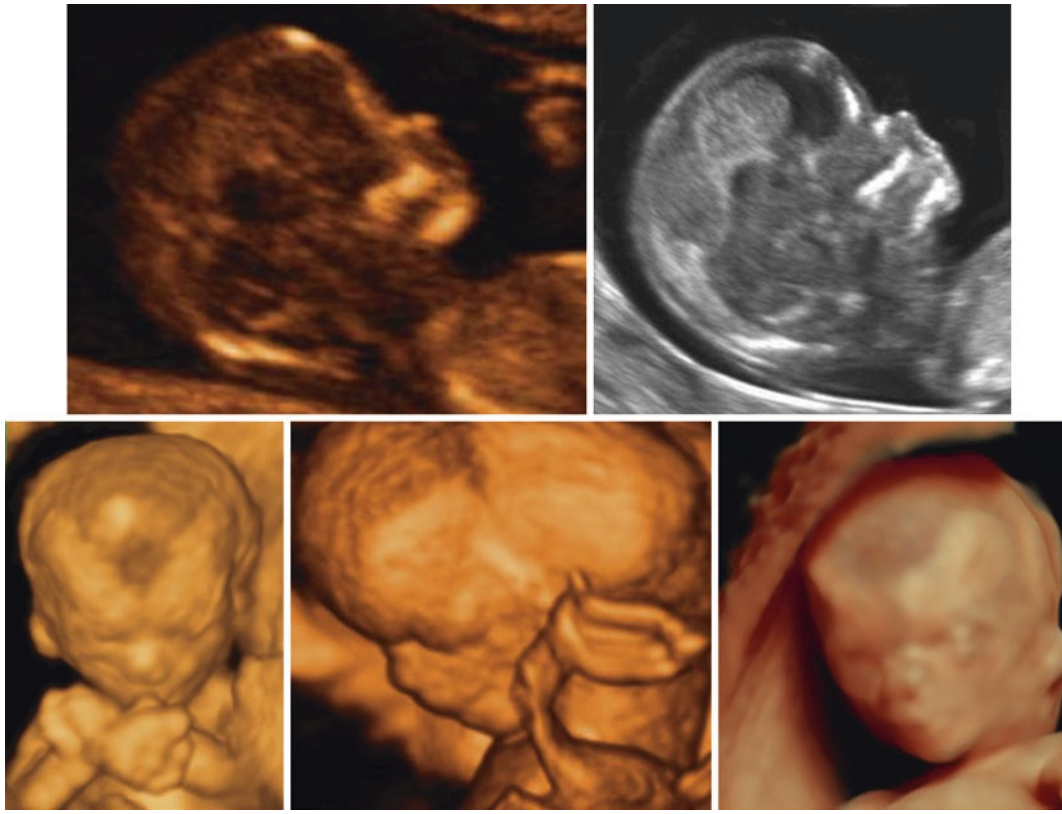

Fig. 3.10 Representative ultrasound views of the fetal face in the first trimester using different ultrasound techniques. *Upper panel*: *left*, transabdominal ultrasound; *right*, transvaginal ultrasound. *Lower panel*: *left and middle*, three-dimensional surface-rendered views of the face in the frontal and lateral views; *right*, fetal face reformatted with the HDLive™ software

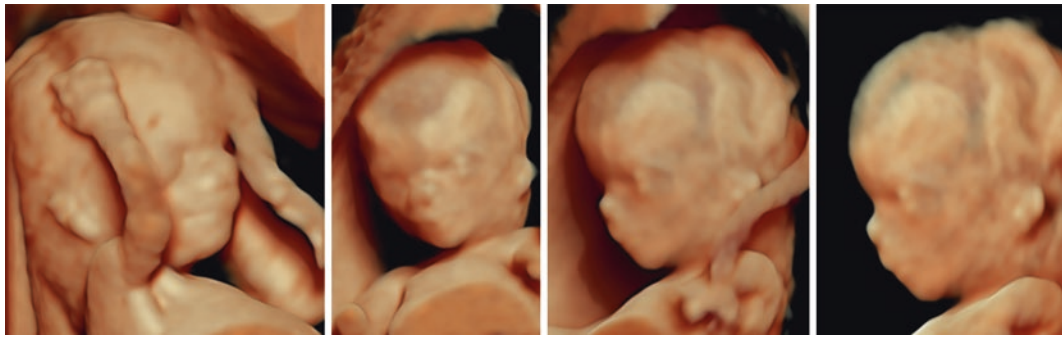

Fig. 3.11 Additional ultrasound images using the HDLive™ software obtained transvaginally from a 13-week fetus show realistic views of the fetal face in the first trimester

to examine properly the facial structures even in the first trimester. Indeed, examination of the fetal face should be an integral part of the workup of first-trimester fetuses with ultrasound suspicion of chromosomal abnormalities and also in chromosomally normal fetuses with increased NT thickness, as the latter group seems to have a higher incidence of CLP than fetuses with normal NT thickness, probably due to a higher prevalence of underlying nonchromosomal genetic

conditions [65]. Nevertheless, the vast majority of fetuses with an isolated CLP present with normal NT thickness; therefore, efforts to visualize the fetal face during the first-trimester ultrasound scan should be made irrespective of the NT thickness.

The diagnosis of CLP in the first trimester, however, is difficult because of the small size of the facial structures, scant subcutaneous tissue present in the premaxillary area, and difficulties in detecting orofacial clefts using the sagittal view of the head [43]. Indeed, a recent review of the literature involving more than 45,000 euploid fetuses undergoing routine first-trimester ultrasound screening in a dedicated Fetal Medicine Center demonstrated that the diagnosis of CLP was only made in less than 5 % of cases [66]. This low detection rate highlights the difficulty in diagnosing CLP during the routine first-trimester scan if a focused examination of the fetal face using high-resolution ultrasound equipment and proper scanning technique are not performed. Moreover, a review of the English literature until 2009 [43, 47], when the RNT view was described, revealed only a few cases of CLP diagnosed in the first trimester in euploid fetuses. In the only two reported cases with detailed ultrasound information available, the condition was severe and involved bilateral CLP with prominent premaxillary protrusion, one of which was diagnosed with transvaginal ultrasound [28] and the other with the adjunct use of 3D ultrasound [68]. This observation is further confirmed by a systematic review of the literature on the efficacy of first-trimester ultrasound scan to detect fetal malformations. The overall first-trimester detection rate for facial abnormalities, including both chromosomally normal and abnormal fetuses, was only 34 % [69].

The discordance between the detection rates of trisomy 21 and CLP in the first trimester (>80 % versus <5 %, respectively) led us to speculate that the most significant limitation to the detection of CLP was the plane of examination employed. Indeed, although the ultrasound technique used for aneuploidy screening, namely, assessment of the NT thickness, nasal bone, and frontomaxillary facial angle in the sagittal plane, is good at detecting trisomy 21, this view is poor at identifying CLP. Occasionally, 2D ultrasound visualization of the fetal profile can detect the characteristic premaxillary protrusion of bilateral CLP (Fig. 3.12); however, even this feature has not been emphasized during routine first-trimester sonographic screening. This limitation led our group to investigate an alternative technique for the detection of CLP in the first trimester, which was based on the visualization of the RNT in the coronal plane of the face [43]. This plane is similar to the one used in the second trimester to visualize the upper lip and nostrils [9, 70] and was brought to our attention by the report of the "premaxillary triangle" view suggested by Suresh et al. [71] for the screening of CLP in the second trimester. In their description, the focus is placed on the soft tissue of the upper lip and the echogenic alveolar ridge in a single coronal view. However, since the upper lip is minimally developed in the first trimester, we chose to depict only the maxilla that forms the base of the RNT. In this view, the presence of a cleft of the primary palate is demonstrated by unilateral, bilateral, or central discontinuity at the level of the alveolar ridge, which is the base of the RNT (Fig. 3.12) [43].

The recent advent of 3D ultrasound technology has allowed closer examination of the fetal anatomic structures even in the first trimester. The evaluation and diagnosis of an orofacial cleft with 3D ultrasound in the first trimester was first reported by Ghi et al. in 2009 [68]. In this case, the authors detect a premaxillary protrusion at the time of a routine scan and further evaluation with 3D surface-rendering ultrasound clearly depicted a bilateral CLP. Since then, 3D ultrasound has played an increasingly important role in the prenatal examination of the fetal face including the detection and confirmation of CLP (Fig. 3.13). The technique for the systematic analysis of 3D volume datasets of the fetal face obtained from first-trimester fetuses undergoing ultrasound screening for aneuploidy was reported by our group (Fig. 3.14) [72]. 3D volume datasets from 240 first-trimester fetuses, including seven cases with CLP, were assessed offline by two independent operators. Coronal views at the level

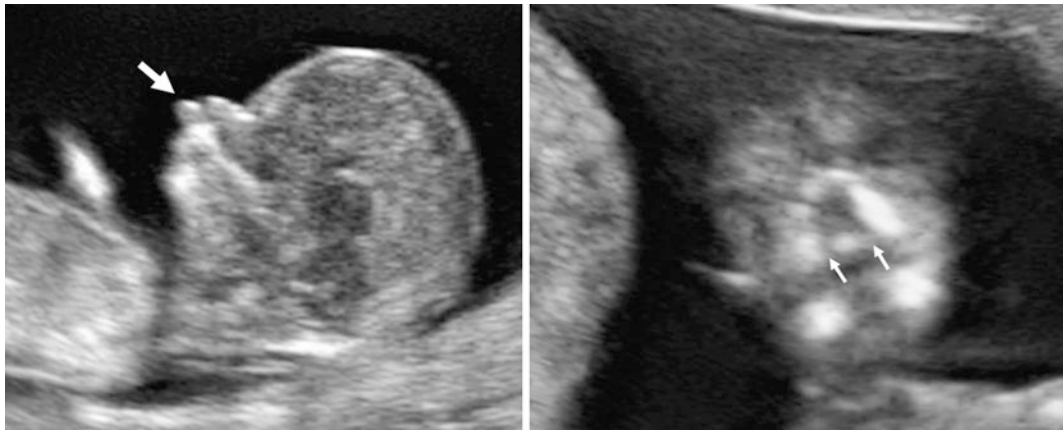

Fig. 3.12 *Left panel*, two-dimensional ultrasound shows premaxillary protrusion in the sagittal view of the face in a first-trimester fetus with bilateral cleft lip and palate (*arrow*). Chromosomal analysis was reported as normal. *Right panel*, coronal view shows an abnormal retronasal triangle. Note the bilateral gaps in the alveolus (*arrows*)

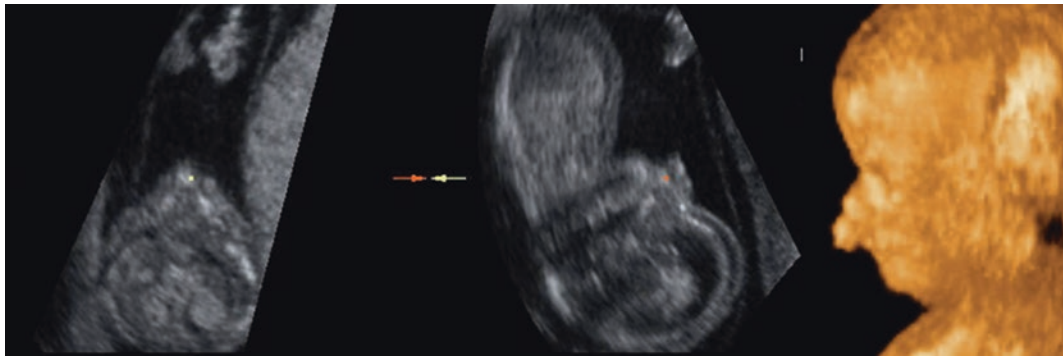

Fig. 3.13 Three-dimensional ultrasound in a first-trimester fetus with premaxillary protrusion. The nuchal translucency thickness was increased and chromosomal analysis revealed trisomy 13

of the RNT were evaluated for possible clefts of the primary palate and axial views were evaluated for possible clefts of the secondary palate (Fig. 3.15). Overall, all fetuses with clefts affecting the primary palate and 86 % of those affecting the secondary palate were detected with a satisfactory false-positive rate [72].

A more sophisticated technique for evaluating the primary and secondary palates using 3D ultrasound involves the use of OmniView™ algorithm, which allows the examination of multiple parallel views to visualize the primary and secondary palates. In a screening study of 100 low-risk and 50 high-risk fetuses, the RNT view was imaged to assess the primary palate and the axial view to assess the secondary palate [61]. The two fetuses affected with CLP in this cohort were correctly identified using this technique and none of the fetuses with normal lip and palate displayed an abnormality on this 3D ultrasound examination. The utility of the HDLive™ technique in fetuses with CLP remains to be determined; however, based on several cases in which it has been used, it seems to be promising (Fig. 3.16) [73].

Recently, another technique to detect clefts of the secondary palate was reported [74]. It is based on the identification of the "maxillary gap," which is displayed in the sagittal view of the head. In this plane, the primary and secondary palates form a continuous thick and straight

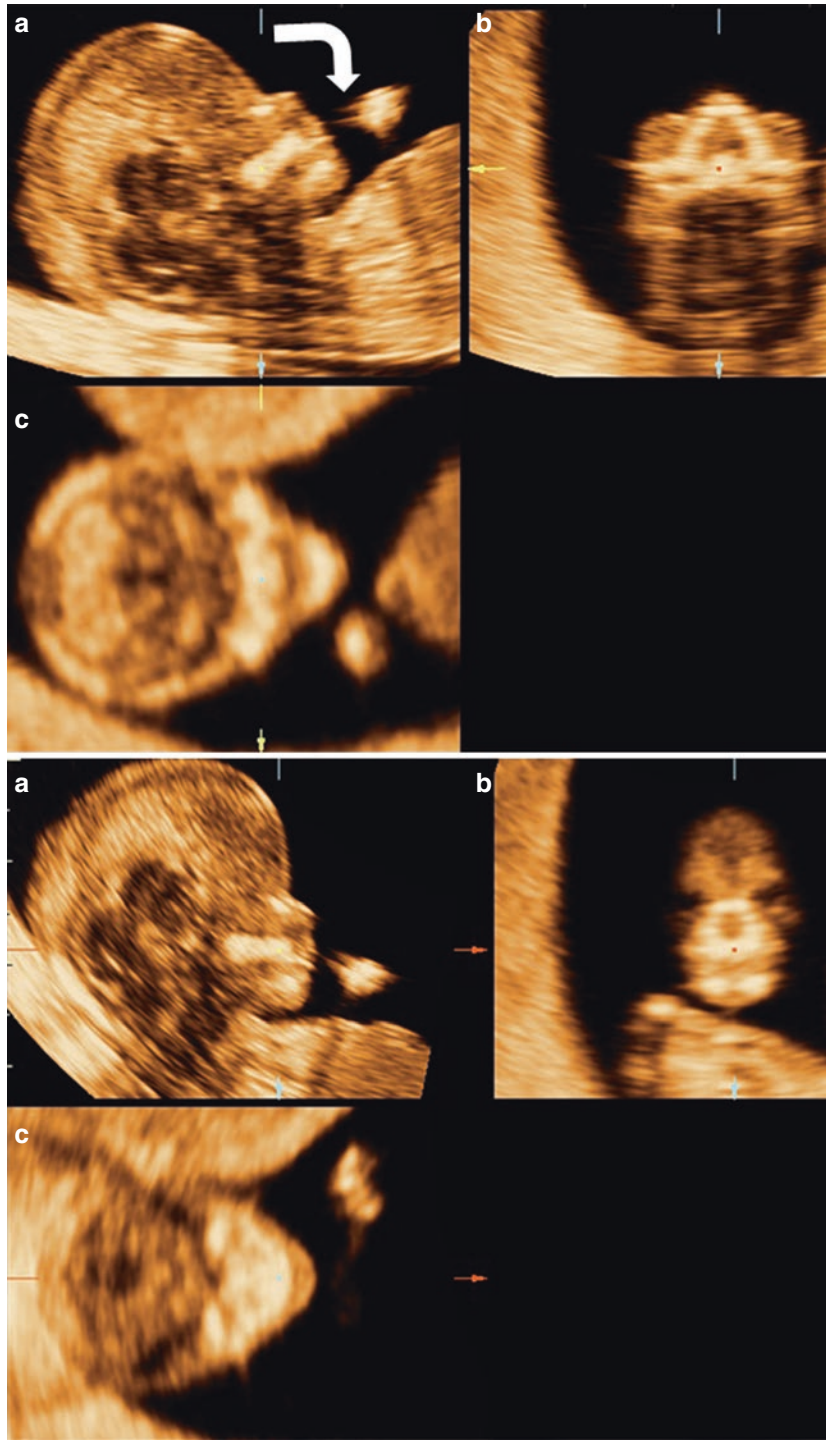

Fig. 3.14 Technique for three-dimensional ultrasound evaluation of the fetal face in the first trimester. *Upper panel* shows the initial plane for acquisition. The sagittal plane is seen in **a**, the axial plane in **b**, and the coronal plane in **c**. *Lower panel* shows the three orthogonal views after rotation in plane **a**. The reference dot is on the primary palate and the palate is horizontal. The retronasal triangle is displayed in plane **b** and the secondary palate in plane **c**

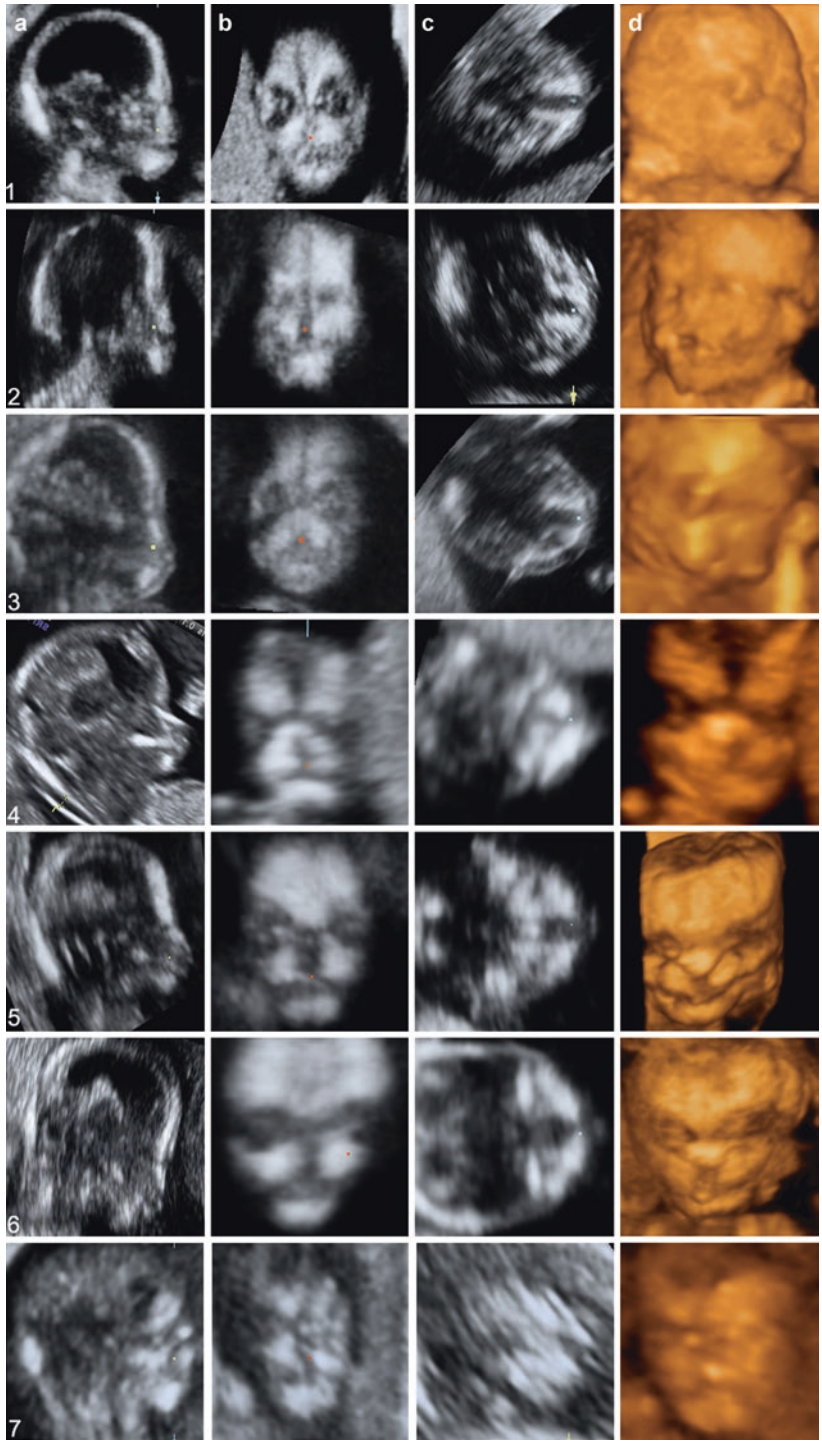

Fig. 3.15 Representative views of the fetal face in the three orthogonal planes and the surface-rendered images in seven first-trimester fetuses with cleft lip and palate as determined by three-dimensional ultrasound. The *numbers* indicate the case and **a**, **b**, and **c** indicate the sagittal, coronal, and axial planes. In **d**, the surface-rendered view is shown

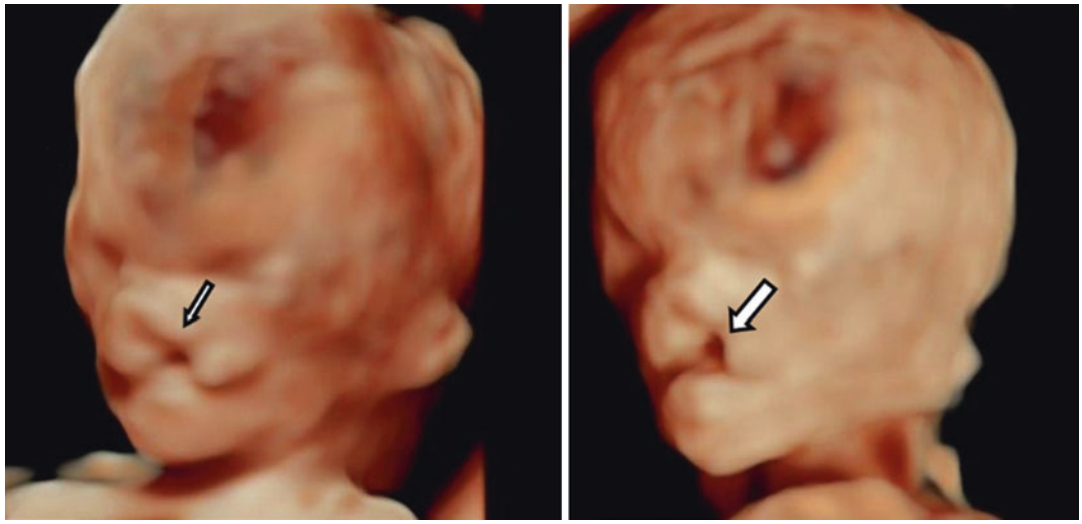

Fig. 3.16 Three-dimensional ultrasound performed with the HDLive™ technique in a first-trimester fetus with unilateral cleft lip (*arrows*) (Courtesy of Prof. F. da Silva Costa, Melbourne)

echogenic line. In fetuses with clefts of the secondary palate, this line is interrupted, yielding a gap (Fig. 3.17). The advantage of this technique is its simplicity, as it can be performed with 2D ultrasound and uses the same view as the one for NT assessment. However, the diagnosis should ideally be confirmed with 3D ultrasound technology. The axial view can also be used to assess the secondary palate for possible clefting. In this plane, the tongue can prevent visualization of the cleft, so it is advised to wait until the fetus swallows and fills the gap with amniotic fluid to enhance identification of the cleft (Fig. 3.18).

3.5.2 Micrognathia

Micrognathia is defined as a small chin, which usually is also displaced posteriorly (retrognathia). Clinically, these two terms are often used synonymously. The prenatal detection of micrognathia is of paramount importance because it is associated with several craniofacial abnormalities, genetic disorders, and chromosomal anomalies [75, 76]. In the first trimester, the diagnosis can be difficult since the normal mandible is poorly developed. However, cases of severe micrognathia can be confidently detected with a proper view of the fetal profile demonstrating the receding chin even at this early stage of development.

The first reported diagnosis of micrognathia in the first trimester was reported by the use of transvaginal 2D ultrasound in a fetus with Robin anomalad [25]. The diagnosis was made at 13 weeks and was based on the subjective impression of a receding chin on the profile view of the fetus. Subsequently, several additional cases have been recently reported by detecting similar features, including one case of severe micrognathia in a fetus with trisomy 9 [77], one case of progressive development of mandibular hypoplasia and microglossia [78], and another with Nager syndrome (acrofacial dysostosis) [79].

We have described an ultrasound screening technique for micrognathia in the first trimester based on the coronal view of the fetal face [46]. In this view, just inferior to the RNT, the two mandibular bones are normally separated by a gap, the "mandibular gap." In fetuses with micrognathia, however, the plane in which the gap is located crosses the chin or is located behind the

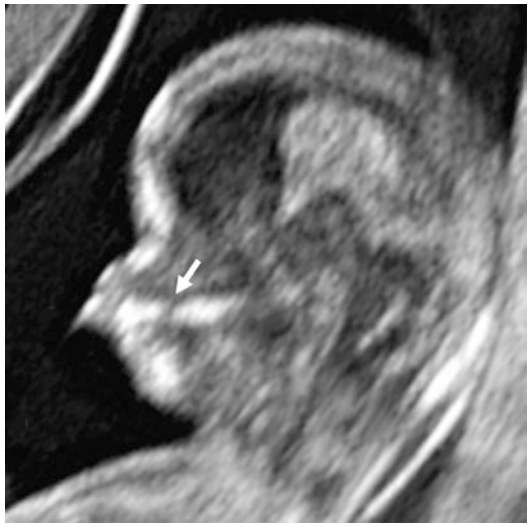

Fig. 3.17 The "maxillary gap" sign. Sagittal view of a fetus with bilateral cleft lip. Note the gap in the secondary palate (*arrow*)

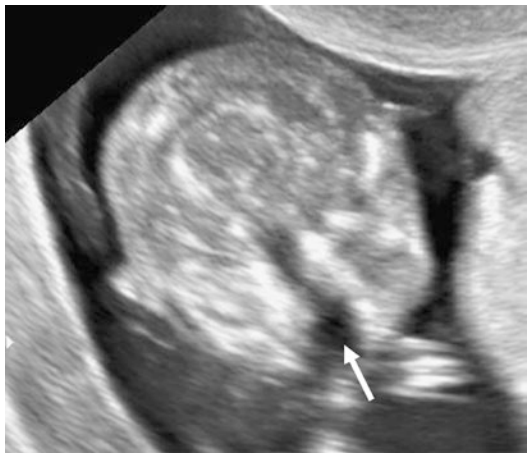

Fig. 3.18 Coronal view of a fetus with complete clefting of the primary and secondary palates (*arrow*)

chin, and the gap is therefore absent or the mandible not seen (Fig. 3.19). The utility of this view was demonstrated in nine fetuses with micrognathia analyzed retrospectively by offline analysis of the corresponding 3D volume datasets [46].

Additional techniques, which do not require 3D ultrasound, include the visualization of the profile and measurement of different angles involving the maxilla and mandible. These include the mandibulo-maxillary facial angle [80] or, an even simpler technique, the frontal space distance technique [59]. In the latter case, a line crossing the anterior aspect of the chin and the maxilla should cross the forehead. In fetuses with micrognathia, this line is deviated anteriorly (Fig. 3.20). This appears to be an excellent, simple ultrasound technique for the screening of micrognathia in the first trimester.

3.5.3 Cyclopia and Proboscis

Cyclopia and proboscis are invariably lethal congenital anomalies affecting the upper face and are closely related to each other as part of the holoprosencephaly sequence. The term cyclopia refers to the fusion of the orbits (the single orbit can contain one or two eyeballs), whereas proboscis is an appendage located above the single orbit corresponding to a nonfunctioning nose. These facial malformations always occur together as the result of abnormal cleavage of the forebrain or prosencephalon resulting in a failure to divide the orbits. The most frequent associated chromosomal abnormality is trisomy 13.

The second-trimester diagnosis of cyclopia and proboscis is simple and includes the visualization of the proboscis as a trunk-like appendage extending from the forehead, a single orbit, and absent nose in the midsegment of the face [17]. In the first trimester, however, the diagnosis can be missed if a detailed examination of the face is not performed. The first-trimester ultrasound diagnosis of cyclopia and proboscis has been reported several times [24, 81–83], with the most striking first-trimester ultrasound finding in affected fetuses being the detection of holoprosencephaly on axial views of the fetal head. Further evaluation of the face in these cases often reveals the cardinal features of cyclopia and proboscis (Fig. 3.21). 3D ultrasound can also help in the diagnosis by demonstrating the proboscis in the surface-rendering mode (Fig. 3.22).

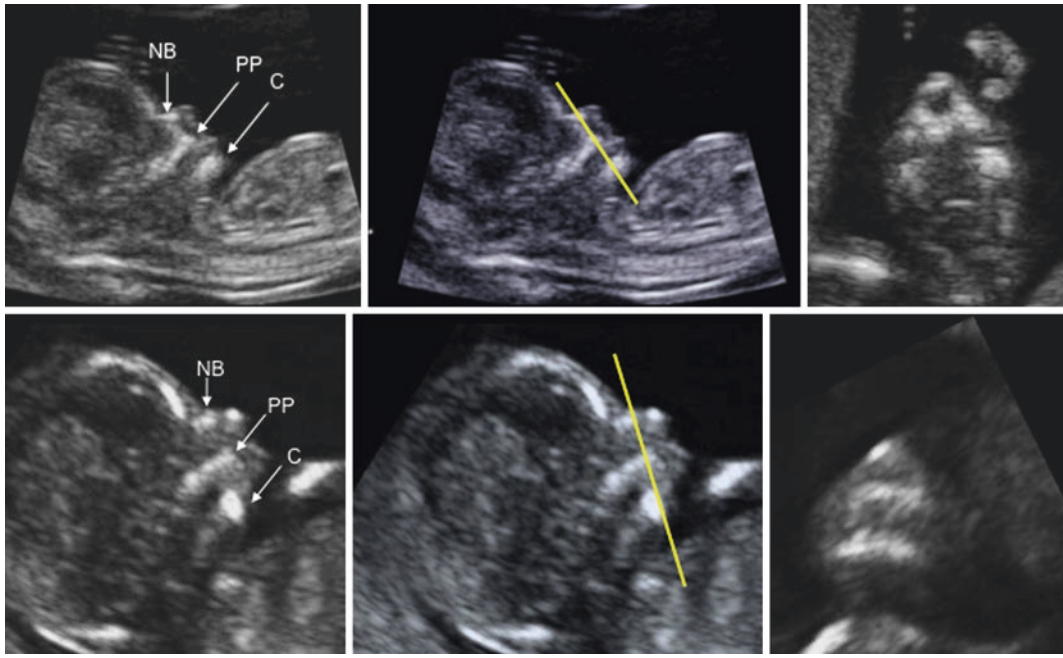

Fig. 3.19 The "mandibular gap" sign. *Upper panel*, in normal fetuses the line crossing through the nasal bone and primary palate passes posterior to the chin, displaying a gap on the coronal view of the face. *Lower panel*, in fetuses with micrognathia, the line passes either anterior to or at the plane of the chin; consequently, the coronal view of the face does not incorpórate the chin or displays an absent mandibular gap. *NB* nasal bone; *PP* primary palate; *C* chin

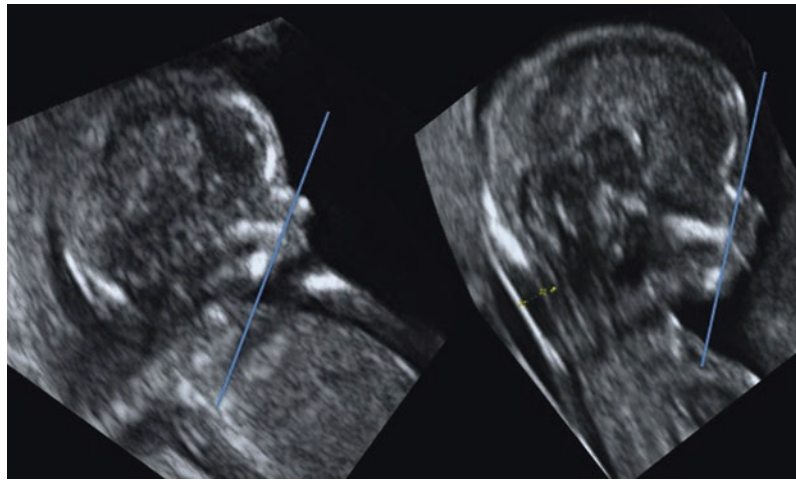

Fig. 3.20 The "frontal space" sign. In fetuses with micrognathia, the line crossing through the anterior aspect of the maxilla and primary palate passes anterior to the frontal bone. In normal fetuses, the line is close to the frontal bone

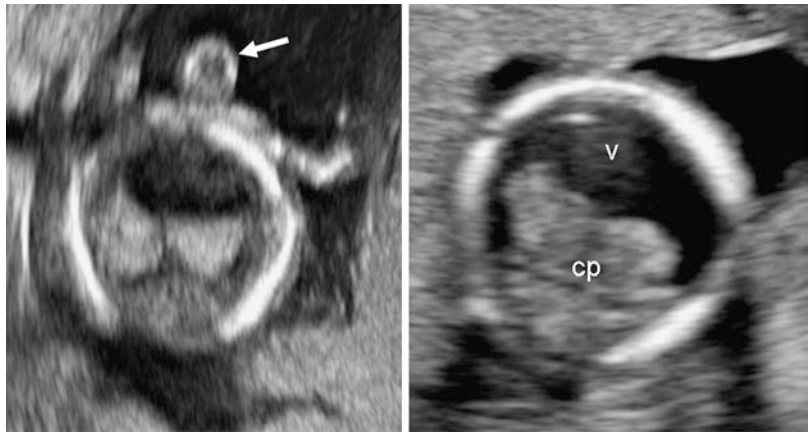

Fig. 3.21 Axial view of the fetal head. Proboscis (*arrow*) in a fetus with holoprosencephaly. *V* monoventricle, *cp* choroid plexuses

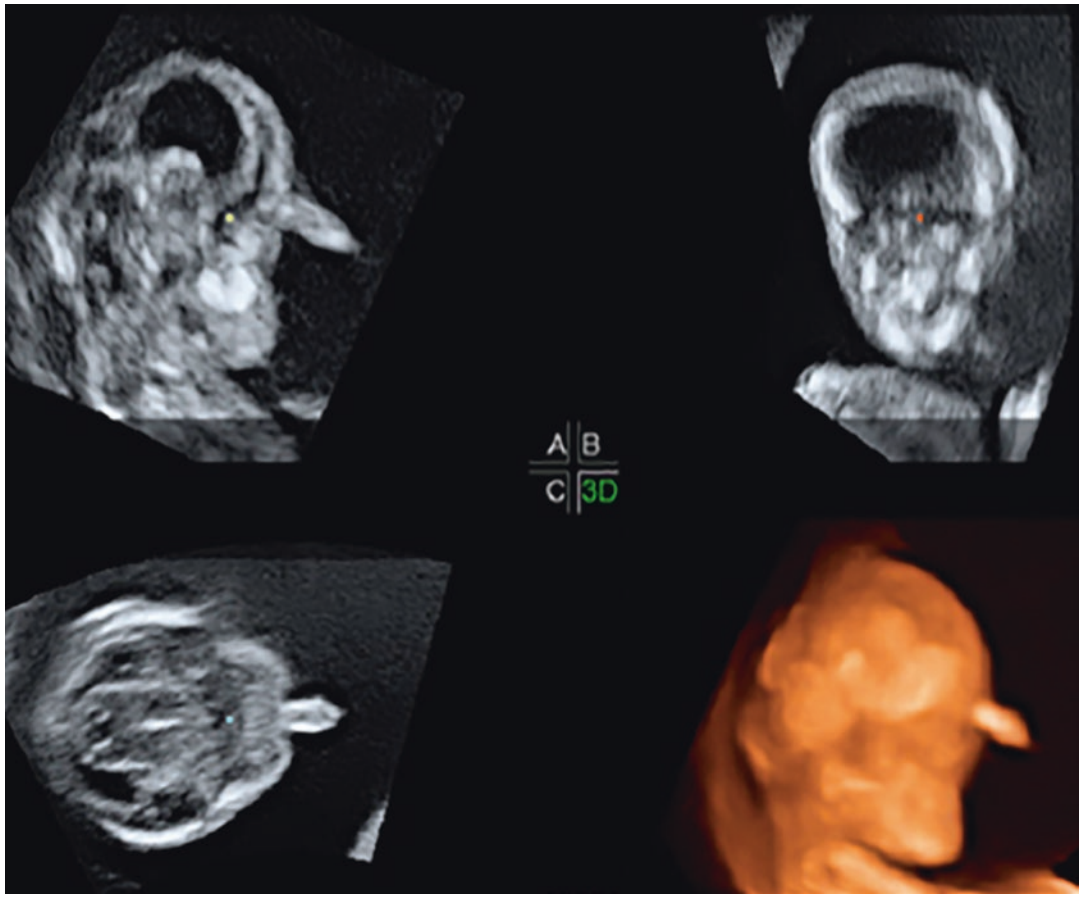

Fig. 3.22 Three-dimensional multiplanar and surface-rendered views of a first-trimester fetus with proboscis

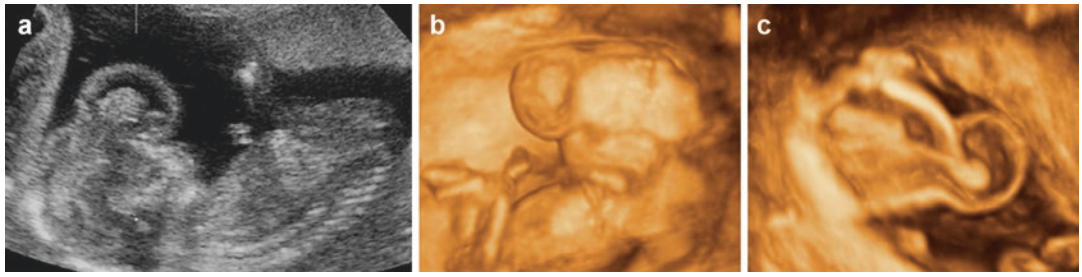

Fig. 3.23 Frontal cephalocele in the first trimester

3.5.4 Frontal Cephalocele

Cephaloceles are open neural tube defects through which cranial contents protrude. In a recent first-trimester study, we noted that frontal cephaloceles seem to be more prevalent in the first trimester compared to the second trimester [84]. Although the diagnosis of any type of cephalocele in the first trimester is typically straightforward, the presence of a frontal cephalocele always produces a bizarre appearance (Fig. 3.23) and is usually associated with a dismal prognosis.

3.5.5 Agnathia-Holoprosencephaly Sequence

This is a lethal anomaly characterized by severe hypoplasia or absence of the mandible in association with holoprosencephaly. It is invariably associated with ventro-caudal displacement of the ears, microstomia, and microglossia. Three cases of agnathia diagnosed in the first trimester have been reported, the most striking antenatal finding being the detection of an abnormal profile and absent mandible in association with holoprosencephaly (Fig. 3.24) [85–87].

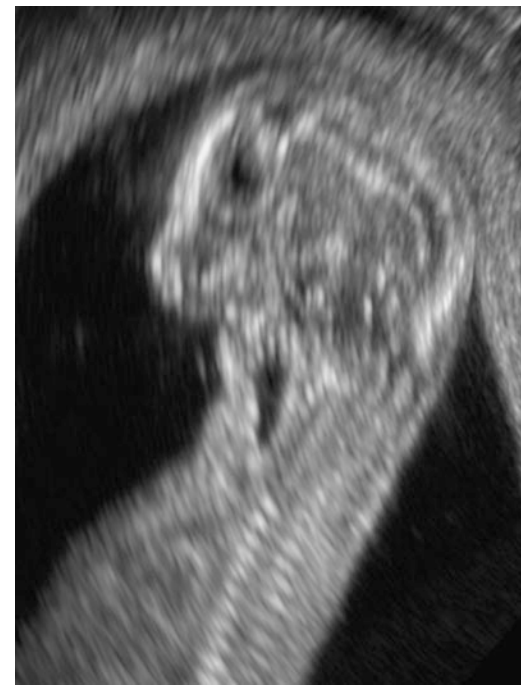

Fig. 3.24 Two-dimensional view of a fetus with agnathia-holoprosencephaly sequence. Note absent mandibular bone (Courtesy of Dr. E. Andreeva, Moscow)

3.5.6 Miscellaneous Conditions

As previously mentioned, case reports of the prenatal diagnosis of extremely rare malformations of the fetal face have been published. These include diprosopus [26] and oculo-auriculo-frontonasal syndrome [27]. With the improved resolution of 2D/3D ultrasound technology, it is expected that the number of these cases will increase in the future.

Conclusions

The early diagnosis of CLP and other malformations affecting the fetal face still requires a high index of clinical suspicion. With current ultrasound image resolution and scanning technique, examination of the fetal face in the

first trimester is feasible and can provide valuable information for the early detection of orofacial defects and other facial malformations. Every attempt should be made to visualize the fetal face during first-trimester ultrasound screening, starting with close examination of the profile in the sagittal plane of the fetal head under appropriate settings. Acquisition of the coronal plane to visualize the RNT should also be mandatory. The latter technique is easily and rapidly performed and can be easily incorporated into the first-trimester scanning protocols. Moreover, it can facilitate the detection of facial anomalies and enhance early prenatal detection of fetuses with chromosomal anomalies and genetic syndromes.

References

1. Cullen MT, Reece EA, Whetham J, Hobbins JC. Embryoscopy: description and utility of a new technique. Am J Obstet Gynecol. 1990;162:82–6.
2. Reece EA. Embryoscopy: new developments in prenatal medicine. Curr Opin Obstet Gynecol. 1992;4:447–55.
3. Pennehouat GH, Thebault Y, Ville Y, Medelenat P, Nicolaides KH. First-trimester transabdominal fetoscopy. Lancet. 1992;340:429.
4. Dommergues M, Lemerrer M, Couly G, Delezoide AL, Dumez Y. Prenatal diagnosis of cleft lip at 11 menstrual weeks using embryoscopy in the van der Woude syndrome. Prenat Diagn. 1995;15:378–81.
5. Ville Y, Bernard JP, Doumerc S, Multon O, Fernandez H, Frydman R, Barki G. Transabdominal fetoscopy in fetal anomalies diagnosed by ultrasound in the first trimester of pregnancy. Ultrasound Obstet Gynecol. 1996;8:11–5.
6. Reece EA. First trimester prenatal diagnosis: embryoscopy and fetoscopy. Semin Perinatol. 1999;23:424–33.
7. Tonni G, Periti E, Rosignoli L. Hysteroscopic fetoscopy: a role as virtuopsy for parents who refuse full autopsy? A case of facial clefting, proboscis, and limb deformities. Taiwan J Obstet Gynecol. 2015;54:608–11.
8. Christ JE, Meininger MG. Ultrasound diagnosis of cleft lip and cleft palate before birth. Plast Reconstr Surg. 1981;68:854–9.
9. Seeds JW, Cefalo RC. Technique of early sonographic diagnosis of bilateral cleft lip and palate. Obstet Gynecol. 1983;62:2s–7.
10. de Elejalde MM, Elejalde BR. Visualization of the fetal face by ultrasound. J Craniofac Genet Dev Biol. 1984;4:251–7.
11. Jeanty P, Romero R, Staudach A, Hobbins JC. Facial anatomy of the fetus. J Ultrasound Med. 1986;5:607–16.
12. American Institute of Ultrasound in Medicine. AIUM Practice Guideline for the performance of an antepartum obstetric ultrasound examination. J Ultrasound Med. 2003;22:1116–25.
13. American Institute of Ultrasound in Medicine. AIUM practice guideline for the performance of obstetric ultrasound examinations. J Ultrasound Med. 2010;29:157–66.
14. Salomon LJ, Alfirevic Z, Berghella V, Bilardo C, Hernandez-Andrade E, Johnsen SL, Kalache K, Leung KY, Malinger G, Munoz H, Prefumo F, Toi A, Lee W, Clinical Standards Committee ISUOG. Practice guidelines for performance of the routine mid-trimester fetal ultrasound scan. Ultrasound Obstet Gynecol. 2011;37:116–26.
15. American Institute of Ultrasound in Medicine. AIUM practice guideline for the performance of obstetric ultrasound examinations. J Ultrasound Med. 2013;32:1083–101.
16. Pilu G, Nicolaides KH. Face. In: Pilu G, Nicolaides KH, editors. Diagnosis of fetal abnormalities. The 18–23-week scan. London: Parthenon Publishing; 1999. p. 19–24.
17. Benacerraf BR, Nyberg DA. The face and neck. In: Nyberg DA, McGahan JP, Pretorius DH, Pilu G, editors. Diagnostic imaging of fetal anomalies. Philadelphia: Lippincott Williams & Wilkins; 2003. p. 335–79.
18. Nyberg DA, Sickler GK, Hegge FN, Kramer DJ, Kropp RJ. Fetal cleft lip with and without cleft palate: US classification and correlation with outcome. Radiology. 1995;195:677–84.
19. Rotten D, Levaillant JM. Two- and three-dimensional sonographic assessment of the fetal face. 2. Analysis of cleft lip, alveolus and palate. Ultrasound Obstet Gynecol. 2004;24:402–11.
20. Maarse W, Pistorius LR, Van Eeten WK, Breugem CC, Kon M, Van den Boogaard MJ, Mink van Der Molen AB. Prenatal ultrasound screening for orofacial clefts. Ultrasound Obstet Gynecol. 2011;38:434–9.
21. Martinez-Ten P, Sepulveda W, Wong AE, Tonni G. The role of 2D/3D/4D ultrasound in the prenatal assessment of cleft lip and palate. In: Tonni G, Sepulveda W, Wong AE, editors. Prenatal diagnosis of orofacial malformations. Berlin: Springer; 2017:43–59.
22. Nyberg DA, Hegge FN, Kramer D, Mahony BS, Kropp RJ. Premaxillary protrusion: a sonographic clue to bilateral cleft lip and palate. J Ultrasound Med. 1993;12:331–5.
23. Gabrielli S, Piva M, Ghi T, Perolo A, De Santis MS, Bevini M, Bonasoni P, Santini D, Rizzo N, Pilu G. Bilateral cleft lip and palate without premaxillary protrusion is associated with lethal aneuploidies. Ultrasound Obstet Gynecol. 2009;34:416–8.

24. Hsu TY, Chang SY, Ou CY, Chen ZH, Tsai WL, Chang MS, Soong YK. First trimester diagnosis of holoprosencephaly and cyclopia with triploidy by transvaginal three-dimensional ultrasonography. Eur J Obstet Gynecol Reprod Biol. 2001;96:235–7.
25. Teoh M, Meagher S. First-trimester diagnosis of micrognathia as a presentation of Pierre Robin syndrome. Ultrasound Obstet Gynecol. 2003;21:616–8.
26. Bulbul Y, Drummond CL, Hillion Y, Bidat L, Ville Y. Diprosopus associated with neural tube defect and facial cleft in the first trimester. Fetal Diagn Ther. 2004;19:246–50.
27. Johnson JM, Benoit B, Pierre-Louis J, Keating S, Chitayat D. Early prenatal diagnosis of oculoauriculofrontonasal syndrome by three-dimensional ultrasound. Ultrasound Obstet Gynecol. 2005;25:184–6.
28. Gullino E, Serra M, Ansaldi C, Massobrio M, Pagliano M. Bilateral cleft lip and palate diagnosed sonographically at 11 weeks of pregnancy. J Clin Ultrasound. 2006;34:398–401.
29. Snijders RJ, Noble P, Sebire N, Souka A, Nicolaides KH. UK multicentre project on assessment of risk of trisomy 21 by maternal age and fetal nuchal-translucency thickness at 10-14 weeks of gestation. Fetal Medicine Foundation First Trimester Screening Group. Lancet. 1998;352:343–6.
30. Nicolaides KH. Nuchal translucency and other first-trimester sonographic markers of chromosomal abnormalities. Am J Obstet Gynecol. 2004;191:45–67.
31. Nicolaides KH. Screening for fetal aneuploidies at 11 to 13 weeks. Prenat Diagn. 2011;31:7–15.
32. Souka AP, Nicolaides KH. Diagnosis of fetal abnormalities at the 10–14-week scan. Ultrasound Obstet Gynecol. 1997;10:429–42.
33. Souka A, Heath V. Increased nuchal translucency with normal karyotype. In: Nicolaides KH, Sebire NJ, Snijders RJM, editors. The 11–14-week scan. The diagnosis of fetal abnormalities. London: Parthenon Publishing; 1999. p. 67–93.
34. Whitlow BJ, Chatzipapas IK, Lazanakis ML, Kadir RA, Economides DL. The value of sonography in early pregnancy for the detection of fetal abnormalities in an unselected population. Br J Obstet Gynaecol. 1999;106:929–36.
35. Carvalho MH, Brizot ML, Lopes LM, Chiba CH, Miyadahira S, Zugaib M. Detection of fetal structural abnormalities at the 11–14 week ultrasound scan. Prenat Diagn. 2002;22:1–4.
36. Fong KW, Toi A, Salem S, Hornberger LK, Chitayat D, Keating SJ, McAuliffe F, Johnson JA. Detection of fetal structural abnormalities with US during early pregnancy. Radiographics. 2004;24:157–74.
37. Weisz B, Pajkrt E, Jauniaux E. Early detection of fetal structural abnormalities. Reprod Biomed Online. 2005;10:541–53.
38. Souka AP, Pilalis A, Kavalakis I, Antsaklis P, Papantoniou N, Mesogitis S, Antsaklis A. Screening for major structural abnormalities at the 11- to 14-week ultrasound scan. Am J Obstet Gynecol. 2006;194:393–6.
39. Sepulveda W, Illescas T, Adiego B, Martinez-Ten P. Prenatal detection of fetal anomalies at the 11- to 13-week scan – part I: brain, face and neck. Donald School J Ultrasound Obstet Gynecol. 2013;7:359–68.
40. Salomon LJ, Alfirevic Z, Bilardo CM, Chalouhi GE, Ghi T, Kagan KO, Lau TK, Papageorghiou AT, Raine-Fenning NJ, Stirnemann J, Suresh S, Tabor A, Timor-Tritsch IE, Toi A, Yeo G. ISUOG practice guidelines: performance of first-trimester fetal ultrasound scan. Ultrasound Obstet Gynecol. 2013;41:102–13.
41. Cicero S, Curcio P, Papageorghiou A, Sonek J, Nicolaides K. Absence of nasal bone in fetuses with trisomy 21 at 11-14 weeks of gestation: an observational study. Lancet. 2001;358:1665–7.
42. Borenstein M, Persico N, Kagan KO, Gazzoni A, Nicolaides KH. Frontomaxillary facial angle in screening for trisomy 21 at 11+0 to 13+6 weeks. Ultrasound Obstet Gynecol. 2008;32:5–11.
43. Sepulveda W, Wong AE, Martinez-Ten P, Perez-Pedregosa J. Retronasal triangle: a sonographic landmark for the screening of cleft palate in the first trimester. Ultrasound Obstet Gynecol. 2010;35:7–13.
44. Martinez-Ten P, Adiego B, Perez-Pedregosa J, Illescas T, Wong AE, Sepulveda W. First-trimester assessment of the nasal bones using the retronasal triangle view: a 3-dimensional sonographic study. J Ultrasound Med. 2010;29:1555–61.
45. Adiego B, Martinez-Ten P, Illescas T, Bermejo C, Sepulveda W. First-trimester assessment of nasal bone using retronasal triangle view: a prospective study. Ultrasound Obstet Gynecol. 2014;43:272–6.
46. Sepulveda W, Wong AE, Viñals F, Andreeva E, Adzehova N, Martinez-Ten P. Absent mandibular gap in the retronasal triangle view: a clue to the diagnosis of micrognathia in the first trimester. Ultrasound Obstet Gynecol. 2012;39:152–6.
47. Souka AP, Pilalis A, Kavalakis Y, Kosmas Y, Antsaklis P, Antsaklis A. Assessment of fetal anatomy at the 11-14-week ultrasound examination. Ultrasound Obstet Gynecol. 2004;24:730–4.
48. McAuliffe FM, Fong KW, Toi A, Chitayat D, Keating S, Johnson JA. Ultrasound detection of fetal anomalies in conjunction with first-trimester nuchal translucency screening: a feasibility study. Am J Obstet Gynecol. 2005;193:1260–5.
49. Cicero S, Bindra R, Rembouskos G, Tripsanas C, Nicolaides KH. Fetal nasal bone length in chromosomally normal and abnormal fetuses at 11-14 weeks of gestation. J Matern Fetal Neonatal Med. 2002;11:400–2.
50. Orlandi F, Bilardo CM, Campogrande M, Krantz D, Hallahan T, Rossi C, Viora E. Measurement of nasal bone length at 11-14 weeks of pregnancy and its potential role in Down syndrome risk assessment. Ultrasound Obstet Gynecol. 2003;22:36–9.
51. Moon MH, Cho JY, Lee YM, Lee YH, Yang JH, Kim MY, Park SH. Nasal bone length at 11-14 weeks of pregnancy in the Korean population. Prenat Diagn. 2006;26:524–7.

52. Casasbuenas A, Wong AE, Sepulveda W. First-trimester nasal bone length in a normal Latin American population. Prenat Diagn. 2009; 29:108–12.
53. Miron JP, Cuckle H, Miron P. Prenasal thickness in first-trimester screening for Down syndrome. Prenat Diagn. 2012;32:695–7.
54. Cicero S, Curcio P, Rembouskos G, Sonek J, Nicolaides KH. Maxillary length at 11-14 weeks of gestation in fetuses with trisomy 21. Ultrasound Obstet Gynecol. 2004;24:19–22.
55. Unsal N, Ozat M, Kanat-Pektas M, Gungor T, Danisman N. The significance of fetal maxillary length in the first trimester screening for trisomy 21. Arch Gynecol Obstet. 2011;283:1199–205.
56. Shyu IL, Yang MJ, Wang HI, Wang PH, Chang CM, Juang CM, Chen YJ, Horng HC, Chen CC, Tseng JY, Sung PL, Yen MS, Chen CY, Chao KC. Fetal maxillary and mandibular length in normal pregnancies from 11 weeks' to 13(+6) weeks' gestation: a Taiwanese study. Taiwan J Obstet Gynecol. 2014;53:53–6.
57. Sepulveda W, Martinez-Ten P, Wong AE, Adiego B, Illescas T. Premaxillary thickness (PMT): a sonographic technique for the evaluation of the upper lip in the first trimester. Presented at the XII world congress in fetal medicine, Marbella, 23–27 June 2013.
58. Yazdi B, Riefler P, Fischmüller K, Sonek J, Hoopmann M, Kagan KO. The frontal space measurement in euploid and aneuploid pregnancies at 11-13 weeks' gestation. Prenat Diagn. 2013;33:1124–30.
59. Hoopmann M, Sonek J, Esser T, Bilardo CM, Wagner P, Abele H, Kagan KO. Frontal space distance in facial clefts and retrognathia at 11-13 weeks' gestation. Ultrasound Obstet Gynecol. 2016;48:171–6.
60. Pooh RK, Kurjak A. Novel application of three-dimensional HDlive imaging in prenatal diagnosis from the first trimester. J Perinat Med. 2015;43:147–58.
61. Tonni G, Grisolia G, Sepulveda W. Early prenatal diagnosis of orofacial clefts: evaluation of the retronasal triangle using a new three-dimensional reslicing technique. Fetal Diagn Ther. 2013;34:31–7.
62. Li WJ, Wang XQ, Yan RL, Xiang JW. Clinical significance of first-trimester screening of the retronasal triangle for identification of primary cleft palate. Fetal Diagn Ther. 2015;38:135–41.
63. Sepulveda W, Dezerega V, Be C. First-trimester sonographic diagnosis of holoprosencephaly: value of the "butterfly" sign. J Ultrasound Med. 2004;23:761–5.
64. Sepulveda W, Cafici D, Bartholomew J, Wong AE, Martinez-Ten P. First-trimester assessment of the fetal palate: a novel application of the Volume NT algorithm. J Ultrasound Med. 2012;31:1443–8.
65. Timmerman E, Pajkrt E, Maas SM, Bilardo CM. Enlarged nuchal translucency in chromosomally normal fetuses: strong association with orofacial clefts. Ultrasound Obstet Gynecol. 2010;36:427–32.
66. Syngelaki A, Chelemen T, Dagklis T, Allan L, Nicolaides KH. Challenges in the diagnosis of fetal non-chromosomal abnormalities at 11-13 weeks. Prenat Diagn. 2011;31:90–102.
67. Tonni G, Rosignoli L, Palmisano M, Sepulveda W. Early detection of cleft lip by three-dimensional transvaginal ultrasound in niche mode in a fetus with trisomy 18 diagnosed by celocentesis. Cleft Palate Craniofac J. 2016;53:745–8.
68. Ghi T, Arcangeli T, Radico D, Cavallotti D, Contro E, Pelusi G. Three-dimensional sonographic imaging of bilateral cleft lip and palate in the first trimester. Ultrasound Obstet Gynecol. 2009;34:119–20.
69. Rossi AC, Prefumo F. Accuracy of ultrasonography at 11-14 weeks of gestation for detection of fetal structural anomalies: a systematic review. Obstet Gynecol. 2013;122:1160–7.
70. Rotten D, Levaillant JM. Two- and three-dimensional sonographic assessment of the fetal face. 1. A systematic analysis of the normal face. Ultrasound Obstet Gynecol. 2004;23:224–31.
71. Suresh S, Vijayalakshmi R, Indrani S, Devaki G, Bhavani K. The premaxillary triangle: clue to the diagnosis of cleft lip and palate. J Ultrasound Med. 2006;25:237–42.
72. Martinez-Ten P, Adiego B, Illescas T, Bermejo C, Wong AE, Sepulveda W. First-trimester diagnosis of cleft lip and palate using three-dimensional ultrasound. Ultrasound Obstet Gynecol. 2012;40:40–6.
73. Tonni G, Castigliego AP, Grisolia G, Lituania M, Meagher S, Da Silva Costa F, Araujo Junior E. Three-dimensional ultrasonography by means of HDlive rendering in the first trimester of pregnancy: a pictorial review. J Turk Ger Gynecol Assoc. 2016;17:110–9.
74. Chaoui R, Orosz G, Heling KS, Sarut-Lopez A, Nicolaides KH. Maxillary gap at 11-13 weeks' gestation: marker of cleft lip and palate. Ultrasound Obstet Gynecol. 2015;46:665–9.
75. Paladini D. Fetal micrognathia: almost always an ominous finding. Ultrasound Obstet Gynecol. 2010;35:377–84.
76. Araujo Junior E, Santana EFM, Tonni G, Wong AE, Sepulveda W. Micrognathia. In: Tonni G, Sepulveda W, Wong AE, editors. Prenatal Diagnosis of Orofacial Malformations. Berlin: Springer; 2017:105–18.
77. Bijok J, Massalska D, Michalowska A, Roszkowski T, Ilnicka A, Pawlowska B, Jakiel G. Severe micrognathia in the first trimester in complete trisomy 9 – a case report and literature review. Arch Perinat Med. 2012;18:173–7.
78. Galvao A, Inocencio G, Rodrigues MC. First trimester ultrasound detection of fetal micrognathia. Acta Obstet Ginecol Port. 2015;9:425–6.
79. Lund IC, Vestergaard EM, Christensen R, Uldbjerg N, Becher N. Prenatal diagnosis of Nager syndrome in a 12-week-old fetus with a whole gene deletion of SF3B4 by chromosomal microarray. Eur J Med Genet. 2016;59:48–51.

80. Borenstein M, Persico N, Strobl I, Sonek J, Nicolaides KH. Frontomaxillary and mandibulomaxillary facial angles at 11 + 0 to 13 + 6 weeks in fetuses with trisomy 18. Ultrasound Obstet Gynecol. 2007;30:928–33.
81. Van Zalen-Sprock R, van Vugt JM, van der Harten HJ, Nieuwint AW, van Geijn HP. First trimester diagnosis of cyclopia and holoprosencephaly. J Ultrasound Med. 1995;14:631–3.
82. Dane B, Dane C, Aksoy F, Yayla M. Semilobar holoprosencephaly with associated cyclopia and radial aplasia: first trimester diagnosis by means of integrating 2D-3D ultrasound. Arch Obstet Gynecol. 2009;280:647–51.
83. Araujo Junior E, Rolo LC, Tonni G, Haeri S, Ruano R. Assessment of fetal malformations in the first trimester of pregnancy by three-dimensional ultrasonography in the rendering mode. Pictorial assay. Med Ultrason. 2015;17:109–14.
84. Sepulveda W, Wong AE, Andreeva E, Odegova N, Martinez-Ten P, Meagher S. Sonographic spectrum of first-trimester fetal cephalocele: review of 35 cases. Ultrasound Obstet Gynecol. 2015;46:29–33.
85. Andeeva E. Otocephaly, agnathia, holoprosencephaly – 12 weeks. www.sonoworld.com/TheFetus/page.aspx?id=2690.
86. Cuillier F, Alessandri JL, Cartault F. Otocephaly-agnathia-holoprosencephaly. www.sonoworld.com/TheFetus/page.aspx?id=3287.
87. Andreeva E. Case of the week #390. March 12, 2015 – March 26, 2015. www.sonoworld.com/TheFetus/Case.aspx?CaseId=3522&answer=1.

The Role of 2D/3D/4D Ultrasound in the Prenatal Assessment of Cleft Lip and Palate

4

Pilar Martínez-Ten, Waldo Sepulveda, Amy E. Wong, and Gabriele Tonni

4.1 Introduction

Orofacial clefting is a significant abnormality because it can be associated with other structural anomalies, chromosomal disorders, and genetic syndromes. The frequency is high, occurring in about 1 in every 700 live births [1]. Due to the visible nature of the abnormality, the parents are often significantly emotionally affected. The children born with defects of the hard palate have difficulties with feeding, ear infections and loss of hearing, difficulties and delay in speaking, and dental problems. These children require complex surgery.

As a result of improvements in ultrasound technology and the routine use of this technique in standard clinical practice, orofacial clefting (with or without associated abnormalities) is being diagnosed in the prenatal period with increasing frequency [2, 3]. The rate of detection, especially of the cleft lip with or without cleft palate (CL/CLP), has risen from 5 % in the 1980s [2] to 26 % in 1990 [4] and was most recently reported to be as high as 65 % [5].

Although there have been many classification systems of clefts described in the literature, none have been universally accepted. The current trend is to classify them as cleft lip (CL), cleft lip-palate (CLP), cleft palate (CP), or medial fissures [3]. Many classifications are modifications of the Y system of Kernahan [6], which defines the lips, primary palate, and secondary palate (hard and soft). The LAHSAL system proposed by Kriens in 1989 [7], also a modification of Y of Kernahan [6], is very common, easy to use, and excellent for teaching purposes (Fig. 4.1). It is the system of classification that our department currently uses. A specific prenatal description of the cleft is useful to counsel the parents on the prognosis and to plan the surgical procedures to be performed on the neonate. Furthermore, because the newborn with CLP requires the involvement of a multidisciplinary team of healthcare professionals, an accurate and precise description of the defect is essential to optimize coordination of care to achieve a favorable outcome.

The role of prenatal ultrasound is to diagnose the cleft, establish the extent of the lesion, and diagnose any associated abnormalities, both structural and chromosomal.

P. Martínez-Ten (✉)
Delta – Ultrasound Diagnostic Center in Obstetrics and Gynecology, Conde de Peñalver 14, esc der, 1° izq., Madrid 28006, Spain
e-mail: pilarmten@gmail.com

W. Sepulveda
Fetalmed – Maternal-Fetal Diagnostic Center, Santiago, Chile

A.E. Wong
Department of Maternal-Fetal Medicine, Palo Alto Medical Foundation, Mountain View, CA, USA

G. Tonni, MD, PhD
Department of Obstetrics and Gynecology, Prenatal Diagnostic Service, Guastalla Civil Hospital, AUSL Reggio Emilia, Reggio Emilia, Italy
e-mail: Tonni.Gabriele@ausl.re.it

G. Tonni, W. Sepulveda, and A.E. Wong (eds.), *Prenatal Diagnosis of Orofacial Malformations*,
DOI 10.1007/978-3-319-32516-3_4

4.2 Assessment with 2D ultrasound

The evaluation with 2D ultrasound of the lip and palate is performed using the three spatial planes: sagittal, coronal, and axial or transverse/cross sectional (Fig. 4.2). The profile is obtained by scanning the face in the sagittal plane. The view of the nose and lips is obtained by scanning the face in an anterior coronal section. Finally, the assessment in an axial or cross-sectional plane just below the nose at the level of the upper lip enables visualization of the integrity of the upper lip, as well as the surrounding alveolus, or primary palate.

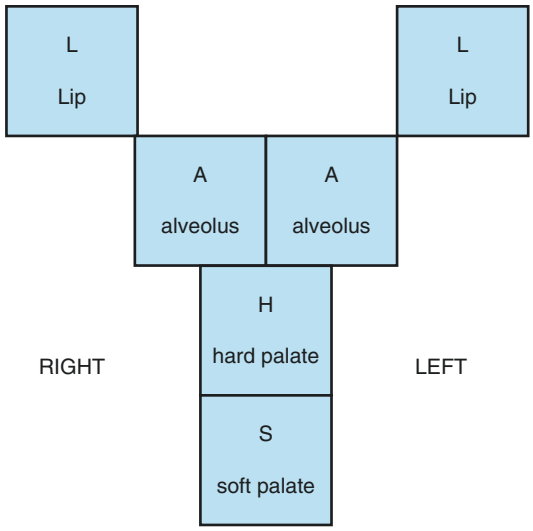

Fig. 4.1 The LAHSAL system, proposed by Kriens in 1989 [7], is a modification of the Y of Kernahan [6]

The sagittal plane can detect a wide variety of profile alterations during the routine anatomy assessment when certain facial anomalies are present. These include anomalies of the orbits, facial mass, micrognathia, retrognathia, and the absence or hypoplasia of the nasal bones.

The *premaxilla, or paranasal protuberance* was described by Nyberg et al. [8, 9] in 1992 and 1993. A paranasal mass identified by ultrasound during the second trimester is an important finding of a complete bilateral CLP (Fig. 4.3). In the studies by Nyberg et al. [8, 9], the majority of the fetuses with bilateral CLP demonstrated presence of this mass. The paranasal protuberance can be seen below the nose and represents the prolabium and the premaxilla, composed of the central portion of the upper lip and the primary palate with the alveolar holes of the two central incisors that are derived from the frontonasal processes. The paranasal protuberance can also be evident in cases of larger unilateral CLP.

A *flat profile* (Fig. 4.4) associated with bilateral clefts with or without palate involvement has been described by Gabrielli et al. [10]. In their retrospective study with 14 fetuses with prenatal diagnosis of bilateral clefts, 9 of 14 fetuses had a premaxilla protuberance and 5 of 14 (approximately one-third) had a flat profile.

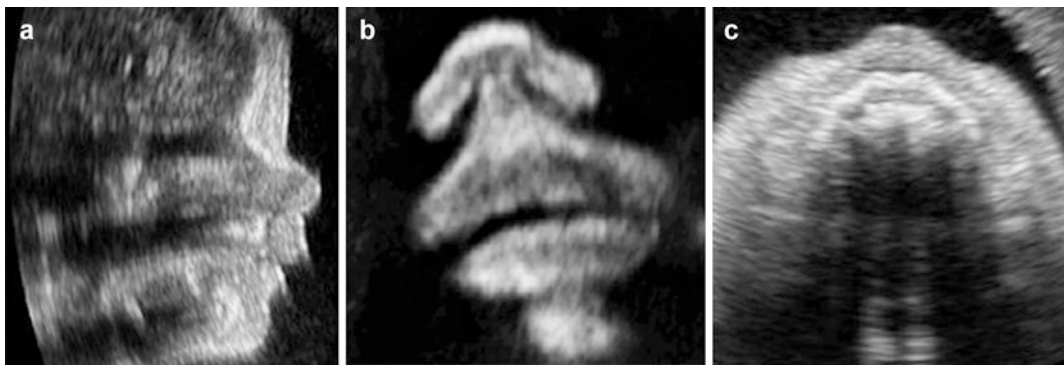

Fig. 4.2 Evaluation with 2D ultrasound of the lips and palate. (**a**) Sagittal plane showing the forehead, nose, upper and lower lips, and the chin. (**b**) Anterior coronal plane showing nasal columella, nostrils, philtrum, upper and lower lips, and chin. (**c**) Axial plane showing upper lip and primary palate with the alveolar holes. The secondary palate is not seen

The 5 fetuses with a flat profile were aneuploid, including three with trisomy 18, one with trisomy 13, and another with mosaic trisomy 8. In the group with premaxilla protuberance, only one of the nine fetuses had trisomy 13. The authors concluded that the flat profile is seen in approximately a third of the cases with prenatal diagnosis of bilateral clefting and that these fetuses are at high risk of having a lethal aneuploidy. The combination of a flat facial profile and a chromosomal abnormality suggests that many of these clefts, which are usually medial fissures, are a consequence of a deficiency during the development of the frontonasal process affecting the forehead and nose.

In the *anterior coronal* plane, in which the tip of the nose and the length of the lip are seen in the same view, the interruption of the surface of the lip can be visualized and classified as unilateral (right or left) or bilateral (Fig. 4.5).

In the *transverse or axial plane performed with 2D ultrasound*, we can identify the alveolar crest of the upper maxilla (Fig. 4.6). However, we cannot see the secondary palate (hard or soft) because of shadowing from the surrounding alveolus and the presence of the tongue.

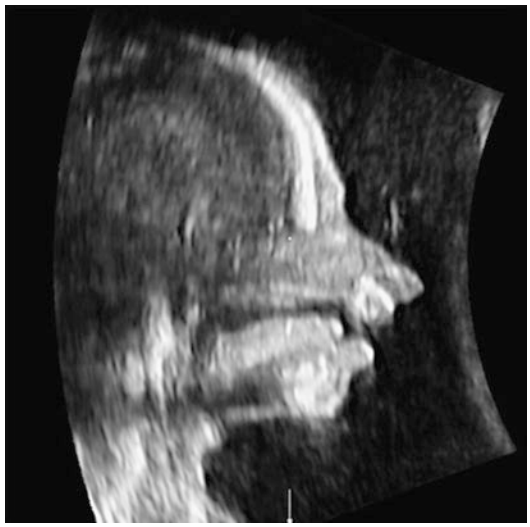

Fig. 4.3 Sagittal plane obtained with 2D ultrasound of a fetus of 22 weeks with a bilateral CLP. A premaxilla or paranasal protuberance is seen, representing the prelabium and the premaxilla projecting anteriorly

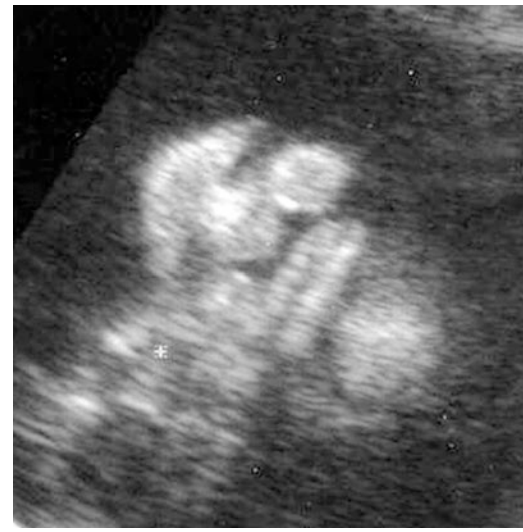

Fig. 4.5 Anterior coronal plane (2D ultrasound) of a bilateral CLP

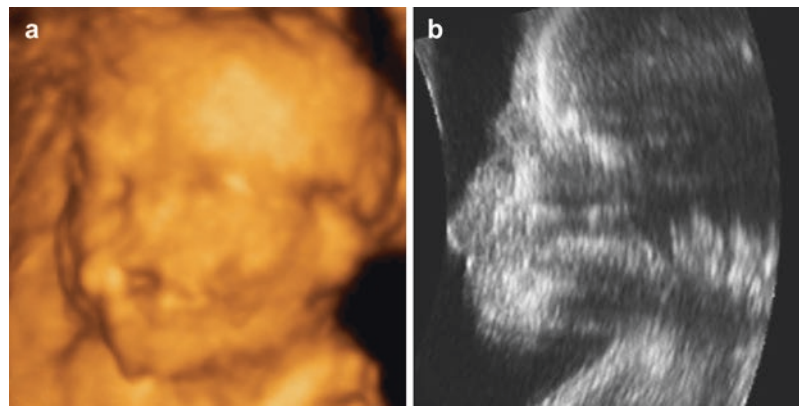

Fig. 4.4 (**a**) Surface rendered image using 3D ultrasound of a 16-week fetus affected with trisomy of chromosome 13 with a midline cleft. (**b**) Sagittal plane (2D ultrasound) of the same fetus illustrating the "flat profile"

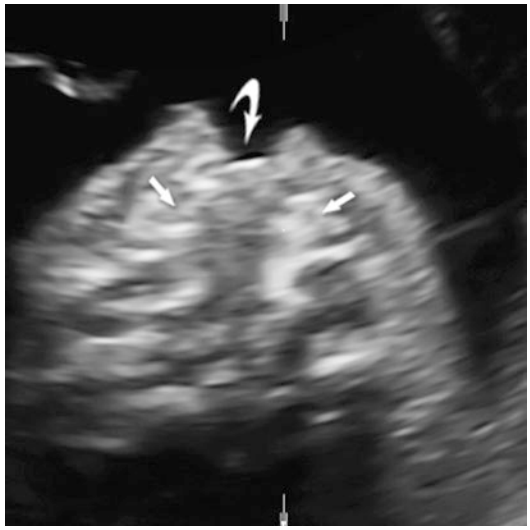

Fig. 4.6 Axial plane (2D ultrasound) of a left CLP showing the lip (*curved arrow*) and the affected border of the alveolus (*straight arrows*). Shadowing from the tongue and the ear precludes visualization of the secondary palate

In addition, evaluation of the uvula can be a helpful in determining if there may be a defect of the soft palate. Sonographic visualization of the uvula can be achieved by obtaining a coronal plane through the neck and pharynx or via a transverse plane with slight tilting of the transducer as demonstrated by Wilhelm and Borgers [11] in 667 consecutive patients with a normal singleton pregnancy between 20 and 25 weeks of gestation. These authors demonstrated that a normal uvula could be visualized with a typical echo pattern (the "equals sign") in 90.7 % of the cases and the soft palate could be completely visualized in a median sagittal section in 85.3 % of the cases. Visualization of at least one of the two structures (either the uvula or the soft palate) was successful in 98.4 % of cases. Ultrasound detection of a bifid uvula (consisting in a cleft at this level) is diagnostic of a soft palatal defect [12].

In addition to the use of conventional 2D ultrasound, color Doppler ultrasound may contribute to the prenatal diagnosis of CP by demonstrating abnormal amniotic fluid flow between the oropharynx and the nasopharynx cavity, either using 2D or 3D ultrasound [13–15]. However, power Doppler may create a "blooming artifact" or "color bleed" [16] compared to high-definition power Doppler. The new bidirectional power Doppler technique combines high axial resolution with reduced spatial overlap of tissue and flow signals [17].

4.3 Exploration with 3D ultrasound

As we have highlighted above, in the second and third trimesters, defects involving the lips and the surrounding alveolus are often successfully diagnosed with relative ease using conventional 2D ultrasound. However, the diagnosis of the secondary palate involvement (hard and soft) continues to be a challenge for the sonographer.

With the arrival of 3D ultrasound, a series of techniques have been developed for exploring the secondary palate. These are the "reverse face" technique published by Campbell et al. [18], the "flipped face" technique developed by Platt et al. [19], and variations of both techniques [11, 20–24]. All seek to evaluate the palate in coronal or axial planes using a multiplanar system and/or rendering provided by 3D ultrasound. Our group published another method [25], which we termed the "oblique face" technique using the Oblique View tool that enables selection of nonconventional planes of volume (oblique or curved). The results are similar to that obtained with the OmniView tool [26].

To view the secondary palate, it is essential that the plane of initial acquisition of volume is very clear. It needs to be a midsagittal plane of the face, restricting the sector over the facial mass. According to the recommendations of Pilu and Segata [27], the fetus should have the head slightly deflected; the face may be gently pressed with the transducer to induce this slight deflection (Fig. 4.7) so that the hard palate and the shadow of the maxilla do not interfere with the ultrasound. We use maximum quality, high harmonics, and an angle of 40–70° depending on gestational age. It does not matter whether the cord or the placenta is in front of the face, but there should not be any limbs because of the shadows created over the upper maxilla or hard palate.

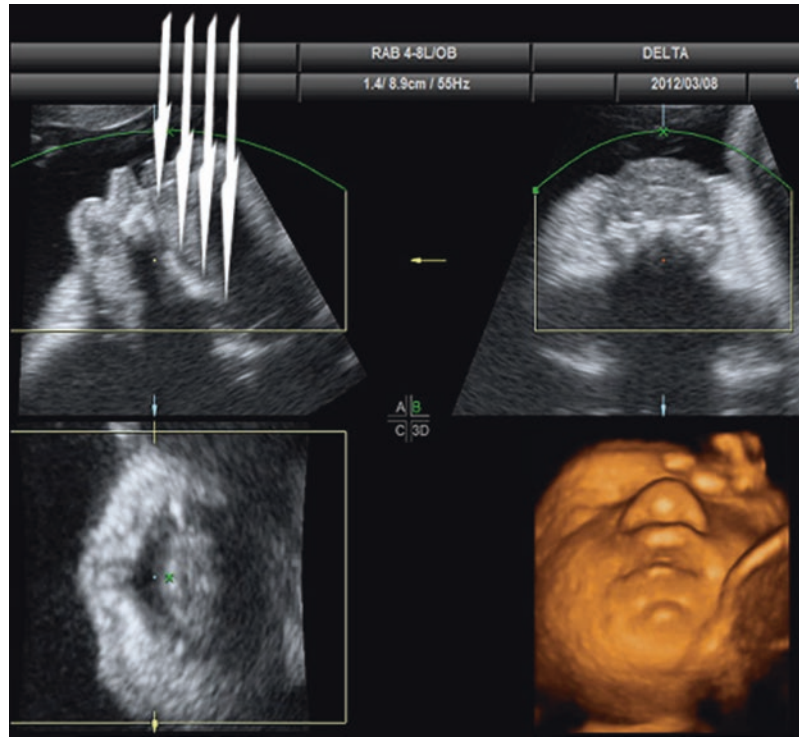

Fig. 4.7 Window A: The initial plane for volume acquisition is a straight midsagittal plane from which the volume is obtained with a sweep angle of 40–70°. The sweep is performed in a lateral direction from one side of the face to the other. The head is slightly deflected so that the ultrasound beams are directed toward the palate at a slightly oblique angle (*arrows*). Window B: coronal plane. Window C: axial plane. Window X: surface rendered image of the face

Below, we describe the techniques that enable us to visualize the secondary palate with 3D ultrasound.

4.3.1 "Reverse Face" View

According to the technique described by Campbell et al. [18], we place the green rendering lines from the posterior part to the anterior part of the palate. This allows coronal reconstructions rendered from the "inside" (Fig. 4.8).

4.3.2 "Flipped Face" View

This technique was described by Platt et al. [19]. We rotate the fetal face 90° from the midsagittal supine position to obtain axial planes of the secondary palate displaced from the chin up to the nose in a rendered surface reconstruction. We have enhanced this technique slightly; given that the form of the palate is concave, we curve the green line over the palate to achieve a better representation of the palate. The green line is curved over the coronal plane of the multiplanar evaluation (demonstrating the laterals borders of the palate) and the sagittal plane (demonstrating the anterior and posterior borders of the palate) (Fig. 4.9).

4.3.3 "Oblique Face" View

To obtain the "oblique face" view, we use the Oblique View tool to obtain a nonstandard plane enhanced with XIMR [25] or the OmniView tool [26]. On a volume represented by the midsagittal section of the face, we specify a surface that traces the lips, the surrounding alveolus, and the palate, and we obtain an axial plane, perpendicular to this previously traced surface, in which the palate is incorporated. Secondly, we trace a line on the profile in the caudal-cranial direction from inside the face, and we obtain a coronal plane that we can shift and rotate along the length of the palate (Fig. 4.10).

Figures 4.11 through 4.19 show different types of clefts and their evaluation with 3D

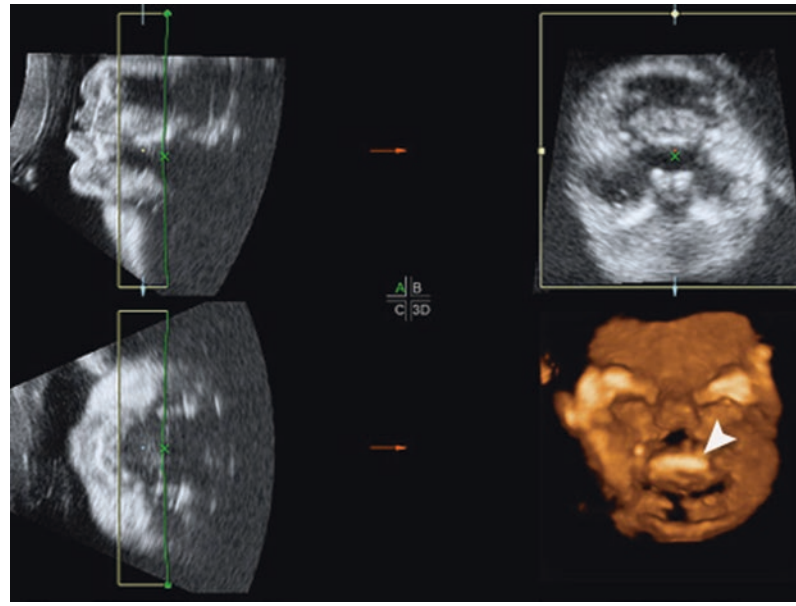

Fig. 4.8 Reverse face technique. Window A: initial plane of volume acquisition with the profile of the face turned 90° and the green rendering line placed to the right, from the inside of the face. Window B: coronal plane of the face. Window C: axial plane at the level of the nasal septum. Window X: surface rendered image demonstrating the hard palate in a coronal plane (*arrow head*)

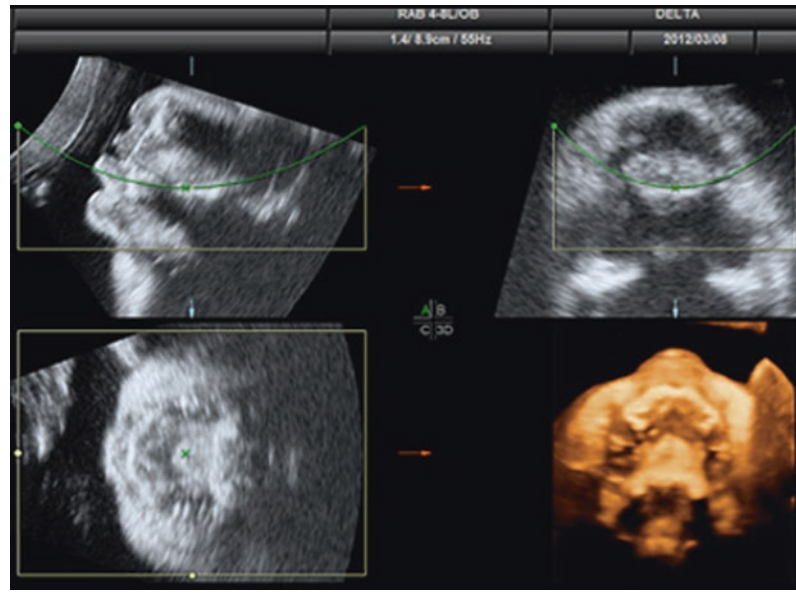

Fig. 4.9 Flipped face technique. Window A: initial plane of volume acquisition with the profile of the face turned 90° and the green line of the rendering box curved so that it is fitted to the location of the hard and soft palate. Window B: coronal plane of the face with the *green line* curved over the hard palate. Window C: axial plane at the level of the nasal septum. Window X: surface rendering on the right shows an axial plane of the maxilla with alveolar ridges, hard palate, and soft palate

ultrasound using these three techniques. We need to take into account that when we see the face using surface rendering, the right side of the fetus is on the left in the image and vice versa (a mirror image). The same mirroring occurs in the axial planes obtained with the "flipped face" technique and with the coronal or axial planes derived using the oblique face technique. Nevertheless, when we employ the reverse face technique of Campbell, since we are looking at the coronal plane from "inside," the right of the face is on the right in the image, and the left side of the face is on the left in the image.

It is most likely that no single method ("reverse face," "flipped face," or "oblique face") is notably superior than the others. All techniques can be applied to each case; the critical factors to achieve an accurate and specific understanding of the abnormality are a good 3D volume and the time to perform thorough evaluation.

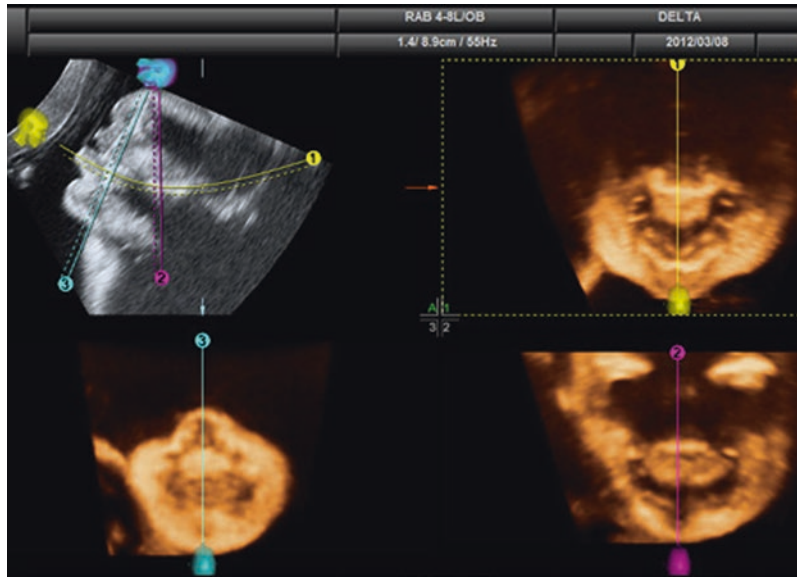

Fig. 4.10 Oblique face technique. We used the OmniView tool (GE Health Care, Zipf, Austria). Window A: initial plane of volume acquisition on which we trace a nonstandard plane (oblique or curved). The first line with volume contrast imaging (VCI) in the 2 mm thickness (1, *yellow*) is curved over the palate to include the upper lip and the central part of the upper maxilla of the hard and soft palate. In Window 1, the plane obtained perpendicular to the traced line is a curved axial plane that shows the lip, the upper maxilla with the alveolar holes, and the hard palate. The second line with VCI with a thickness of 2 mm (2, *purple*) is perpendicular to the hard palate. In Window 2, we see the obtained coronal plane that traverses the hard palate and is similar to that obtained with the Campbell (2007) technique. The third line with VCI in thickness of 2 mm is oblique (3, *blue*) and incorporates the more anterior part of the facial mass. In Window 3, we see an anterior coronal plane of the face with the central portion of the upper maxilla

4.4 Do We Need to Include the 3D Ultrasound Evaluation of the Secondary Palate in the Anatomy Assessment in the Second Trimester?

In a recent study [28], we applied the "flipped face" technique to 97 consecutive pregnancies between 18 and 23 weeks during our routine midtrimester anatomic assessments. It was not possible to obtain a volume in 13 patients. Of the 84 cases in which it was possible to capture a volume, the assessment of the secondary palate was acceptable in only 34 cases. In the remaining 50 cases, the positioning of the limbs, shadows generated by the superior maxilla, or the poor quality of the volumes prevented an adequate view of the secondary palate.

From this study, we concluded that 3D ultrasound evaluation should not be used routinely. However, it may be offered as a special ultrasound study such as a *maxillofacial ultrasound* similar to the indications for an echocardiogram or a neurosonographic exam in specific circumstances. The indications for maxillofacial ultrasound would consist of:

1. Finding of cleft lip on 2D ultrasound. Attempts should be made to assess the full extent of the lesion to appropriately counsel the parents and the multidisciplinary team regarding whether the maxilla and the secondary palate are also involved.
2. Pregnancies with high risk of clefting of the secondary palate. When structural anomalies, intrauterine growth restriction, polyhydramnios, or a syndrome or a chromosomal abnormality is suspected, it is reasonable to perform a detailed assessment of the palate [29].

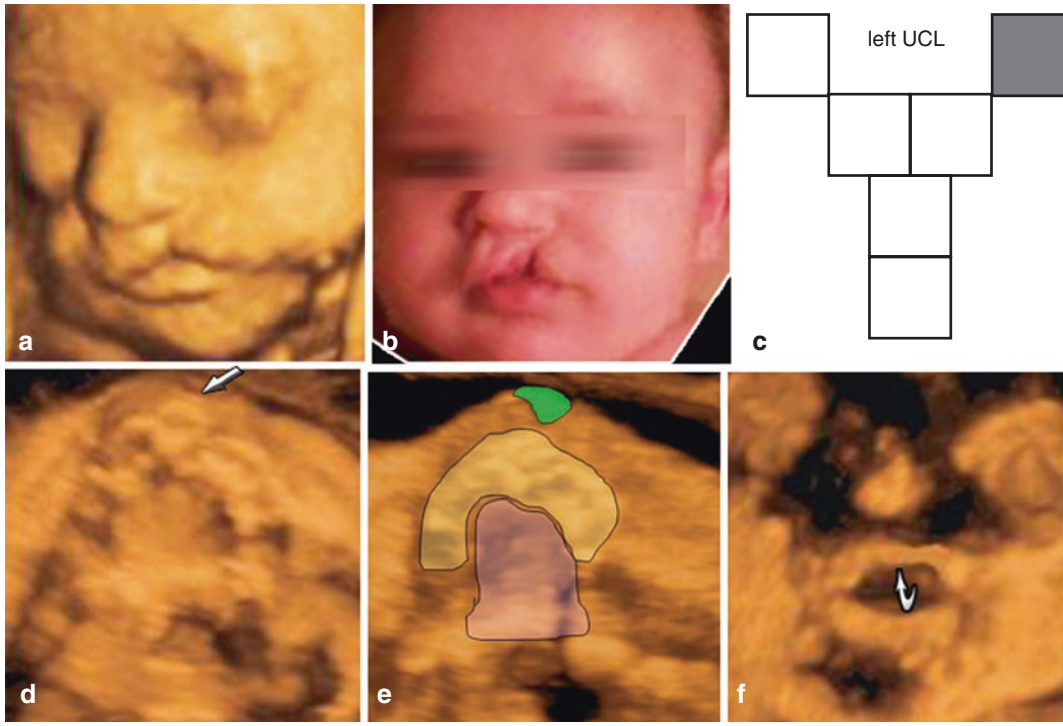

Fig. 4.11 Unilateral left lip cleft. (**a**) Surface rendering of the fetal face showing the cleft of the left lip. (**b**) Newborn. (**c**) Kernahan Y simplified [6]. (**d**) Surface rendering of the axial plane of the palate with the flipped face technique showing the affected left lip (*arrow*) and the surrounding alveolus and normal secondary palate. (**e**) The same image of (d) highlighting the cleft lip (*green*), the upper maxilla (*yellow*), and the secondary palate (*pink*). (**f**) Coronal plane obtained with the reverse face technique. The *curved arrow* highlights the non-affected secondary palate

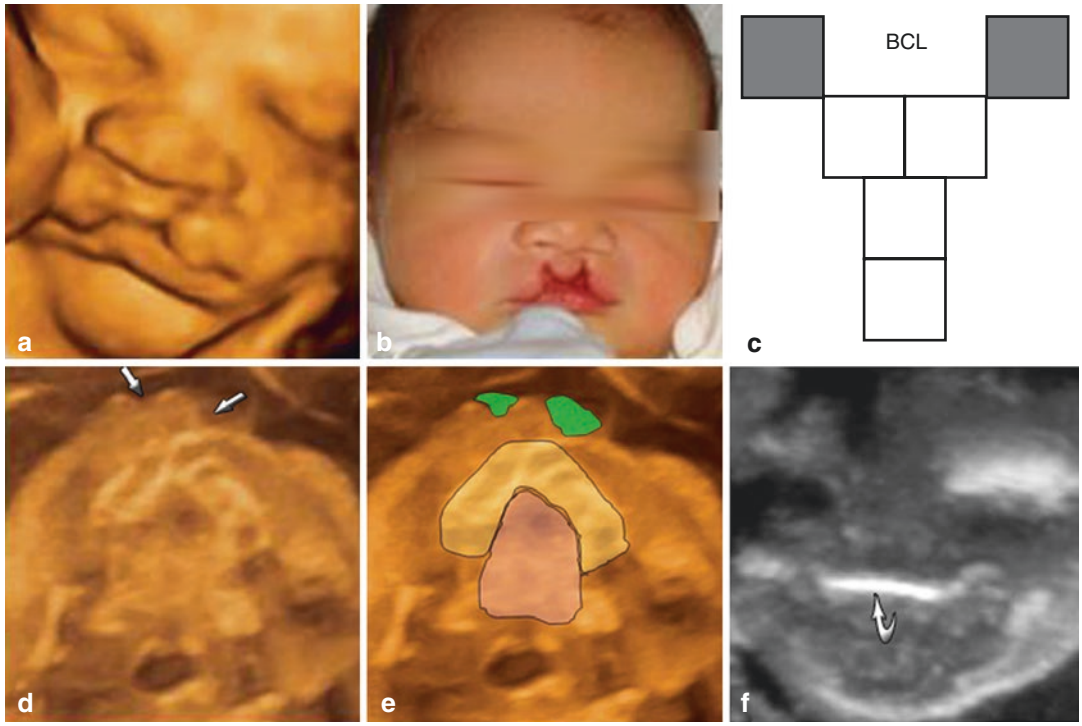

Fig. 4.12 Bilateral cleft lip: (**a**) surface rendering of the fetus showing the bilateral cleft lip at 32 weeks. (**b**) Newborn. (**c**) Simplified Y of Kernahan [6]. (**d**) Surface rendering of the axial plane of the palate with the flipped face technique showing the affected lips on both the left and right sides (*arrows*), the surrounding alveolus, and unaffected secondary palate. (**e**) The same image of (d) highlighting the cleft lip (*green*), upper maxilla (*yellow*), and secondary palate (*pink*). (**f**) Coronal plane obtained with the reverse face technique. The *curved arrow* indicates the non-affected secondary palate

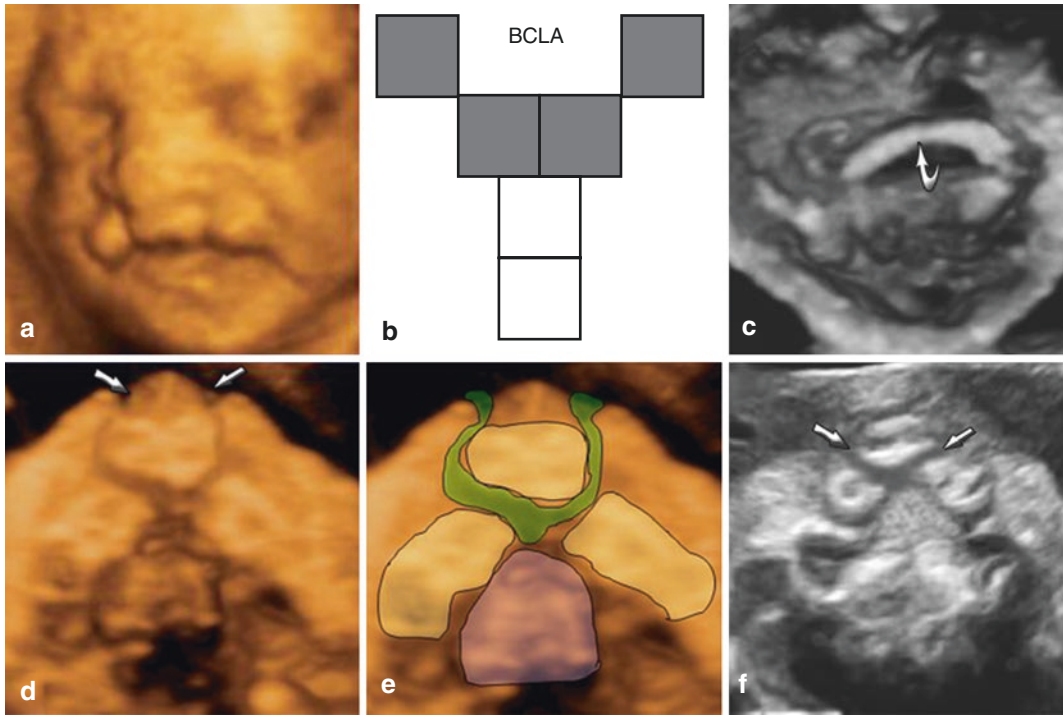

Fig. 4.13 Bilateral cleft lip-palate. (**a**) Surface rendering showing the bilateral fissure of the lip. (**b**) Simplified Y of Kernahan [6]. (**c**) Coronal plane obtained with reverse face technique. The *curved arrow* shows the non-affected secondary palate. (**d**) Surface rendering of the axial plane of the palate with the flipped face technique showing the bilaterally affected lip (*arrows*). The cleft of the primary palate extends up to the incisor foramen. The secondary palate is non-affected. (**e**) The same image as (c) with the cleft lips and the upper maxilla at the site of the lateral foramen highlighted in *green. Yellow* highlights are the central parts of the upper maxilla with the two central incisors, and the remainder of the maxilla lateral to the defect. *Pink* highlights are the secondary palate. (**f**) Oblique face technique showing the axial plane with the affected lip (*arrows*), the primary palate at the site of the lateral incisor foramen, and the secondary palate

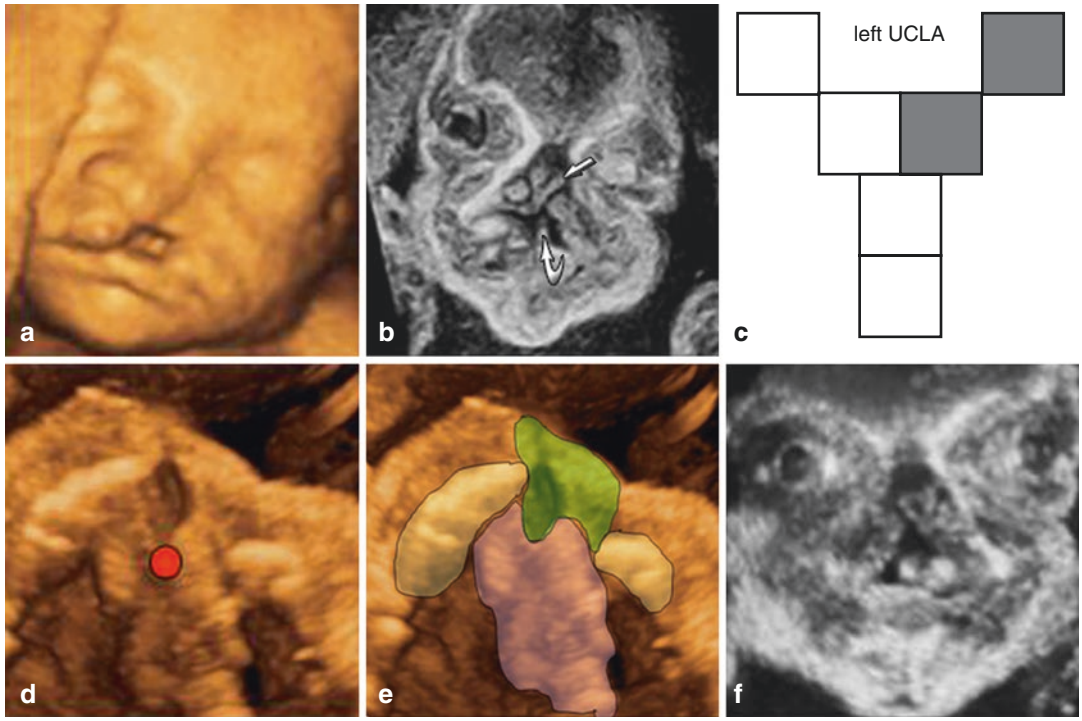

Fig. 4.14 Left unilateral lip-alveolus cleft. (**a**) Surface rendering of the face of a fetus at 27 weeks showing a defect of the lip from the base of the nose producing an asymmetric nose with deviation of the septum and flattening of the alar cartilage. (**b**) With the oblique face technique, we traced a line in the caudal-cranial direction that crosses the upper maxilla. The plane obtained is in the coronal plane similar to that obtained in the reverse face method showing the orbits, the frontal processes, nasal septum deviated to the right (*arrow*), the fissured upper maxilla, and the communication between the oral cavity and the nasal cavity (*curved arrow*). (**c**) Simplified Y of Kernahan [6]. (**d**) Surface rendering of the axial plane of the palate with the flipped face technique showing the maxilla interrupted laterally, lacking the segment of the maxilla that will begin the lateral incisor of the affected side. The defect will reach the point of separation of the primary palate from the secondary, i.e., up to the incisor foramen (*red dot*). (**e**) The same image as (**d**) with *green* showing the fissures of the lip and the upper maxilla up to the incisor foramen. *Yellow* highlights the surrounding non-affected alveolus. *Pink* shows the secondary palate. (**f**) Coronal plane obtained with the reverse face technique. Note the affected secondary palate

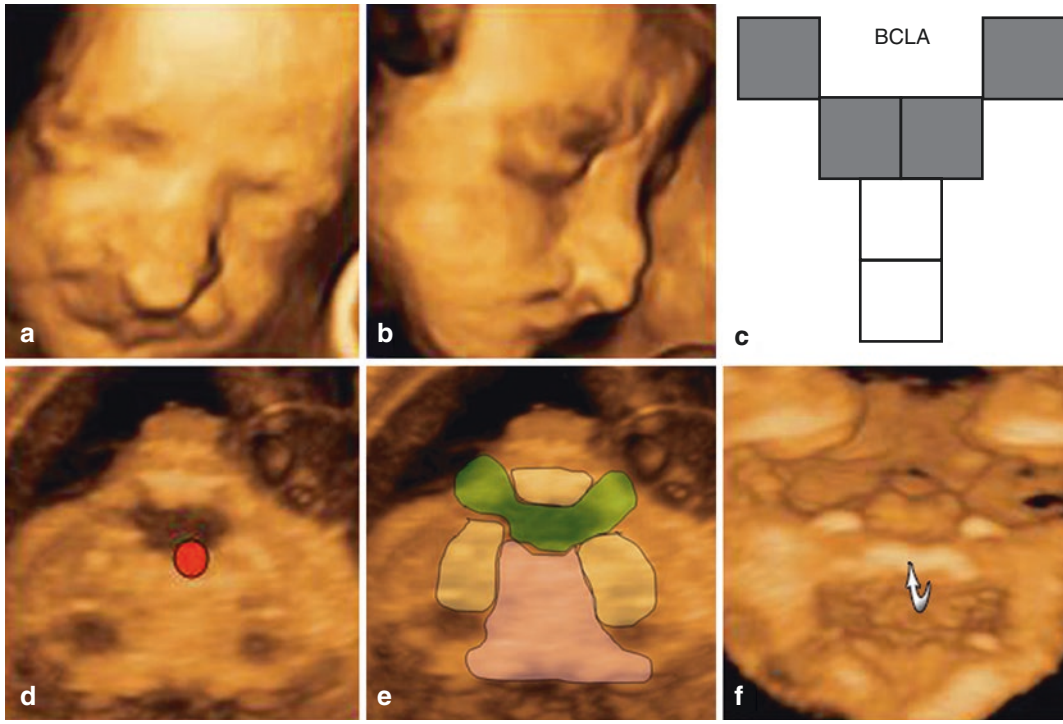

Fig. 4.15 Bilateral alveolar-lip fissure. (**a**) and (**b**) surface rendering showing the bilateral fissure of the lip with the prolabium projecting anteriorly. (**c**) Simplified Y of Kernahan [6]. (**d**) Surface rendering of the axial plane of the palate with the flipped face technique showing the bilaterally affected lip. The primary palate is fissured up to the incisor foramen (*red dot*). The secondary palate is non-affected. (**e**) The same image as (d) with *green* highlighting the fissures of the lip and upper maxilla at the site of the lateral incisor foramen. *Yellow* highlights the central part, the upper maxilla with the two incisors central and lateral to the defect, and the rest of the maxilla. *Pink* highlights the secondary palate. (**f**) Coronal plane obtained with the reverse face technique showing the intact hard palate (*curved arrow*)

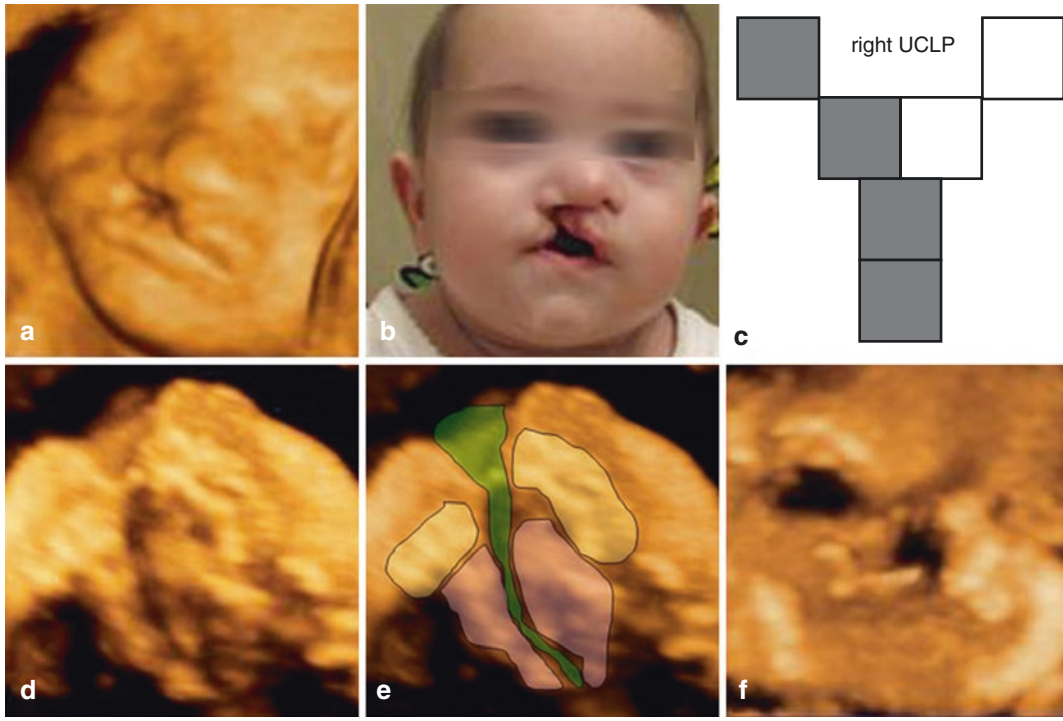

Fig 4.16 Right unilateral cleft lip-palate. (**a**) Surface rendering of the fetal face showing the right lip fissure. (**b**) Newborn. (**c**) Simplified Y of Kernahan [6]. (**d**) Surface rendering of the axial plane of the palate with the flipped face technique showing the lip, the surrounding alveolus, and the secondary palate affected on the right side. (**e**) The same image as in (d) with *green* highlighting the lip fissures, the upper maxilla, and the secondary palate. *Yellow* highlights the non-affected maxilla. *Pink* shows the entire secondary palate to the side of the defect. (**f**) Coronal plane obtained with the reverse face technique showing the fissure in the secondary palate

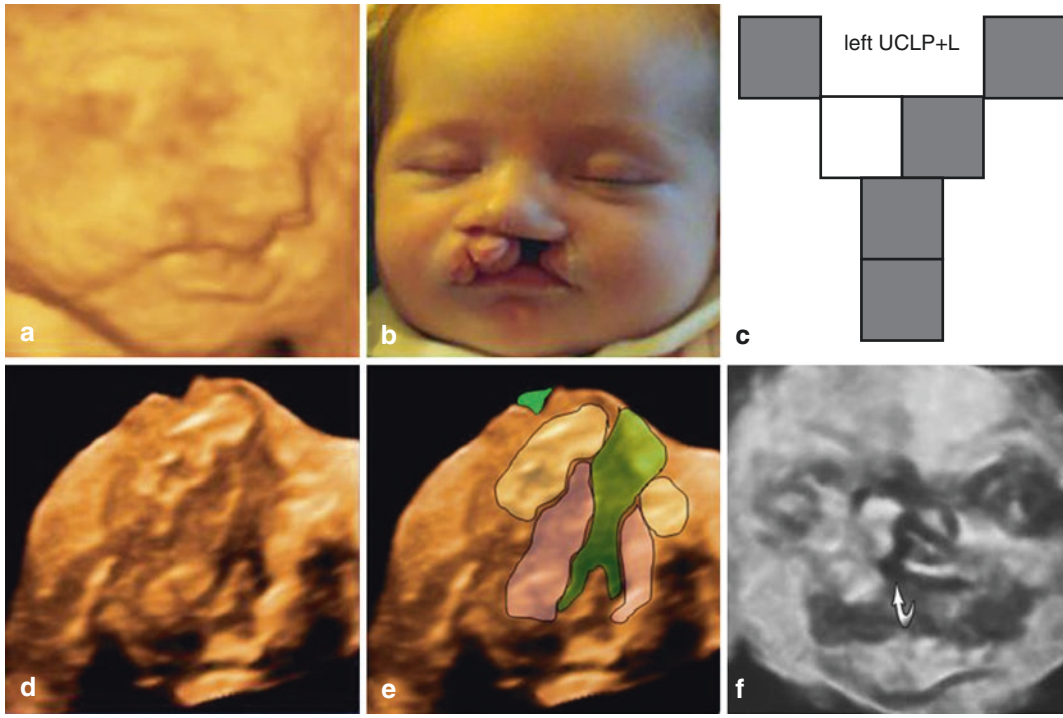

Fig. 4.17 Unilateral left cleft lip-palate + right lip fissure. (**a**) Surface rendering showing the bilateral fissure of the lip. (**b**) Newborn. (**c**) Simplified Y of Kernahan [6]. (**d**) Surface rendering of the axial plane of the palate with the flipped face technique showing the lip, surrounding alveolus, and the affected left secondary palate as well as the affected lip, on the right side. (**e**) The same image as (d) with *green* highlighting the fissures of the lip, upper maxilla, and the secondary palate. *Yellow* highlights the non-affected maxilla. *Pink* shows the secondary palate to the sides of the defect. *Dark green* shows the notch in the lip on the right side. (**f**) Coronal plane obtained with the reverse face technique showing the fissure in the secondary palate (*curved arrow*) and the central communication between the oral cavity and the nose

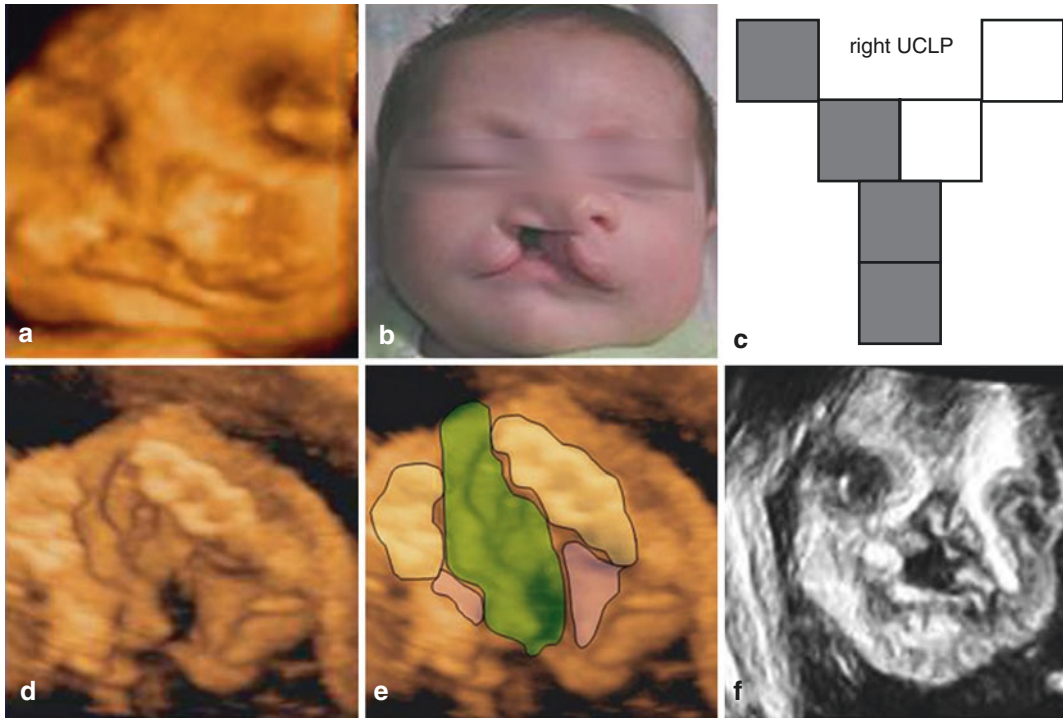

Fig. 4.18 Unilateral right CLP. (**a**) Surface rendering showing the right lip cleft with a large fissure. (**b**) Newborn. (**c**) Simplified Y of Kernahan [6]. (**d**) Surface rendering of the axial plane of the palate with the flipped face technique showing the lip, the surrounding alveolus, and the secondary palate affected on the right side. This defect is very severe, with wide separation of the structures. (**e**) The same image as (**d**) with green showing the wide fissure of the lip, the upper maxilla, and the secondary palate. *Yellow* highlights the non-affected maxilla. *Pink* shows the secondary palate lateral to the defect. (**f**) With the oblique face technique, we traced a line in the caudal-cranial direction. The plane obtained is coronal showing the orbits, the frontal processes, and the nasal septum deviated to the left and the wide communication between the oral cavity and the nasal cavity

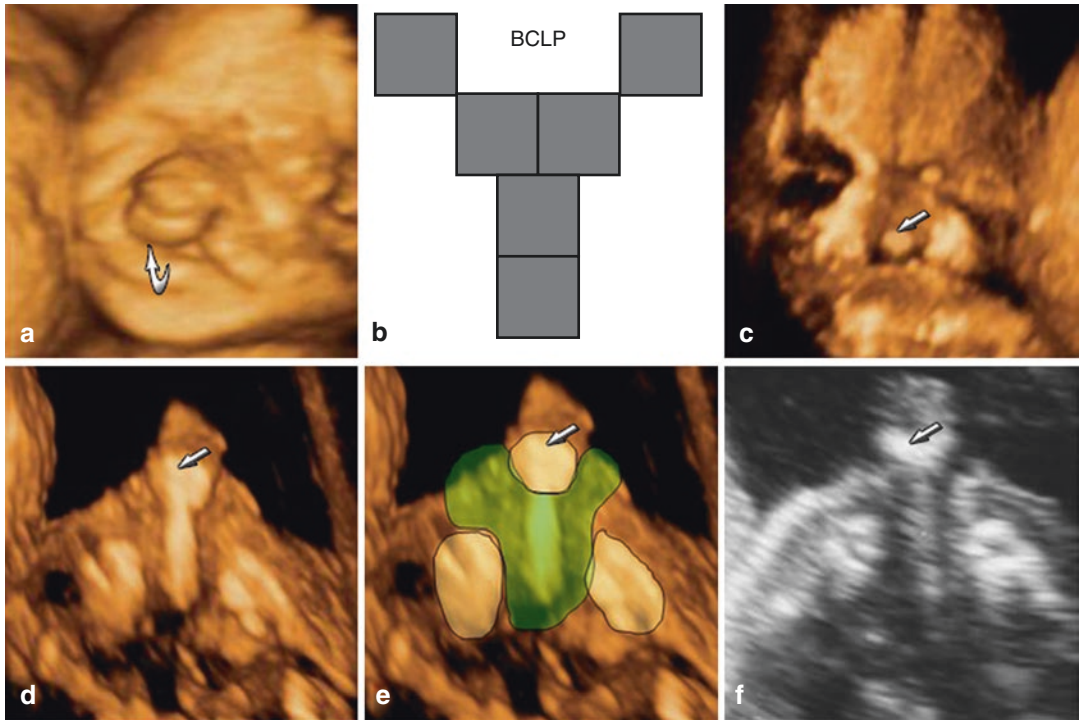

Fig. 4.19 Bilateral lip-palate cleft. (**a**) Surface rendering of the face of a fetus of 23 weeks with a bilateral CLP affecting the lip, maxilla, hard palate, and soft palate. The cleft completely involves the two sides of the lip. The premaxilla and prolabium (*arrow*) unite into the vomer, projecting anteriorly and separated from the maxilla. The facial appearance is very characteristic of orofacial clefting. (**b**) Simplified Y of Kernahan [6]. (**c**) Coronal plane obtained with the reverse face technique. The *arrow* shows the premaxilla. (**d**) Axial plane showing the maxilla interrupted laterally and the premaxilla with the foramen of the central incisors projecting anteriorly. Not observed is the maxilla that will give rise to the lateral incisors. There is no secondary palate, and the central line of the image is the vomer. As such, there is total communication between the oral cavity and the nose. (**e**) The same image as in (d) where *green* highlights the wide cleft lip, the upper maxilla, and the secondary palate. *Yellow* shows the non-affected maxilla. (**f**) Image very similar to (a) and (c) obtained with the oblique face technique

References

1. Mossey PA, Little J, Munger RG, Dixon MJ, Shaw WC. Cleft lip and palate. Lancet. 2009;374:1773–85.
2. Maarse W, Berge SJ, Pistorius L, Van Barneveld T, Kon M, Breugem C, et al. Diagnostic accuracy of transabdominal ultrasound in detecting prenatal cleft lip and palate: a systematic review. Ultrasound Obstet Gynecol. 2010;35:495–502.
3. Maarse W, Rozendaal AM, Pajkrt E, et al. A systematic review of associated structural and chromosomal defects in oral clefts: when is prenatal genetic analysis indicated? J Med Genet. 2012;49:490–8.
4. Stoll C, Dott B, Alembik Y, Roth M. Evaluation of prenatal diagnosis of cleft lip/palate by foetal ultrasonographic examination. Ann Genet. 2000;43:11–4.
5. Maarse W, Pistorius LR, Van Eeten WK, Breugem CC, Kon M, Van den Boogaard MJ, Mink van Der Molen AB. Prenatal ultrasound screening for orofacial clefts. Ultrasound Obstet Gynecol. 2011;38:434–9.
6. Kernahan DA. The striped Y—a symbolic classification for cleft lip and palate. Plast Reconstr Surg. 1971;47:469–70.
7. Kriens O. LAHSAL—a concise documentation system for cleft lip, alveolus and palate diagnoses. In: What is cleft lip and palate? A multidisciplinary update. Stuttgart: Thieme; 1989.
8. Nyberg DA, Mahony BS, Kramer D. Paranasal echogenic mass: sonographic sign of bilateral complete cleft lip and palate before 20 menstrual weeks. Radiology. 1992;184:757–9.
9. Nyberg DA, Hegge FN, Kramer D, Mahony BS, Kropp RJ. Premaxillary protrusion: a sonographic clue to bilateral cleft lip and palate. J Ultrasound Med. 1993;12:331–5.
10. Gabrielli S, Piva M, Ghi T, Perolo A, De Santis MS, Bevini M, et al. Bilateral cleft lip and palate without premaxillary protrusion is associated with lethal aneuploidies. Ultrasound Obstet Gynecol. 2009;34:416–8.
11. Wilhelm I, Borgers H. The "equals sign": a novel marker in the diagnosis of fetal isolated cleft palate. Ultrasound Obstet Gynecol. 2010;36:439–44.

12. Lituania M, Tonni G. Bifid uvula and familial Stickler syndrome diagnosed prenatally before the sonographic "equals sign" landmark. Arch Gynecol Obstet. 2013;288:483–7.
13. Aubry MC, Aubry JP. Prenatal diagnosis of cleft palate: contribution of color Doppler ultrasound. Ultrasound Obstet Gynecol. 1992;2:221–4.
14. Sherer DM, Abramowicz JS, Jaffe R, Woods JR Jr. Cleft palate: confirmation of prenatal diagnosis by colour Doppler ultrasound. Prenat Diagn. 1993;13:953–6.
15. Lee W, Kalache KD, Chaiworapongsa T, Londono J, Treadwell MC, Johnson A, Romero R. Three-dimensional power Doppler ultrasonography during pregnancy. J Ultrasound Med. 2003;22:91–7.
16. Nilsson A. Artefacts in sonography and Doppler. Eur Radiol. 2001;11:1308–15.
17. Kennelly MM, Moran P. Directional Power Doppler in the midsagittal plane as an aid to the prenatal diagnosis of cleft lip and palate. Prenat Diagn. 2008;28:56–8.
18. Campbell S, Lees C, Moscoso G, Hall P. Ultrasound antenatal diagnosis of cleft palate by a new technique: the 3D 'reverse face' view. Ultrasound Obstet Gynecol. 2005;25:12–8.
19. Platt LD, Devore GR, Pretorius DH. Improving cleft palate/cleft lip antenatal diagnosis by 3-dimensional sonography: the 'flipped face' view. J Ultrasound Med. 2006;25:1423–30.
20. Tonni G, Ventura A, Centini G, Rosignoli L. Sonographic imaging of the fetal hard palate during second-third trimester pregnancy scan: setting the standard for 3D sonography in a training program. J Diagn Med Sonography. 2009;25:179–84.
21. Tonni G, Grisolia G. Fetal uvula: navigating and lightening the soft palate using HDlive. Arch Gynecol Obstet. 2013;288:239–44.
22. Faure JM, Captier G, Baumler M, Boulot P. Sonographic assessment of normal fetal palate using three-dimensional imaging: a new technique. Ultrasound Obstet Gynecol. 2007;29:159–65.
23. Wong HS, Tait J, Pringle KC. Examination of the secondary palate on stored 3D ultrasound volumes of the fetal face. Ultrasound Obstet Gynecol. 2009;33:407–11.
24. Wang LM, Leung KY, Tang M. Prenatal evaluation of facial clefts by three-dimensional extended imaging. Prenat Diagn. 2007;27:722–9.
25. Martinez-Ten P, Perez-Pedregosa J, Santacruz B, Adiego B, Barron E, Sepulveda W. Three-dimensional ultrasound diagnosis of cleft palate: 'reverse face', 'flipped face' or 'oblique face' – which method is best? Ultrasound Obstet Gynecol. 2009;33:399–406.
26. Tonni G, Lituania M. OmniView algorithm: a novel 3-dimensional sonographic technique in the study of the fetal hard and soft palates. J Ultrasound Med. 2012;31:313–8.
27. Pilu G, Segata M. A novel technique for visualization of the normal and cleft fetal secondary palate: angled insonation and three-dimensional ultrasound. Ultrasound Obstet Gynecol. 2007;29:166–9.
28. Sepulveda W, Wong AE, Castro-Vargas F, Adiego B, Martinez-Ten P. Three-dimensional sonographic examination of the fetal secondary palate at the second-trimester anatomy scan: a feasibility study. J Ultrasound Med. 2011;30:1619–24.
29. Gillaham JC, Anad S, Bullen PJ. Antenatal detection of cleft lip with or without cleft palate. Ultrasound Obstet Gynecol. 2009;34:410–5.

2D/3D/4D Ultrasound of the Fetal Face in Genetic Syndromes

5

Pilar Martínez-Ten, Waldo Sepulveda, and Gabriele Tonni

5.1 Introduction

Clinical dysmorphology is the study of rare syndromes that accompany malformations and/or phenotypic abnormalities. Around 2500 dysmorphology syndromes or malformations have been described, the great majority accompanied by mental retardation. Combinations of small phenotype variations characterize a large number of them, without there being a principal malformation. The examination of the face and, to a less extent, the extremities is the element that most often determines the diagnosis.

Progress in prenatal diagnosis and, in particular, the development of three-dimensional (3D) ultrasound is facilitating dysmorphography examination of the fetus. The dysmorphology analysis requires a sonologist with experience in rare syndromes as well as an extensive knowledge. In utero, this focus can only be achieved in a multidisciplinary field combining, if possible, the participation of an expert sonologist in the field of normal fetal face and an expert in dysmorphology. A thorough evaluation including family history, fetal biometry, study of stages of psychomotor development of the relatives, outcomes of para-clinical tests, and examination of the parents should be performed. The dysmorphology examination should be an additional diagnostic tool in prenatal study. In particular, the systematic examination of the face can reveal abnormalities that could provide key clues in the diagnosis of fetal diseases and syndromes.

The study of the fetal face needs to be systematic in order to identify malformations (cleft lips, ocular abnormalities, etc.), but the dysmorphology examination needs to be a dedicated test similar to echocardiography or neurosonography that assesses whether an abnormality is isolated or occurs in association with other abnormalities as part of a possible syndrome [1].

5.2 The Dysmorphology Examination

Genetic syndromes that can be diagnosed in the first trimester usually involve large malformations, not merely dysmorphisms. Further, facial morphology evolves with gestational age. In the first trimester, the lower third of the face are more developed compared to the upper third, and as such, the ears have a very low position. The

P. Martínez-Ten (✉)
Delta – Ultrasound Diagnostic Center in Obstetrics and Gynecology, Conde de Peñalver 14, esc der, 1° izq., Madrid 28006, Spain
e-mail: pilarmten@gmail.com

W. Sepulveda
Fetalmed – Maternal-Fetal Diagnostic Center, Santiago, Chile

G. Tonni, MD, PhD
Department of Obstetrics and Gynecology, Prenatal Diagnostic Service, Guastalla Civil Hospital, AUSL Reggio Emilia, Reggio Emilia, Italy
e-mail: Tonni.Gabriele@ausl.re.it

G. Tonni, W. Sepulveda, and A.E. Wong (eds.), *Prenatal Diagnosis of Orofacial Malformations*,
DOI 10.1007/978-3-319-32516-3_5

dysmorphology discussed in this chapter refers to findings in the second and third trimesters.

5.2.1 The Face

The dysmorphology examination of the fetal face needs to be the same as that of the newborn or infant [2, 3]. It needs to be systematic while examining the front of the face and the profile with two-dimensional (2D) ultrasound and 3D ultrasound (Fig. 5.1).

5.2.2 Profile Views

In the profile view we study:

1. The forehead (elusive or convex) and discard prefrontal edema (Fig. 5.2).
2. The nasal root (hypoplastic or very prominent) (Fig. 5.3).
3. The size of the chin (micrognathia and/or retrognathia) (Figs. 5.4 and 5.5). The mandibular disorders have been traditionally diagnosed by subjective evaluation of the chin in the profile study. In an attempt to use objective measures, Rotten et al. [4] described two indices to help diagnosis; the inferior facial angle (IFA) and the ratio of "mandibular width (MD)" and "maxilla height (MX)". The IFA is obtained in a midsagittal plane of the face tracing a line perpendicular to the forehead at the level of the union of the two nasal bones. The second line links the more anterior portion of the lips and the extremity of the chin. The mean value of this angle is 65.5° and values below 49.2° are considered retrognathia.
4. The philtrum (located between the columella that separates the nose and the upper lip) (Fig. 5.2c).
5. The ears. The size needs to be compared with the published nomograms. The evaluation of the position must be carefully performed because an abnormally positioned ear can present in very subtle fashion, and the gestational age needs to be taken into account (Fig. 5.6).

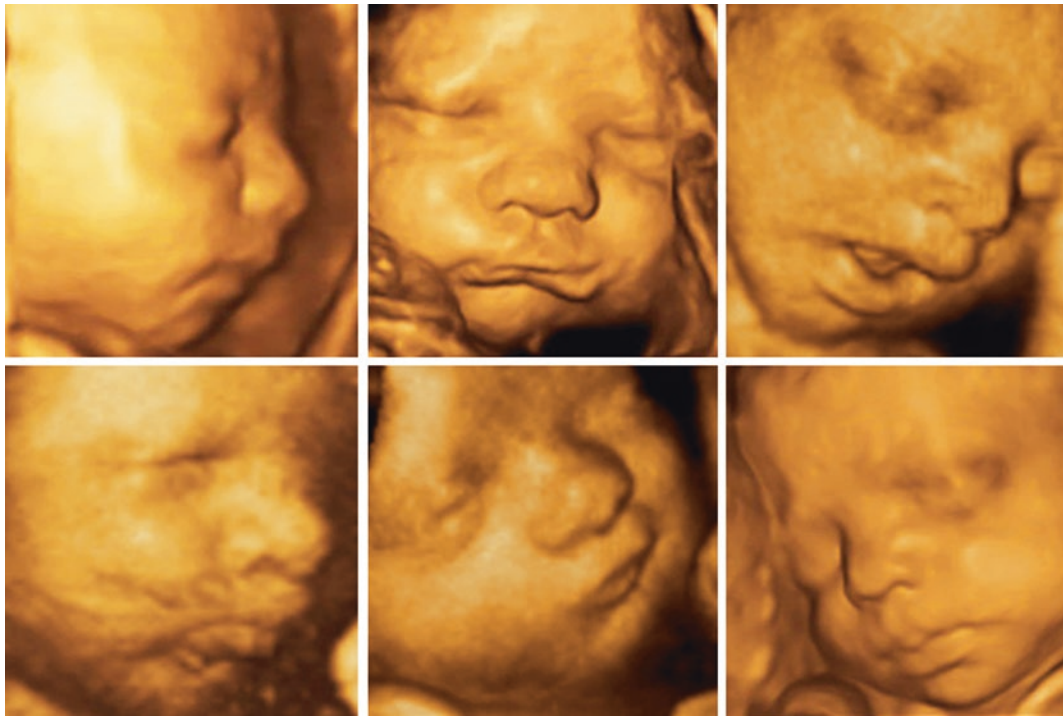

Fig. 5.1 Images obtained with 3D ultrasound in which the surface renderization enables us to obtain coronal, oblique, and sagittal planes of normal fetuses with gestational ages between 27 and 33 weeks

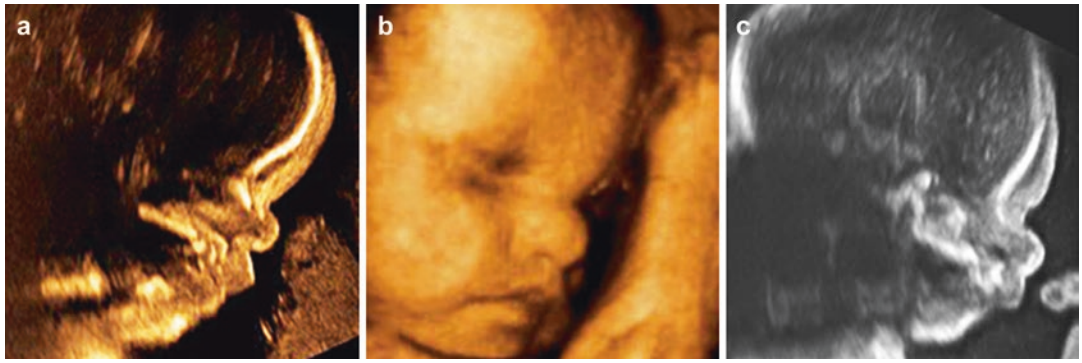

Fig. 5.2 Different pathologies assessed in the fetal profile. (**a**) 2D ultrasound of achondroplasia at 33 weeks; (**b**) 3D ultrasound of a 35 week fetus with severe cerebral ventriculomegaly (35 weeks); (**c**) 2D ultrasound of a fetus with Cornelia de Lange syndrome with Long and prominent philtrum, prefrontal edema, and retromicrognathia

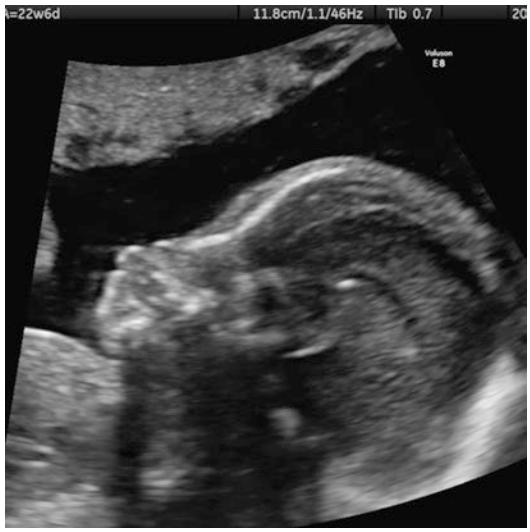

Fig. 5.3 2D ultrasound of a fetus with Binder phenotype. Combination of abnormalities that are characteristic, such as underdevelopment of the middle third of the face; absence of the frontal-nasal angle with flattening of the glabella and verticalization of the nasal pyramid. The nose is short with flattened dorsal and nasal tip and shortened columella; prenasal hypoplastic maxilla with acute angle nasal lip and convex upper lip (Courtesy of Dr. Nerea Maiz Elizaran, Spain)

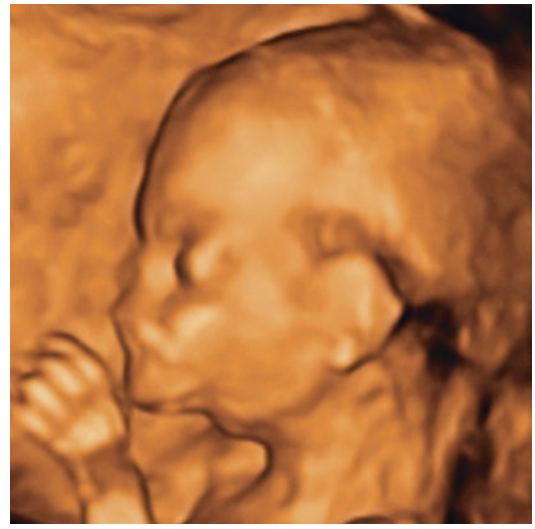

Fig. 5.4 Surface renderization with 3D ultrasound of a fetus of 15 weeks, with retrognathia/micrognathia

5.2.3 Coronal Views

In the coronal plane we assess:

1. Orientation and size of the palpebral fissures
2. Hypertelorism or hypotelorism (Fig. 5.7)
3. Microphthalmia or anophthalmia (Fig. 5.8)
4. Shape of the nose
5. Microstomia or macrostomia
6. Tongue (possible macroglossia) (Fig. 5.9)
7. Lips (discard fissures)

Reference values have been published for the majority of these measurements (width of the eyelids, area of the ears, height of the front, size of the philtrum, etc.) [5].

5.2.4 The Rest of the Examination

The majority of syndromes have extrafacial abnormalities and, in particular, abnormalities of the extremities. The dysmorphology examination, hence, includes detailed analysis of the limbs (Figs. 5.10 and 5.11). The number of fingers and toes should be counted. A postaxial

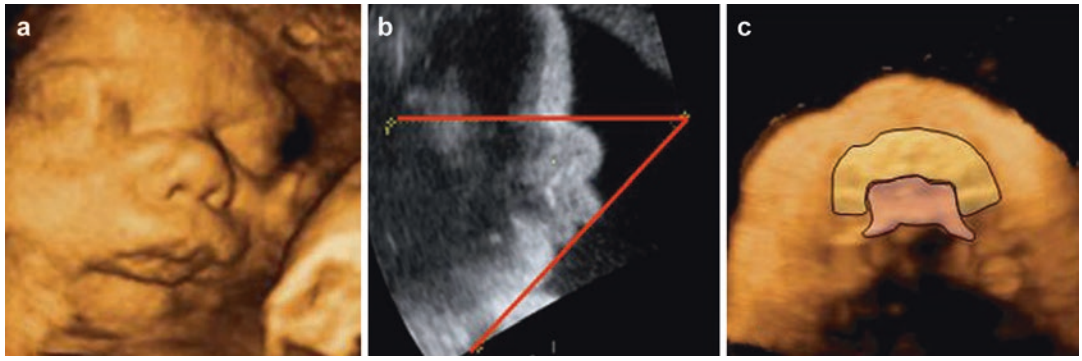

Fig. 5.5 (**a**) 3D ultrasound of the face of a fetus of 34 weeks with retrognathia/micrognathia; (**b**) 2D ultrasound of the fetal profile in which the measured lower face angle is 47.06 (normal defined as >49.2°) [4]; (**c**) 3D ultrasound surface rendering of the axial plane with the "flipped face" technique; the hard palate is very short and small (highlighted in *pink*). The newborn presented with obstruction of the airway due to the abnormal location of the tongue; absence of the soft palate was diagnosed postnatally

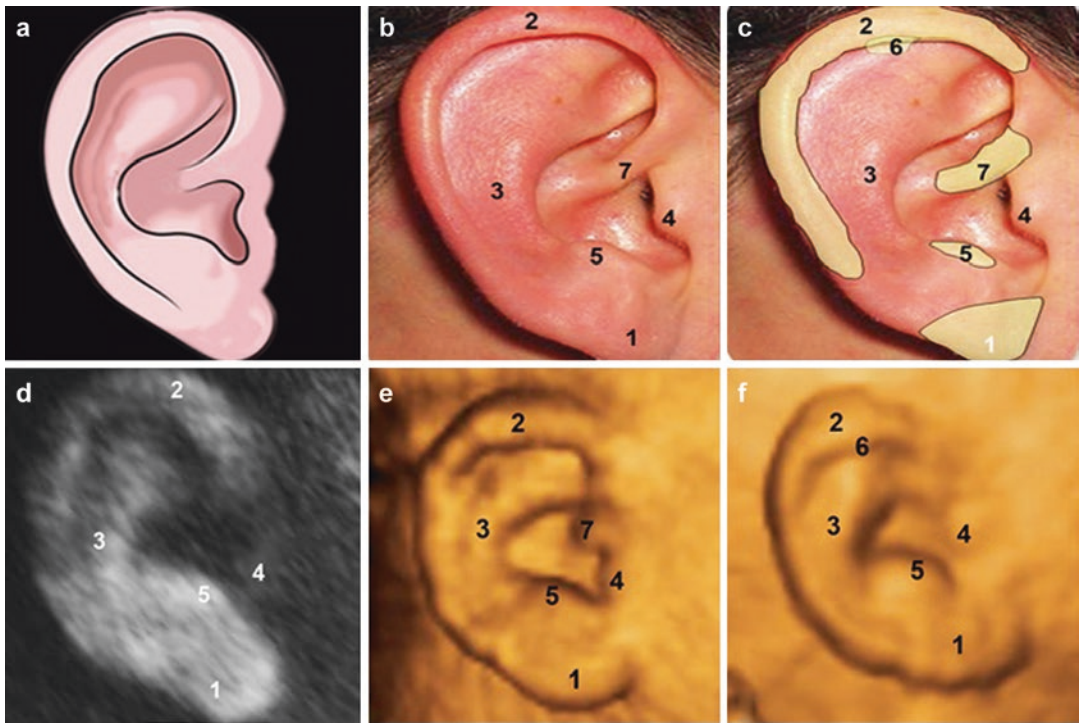

Fig. 5.6 (**a**–**c**) Outline and ear of a newborn showing different components; (**d**) fetal ear view with 3D ultrasound; (**e**, **f**) fetal ear with 3D ultrasound surface renderization; *1* lobe, *2* helix, *3* antihelix, *4* trago, *5* antitrago, *6* auricular tubercle, *7* cross of the helix

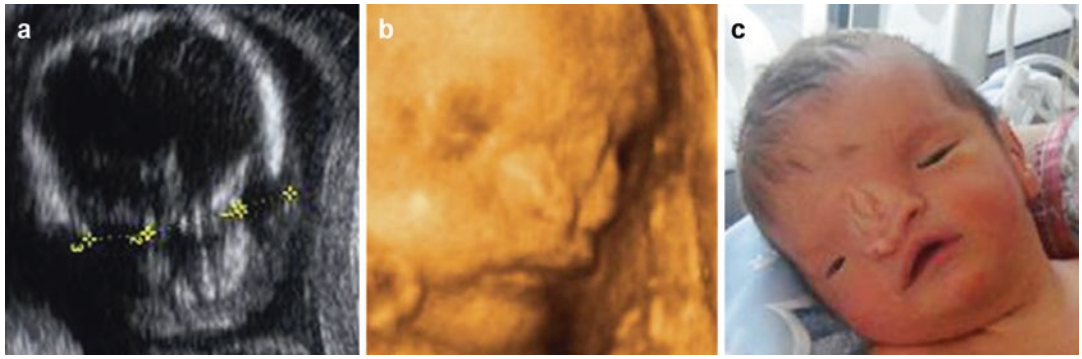

Fig. 5.7 Frontal-nasal dysplasia with nose involvement and hypertelorism. (**a**) Coronal plane with 2D ultrasound showing the intraorbital distance greater than the transverse diameter distance of each orbit. (**b**) Image with 3D ultrasound with renderization showing the dysplasia at the level of the nose. (**c**) Newborn

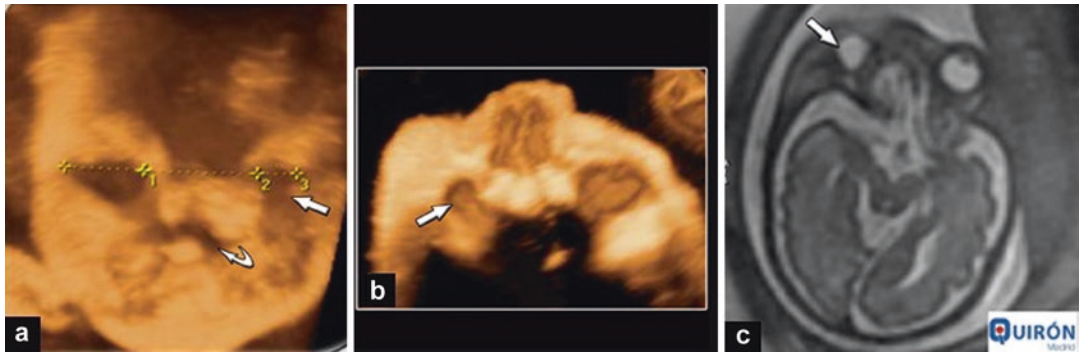

Fig. 5.8 Right lip-palate cleft with right microphthalmia. (**a**) Evaluation using the "reverse face" technique of the coronal plane; microphthalmia (*arrow*) and the affected secondary palate (*curved arrow*); (**b**) 3D ultrasound, high axial plane in which the *arrow* highlights the small right orbit, and without lens. (**c**) Fetal MRI; coronal plane showing affected orbit

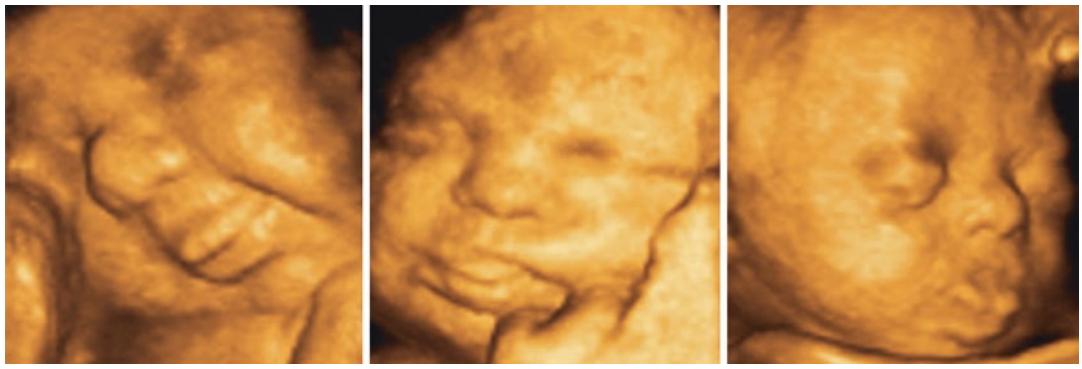

Fig. 5.9 Macroglossia in Down syndrome. It is "relative" macroglossia in that the tongue protrudes beyond the surrounding alveolar ridge due to the hypoplasia of the lower third of the face that is present in this syndrome

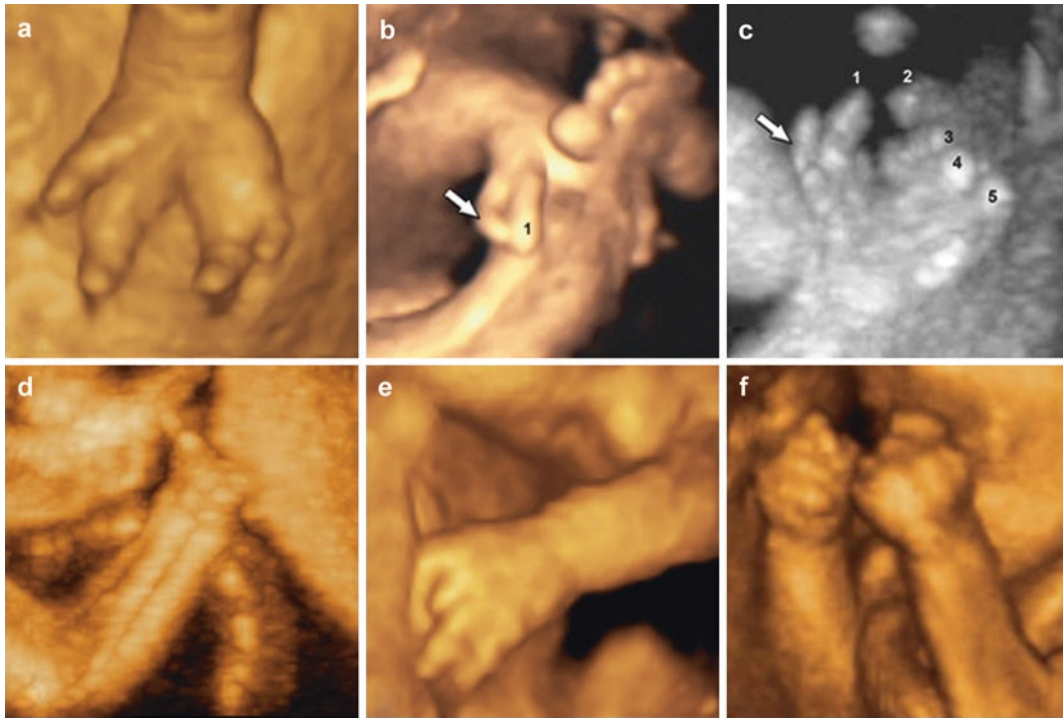

Fig. 5.10 (**a**) Surface rendering with 3D ultrasound of fetal hand with typical ectrodactyly (29 weeks). (**b**) Preaxial polydactyly. The extra finger (arrow) is encountered in the radial axis of the hand. (**c**) The same case as in (b) evaluated with 3D ultrasound in skeletal mode. Arrow showing the extra finger. (**d**) A typical ectrodactyly in a fetus of 33 weeks, 3D ultrasound in skeletal mode. (**e**) 3D ultrasound surface renderization: absence of first and second phalanges of the third finger. (**f**) "Claw hand," superimposition of the fifth finger on the fourth and of the second on the third. Assessment with 3D ultrasound, surface renderization of a case of trisomy 18

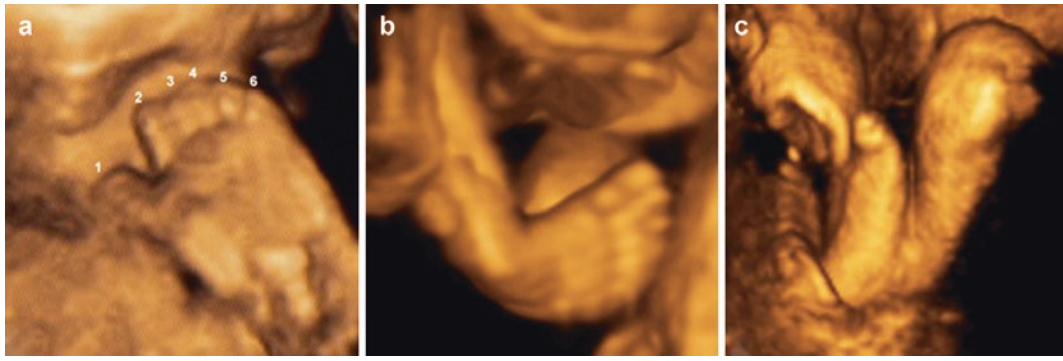

Fig. 5.11 3D ultrasound surface rendering of abnormalities of the feet. (**a**) Postaxial polydactyly. (**b**) Club foot. (**c**) Metatarsus varus foot

polydactyly of only one hand can have the same semiological value as polydactyly of the four limbs. In addition, we should look at the orientation of the fingers and toes and the number of phalanges. The diagnosis of syndactyly, although difficult, may be possible with 3D ultrasound. However, parents should also be counseled that abnormalities of the fingers/toes can occur as isolated malformations without severe clinical significance.

5.3 Facial Malformation as a Sign of a Complex Syndrome

As we have commented, the analysis of the face forms part of the routine examination. It is necessary to emphasize the risk associated with performing a very detailed analysis of the face in the absence of a high level of suspicion of abnormality due to the precence of other abnormalities and/or family history. Many isolated dymorphology features may be encountered in normal individuals and should not be of concern to the parents. However, significant facial abnormalities (Figs. 5.12, 5.13, 5.14, and 5.15) can be the entry point for the diagnosis of fetal diseases and syndromes and can facilitate an overall fetal evaluation using the same criteria that we employ when we diagnose, for example, visceral malformations.

5.3.1 The Cleft Lip-Palate

As we have commented in Chapter 3, the cleft lip and palate (CLP) can be associated with a number of chromosomal syndromes or genetic errors [8, 9]. In the LDDB database [23] (http://www.lmdatabases.com), there are 189 syndromes with non-medial CLP, of which 77 are associated with mental retardation and 41 with medial fissures of which the majority are associated with mental retardation or death. Figures 5.16 and 5.17 show CLP associated with syndromes [10].

5.3.2 Abnormalities of the Ears

These are difficult to evaluate in detail with 2D ultrasound but very accessible with 3D ultrasound.

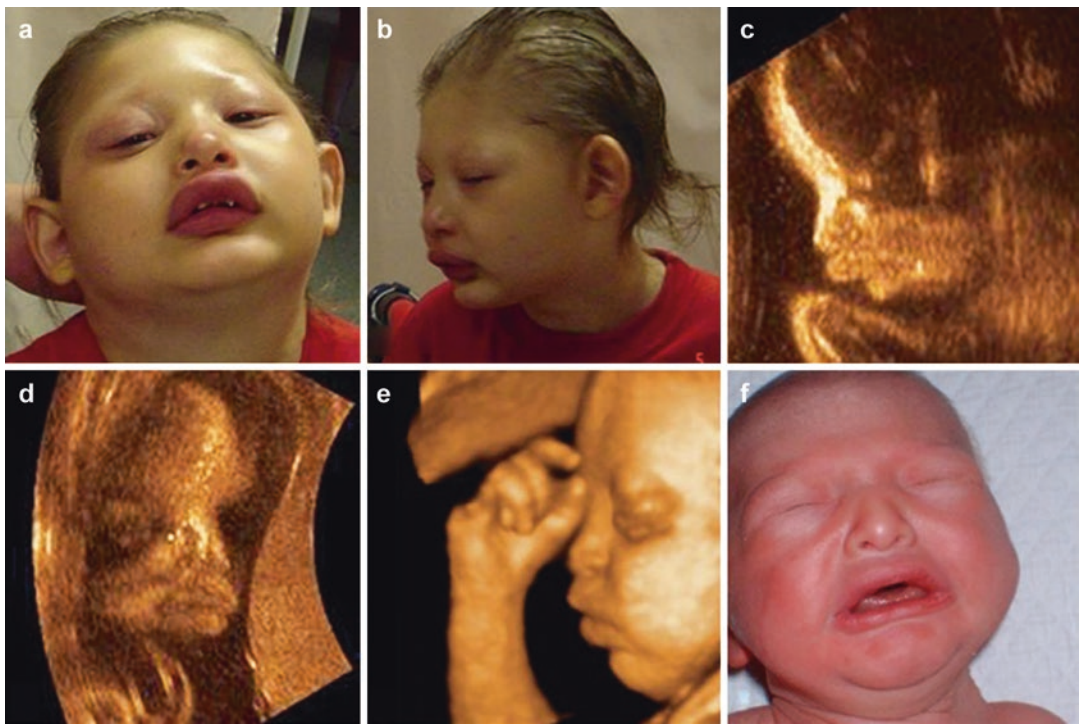

Fig. 5.12 Hypohidrotic ectodermal dysplaisa, a rare disease (1/10,000 to 100,000 newborns) caused by an abnormal development of the tissues derived from the ectoderm. These children have problems with the sweat glands, are incapable of sweating and, as such, have febrile confulsions. Further, they have thinning hair and hypoplasia of the dental arch with prominent lips and teeth that are pointed and separated. (**a**, **b**) Photographs of child affected with hypohidrotic ectodermal dysplasia. (**c**–**e**) 2D and 3D ultrasound performed prenatally showed the face to have very prominent lips and a small nose. (**f**) Newborn with the charactistic facial features of hypohidrotic ectodermal dysplasia [28]

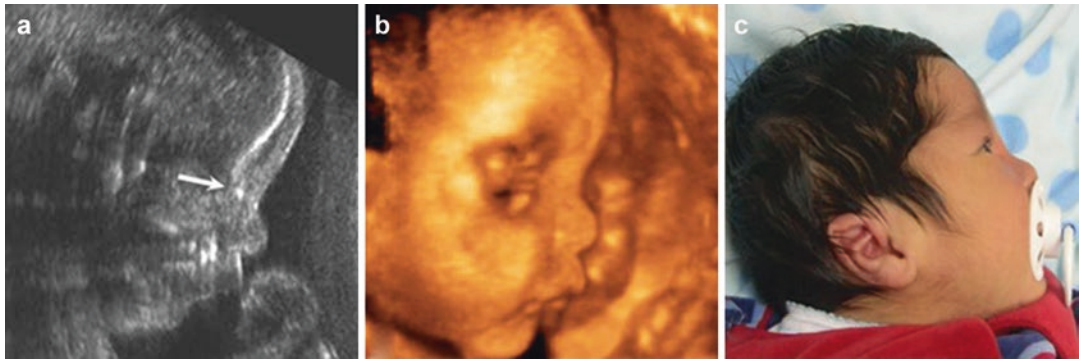

Fig. 5.13 Partial trisomy of chromosome 20. Fetus assessed at 28 weeks showed shortened femur, slight ventriculomegaly with cephalic perimeter increased relative to gestational age, and hypoplasia of the nasal bones. The rest of the morphology assessment was normal. The karyotype showed a duplication of part of the material of the long arm of chromosome 20 (46 XY, dup (20) (q11.2q13.2). The child of 5 years of age has dysplasia of the corpus callosum, microcephaly, and moderate-severe mental retardation. (**a**) Hypoplasia of the nasal bones (*arrow*). (**b**) Facial profile obtained with 3D ultrasound surface renderization, showing the small nose but otherwise normal-appearing profile that would lead to a suspicion of trisomy 21. (**c**) Newborn [6]

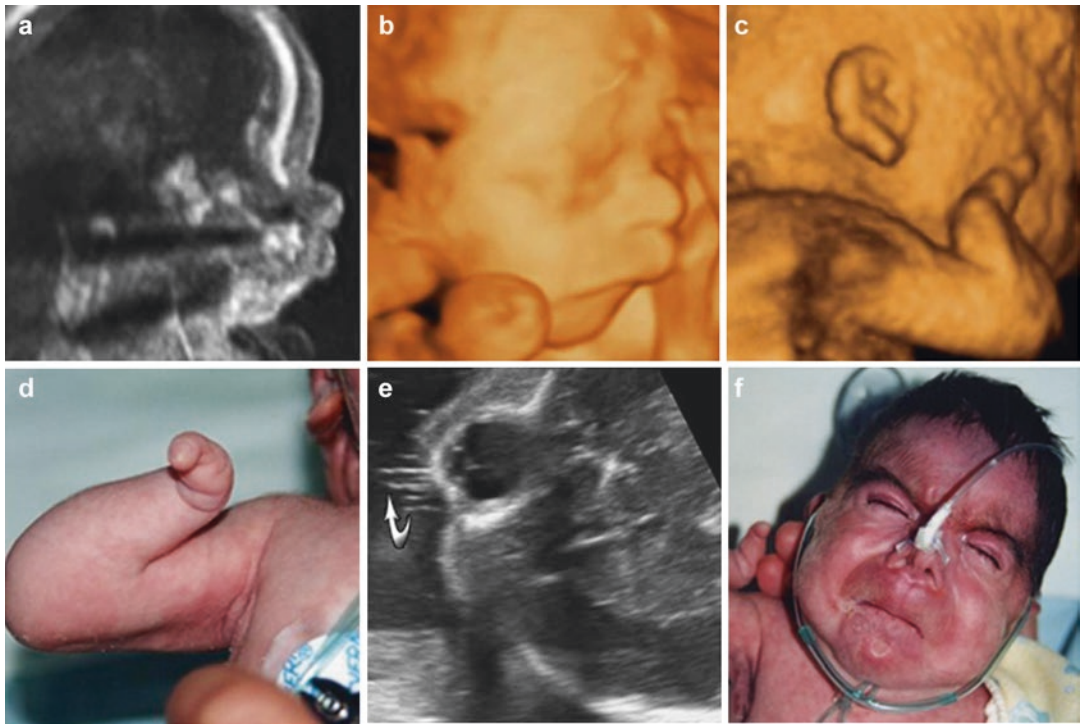

Fig. 5.14 Cornelia de Lange syndrome. Rare syndrome (1/80,000 newborns) and sporadic, described by Cornelia de Lange in 1933. The syndrome has various characteristics, among which is a severe psychomotor delay. The fetus presents, at 26 weeks, micromelia in one arm with monodactyly and facial dysmorphism. There are no nasal bones and prefrontal edema is present; the nasal philtrum is very prominent due to excessive development of the upper maxilla. Micrognathia and retrognathia are present. The eyelashes (*arrow*) are long which indicate hirsutism; (**a**) and (**b**): in the assessment with 2D and 3D ultrasound, the philtrum is very large and prominent, with prefrontal edema and retromicrognathia; (**c**) and (**d**) show micromyelia of the arm with monodactyly in the assessment with 3D ultrasound, and following birth. (**e**) and (**f**) Eyelashes are extraordinarily long, an indication of hirsutism, as can be seen in the newborn [7]

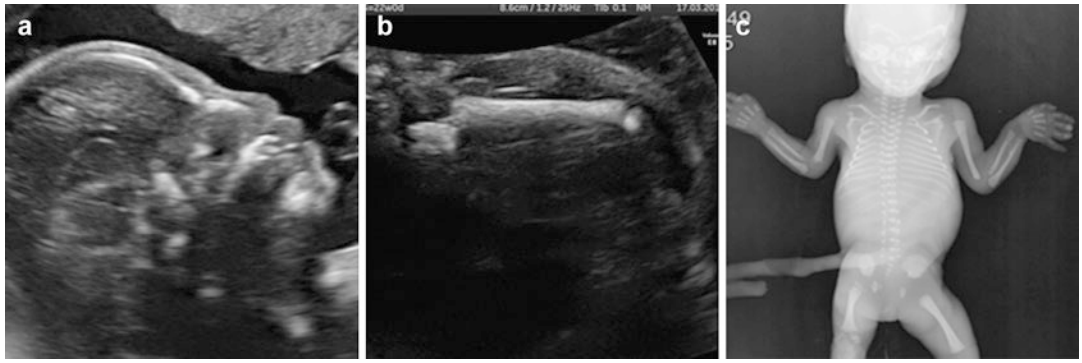

Fig. 5.15 Binder syndrome. (**a**) 2D ultrasound profile of the Binder phenotype with flat profile without nasal eminence. (**b**) 2D ultrasound showing a thick and striking femur due to calcification of the hypophysis, consistent with chondrodysplasia punctata associated with Binder syndrome. (**c**) Fetal X-ray showing asymmetry in the long bones and unilateral calcification of the epiphyses of the femur and humerus, as well as the vertebra-rib junction (Courtesy of Dr. Nerea Maiz Elizaran, Spain)

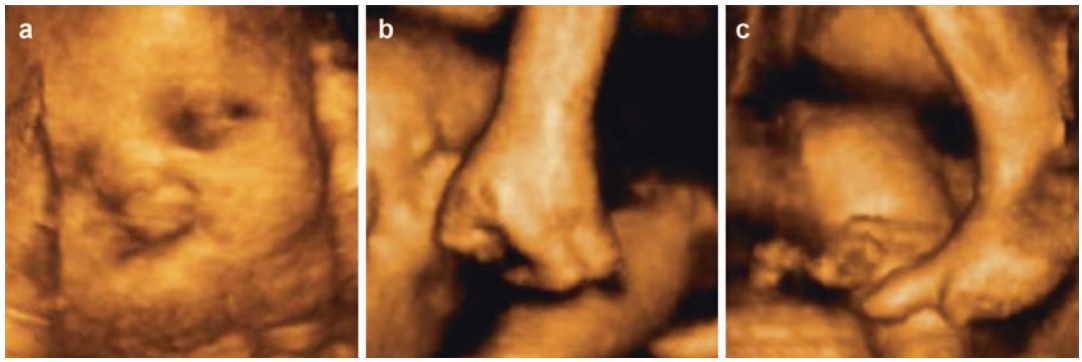

Fig. 5.16 Ectrodactyly-ectodermal dysplasia-left syndrome (EEC syndrome). (**a**) Surface renderization showing the bilateral cleft of the lip. (**b–c**) Surface renderization of the hand and foot with ectrodactyly

We need to distinguish among ears that are small, large, abnormally shaped, asymmetric, or of a low-set position, as these characteristics would direct the diagnostician to a particular syndrome. For example, a small ear would prompt assessment of the other ear and the face to search for signs of Franceschetti syndrome or Treacher Collins syndrome. Or, we may be directed toward performing a detailed study of the heart and spine to assess for possible Goldenhar syndrome or facial-auricle-vertebral malformation, or a careful analysis of the limbs looking for a defect of the radial ray abnormality of Nager syndrome. Asymmetric and abnormally shaped pinnas of the ears would sugest CHARGE syndrome.

5.3.3 Micrognathia

In the LDDB database [23] (http://www.lmdatabases.com), there are 824 syndromes that involve micrognathia/retrognathia. These include the Pierre Robin and Treacher Collins syndromes and chromosome abnormalities such as trisomy 13 and 18, triploidy, translocations, and deletions. This abnormality can produce obstruction of the airway due to abnormal location of the tongue (Fig. 5.5). As such, prenatal diagnosis is important so delivery can be planned with the appropriate resources available to a neonate who is suspected to have respiratory difficulties after birth [11].

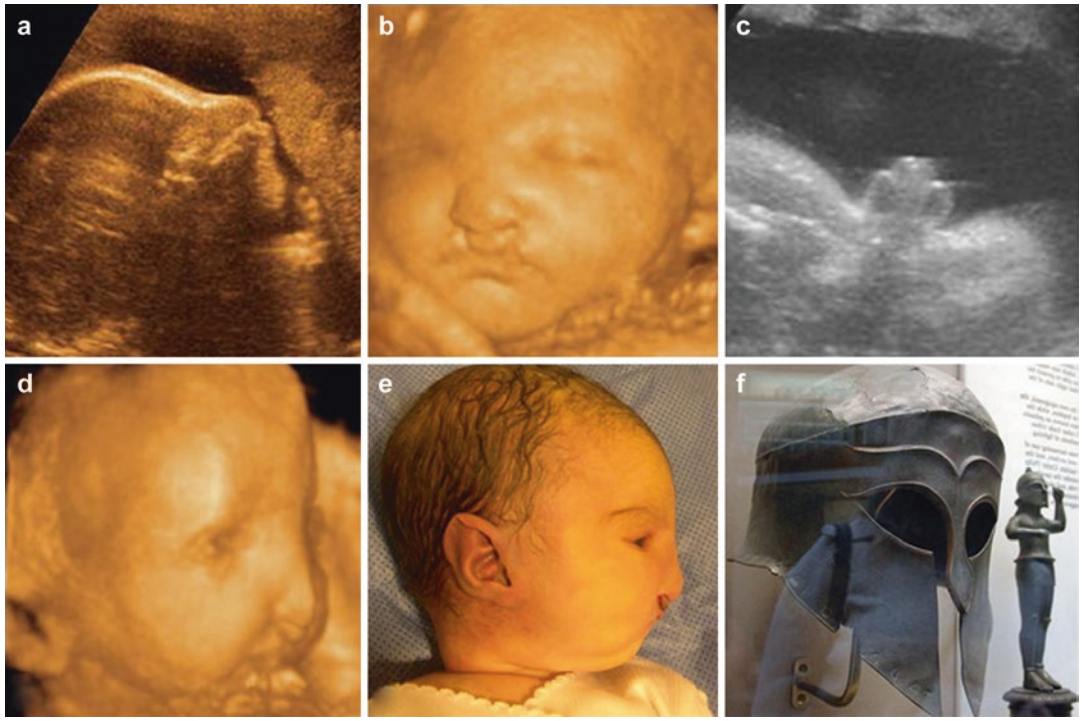

Fig. 5.17 Wolf-Hirschhorn syndrome: ultrasound assessment at 29 weeks demonstrated bilateral cleft lip and palate, hypertelorism, very prominent glabella with absence of nasal bridge, prenasal edema, agenesis of the corpus callosum, and hypospadias. Karyotype analysis showed a chromosomal structural alteration in the male fetus, identified as a deletion in the short arm of chromosome 4. (**a**) 2D ultrasound It is as if the front continues with the showing an abnormal profile in which the forehead is continuous with the nose. (**b**) Coronal plane obtained with 3D ultrasound showing the bilateral lip cleft, slight hypertelorism, and absence of nasal bridge with a very prominent glabella. (**c**) Coronal plane with 2D ultrasound showing genitals having the typical tulip form characteristic of hypospadias. (**d**) and (**e**) Facial profile in the third trimester and following birth. The profile appears to have the shape of the Greek war helmet (**f**)

5.3.4 Profile Abnormalities

An abnormal profile is associated with >100 syndromes. Hypoplasia of the middle third of the face can present in some skeletal dysplasias such as achondroplasia or thanatophoric dysplasia.

5.4 Down Syndrome

Down syndrome (DS) is the chromosomal alteration most frequently seen in humans. It is the principal congenital cause of mental retardation. The neonatal prevalance is around 7.11/10,000 newborns; there has been a statistically significant linear decrease in the prevalance over the years, possibly due to the impact voluntary terminations of pregnancy since it is a defect amenable to prenatal diagnosis.

Trisomy of chromosome 21 has profound effects on fetal development that can give rise to a constellation of peculiarities in the phenotype that has become known as DS. Children with DS present with very characteristic and recognizable features at birth [12–17]. The abnormalities in the development of the cranial-facial skeleton serve to explain, at least in part, the specific appearance of these subjects.

The characteristics of the phenotype are:

Head and Neck There is mild microcephaly with brachycephaly and occipital flattening. The neck is short. The ears are small with a highly

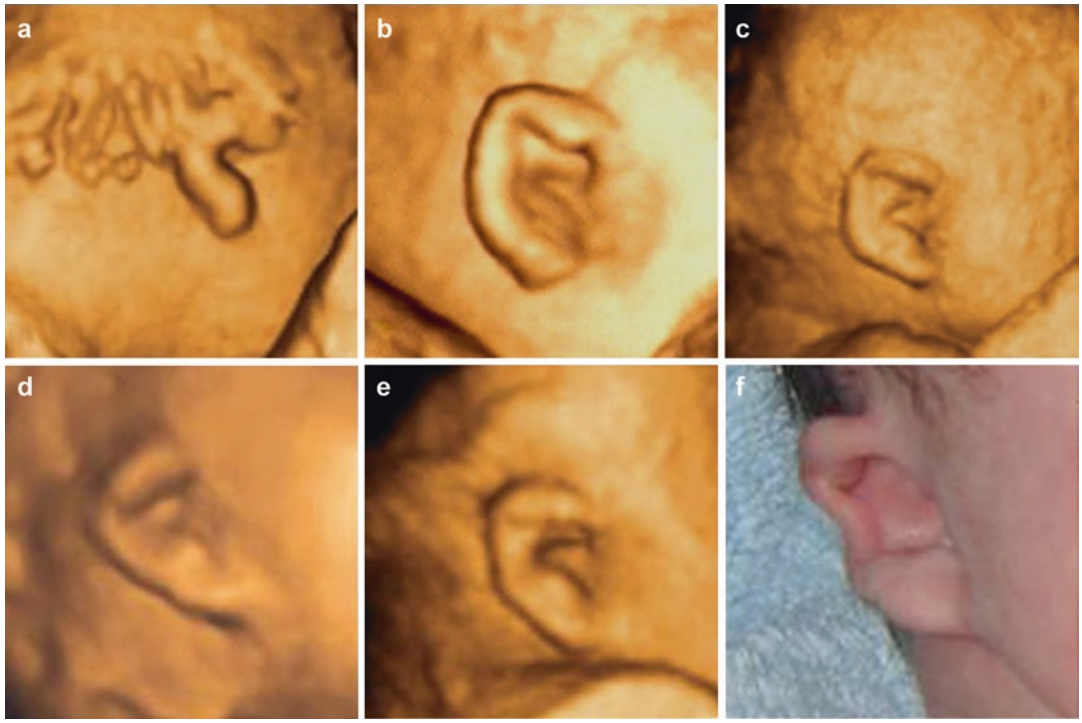

Fig. 5.18 Five fetuses with Down syndrome, with ears characteristic of the syndrome that are small with a highly folded helix and absence of pendulous earlobes. (**a**) and (**b**) demonstrate a highly folded helix. Images (**c**–**f**) demonstrate the characteristic small ear which is narrow with the helix folded in the upper portion. Image (**f**) is of a newborn.

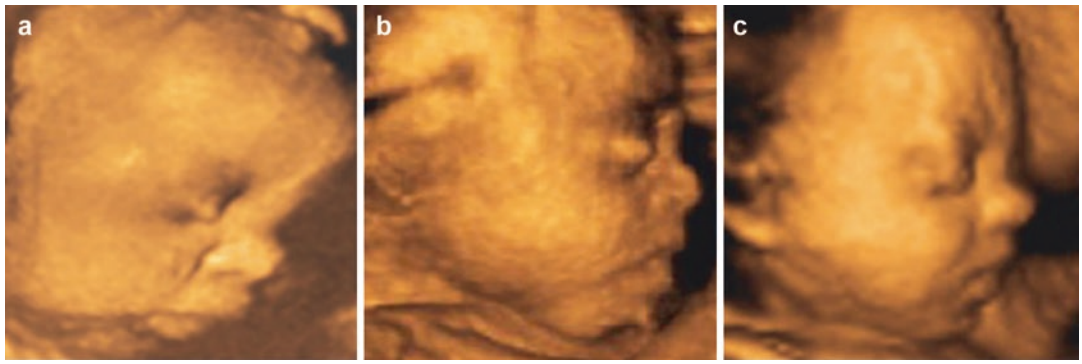

Fig. 5.19 Three fetuses with DS, in the third trimester. All three have an abnormal profile, with a depressed and saddle-shaped nasal bridge and hypoplasia of the middle third of the face. In the central image, the fetus has clear retrognathia

folded helix and, usually, with absence of earlobe, i.e., non-pendulous. Hearing may be very reduced (Fig. 5.18).

Face Hypoplasia is present of the middle third of the face with a characteristic profile with the front unusually flat with depressed nasal bridge, like a saddle. The nose is small with the nasal root flattened (Fig. 5.19). The mouth is small with a characteristic protruding tongue. When in repose, the tongue is held between the teeth so as to be away from the surrounding alveolus (Fig. 5.20). This apparent macroglossia is due to the hypoplasia of the upper maxilla. When active,

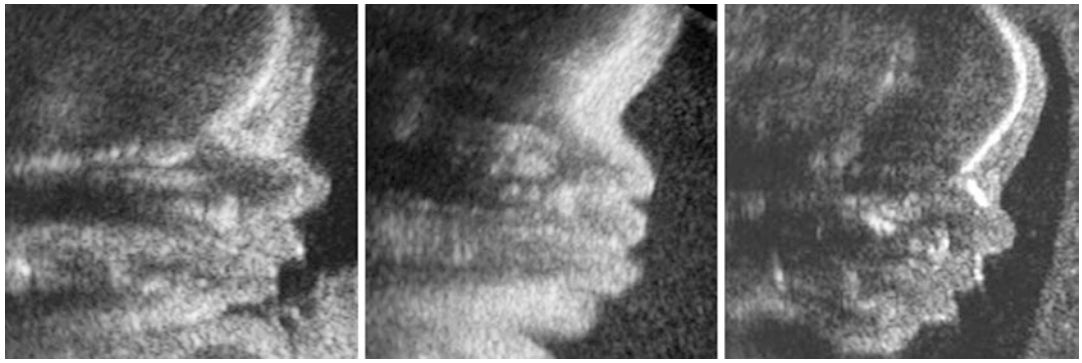

Fig. 5.20 Three fetuses with DS with macroglossia. The tongue appears to be constantly away from the surrounding alveolar ridge. Although there is the impression of macroglossia, in reality, the tongue is not large but the buccal cavity is small due to a hypoplastic upper maxilla

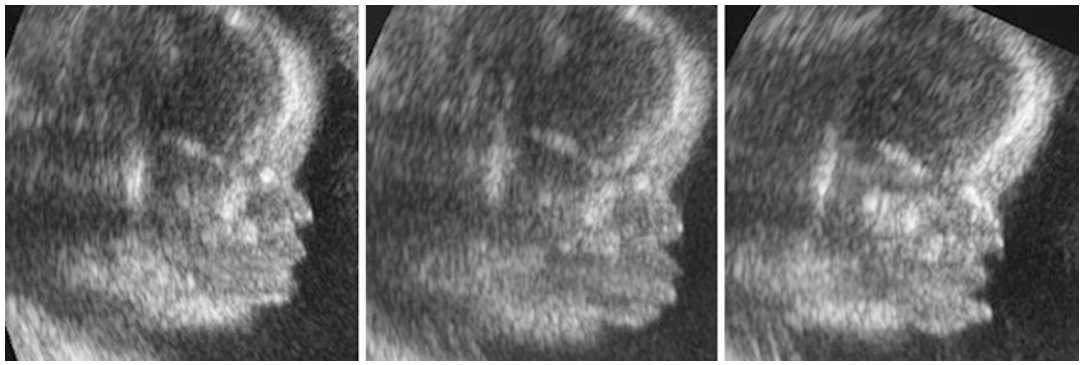

Fig. 5.21 Tongue thrust: sequence of the fetal profile with 2D ultrasound showing movement of the tongue

the tongue is repeatedly withdrawn in a movement known as "tongue thrust" (Figs. 5.9 and 5.21). The mouth is maintained ajar at rest (Fig. 5.22), and when closed, it appears that the tongue is contained within the mouth (Fig. 5.23).

The Eyes The eyes are almond shaped, and if the iris is clear, a mottled pigmentation can be seen (*Brushfield stains*). The palpebral fissures continue in an oblique direction superiorly and laterally and have a skinfold that covers the interanl angle (epicanthal fold).

Hands and Feet Affected infants have small, square-shaped hands with short metacarpals and phalangies (brachydactyly) (Fig. 5.24) and clinodactyly due to hypoplasia of the middle phalange

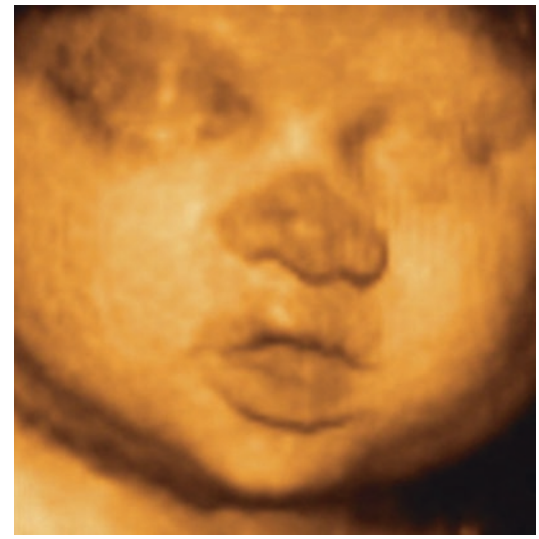

Fig. 5.22 Fetus with DS. Hypoplasia of the upper maxilla and, as such, an "apparent" macroglossia. It is common to see these fetuses in the third trimster with the mouth ajar

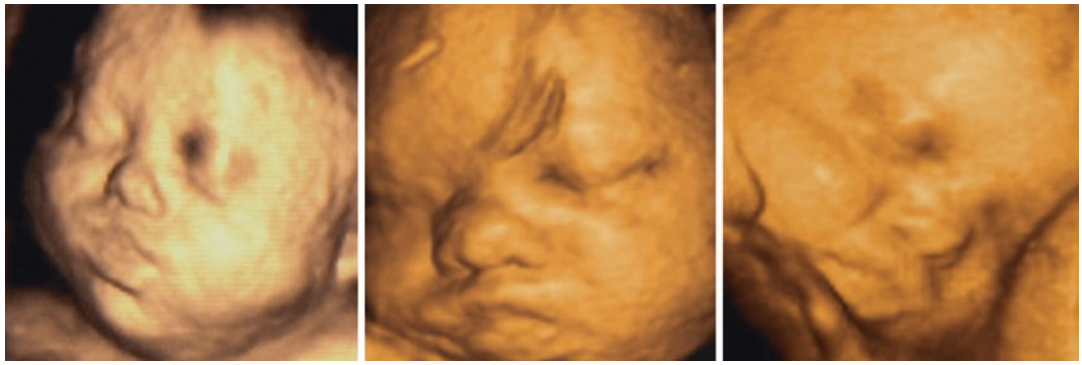

Fig. 5.23 Three DS fetsus with the mouth closed but with the impression of a large tongue due to a small buccal cavity

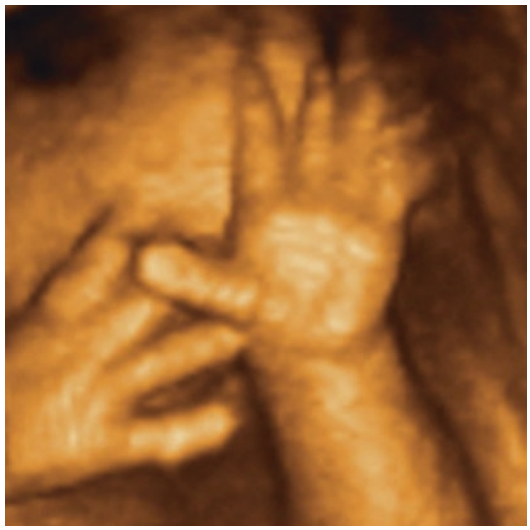

Fig. 5.24 DS hand. Brachydactyly: short fingers

of the fifth finger (Fig. 5.25). A single palmar groove can be observed. In the foot, there is a gap between the first and second toe (sandal sign) (Fig. 5.26).

Genitals The size of the penis is somewhat small and the testicular volume is less than that of the children of the same age. Cryptorchidism is relatively frequent in these individuals.

Skin and Appendages The skin is redundant in the cervical regions, primarily in the fetal and neonatal periods (Fig. 5.27). They present large ligamentous hypotony and articular hypermobility.

Although many of these are non-specific features, they are considered as distinctive of DS when they occur in combination. They have a wide degree of variability and, according to some authors, are more or less pronounced.

About 40 % of children with DS have an associated anatomic malformation, half of which are cardiovascular or gastrointestinal. The malformations can occur in the non-DS child, but with lower frequency.

In the past decade, screening in the first trimester of gestation using US and maternal biochemistry has become a reliable method for the screening of DS. Also, the second-trimester sonogram is a genetic screen that assesses risk of chromosomal abnormalities [18]. The genetic sonograph includes a detailed study to evaluate the presence of both large malformations and ultrasound soft markers for aneuploidy such as nuchal fold, shortening of long bones, echogenic intracardiac focus (EIF), echogenic bowel (EB), pyelectasis (PE), choroid plexus cysts (CPCs), and aberrant right subclavian artery. Although these lesser ultrasound markers can be present in normal fetuses, they are encountered with higher frequency in aneuploid fetuses, and their presence/absence has become an important element in adjusting the risk of syndromes or malformations in the second half of pregnancy.

Echographic markers of DS, which we use in the first and second trimesters, may not be valid in the third trimester. Many are transitory and can disappear according to how the gestation week

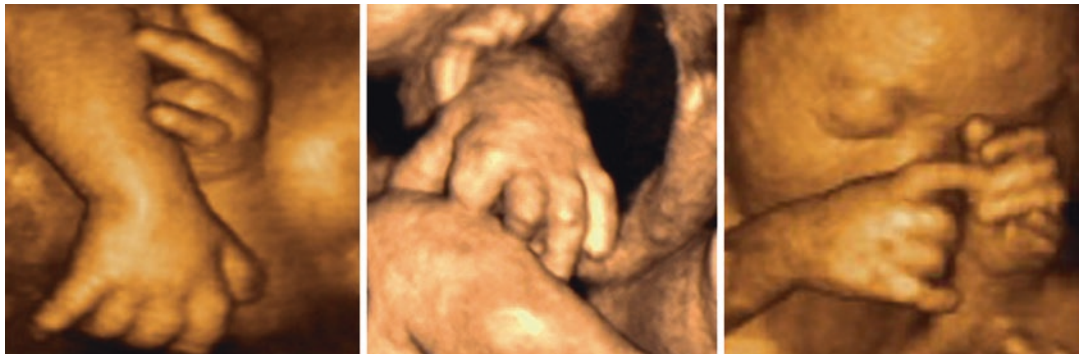

Fig. 5.25 Clinodactyly in DS: persistent radial deviation of fifth finger of the hand as a result of agenesis or, more frequently, hypoplasia of the second phalange of the fifth finger. This sign can be very subtle and difficult to identify in the third trimester

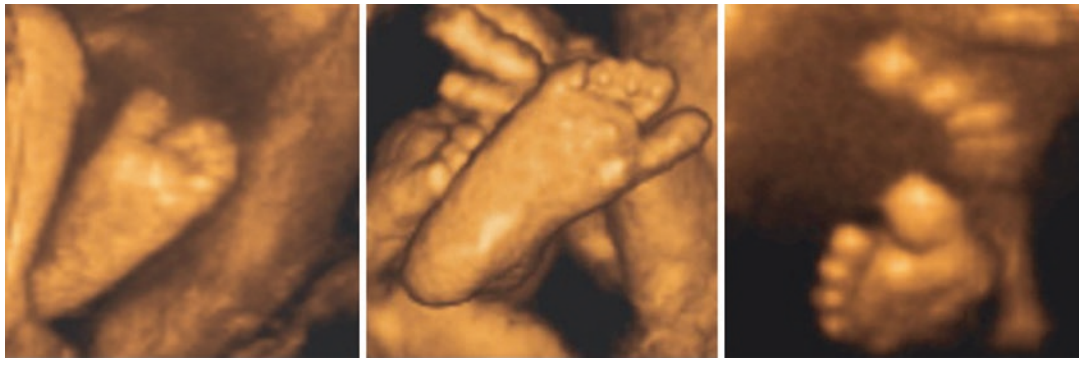

Fig. 5.26 Sandal foot in DS: characterized by a gap between the first and second toes

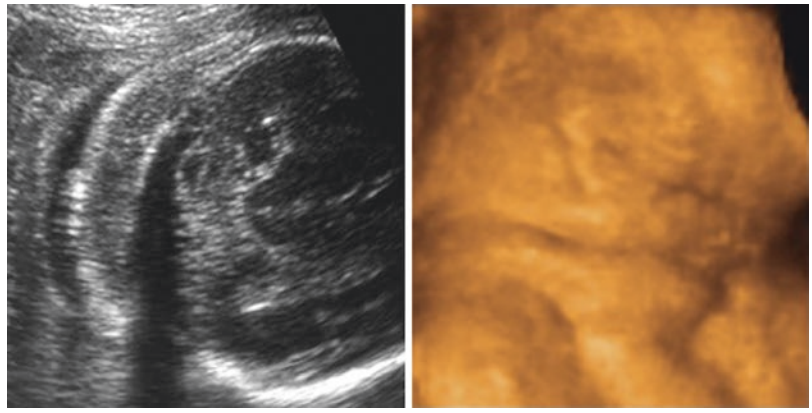

Fig. 5.27 Nuchal edema. Nuchal thickening >5 mm in the second and third trimesters in DS assessed by 2D and 3D ultrasound

progress, as occurs with the cardiac echogenic focus or the choroid plexus cysts. Others can be delayed in their formation, as occurs in the shortening of the long bones.

However, in the third trimester, the fetus with T21 has the same phenotype characteristics (Fig. 5.28) and the same neurological status as the newborn and young children with

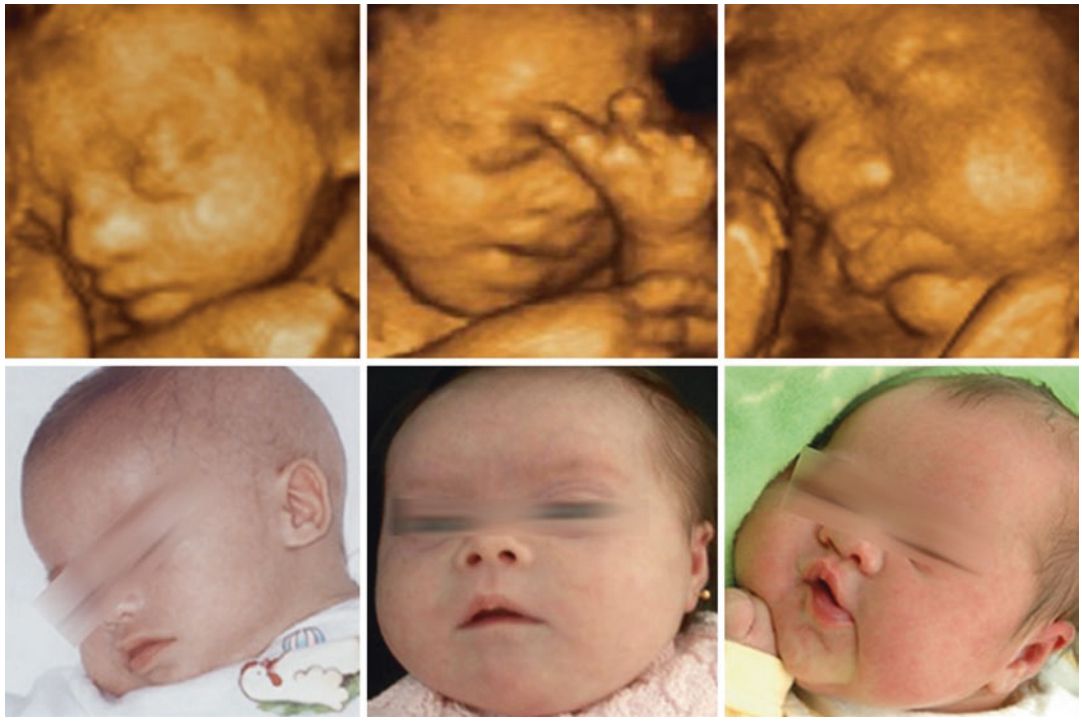

Fig. 5.28 Surface renderization with 3D ultrasound of the face of three fetuses with DS at 26, 27, and 36 weeks. *Lower panels*: images of the newborns

this chromosome abnormality. Current ultrasound equipment enables us to get more detailed information with high precision not only in the assessment of small changes such as the ears, but also some characteristic facial gestures such as the movements of the mouth and the tongue.

There are very few publications that present data on the usefulness of echography to identify the fetus with T21 in the third trimester [19–22]. Rotmensch et al. [20] studied 14 fetuses with 24 structural abnormalities detected in 24 and 28 weeks, as part of a more extensive study looking at the abnormalities in DS fetuses between 9 and 28 weeks. Nyberg et al. [21] described the anomalies observed in 12 of 15 fetuses, also part of a broader study for the detection of DS. The most common abnormalities encountered in DS fetuses in these studies were hydrops, duodenal atresica, and cardiac defects. However, these studies did not investigate all soft markers or abnormal length in the long bones. Only Nyberg et al. [21] reported the number of fetuses that, in the third trimester, were echographically normal (3 of 15).

Picklesimier et al. [22] suggested that the markers of chromosome abnormalities change over the time of the pregnancy. The soft markers (CPC, EB, short femur, short humerous, EIF, nuchal edema, and PE) are more common in the first and second trimesters, and the major markers (structural abnormalities) are diagnosed more frequently in the third trimester. Ranzini et al. [19] studied 17 fetuses with T21 in whom echography had been performed between 24 and 41 weeks. They retrospectively studied cardiac abnormalities, lesser phenotypic markers, relationship of the femur with the biparietal diameter (PBD), the abdominal circumference (AC), and one or more long bones below the 5th percentile. In 15 of the 17 fetuses, there had been some abnormality and alterations of the femur/PBD ratio or femur/AC ratio in 13. The authors concluded that an abnormal biometry in the third trimester should highlight suspicion of T21.

5.5 Binder Syndrome

Binder syndrome is a rare congenital anomaly with heterogeneous etiology including genetic factors, alloimmune maternal diseases, deficiency of vitamin K, and exposure of warfarin or alcohol, among others.

Fetuses may exhibit the typical phenotypic characteristics of Binder syndrome that include nasal hypoplaisa with reduced nasofrontal angle. Binder (1962) [24] described three cases characterized by a short nose with flat bridge, a short columella, an acute nasolabial angle, perialar flatness, a convex upper lip, and a tendency toward angle class III malocclusion.

5.5.1 Associated Malformations

5.5.1.1 Skin and Skeleton

Binder syndrome is associated with chondrodysplasia punctata in most cases and vertebral anomalies of the cervical spine in 50 % of cases. It has been questioned if Binder syndrome may represent a phenotypic variation of chondrodysplasia punctata (Nino et al. 2008) [25].

Chondrodysplasia punctata-2 (CDPX2) is an X-linked dominant disease caused by a mutation in the gene encoding delta(8)-delta(7) sterol isomerase emopamil-binding protein on chromosome Xp11. The phenotype is heterogeneous and may be characterized by pigmentary lesions, striated hyperkeratosis, coarse lusterless hair and alopecia, cataracts, and skeletal abnormalities including short stature, rhizomelic shortening of the limbs, epiphyseal stippling, and craniofacial defects (Derry et al. 1999) [26].

Malformations of the cervical spine can occur in 50 % of patients, involving an abnormal posterior or anterior wall of the atlas and axis, fused vertebrae and persistence of chorda dorsalis. In addition, separate odontoid process, spina bifida occulta, and mild scoliosis and/or kyphosis also have been described (Olow-Nordenram et al. 1984) [27].

Conclusion

Although prenatal dysmorphology can help us in the diagnosis of syndromes that have a high impact on parents, healthcare professionals, and in overall society, we must be very cautious. Experts in neonatal dysmorphology often dely diagnosing a rare disease for years despite being able to perform a direct physical evaluation and a wide variety of diagnostic tests (Fig. 5.29). Figure 5.30

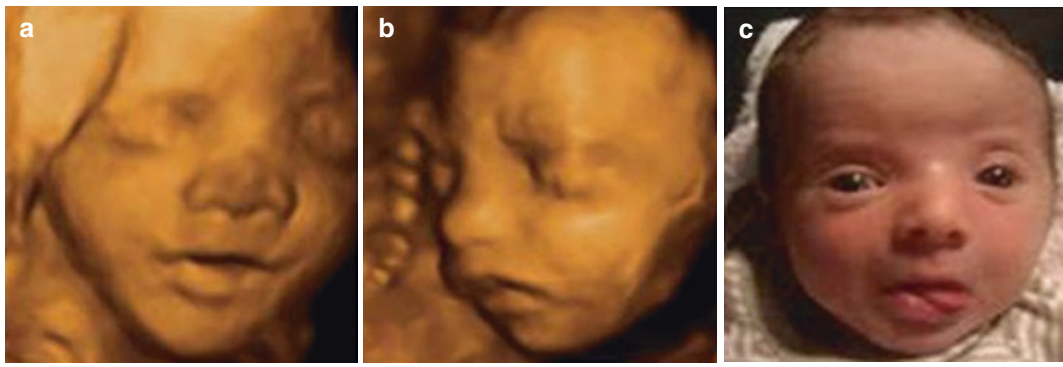

Fig. 5.29 Rubinstein-Taybi syndrome. The etiology of the syndrome is an error in chromosome 16 in which a gene at this locus does not bind well with the cAMP response element-binding (CREB) protein. It is characterized by mental retardation, thus and big toes that are widened and arched, short stature, and characteristic facial features (hypertelorism, wide nasal brige, abnormally large nasa orifices, micrognathia, palpebral ptosis, and epicanthus). Ultrasound performed at 27 weeks of an affected fetus did not detect any facial abnormalities (**a**, **b**). The female infant was diagnosed with this syndrome at birth (**c**, **d**). Postnatal review of the stored prenatal ultrasound images showed slightly enlarged thumbs (**e**) and big toe (**f**)

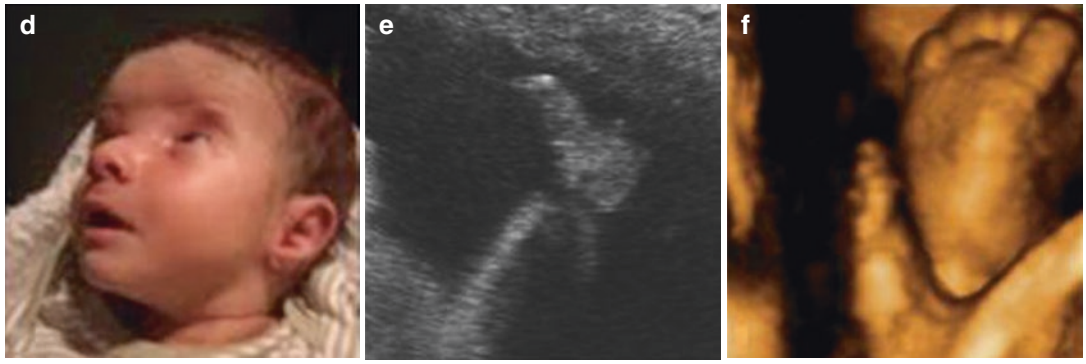

Fig. 5.29 (Continued)

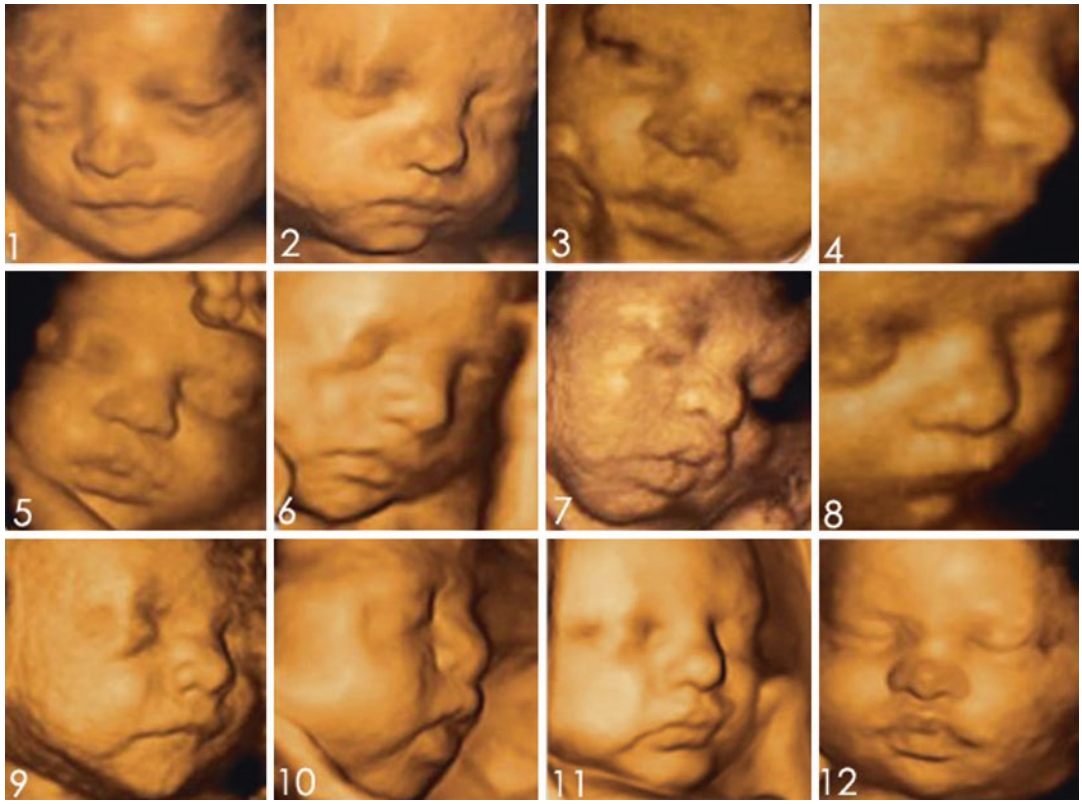

Fig. 5.30 Surface rendering with 3D ultrasound of 16 fetuses between 25 and 36 weeks, four of which with DS (2, 7, 10, 12)

shows the faces of 12 fetuses in the third trimester of gestation, 4 of whom have Down syndrome (2, 7, 10, and 12). Although this syndrome is familiar to most, it has subtle features that may be difficult to detect prenatally using ultrasound.

Finally, we must not forget that many phenotypic variations such as of the limbs (Fig. 5.31), face, and ears, when isolated, may not have any pathologic significance and care needs to be taken not to cause unncessary parental anxiety.

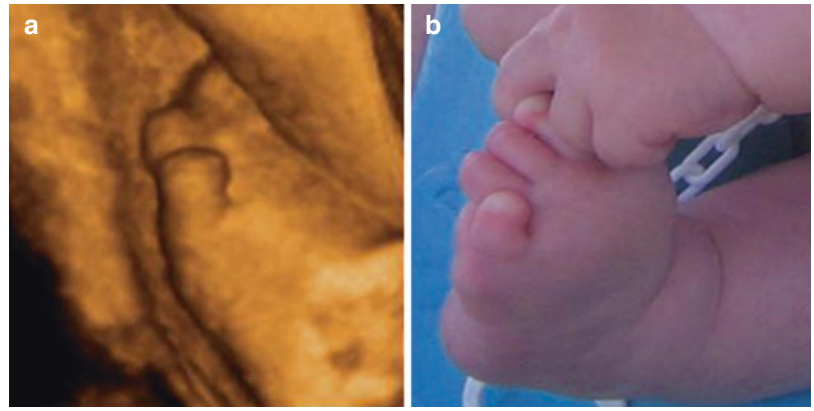

Fig. 5.31 Overlapping toes. The fifth toe overlaps the fourth, as seen by 3D ultrasound of fetus (**a**) and in the newborn (**b**)

References

1. Philip N, Quarello E, Gorincour G, Sigaudy S. Approche de la dysmorphologiefoetale in utero. Fetal dysmorphology: A practical approach in utero. Gynecol Obstet Fertil. 2010;38:677–85.
2. Philip N. Conseilgénétique et examendysmorphologiqueennéonatologie. In: Laugier J, Rozier JC, Simeoni U, Saliba E, editors. Soins aux nouveau-nés: avant, pendant et après la naissance. Paris: Masson; 2006. p. 150–7.
3. Shojaei T, Lacombe D, Lyonnet S, Amiel J, Philip N. Approcheclinique de l'enfantdysmorphique. J Pediatr Pueric. 1999;12:75–80.
4. Rotten D, Levaillant JM, Martinez H, Ducou le Pointe H, Vicaut E. The fetal mandible: a 2D and 3D sonographic approach to the diagnosis of retrognathia and micrognathia. Ultrasound Obstet Gynecol. 2002; 19:122–30.
5. Goldstein I, Tamir A, Weiner Z, Jakobi P. Dimensions of the fetal facial profile in normal pregnancy. Ultrasound Obstet Gynecol. 2010;35:191–4.
6. Sepulveda W, Be C. Partial trisomy 20q in a fetus with hypoplastic nasal bone, mild ventriculomegaly, and short femur. Prenat Diagn. 2008;28:868–70.
7. Sepulveda W, Wong AE, Dezerega V. Brachmann-de Lange Syndrome: prenatal diagnosis with 2- and 3-dimensional sonography. J Ultrasound Med. 2009; 28:401–4.
8. Bergé SJ, Plath H, Van de Vondel PT, Appel T, Niederhagen B, Von Lindern JJ, Reich RH, Hansmann M. Fetal cleft lip and palate: sonographic diagnosis, chromosomal abnormalities, associated anomalies and postnatal outcome in 70 fetuses. Ultrasound Obstet Gynecol. 2001;18:422–31.
9. Maarse W, Rozendaal AM, Pajkrt E, Vermeij-Keers C, Mink van der Molen AB, van den Boogaard MJ. A systematic review of associated structural and chromosomal defects in oral clefts: when is prenatal genetic analysis indicated? J Med Genet. 2012;49:490–8.
10. Sepulveda W. Prenatal 3-dimensional sonographic depiction of the Wolf-Hirschhorn phenotype: the "Greek warrior helmet" and "tulip" signs. J Ultrasound Med. 2007;26:407–10.
11. Ramos GA, Ylagan MV, Romine LE, D'Agostini DA, Pretorius DH. Diagnostic evaluation of the fetal face using 3-dimensional ultrasound. Ultrasound Q. 2008; 24:215–23.
12. Bagic I, Verzak Z. Craniofacial anthropometric analysis in Down's syndrome patients. Coll Antropol. 2003;27 Suppl 2:23–30.
13. Farkas LG, Katic MJ, Forrest CR. Surface anatomy of the face in Down's syndrome: anthropometric proportion indices in the craniofacial regions. J Craniofac Surg. 2001;12:519–26.
14. Richtsmeier JT, Zumwalt A, Carlson EJ, Epstein CJ, Reeves RH. Craniofacial phenotypes in segmentally trisomic mouse models for Down syndrome. Am J Med Genet. 2002;107:317–24.
15. Roizen NJ, Patterson D. Down's syndrome. Lancet. 2003;361:1281–9.
16. Richtsmeier JT, Baxter LL, Reeves RH. Parallels of craniofacial maldevelopment in Down syndrome and Ts65Dn mice. Dev Dyn. 2000;217:137–45.
17. Sforza C, Elamin F, Rosati R, Lucchini MA, De Menezes M, Ferrario VF. Morphometry of the ear in north Sudanese subjects with Down syndrome: a three-dimensional computerized assessment. J Craniofac Surg. 2011;22:297–301.
18. Agathokleous M, Chaveev P, Poo L, Kosinski P, Nicolaides KH. Meta-analysis of second-trimester markers for trisomy 21. Ultrasound Obstet Gynecol. 2013;1:247–61.
19. Ranzini AC, Guzman ER, Ananth CV, Day-Salvatore D, Fisher AJ, Vintzileos AM. Sonographic identification of fetuses with Down syndrome in the third trimester: a matched control study. Obstet Gynecol. 1999;93:702–6.
20. Rotmensch S, Liberati M, Bronshtein M, Schoenfeld-Dimaio M, Shalev J, Ben-Rafael Z, Copel JA. Prenatal sonographic findings in 187 fetuses with Down syndrome. Prenat Diagn. 1997;17:1001–9.

21. Nyberg DA, Luthy DA, Cheng EY, Sheley RC, Resta RG, Williams MA. Role of prenatal ultrasonography in women with positive screen for Down syndrome on the basis of maternal serum markers. Am J Obstet Gynecol. 1995;173:1030–5.
22. Picklesimer AH, Moise KJ, Wolfe HM. The impact of gestational age on the sonographic detection of aneuploidy. Am J Obstet Gynecol. 2005;193:1243–7.
23. Winter-Baraitser dysmorphology database. London Medical Databases. http://www.lmdatabases.com.
24. Binder KH. Dysostosis maxillo-nasalis, ein arhinencephaler Missbildungkomplex. Dtsch Zahnaerztl Z. 1962; 438.
25. Nino M, Matos-Miranda C, Maeda M, Chen L, Allanson J, Armour C et al. Clinical and molecular analysis of arysulfatase E in patients with brachytelephalangic chondrodysplasia punctata. Am J Med Genet A. 2008;146:997–1008.
26. Derry JM, Gormally E, Means GD, Zhao W, Meindl A, Kelley RI, Boyd Y, Herman GE. Mutations in a delta 8-delta 7 sterol isomerase in the tattered mouse and X-linked dominant chondrodysplasia punctata. Nat Genet. 1999;22:286–90.
27. Olow-Nordenram MAK, Radberg CT. Maxillonasal dysplasia (Binder's Syndrome) and associated malformations of the cervical spine. Acta Radiol 1984;25:353.
28. Sepulveda W, Sandoval R, Carstens E, Gutierrez J, Vasquez P. Hypohidrotic ectodermal dysplasia: prenatal diagnosis by three-dimensional ultrasonography. J Ultrasound Med. 2003;22: 731–5.

Prenatal Diagnosis of Orofacial and Neck Tumors

6

Gabriele Tonni, Marcella Palmisano,
Roberta Granese, and Maria Paola Bonasoni

The prenatal finding of a fetal face and neck tumor poses a challenge because they are very rare lesions that are difficult to evaluate due to their frequent large dimensions, heterogeneous features, and irregular extension into adjacent organs. Development of a differential diagnosis of a facial mass in the fetus is essential in guiding the prenatal counseling of the parents and the prenatal and/or postnatal management.

Two-dimensional (2D) ultrasound may allow identification of these lesions as early as 15–17 weeks' gestation. However, most reports describe findings later in the second trimester and in the third trimester [1], suggesting that these tumors may develop later in pregnancy.

Three-dimensional (3D) ultrasound must be considered a complementary diagnostic tool because it enables spatial evaluation of the lesion, enhances analysis of its relationship with the anatomic structures of the face including the eyes and nose, and assists in communication of the significance of the anomaly during counseling of the parents. Magnetic resonance imaging (MRI) also has proved to be very useful in diagnosis, especially in the evaluation of involvement of the central nervous system (CNS). The combination of 2D-3D ultrasound and MRI provides unquestionable benefits that, together with genetic counseling, allows provision of information to the future parent-to-be and preparation of the multidisciplinary team for delivery [2].

6.1 Tumor of the Face

Nasal glioma is a rare, benign congenital midline facial lesion with an estimated incidence of only 1:20,000–1:40,000 live births and with a female-to-male ratio of 3:2 [4].

These lesions are located extranasally in 60 % of cases and intranasally in 30 % of cases and involve both the extra- and intranasal areas in 10 % of cases. Nasal gliomas or heterotopic central nervous system tissue (HCNST) are considered nonneoplastic glial heterotopia in an extracranial site [5].

G. Tonni, MD, PhD (✉)
Department of Obstetrics and Gynecology, Prenatal Diagnostic Service, Guastalla Civil Hospital, AUSL Reggio Emilia, Reggio Emilia, Italy
e-mail: Tonni.Gabriele@ausl.re.it

M. Palmisano
Department of Obstetrics and Gynecology, Prenatal Diagnostic Service, AUSL Reggio Emilia, Guastalla Civil Hospital, Reggio Emilia, Italy

R. Granese
Department of Obstetrics and Gynecology, Azienda Ospedaliera Universitaria di Messina, G. Martino, Italy

M.P. Bonasoni
Pathology Service, IRCCS Arcispedale "Santa Maria Nuova", Reggio Emilia, Italy

G. Tonni, W. Sepulveda, and A.E. Wong (eds.), *Prenatal Diagnosis of Orofacial Malformations*,
DOI 10.1007/978-3-319-32516-3_6

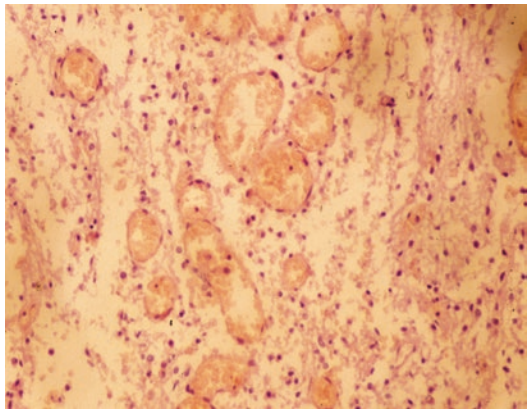

Fig. 6.1 Glial fibers intermixed with a rich vascular network

The most accepted embryological theory was described by Grümwald in 1910 and is called the "prenasal space" theory. This theory is very appealing because of the embryopathogenic continuum proposed among dermoids, gliomas, and encephaloceles. The differential diagnosis of nasal gliomas includes other masses of the "prenasal space," such as nasoethmoidal meningoencephaloceles, nasal dermoids, epidermoid cysts [6], dacryocystocele, retinoblastoma, and hemangioma [7].

Gliomas are composed of heterotopic neuroglial tissue with a potential for intracranial extension through a bony defect in the skull base (Fig. 6.1). Neuroimaging is essential for identifying nasal lesions and for determining its exact location and any possible intracranial extension [8].

Its diagnosis is rarely described prenatally; in cases reported, the finding was usually during the second or third trimester when ultrasound demonstrated a voluminous mass extending from the internal canthus to the nasal bridge [9–12] (Figs. 6.2, 6.3, and 6.4).

Postnatally, CT scan is often the initial imaging study obtained because it provides good visualization of the bony landmarks of the skull base. MRI has better soft tissue resolution and may be the best initial study in patients seen early in life because the anterior skull base consists of unossified cartilage and may falsely appear as if there is a bony dehiscence on computed tomography [8]. T1-weighted imaging demonstrates the mass to be isointense to gray matter with moderate

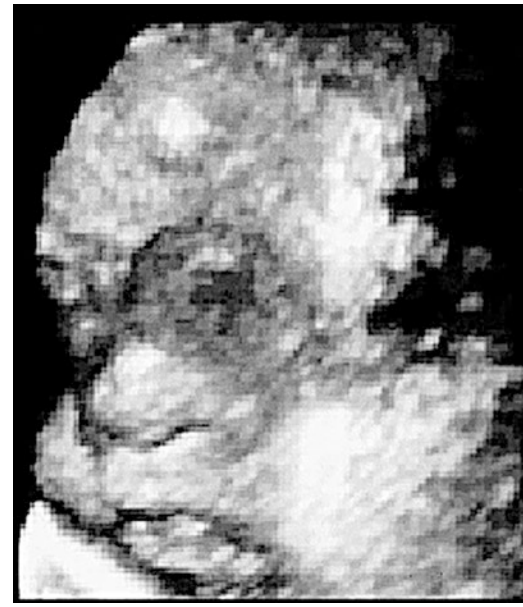

Fig. 6.2 Three-dimensional ultarsond in third trimester with surface rendering mode showing a circular mass at the level of the left nasal ala

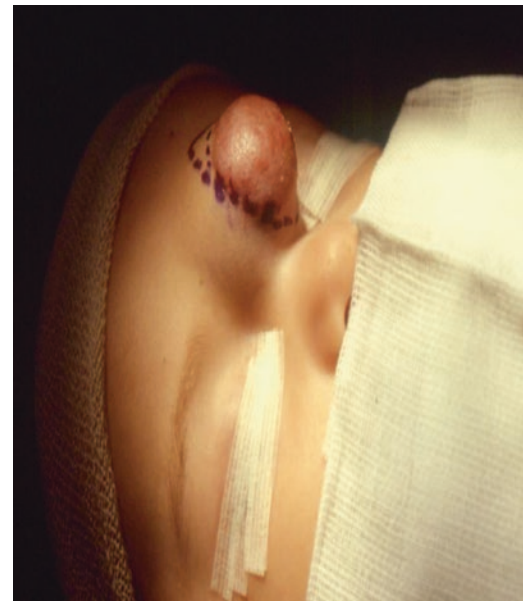

Fig. 6.3 Intraoperative finding in the same case

enhancement with contrast [10]. On T2-weighted imaging, these lesions appear hypointense [13] (Fig. 6.5).

Regarding management, endoscopic surgery is considered appropriate for the removal of an intranasal glioma without intracranial extension

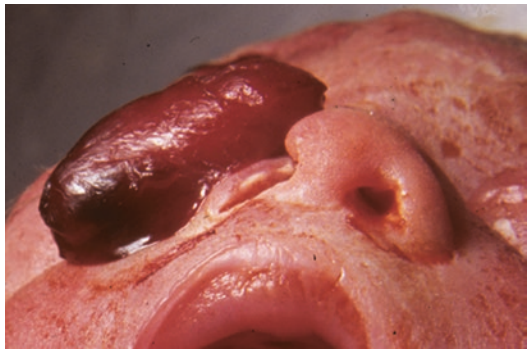

Fig. 6.4 Large nasal glioma in a postmortem specimen demonstrating a large nasal glioma involving the right nasal ala

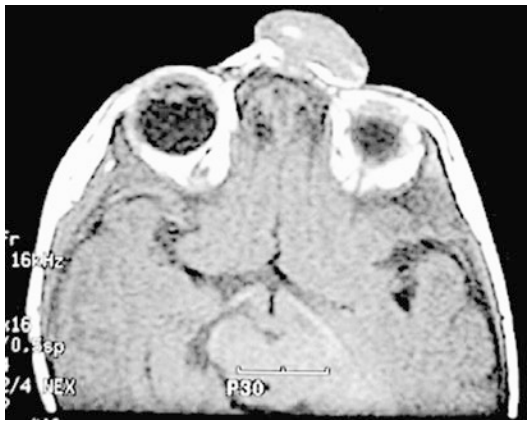

Fig. 6.5 Postnatal T1-weighted MRI confirming a mass protruding at the level of the left nasal ala: note the isointensity of the lesion compared to gray matter

glioma or nasal glial heterotopia may recur following incomplete surgical resection [15].

6.2 Vascular Anomalies

Vascular anomalies can be divided into two main groups: vascular tumors and vascular malformations.

6.2.1 Embryology and Pathology

In general, vascular tumors demonstrate endothelial cell proliferation in contrast to vascular malformations, in which mitotic activity is typically very low or absent. However, exceptions occur. For example, in the involuting phase of infantile hemangioma, cellular proliferation is extremely reduced. On the other hand, capillary expansion may be particularly active in arteriovenous malformations [16].

Congenital nonprogressive hemangioma includes two clinical entities according to their postnatal progression: rapidly involuting congenital hemangiomas (RICHs) and noninvoluting congenital hemangiomas (NICHs). RICHs tend to fully regress after birth leaving a soft tissue defect with local loss of dermal and subcutaneous tissue. Histologically, they appear as NICHs, but with smaller lobules. NICHs are composed of large lobules of small, thin-walled vessels with curved lumina and a large, often stellate, central vessel. Endothelial cells may be hobnailed with eosinophilic cytoplasmic inclusions. Hemosiderin or extramedullary hematopoiesis may also be observed [17].

Histogenesis of congenital hemangiomas is controversial; few theories have been suggested. One theory proposes that placental trophoblasts and endothelial progenitor cells proliferate in an environment of cytokines and estrogen. Indeed, angiopoietin growth factors and cytokines (VEGF, b-FGF, IGF, and matrix metalloproteinase-9) increase during the progression phase of hemangioma formation and subsequently decrease during the involution process. Moreover, in some familial hemangiomas, mutations have been found in growth factor receptors (FGFR4, PDGFRB, VEGFR2, and Flt-4) [18–21].

Vascular malformations are considered to be the result of defective morphogenesis. They include *capillary malformations* (CMs), *venous malformation* (VMs), *lymphatic malformations* (LMs), and *arteriovenous malformations* (AVMs). CMs are the most common and usually arise along the trigeminal nerve. Light microscopy reveals dilation of venules and capillaries within the papillary and reticular dermis, sometimes extending to the superficial subcutis (Figs. 6.6–6.13).

6.2.2 Embryology and Pathology

VMs are soft tissue lesions that may be multifocal or segmental and may occur on mucosal surfaces. They are composed of variably sized, thin-walled, dilated veins with scant mural smooth muscle.

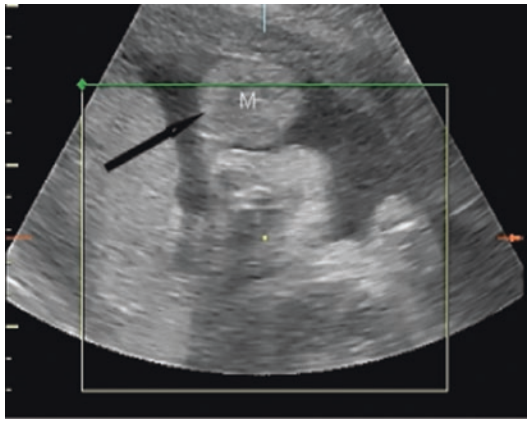

Fig. 6.6 Three-dimensional ultrasound in multiplanar mode performed at 34 weeks of gestation: a superficial mass involving the left side of the fetal profile is visible (*black arrow*) (*M* mass)

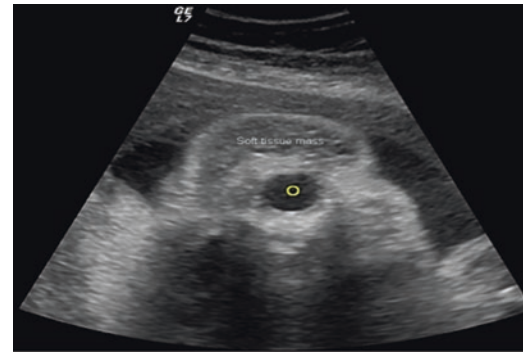

Fig. 6.7 Two-dimensional ultrasound: note the soft tissue mass located superiorly to the left fetal orbit

Fig. 6.8 Doppler ultrasound waveform analysis demonstrating a low velocity arterial flow (peak systolic velocity: 11.5 cm/s) pattern at the level of the peripheral vascular branching

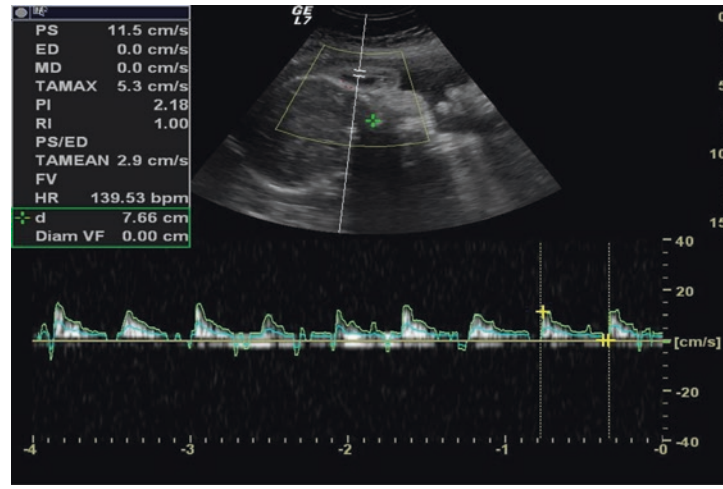

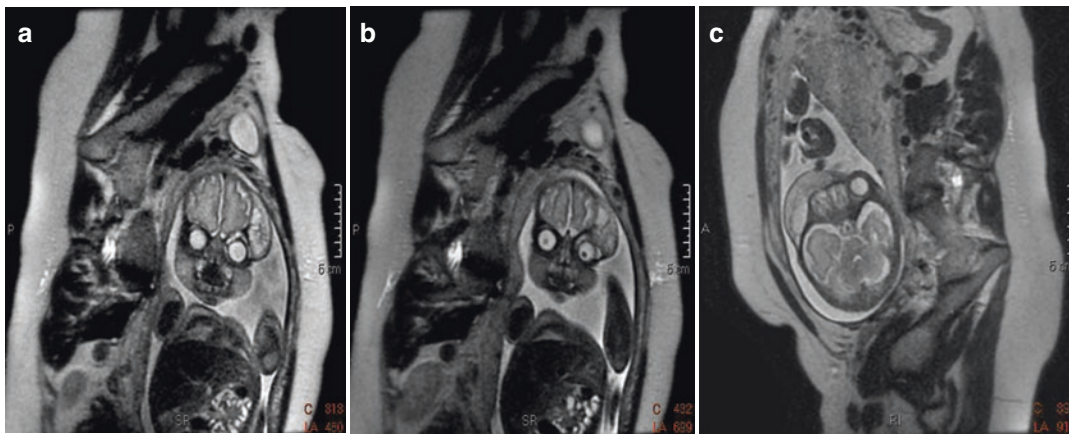

Fig. 6.9 Fetal T2-weighted MRI in coronal planes (**a**, **b**) confirming the presence of a heterogeneous, hyperintense superficial lesion extending from the left temporal region and involving the conic portion of the ipsilateral orbit. Axial plane (**c**) demonstrating integrity of the skin overlying the lesion which extends from the left temporal region to the left fetal orbit and abutting the most medial portion of the contralateral orbit

Fig. 6.10 Infant with capillary malformation

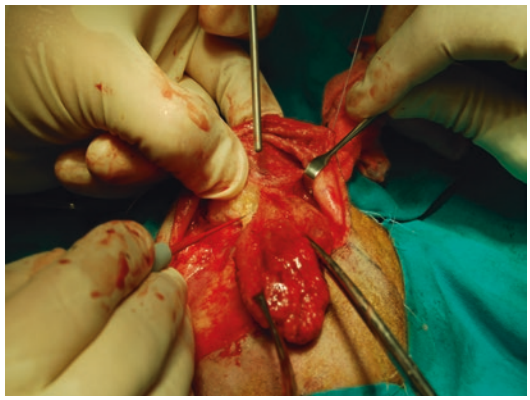

Fig. 6.11 Intraoperative finding at the time of excision of capillary malformation

Due to the slow velocity of blood flow within them, thrombosis is frequent with consequent organization and recanalization, inducing endothelial hyperplasia known as Masson vegetant intravascular hemangioendothelioma.

Venous maldevelopment seems to be caused by abnormalities in the TIE-2 receptor. Mutations in the TIE-2/TEK gene on chromosome 9p21–22 lead to increased autophosphorylation of the receptor, resulting in alterations in endothelial migration and vascular growth. Activating mutations of TIE-2/TEK have been identified in some forms of hereditary VMs.

LMs may be macrocystic or microcystic. Macrocystic variants include large interconnected lymphatic vessels lined by endothelium containing proteinaceous fluid, some lymphocytes, macrophages, and erythrocytes. Some vessels may have valves and an incomplete

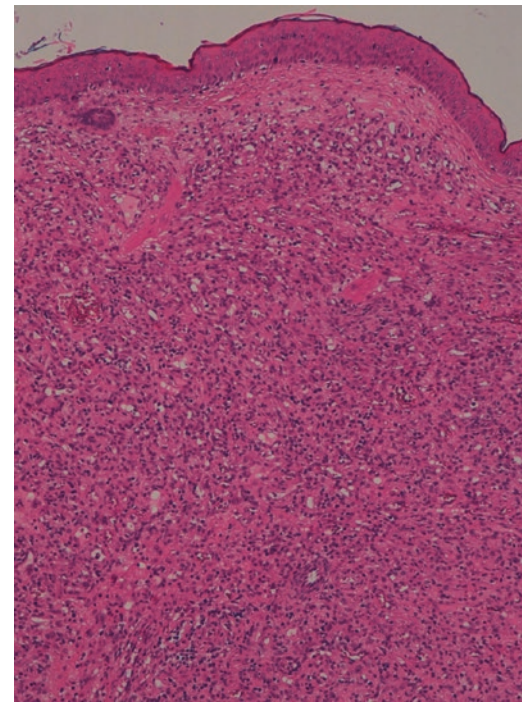

Fig. 6.12 Lobular capillary hemangioma is composed of small vascular channels separated in lobules by fibrous connective tissue (hematoxylin and eosin, 4 HPF). (Courtesy of Prof. N. Sebire)

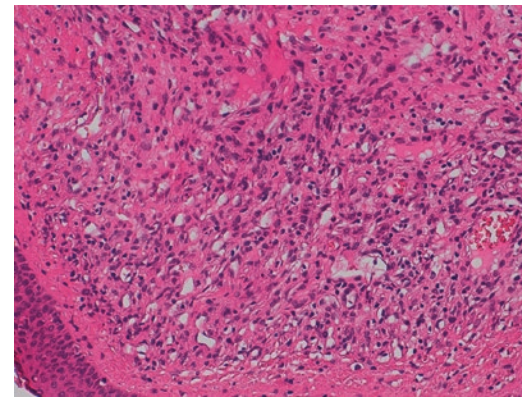

Fig. 6.13 The capillaries are lined by plump endothelial cells supported by pericytic elements (hematoxylin and eosin, 20 HPF). (Courtesy of Prof. N. Sebire)

smooth muscular wall. Mural lymphoid aggregates are frequently observed [1]. Cystic hygromas, typically located in the neck and axillae, show marked dilatation of the lymphatic spaces.

Microcystic LMs are made of smaller lymphatic vessels that may infiltrate and expand into

adjacent tissues. In superficial lesions, they can form lymph-filled vesicles due to protrusion and expansion of dermal papillae.

AVMs lack a normal capillary bed between arteries and veins. Histologically, they appear as a conglomerate of arterioles, venules, and capillaries that are haphazardly connected within a densely fibrous or fibromyxomatous dermis. Larger caliber arteries and thick-walled veins are also present. Veins are often characterized by adventitial fibrosis and irregular intimal hyperplasia [22].

6.3 Tumors of the Oral Cavity and Oropharynx Teratomas

6.3.1 Classification

Teratomas of the oral cavity can be classified according to the site of origin as episphenoid, epipalatine or epignathus.

6.3.2 Embryology and Pathology

Histologically, these tumors can be divided into (1) dermoids or hairy polyps, composed of mesodermal and ectodermal elements; (2) teratoids and teratomas, which include all three germ layer components with scarce or intermediate differentiation; and (3) epignathus, which also comprises fetiform structures. The term *fetus in fetu* should be reserved to tumors in which it is possible to recognize axial differentiation of limbs and organs [23]. This may be the result of an arrested development of a conjoined twin from the third week of gestation. However, epignathus is commonly thought to arise from pluripotent cells in the region of Rathke's pouch, in particular the craniopharyngeal canal, within the sphenoid bone where during early gestation, the oropharyngeal membrane, Rathke's pouch, and the notochord are closely related [24].

Regarding the formation of congenital masses (either teratomas or hamartomas), the coexistence of collapse and expansion of the cephalic midline is observed in cases of cephalic teratomas (CTS) and holoprosencephaly diencephalic hamartoma association [25]. Therefore, midline CTS and hamartomas may be interpreted as clonal expansion of cells that escape differentiation due to the collapse (holoprosencephaly) or splitting at the midline (craniofacial duplication) of the normal process of lateralization starting during gastrulation at the cephalic pole. Nasopharyngeal teratoma predominantly develops during splitting phase of gastrulation, while diencephalic hamartoma results from with defective cleavage of the prosencephalon [26].

Dermoid or hairy polyps are polypoidal masses covered by the skin and composed of mature elements derived from ectoderm (skin and neural tissue) and mesoderm (adipose tissue, muscle, and cartilage) [27] (Figs. 6.14 and 6.15).

Teratoids include the three germ layers with poor differentiation and organization [28]. However, teratoid cysts of the floor of the mouth are complex structures with an outer layer containing epithelial and non-epithelial components such as bone, muscle, blood vessels, collagen fibers, and respiratory and gastrointestinal tissue [29].

Teratomas are composed of a variable admixture of skin, skin appendages, smooth muscle, cartilage, and respiratory and gastrointestinal epithelium. Neural tissue may be present and is

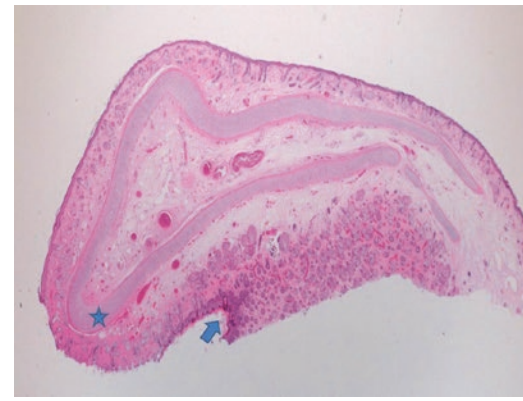

Fig. 6.14 Hairy polyp is a congenital malformation arising from the oropharynx or nasopharynx. The lesion is polypoid and layered by epidermis (*blue star*), hair follicles, and sebaceous glands (*blue arrow*). Cartilage may be found within the polyp core (hematoxylin and eosin, 2 HPF). (Courtesy of Prof. N. Sebire)

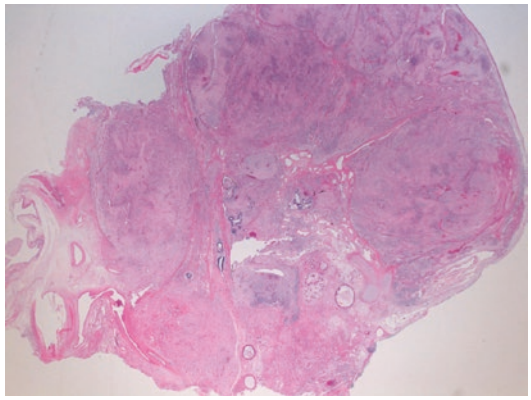

Fig. 6.15 Grossly, the teratoma is encapsulated and lobulated. Histologically, the tumor is composed of mature or immature tissues from the three embryonic germ cell layers: ectoderm, endoderm, and mesoderm (hematoxylin and eosin, 2 HPF). (Courtesy of Prof. N. Sebire)

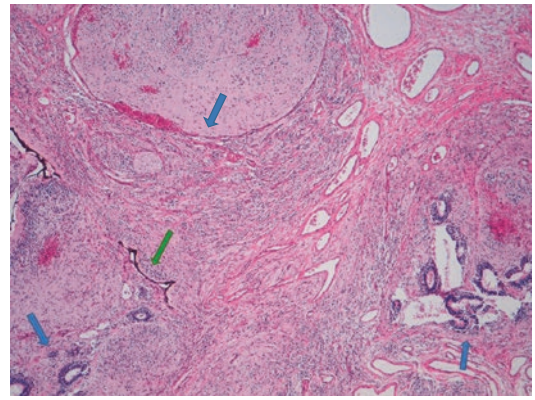

Fig. 6.16 In the teratoma tumors, the most common finding is neural and glial tissue, usually organized in islands (*blue star*), and rosette-like formations of immature ependymal epithelium (*blue arrow*). Sometimes, it is possible to observe retinal anlage epithelium (*green arrow*) (hematoxylin and eosin, 10 HPF). (Courtesy of Prof. N. Sebire)

usually immature ("immature teratoma") including neuroblasts, ependymal rosettes, and retinal anlage [30]. Teratomas are usually benign (Fig. 6.16).

Epignathus is a congenital oropharyngeal teratoma originating from the base of the skull and usually involves the posterior nasopharynx, hard palate, or sphenoid bone.

The incidence for epignathus is estimated to be between 1:35,000 and 1:200,000 live births [31]. Females are more likely to be affected than males with a female-to-male ratio of 3:1 [32].

6.3.3 Embryology and Pathology

Epignathus has various etiologies, including chromosomal abnormalities (such as trisomy 13 [33]), ring X-chromosome mosaicism with inactive ring X-chromosome [34, 35], gonosomal pentasomy 49, XXXXY karyotype [36], gene mutations (e.g., HLXB9) [37], or abnormalities in early embryonic development [38]. Epignathus may be a part of genetic syndromes, such as Aicardi syndrome (agenesis of the corpus callosum, infantile spasm, and ocular anomalies) [39] and Pierre Robin syndrome [40]. Although usually benign, 10 cases of malignant teratoma have been reported in the medical literature [41–45].

6.3.4 Diagnosis

Two-dimensional (2D) ultrasound has accurately identified these lesions, even at the early gestational ages of 15–17 weeks [46, 47]. However, the vast majority of tumors are usually detected in the late second and third trimesters [1], which suggests that the tumor can develop later in pregnancy [31, 48–55].

The ultrasonographic findings of epignathus is characterized by the presence of a solid or mixed cystic/solid mass and calcifications within the mass, which are virtually pathognomonic of teratoma. Color Doppler ultrasound of the solid portions shows extensive vascularization [56] (Fig. 6.17).

The neck is often hyperextended and polyhydramnios is usually associated. The importance of applying three-dimensional ultrasonography with rendering mode to demonstrate the spatial relationships of the tumor with the oral cavity and to provide correlations between the ultrasound images and the postnatal anatomic findings has been recently stressed [57].

Magnetic resonance (MR) imaging can be particularly useful in identifying bidirectional lesions with intracranial extension; these masses are invariably associated with a poor prognosis [58, 59] (Figs. 6.18–6.20).

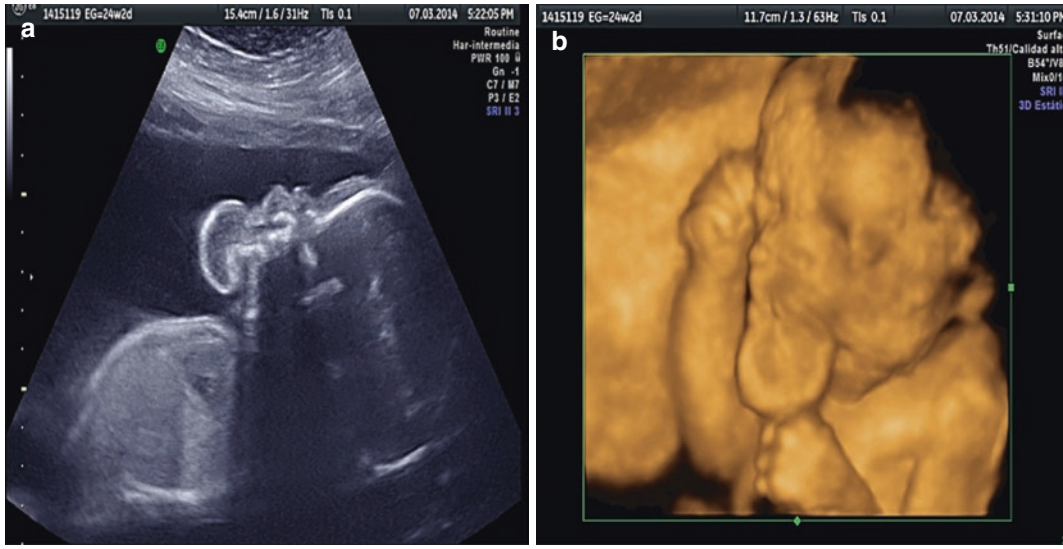

Fig. 6.17 Two-dimensional ultrasound performed at 24w2d showing, in sagittal plane, a heterogeneous mass protruding from the fetal mouth. Polyhydramnios was an associated finding (**a**). Three-dimensional ultrasound with surface rendering confirming the presence of an oral mass (**b**). (Courtesy of Prof. W. Sepulveda)

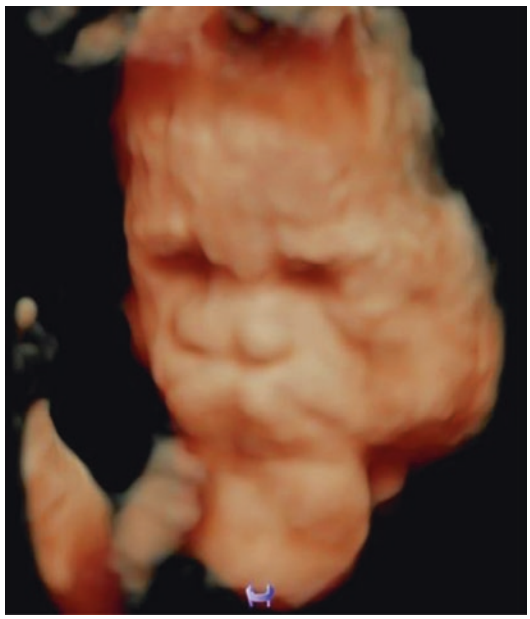

Fig. 6.18 Three-dimensional ultrasound in a second trimester fetus with epignathus using HDLive™ mode. (Courtesy of Prof. W. Sepulveda)

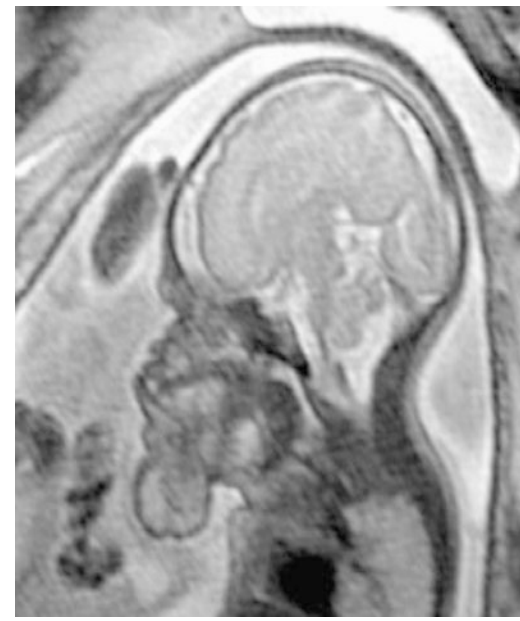

Fig. 6.19 T2-weighted fetal MRI. In the sagittal plane, a bulky mass is seen that is in direct communication with the oral cavity but the upper airway remains unobstructed (Courtesy of Prof. W. Sepulveda)

MR imaging also delineates the level and extent of airway obstruction and can quantify fetal lung volumes. MR imaging can be used with either single-shot spin echo (SSSE) or half-Fourier single-shot turbo spin echo (HASTE) techniques. The latter technology enables rapid imaging in steady-state procession (FISP) to be performed in approximately 20 s and provides

superior contrast resolution compared to the T2-weighted HASTE technique [30]. MR imaging is critical to accurate diagnosis, especially in confirming whether the CNS is involved, and for optimal delivery planning for fetuses in which an EXIT (ex utero intrapartum treatment) procedure may be indicated [60].

Very recently, Heron et al. have demonstrated the utility of integrating 3D ultrasound with MRI volume data to reconstruct a physical model of the lesion and to evaluate for the possibility of fetal upper airway obstruction. To construct the physical model from 3D ultrasound and MRI, the first step is to create a virtual 3D model. All the images obtained through 3D ultrasound and MRI are exported to a workstation in DICOM format. The 3D structure of the fetus is reconstructed by generating its surface using software with the capacity to convert the images obtained into numerical models. These reconstructed images are then exported using STL (standard triangular language) and converted to the file extension 3D polygonal modeling software. The 3D model is converted back to the "STL" extension and exported to the Mimics software, which correlates the shapes and outlines observed from 3D ultrasound. Finally, to determine the physical model of the fetus, ultraviolet spot laser beams are guided through a reservoir of photosensitive resin to model the fetal shape based on the data stored in the 3D geometry software, sliced into transverse planes of predefined thickness of 0.1–0.2 mm [61] (Fig. 6.21).

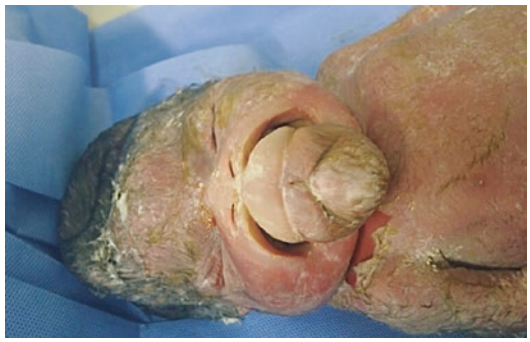

Fig. 6.20 Postmortem finding in a case of epignathus. Note the associated hypertelorism (Courtesy of Prof. W. Sepulveda)

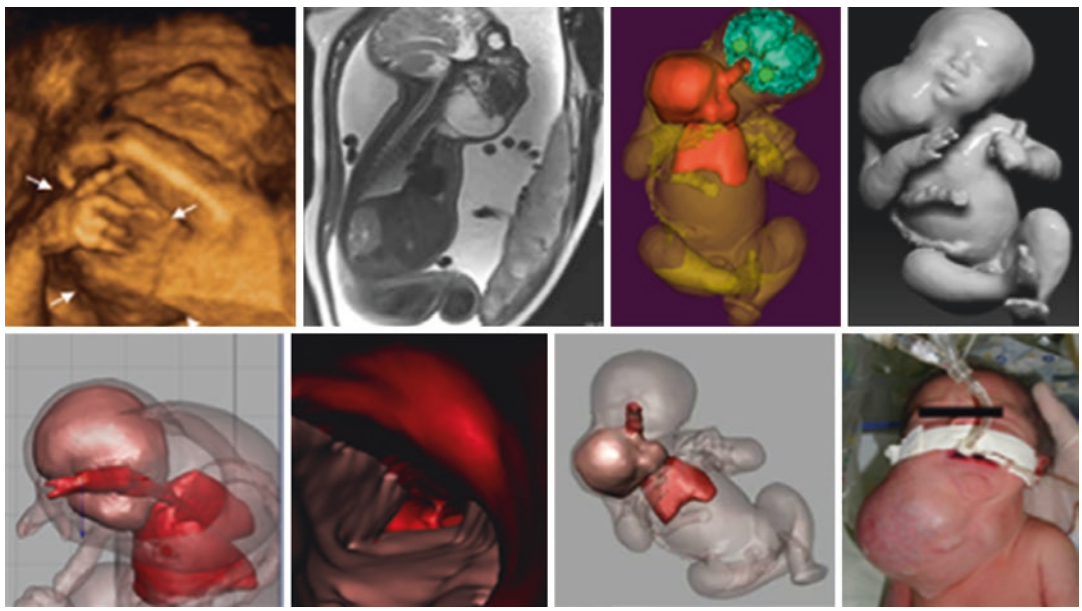

Fig. 6.21 Giant latero-cervical teratoma. (**a**) 3D ultrasound demonstrates the mass (*arrows*) extending from the neck region (**b**) Fetal T2-weighted MRI confirmed heterogeneous hyperintense as well as hypointense signals within the mass (**c**–**g**) Physical models obtained from fetal MRI volumes with reconstruction of the airway and larynx, including demonstration of the anatomic relationship between the teratoma and the airway (**h**) EXIT procedure following delivery by Cesarean section (Courtesy of Dr. W. Heron)

6.3.5 Associated Anomalies

Epignathus should be differentiated from cervical teratoma, cystic hygroma, congenital goiter, branchial cyst, parotid tumor, carcinoma of the thyroid [43], and other rare tumors involving the soft tissue such as hemangioma, fibromatosis, fibrosarcoma, rhabdomyosarcoma [62], cervical neuroblastoma, anterior encephalomyelocele [63, 64], and cavernous lymphangioma of the face and neck, which is a rare variant of cystic hygroma colli characterized by the involvement of deep subcutaneous tissues and muscular septa [65].

Epignathus is often associated with a markedly elevated α-fetoprotein level on second trimester aneuploidy screening [32]. In addition, epignathus is frequently associated with polyhydramnios (in approximately 30 % of cases) due to obstruction of the fetal mouth and impaired fetal swallowing of amniotic fluid [48, 60] that may cause severe respiratory compromise at delivery.

6.3.6 Prognosis

Although usually benign, 10 cases of malignant teratoma have been reported in the medical literature [31, 45–48]. Prognosis depends on size and location of the tumor, rate of growth, associated polyhydramnios, and degree of intracranial spread [66].

Poor prognostic indicators on prenatal sonography include tumors of large size (>5 cm), polyhydramnios, and hydrops fetalis [39, 64, 67, 68].

In cases of giant epignathus and/or cervical teratoma, obstruction of circulation may also lead to high-output cardiac failure, with subsequent development of polyhydramnios and nonimmune hydrops fetalis, a finding that is strongly associated with intrauterine fetal demise [30]. In such cases, the perinatal mortality rate approaches 100 % if immediate critical neonatal intervention and prompt resection of the tumor is not performed [69].

6.3.7 Recurrence Risk

Congenital epignathus is not known to be associated with an increased risk of recurrence in subsequent pregnancies.

6.4 Tumors of the Tongue and Gingiva

These tumors include congenital epulis, congenital lingual dermoid cyst, oral foregut cyst, congenital ranula, teratoid cyst of the tongue, and teratoma of the tongue.

Epulis is a Greek term that means "swelling on the gingiva." It is a rare benign tumor that usually arises from the mucosa of the anterior part of the maxillary alveolar ridge, but may be located in the mandible, maxilla, or tongue. It may be a single mass or occur as multiple lesions [70, 71].

Epulis has an estimated incidence of 1:7000 newborns with a significant female preponderance; it occurs 8–10 times more frequently in females (compared to males) [70, 71]. This discordance may be suggestive of a hormonal component to its development.

6.4.1 Embryology and Pathology

The etiology of congenital epulis remains uncertain. The tumor is also postulated to originate from undifferentiated mesenchymal cells, fibroblasts, myofibroblasts, histiocytes, pericytes, Schwann cells, or odontogenic epithelial cells. Several immunohistochemical studies also support a mesenchymal origin [72, 73].

Histologically, epulis is a well-defined lesion composed of polygonal cells with a granular, eosinophilic cytoplasm. Cells are of medium to large size, and nuclei are eccentric with small nucleoli. Atypical nuclei may be seen, but the overall appearance is bland. The lesion is covered by a thin stratified squamous epithelium with a variable degree of keratinization and absence of rete ridges. Epulis variants have been described such as increased fibrosis and

spindle cell features. Staghorn-like vascular channels, occasional nests or cords of odontogenic epithelium, and lymphohistiocytic infiltration have also been reported. Epulis immunoreactivity is for vimentin and neuron-specific enolase (NSE).

Histogenesis of this entity is controversial and mainly unknown. Many hypotheses have been considered, including a form of odontogenic dysgenesis, which is maldevelopment of the tooth germ. However, the presence of occasional ameloblast-like cells among the granular cells is not sufficient evidence because epithelial residues can be found in all gingival tissues. Other theories consider possible odontogenic, fibroblastic, histiocytic, myogenic, and neurogenic origins. Among the numerous hypotheses, the most widely recognized is a degenerative process of undifferentiated mesenchymal cells [74–76] (Figs. 6.22).

Ultrastructural studies of epulis demonstrate the presence of many autophagosomes containing collagen precursors, suggesting the tumor cells represent early mesodermal cells that express pericytic and myofibroblastic features that undergo cytoplasmic autophagocytosis [77].

Congenital epulis is usually seen at birth and has a predilection for the maxillary alveolar process, lateral to the midline in the region of the primary canine and lateral incisor. Less frequently, it has been reported to occur on the mandibular alveolus and tongue, and in one case with the involvement of the alveolar ridge as well as the tongue [78]. Typically, a single tumor is present (90 %), ranging in size from several millimeters to several centimeters [79].

6.4.2 Diagnosis

Since its first description in 1871 in Germany as "congenital epulis" by Neumann [78], over 200 cases of this rare lesion have been reported [70].

Congenital epulis appears on ultrasound as a well-defined, round, hypoechoic mass protruding from the mouth and with a branching pattern of feeder vessels [79–81] (Fig. 6.23). MRI features of epulis are characterized by a hypointense T2-weighted signal (Fig. 6.24).

Accelerated growth during the third trimester has been reported in some cases; thus, periodic ultrasonographic evaluation is recommended. Repeat exams should focus on changes in the size of the mass and attempt to evaluate fetal breathing and swallowing, including monitoring for increased amniotic fluid volume or absence of a full stomach that would suggest impairment of fetal swallowing [82–84].

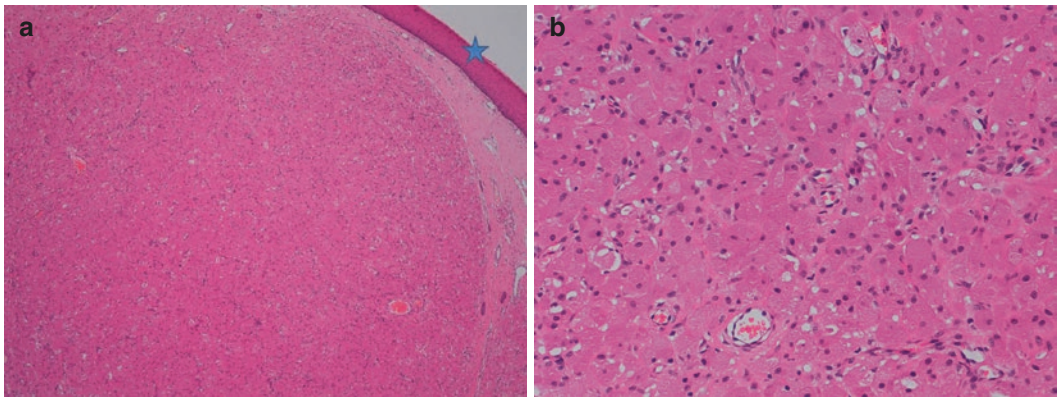

Fig. 6.22 (**a**) The congenital epulis is usually a submucosal lesion with overlying intact epithelium (*blue star*). Cells grow in a typical sheet-like pattern surrounded by fibrovascular septa (hematoxylin and eosin, 4 HPF) (**b**) The epulis is composed of large, granular cells with abundant eosinophilic cytoplasm. The nuclei are round and basophilic (hematoxylin and eosin, 40 HPF). (Courtesy of Prof. N. Sebire)

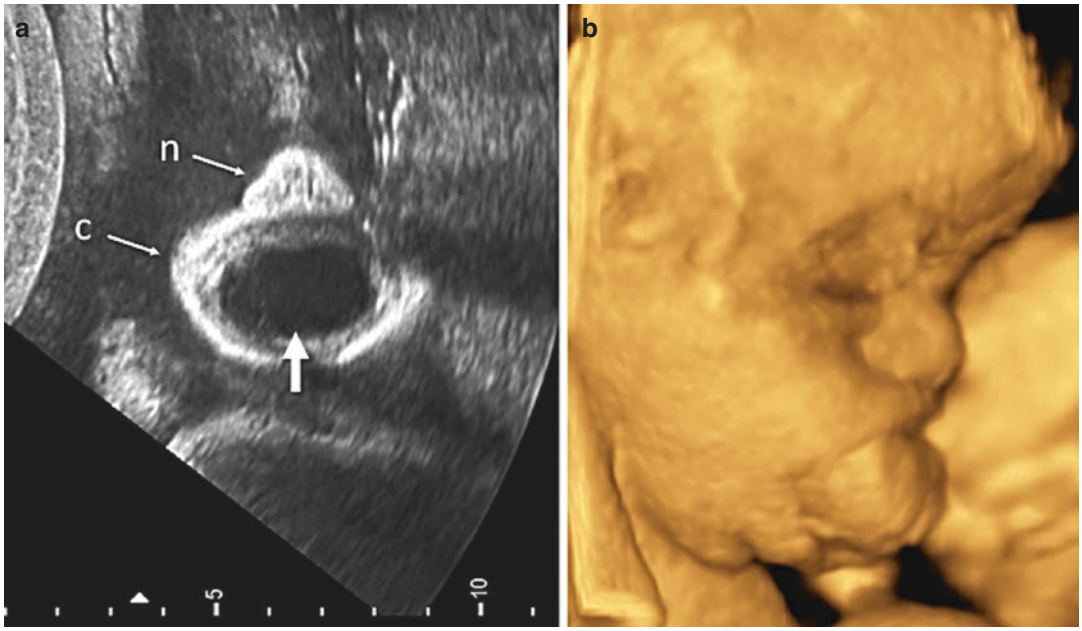

Fig. 6.23 Prenatal imaging of a fetus at 31 weeks 1 day with epulus. (**a**) Two-dimensional ultrasound demonstrated persistent opening of the mouth due to a protruding cystic mass (arrow). n, nose, c, chin. (**b**) Three-dimensional surface-rendered ultrasound clearly depicting the protruding mass (Courtesy of Prof. W. Sepulveda)

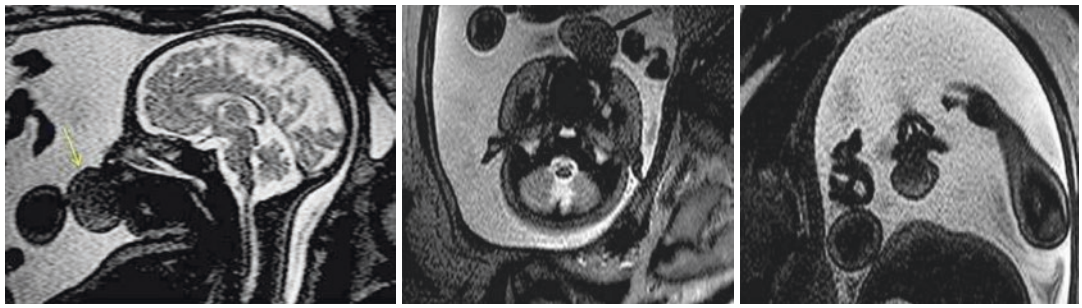

Fig. 6.24 Fetal MRI with hypointense T2-weighted signal in a fetus at 35 weeks of gestation with epulis (*yellow arrow*) in sagittal, axial, and coronal plane, respectively. (Courtesy of Dr. A. Rossi)

6.4.3 Associated Anomalies

There are usually no associated dental abnormalities or congenital malformations, except for occasional reports of a hypoplastic or absent tooth and the possibility of mild midface hypoplasia [70]. Congenital epulis has been reported in infants with polydactyly, goiter, triple X syndrome, maxillary hypoplasia, neurofibromatosis, and polyhydramnios [85].

6.4.4 Prognosis

The overall prognosis for congenital epulis is excellent. After birth, the tumor appears to stop growing and may diminish in size [82]. There are no reported cases of malignant degeneration or posttreatment recurrence, even following incomplete removal, and the cosmetic outcome is excellent [86].

6.4.5 Management

Arising from the mucosa of the gingiva and protruding out of the infant's mouth, a very large epulus can potentially obstruct the airway so early surgical resection is recommended. An EXIT procedure is the ideal delivery strategy for fetuses with a prenatally diagnosed epulis that is sufficiently large to pose concern for potential airway obstruction at birth. Laje et al. [87] performed a retrospective review on four newborns delivered by an EXIT procedure, two of whom were prenatally diagnosed with congenital epulis and two with epignathus. The study analyzed multiple parameters including maternal time under anesthesia, maternal operative time, maternal blood loss, maternal hospital stay, and hysterotomy-to-cord clamp time. The airway was successfully accessed *via* direct laryngoscopy before the umbilical cord was clamped. Some authors indicate that 60 min is the limit for placental support while performing the EXIT procedure [88].

6.4.6 Recurrence Risk

Congenital epulis is not known to be associated with an increased risk of recurrence in subsequent pregnancies.

Congenital lingual dermoid cysts are squamous epithelial-lined cavities with variable numbers of skin appendages in the capsule and are rare entities in the head and neck. Lingual dermoid cysts are most commonly present in early childhood or adolescence and are located in the anterior two-thirds of the tongue. Treatment of these lesions consists of complete surgical excision; however, midline sagittal glossotomy incision using the CO_2 laser has been proposed as it offers surgical precision, superior hemostasis and wound healing, and minimal postoperative edema [89].

Oral foregut cyst is a rare congenital choristoma lined by respiratory and/or gastrointestinal epithelium that should also be considered in the differential diagnosis of an oral tumor. The exact etiology has not been fully identified, but it is thought to arise from misplaced primitive foregut. This lesion initially develops without symptoms but may then lead to difficulty with swallowing and speech depending on its size. Thus, the first choice of treatment is surgical excision. Surgeons should include the oral foregut cyst in the differential diagnosis for ranula, dermoid cyst, thyroglossal duct cyst, and lymphangioma in cases of pediatric head and neck lesions [90]. MR imaging demonstrates a low attenuated T1-weighted signal in the ventral tongue and a high attenuated T2-weighted signal, consistent with a fluid accumulation lesion [91].

Ranulas are mucoid retention cysts, or mucoceles, arising from the sublingual gland or its ductal system secondary to obstruction. A ranula may rarely extend inferomedially into the inferior portion of the tongue resulting in a cystic tongue lesion [92]. Ranulas are extremely rare tumors without a known incidence.

6.4.7 Embryology and Pathology

Ranulas may remain in the floor of the mouth or extend below the mylohyoid sling ("plunging" or "diving" ranula). Cervical ranulas are those that have paracervical extension and plunging ranulas are those that extend toward the superior airway. Another possibility is that a lingual ranula may arise from obstruction of a minor salivary gland or embryologically ectopic salivary tissue [93–95].

6.4.8 Diagnosis

Garcia et al. [96] reported that a lingual ranula appears on ultrasound as a cystic mass that may contain internal septations or echos.

6.4.9 Associated Anomalies

Congenital anomalies that may cause a focal tongue mass include a high thyroglossal duct cyst, lingual thyroid, and foregut duplication cyst

(i.e., an enterocystoma from embryologically entrapped endodermal cells). Other even more unusual etiologies are fibrosarcoma, rhabdomyosarcoma, and synovial sarcomas [96].

6.4.10 Prognosis

Although congenital ranulas have a favorable prognosis, massive sublingual ranulas with a contralateral lesion and macroglossia causing serious neonatal airway obstruction has been observed [97].

6.4.11 Recurrence Risk

Congenital ranulas are not known to be associated with an increased risk of recurrence in subsequent pregnancies.

Teratoid cyst of the tongue may also rarely be observed. This lesion is associated with bronchogenic epithelium characterized by multiple cystic cavities lined by a keratinized squamous epithelium with skin appendages and fatty tissue intermixed with cylindrical, ciliated epithelial cells of respiratory type. Surgical removal via sagittal glossotomy is the treatment of choice [88].

6.4.12 Recurrence Risk

Teratoid cyst of the tongue is not known to be associated with an increased risk of recurrence in subsequent pregnancies.

6.5 Teratoma of the Tongue

Teratomas are one of the most common tumors in infants, especially in the sacrococcygeal region, gonads, retroperitoneum, and mediastinum. However, they account for only 6% of tumors involving the head and neck region [98].

Congenital lingual teratomas are rare with fewer than 20 cases reported in the literature [90, 99–110].

6.5.1 Embryology and Pathology

Histologically, this lesion is benign with a good prognosis without risk of malignancy or recurrence.

6.5.2 Diagnosis

The precise diagnosis and appropriate management of teratoma of the tongue can be achieved by ultrasonography and MRI. Ultrasound demonstrates a multilobular free-floating mass arising from the mouth but mainly growing outside it, with lips intact. It may move slowly and independently if there is a stalk between the mass and the base of the tongue. MRI can confirm the presence of a vascular stalk and the patent airway. The differential diagnosis of congenital oral tumors of the mouth includes congenital epulis, teratomas, encephalocele, lymphatic malformation, hemangiomas, and neuroectodermal tumors [102].

Rarely, a congenital lingual or salivary gland choristoma (teratoid cysts containing respiratory and gastrointestinal epithelium) can occur. This lesion may be associated with bifid tongue and cleft palate; only nine cases of congenital lingual mass, bifid tongue, and cleft palate have ever been reported. Histologically, the most common type was hamartoma (40%), but the differential diagnosis includes hamartoma, teratoma, and salivary choristoma [101, 103].

6.5.3 Management

Teratomas of the tongue may be occasionally associated with feeding and respiratory difficulties. Surgical excision is the management of choice. EXIT is not typically necessary except in cases of extremely massive lesions [104].

6.6 Tumors of the Neck

These masses include branchial cleft cyst, carcinoma of the thyroid, cystic hygroma, congenital goiter, and parathyroid tumor.

6.6.1 Embryology and Pathology

The branchial apparatus appears from the 4th to 7th week of gestation and completes its development by the 20th week of gestation. *A branchial cleft cyst (BBC)* is understood to be the result of incomplete involution of the branchial apparatus [105]. Histology shows BBC to be lined by squamous epithelium with abundant subepithelial lymphoid tissue [106].

6.6.2 Diagnosis

Sixty-four percent of BBCs are anterior to the sternocleidomastoid muscle in the upper third of the neck. It appears on 2D ultrasound as an anterior cystic mass. 3D ultrasound in surface rendering mode shows a well-defined cyst with smooth surface of uniform echogenicity with a thin wall without internal septa [107].

The absence of any solid elements or septations is a useful distinction when differentiating BBCs from teratomas [105].

MR imaging demonstrates a thin-walled cyst with an air–fluid level and can reveal, better than ultrasound, any displacement of the trachea.

6.6.3 Management

Because BBC is associated with a high risk of infection and can potentially cause high-airway obstruction, surgical excision is recommended. After surgical treatment, there is a good prognosis [108].

Congenital goiter can result from either hypo- or hyperthyroidism.

6.6.4 Genetics

Mutation at the level of the dual-oxidase maturation factor 2 (DUOXA2), a component of the thyroid hydrogen peroxidase generator, has been shown proved to cause congenital hypothyroidism with goiter.

6.6.5 Diagnosis

Prenatal diagnosis of fetal goiter can be made by ultrasound by visualization of an enlarged thyroid causing increased thyroid diameter and volume, irregular profile of the anterior aspect of the neck, hyperextension of the neck, and polyhydramnios. Nomograms for fetal thyroid size have been published [109].

Sonographically, the goiter usually appears as a bilobed, solid and hypoechoic mass in the anterior aspect of the fetal neck although cystic components may be seen (Fig. 6.25).

On T1-weighted MR imaging, an anterior, heterogeneous high-signal intensity mass is seen. Congenital hypothyroidism can be confirmed by fetal blood sampling [110, 111]. As demonstrated in cases of giant latero-cervical teratoma, fetal MRI and physical model can evaluate possible airway obstruction [61] (Figs. 6.26, 6.27, and 6.28).

6.6.6 Management

Treatment of congenital goiter has been reported using weekly intra-amniotic injections of L-thyroxin, ranging from 200 to 400 μgm of L-thyroxin [112, 113].

6.7 Hemangioma and Lymphangioma

Hemangioma is a rare a benign vascular tumor of the fetus, where as *lymphangioma* refers to a congenital malformation of the lymphatic vessels. The notion of congenital hemangioma was introduced in 1996 by Boon et al. [114] as a hemangioma-like lesion that has developed to or past its proliferative peak at birth.

6.7.1 Embryology and Pathology

Hemangiomas may be of capillary, cavernous, or mixed morphologic types. Capillary hemangiomas, defined as strawberry marks, are composed

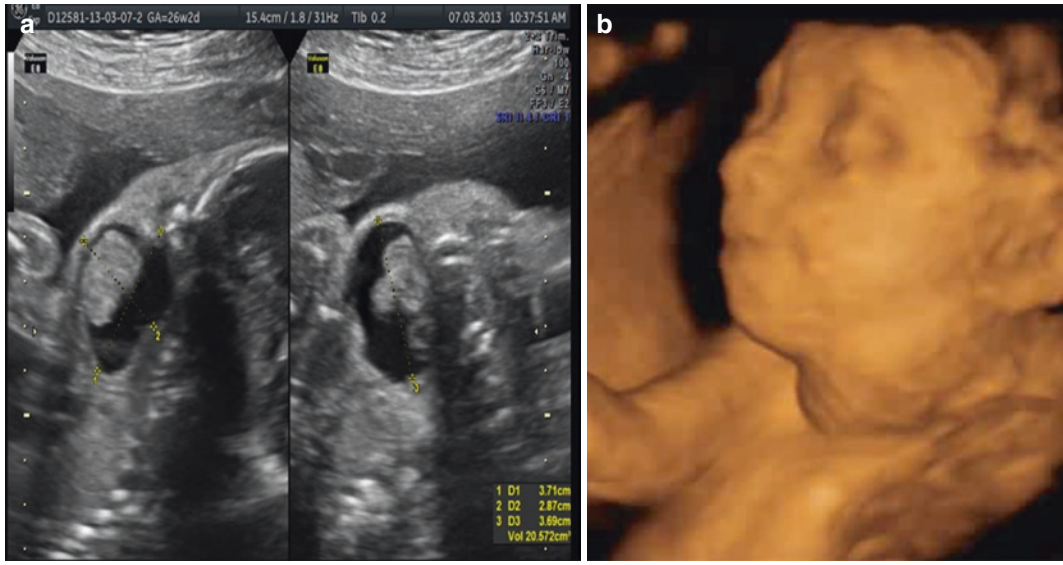

Fig. 6.25 Two-dimensional ultrasound in a fetus at 25 weeks and 2 days demonstrating a partly solid and partly fluid mass occupying the mid-portion of the fetal neck (**a**). Three-dimensional ultrasound in surface mode: a goiter is clearly rendered (**b**) (Courtesy of Dr. W. Heron)

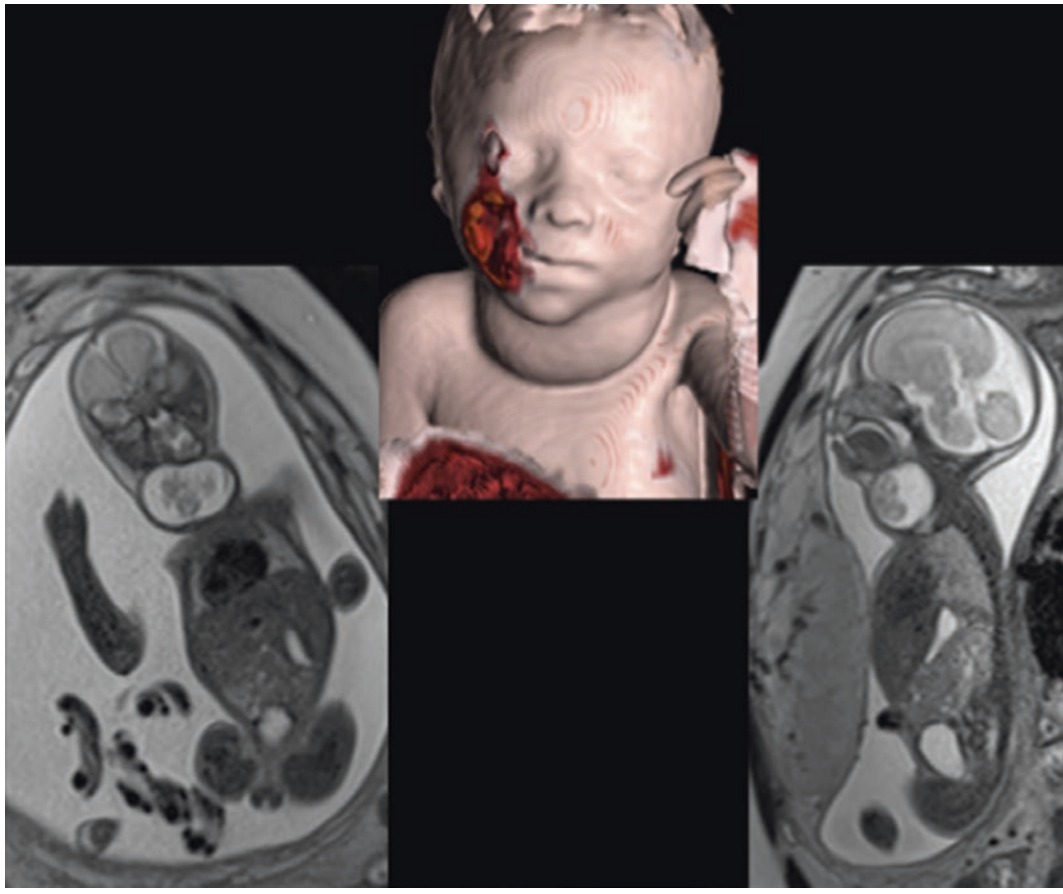

Fig. 6.26 Fetal MRI in coronal and sagittal planes displaying a mass located in the midportion of the fetal neck with heterogeneous lesion with both hyperintense and hypointense components consistent with congenital goiter. The 3D virtual physical model of the goiter is created from the MRI volume data (Courtesy of Dr. W. Heron)

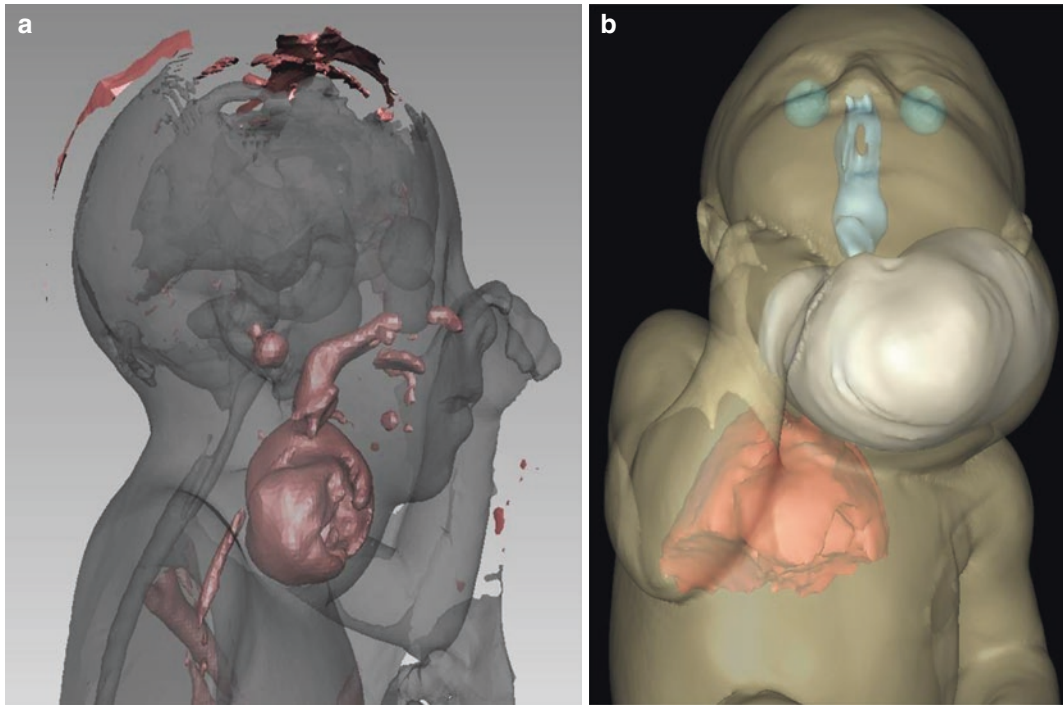

Fig. 6.27 Fetal MRI with 3D volume rendering (**a**) and physical model with rendering (**b**) demonstrating the spatial relationship between the congenital goiter and the fetal airway structure (Courtesy of Dr. W. Heron)

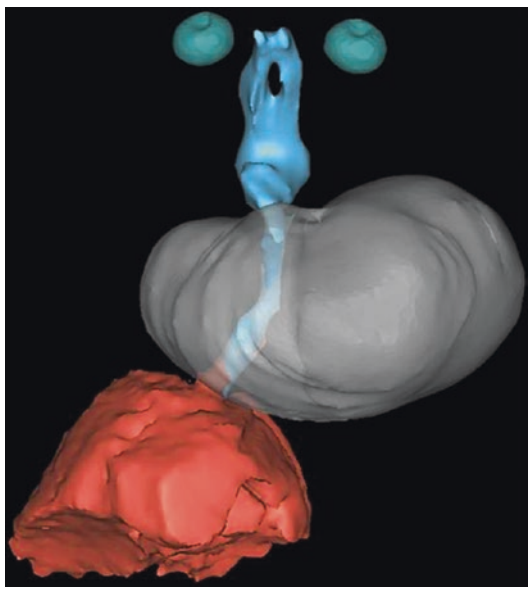

Fig. 6.28 3D details showing the anatomical spatial relationship between the tumoral mass (congenital goiter) and fetal airway structure reconstructed from fetal MRI volume data (Courtesy of Dr. W. Heron)

of small-diameter vessels lined by endothelial cells and surrounded by a single discontinuous layer of pericytes. Differentiation to smooth muscle is not observed. Cavernous hemangiomas have well-differentiated smooth muscle cells surrounding the large-diameter endothelium-lined spaces [115]. They are the only types detectable prenatally and affect 2 % of infants. They demonstrate a relatively slow growth rate and regression is rare and incomplete [116]. They are localized in the lower dermis or subcutaneous tissue and are composed of endothelium-lined spaces and a fibrous or fibromucinous stroma. The pathological classification is based on the nature of the stroma cellularity and the prominence of endothelial components [117].

Three quarters of all hemangiomas are present at birth, with 60 % of them occurring in the head and neck region. The incidence is higher in premature births (20 %), female infants, Caucasian race, advanced maternal age, multiple

gestations, and fetuses with a history of chorionic villus sampling [118].

The mechanisms by which chorionic villus sampling is associated with the occurrence of infantile hemangiomas are believed to be based on the effects on the placenta itself. Quintero et al. [18] showed the dramatic occurrence of numerous ecchymoses on the head and neck after blunt trauma to the placenta. North et al. [119] suggested that infantile hemangiomas are of placental origin.

Immunochemical studies have shown similarity between the vasculature of infantile hemangiomas and the placenta by identifying several tissue-specific markers that are coexpressed by blood vessels in the placenta and in infantile hemangiomas. The researchers postulated that the placenta makes substances, such as Flt-1 (a transmembrane receptor for vascular endothelial growth factor and placental growth factor), which antagonizes angiogenesis. After birth, these placental substances are removed, and the precursor lesions of infantile hemangiomas proliferate within weeks. Presumably, these precursor lesions in the infant's skin have embolized from the infant's placenta. It is possible that a single endothelial cell undergoes monoclonal expansion to become infantile hemangiomas [20].

6.7.2 Diagnosis

The earliest reported diagnosis of hemangioma in the literature is at 14 weeks of gestation [120].

The largest series of prenatal diagnosis of hemangiomas was published by Yang et al. who reported their experience with 23 cases. The sonographic appearance of congenital hemangiomas varies. Masses that are cystic, solid, or mixed, including areas with echogenicity similar to that of the placenta, have been described. Rarely, they may also have internal hyperechogenic areas representing calcification [120–122]. The formation of hypoechoic and cystic spaces has been attributed to cavernous lakes and degeneration [123].

Lymphangioma appears as a cystic structure that is often multilocular. Prenatal diagnosis is greatly facilitated by the use of color and/or power Doppler imaging. The presence of flow depends on the vascular type, amount of arteriovenous shunting, and proliferation of endothelial cells [124]. Features suggestive of hemangiomas are sonographically visible vessels with high vessel density and high peak systolic velocity [118, 124] (Fig. 6.29).

Recently, this lesion has been classified into rapidly involuting congenital hemangioma (RICH) and noninvoluting congenital hemangioma (NICH). A RICH, which is more frequent, spontaneously and completely resolves before the age of 14 months of postnatal life. A NICH, in contrast, grows proportionally with the child; there is no regression of the lesion and excision is eventually required [125].

Few reports are available concerning the clinical prognosis and imaging features of these entities.

NICH and RICH have overlapping clinical features [126]: they have an almost equal sex distribution and a violet color, are usually solitary, and have a similar average diameter and a predilection for the same cutaneous locations (head or limbs near a joint). Pathologically, both RICH and NICH are lobular tumors, the lobules typically smaller in RICH [17]. RICH and NICH are more likely to be heterogeneous on sonography and are much more likely to contain identifiable calcifications. On MRI, these lesions are hyperintense on T2-weighted images and isointense on T1; prior to involution, they enhance avidly and homogeneously [127]. Arteriography may show large tumor vessels containing aneurysms, with arteriovenous shunting [128].

In cavernous hemangiomas, the increased T2 signal is a reflection of the increased fluid volume resulting from slowly flowing blood in vascular spaces [129]. In contrast, a fetal capillary hemangioma has diffuse T2 hypointensity likely because of its compact vascular spaces and low free water content [130] (Fig. 6.30).

6.7.3 Associated Anomalies

Hemangiomas can be associated with cardiac anomalies, central nervous system malformations [122, 131–133], platelet trapping with

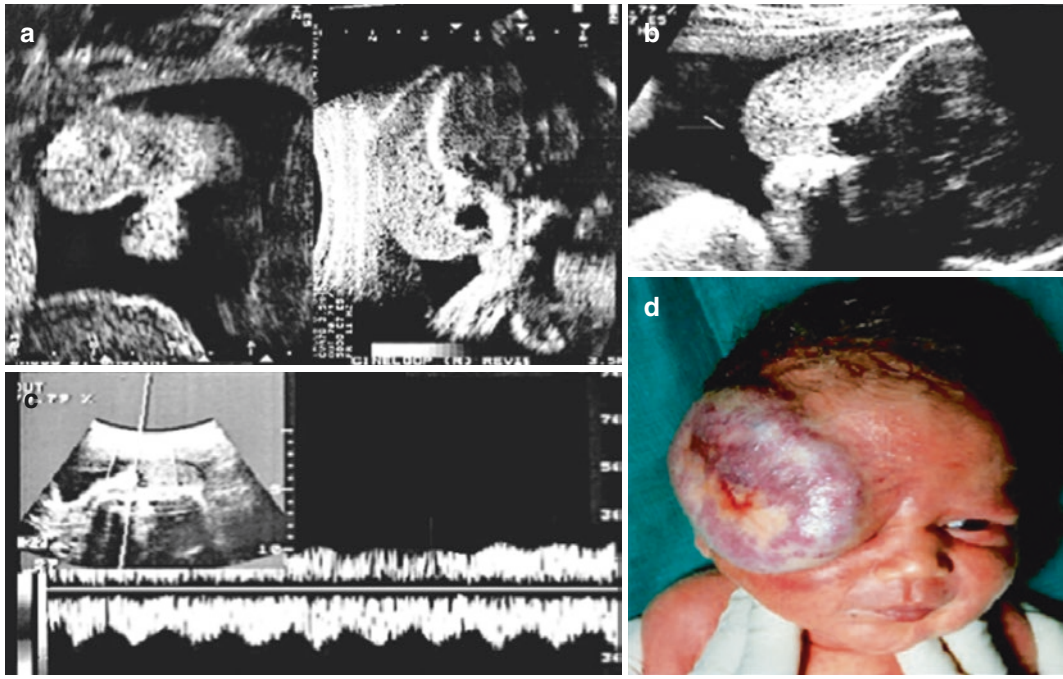

Fig. 6.29 (**a**) Two-dimensional ultrasound in coronal plane and (**b**) in sagittal plane of a third-trimester fetus with a hemangioma. A soft tissue lesion on the right side of the temporal region involving almost the entire ipsilateral orbital region is present. (**c**) Doppler ultrasound shows a low-velocity arterial flow pattern. (**d**) Photograph of the lesion at birth of the infant (Courtesy of Dr. M. Lituania)

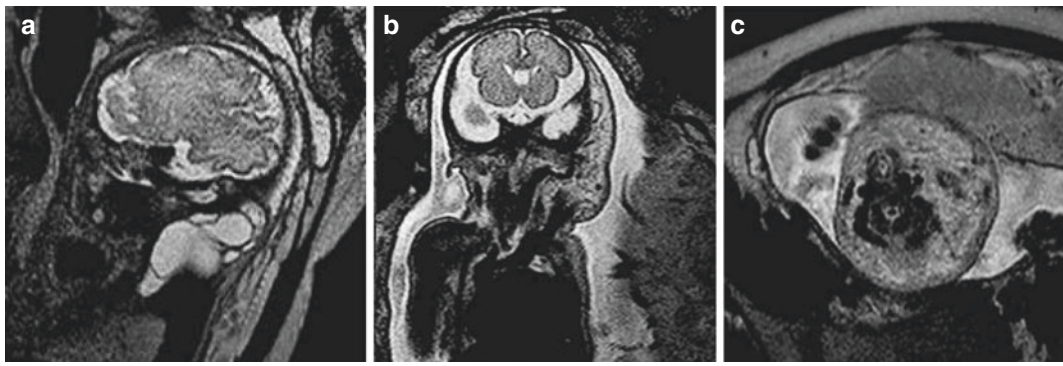

Fig. 6.30 Sagittal (**a**) and axial (**b**) planes of fetal MRI showing a fetus with lymphangioma diagnosed at 32 weeks of gestation. (**c**) Capillary hemangioma detected in a fetus at 29 weeks of gestation (Courtesy of Dr. A. Rossi)

severe consumption coagulopathy, microangiopathic hemolytic anemia, thrombocytopenia Kasabach-Merritt syndrome [116], and profound hypotension leading to brain death. A hemangioma or lymphangioma may be mistaken for an encephalocele, particularly if the lesion involves the occipital region.

6.7.4 Prognosis

Most of these lesions have no clinical significance and resolve spontaneously during infancy. The prognosis is affected by the size and location of the lesion, as well as by the presence of associated anomalies.

If the hemangioma is around the neck, it can cause polyhydramnios and dystocia, airway obstruction, or swallowing difficulties after birth. Large hemangiomas can be associated with hydrops or congestive heart failure, but these hemodynamic complications are poorly linked to RICH [134].

6.7.5 Management

Congenital hemangiomas with characteristic features on ultrasound, CT, and MRI are typically expectantly managed because spontaneous RICHs involute. Complications associated with RICH tumors include intralesional bleeding, high-output cardiac failure, and localized intravascular coagulation [135]. These complications may necessitate more aggressive treatment. If the lesion does not involute, consistent with NICH, excision is required.

6.7.6 Recurrence Risk

Hemangiomas and lymphangiomas are not known to be associated with an increased risk of recurrence in subsequent pregnancies [136].

References

1. Daskalakis G, Efthimiou T, Pilalis A, Papadopoulos D, Anastasakis E, Fotinos G, Antsaklis A. Prenatal diagnosis and management of fetal pharyngeal teratoma: a case report and review of the literature. J Clin Ultrasound. 2007;35:159–63.
2. Santana EF, Helfer TM, Piassi Passos J, Araujo Júnior E. Prenatal diagnosis of a giant epignathus teratoma in the third trimester of pregnancy using three-dimensional ultrasound and magnetic resonance imaging. Case report. Med Ultrason. 2014;16:168–71.
3. Morselli PG, Morellini A, Sgarzani R, Ghi T, Galassi E. Congenital cystic eye: from prenatal diagnosis to therapeutic management and surgical treatment. J Craniofac Surg. 2011;22:360–3.
4. Strauss RB, Callicott JH, Hargett IR. Intranasal heterotopia. So-called nasal glioma. Am J Dis Child. 1966;111:317–20.
5. Fletcher C, editor. Diagnostic histopathology of tumors, vol. 1. 3rd ed. Philadelphia: Churchill Livingstone Elsevier; 2007. p. 135. Chap. 4.
6. Charrier JB, Leboulanger N, Roger G, Denoyelle F, Garabédian EN, Monteil JP. Nasal glioma heterotopia: embryological and clinical approaches. Rev Stomatol Chir Maxillofac. 2006;107:44–9.
7. Shipp TD, Bromley B, Benacerraf B. The ultrasonographic appearance and outcome for fetuses with masses distorting the fetal face. J Ultrasound Med. 1995;14:673–8.
8. Okumura M, Francisco RP, Lucato LT, Zerbini MC, Zugaib M. Prenatal detection and postnatal management of an intranasal glioma. J Pediatr Surg. 2012;4:1951–4.
9. De Biasio P, Scarso E, Prefumo F, Odella C, Rossi A, Venturini P. Prenatal diagnosis of a nasal glioma in the mid trimester. Ultrasound Obstet Gynecol. 2006;7:571–3.
10. Grzegorezyk V, Brausser-Daudruy M, Labadie G, Cellier C, Verspyck E. Prenatal diagnosis of a nasal glioma. Pediatr Radiol. 2010;40:1706–9.
11. Chmait RH, Pretorius DH, Hull AD. Picture of the month. Ultrasound Obstet Gynecol. 2002;20:417–8.
12. Beegun I, Dua R, Connor S, Bentley R. Prenatal diagnosis and management of a craniofacial glioma detected at 20 weeks' gestation. Case report and review of the literature. Int J Oral Maxillofac Surg. 2012;41:200–2.
13. Elia D, Garel C, Enjolras O, Vermouneix L, Soupre V, Oury JF, Guibaud L. Prenatal imaging findings in rapidly involuting congenital hemangioma of the skull. Ultrasound Obstet Gynecol. 2008;31:572–5.
14. Park YH, Kim SW, Cho SH, Choi YW. Nasopharyngeal glioma causing respiratory distress in a neonate: transoral endoscopic excision. Ear Nose Throat. 2010;89:E11–3.
15. Cerdá-Nicolá M, Sanchez Fernandez de Sevilla C, Lopez-Ginés C, Peydro-Olaya A, Llombart-Bosch A. Nasal glioma or nasal glial heterotopia? Morphological, immunohistochemical and ultrastructural study of two cases. Clin Neuropathol. 2002;21:66–71.
16. Viora E, Grassi Pirrone P, Comoglio F, Bastonero S, Campogrande M. Ultrasonographic detection of fetal cranio-facial hemangioma: case report and review of the literature. Ultrasound Obstet Gynecol. 2000;15:431–4.
17. Berenguer B, Mulliken JB, Enjolras O, et al. Rapidly involuting congenital hemangioma: clinical and histopathologic features. Pediatr Dev Pathol. 2003;6:495–510.
18. Quintero RA, Romero R, Mahoney MJ. Embryoscopic demonstration of hemorrhagic lesions on the human embryo after placental trauma. Am J Obstet Gynecol. 1993;168:756–9.
19. North PE, Waner M, Brodsky MC. Are infantile hemangiomas of placental origin? Ophthalmology. 2002;109:633–4.
20. Bischoff J. Monoclonal expansion of endothelial cells in hemangiomas: an intrinsic defect with extrinsic consequences? Trends Cardiovasc Med. 2002;12:220–4.

21. Eivazi B, Ardelean M, Bäumler W, Berlien HP, Cremer H, Elluru R, Koltai P, Olofsson J, Richter G, Schick B, Werner JA. Update on hemangiomas and vascular malformations of the head and neck. Eur Arch Otorhinolaryngol. 2009;266:187–97.
22. Aboutalebi A, Jessup CJ, North PE, Mihm Jr MC. Histopathology of vascular anomalies. Facial Plast Surg. 2012;28:545–53.
23. Prakash A, Parelkar SV, Oak SN, Gupta RK, Sanghvi BV. Giant epignathus with midline mandibular cleft: Insights in embryology and management. Ann Maxillofac Surg. 2012;2:56–9.
24. Nagy GR, Neducsin BP, Lázár L, Stenczer B, Csapó Z, Rigó Jr J. Early prenatal detection of a fast-growing fetal epignathus. J Obstet Gynaecol Res. 2012;38:1328–30.
25. Castori M. Holoprosencephaly-diencephalic hamartoma: sequence or pleiotropy? Am J Med Genet A. 2010;152A:264–6.
26. Morlino S, Castori M, Servadei F, Laino L, Silvestri E; Pediatric Craniofacial Malformation (PECRAM) Study Group, Grammatico P. Oropharyngeal teratoma, oral duplication, cervical diplomyelia and anencephaly in a 22-week fetus: a review of the craniofacial teratoma syndrome. Birth Defects Res A Clin Mol Teratol. 2015;103:554–66.
27. Tariq MU, Din NU, Bashir MR. Hairy polyp, a clinicopathologic study of four cases. Head Neck Pathol. 2013;7:232–5.
28. Jarrahy R, Cha ST, Mathiasen RA, Shahinian HK. Congenital teratoma of the oropharyngeal cavity with intracranial extension: case report and literature review. J Craniofac Surg. 2000;11:106–12.
29. Bonilla JA, Szeremeta W, Yellon RF, Nazif MM. Teratoid cyst of the floor of the mouth. Int J Pediatr Otorhinolaryngol. 1996;38:71–5.
30. Tonni G, De Felice C, Centini G, Ginanneschi C. Cervical and oral teratoma in the fetus: a systematic review of etiology, pathology, diagnosis, treatment and prognosis. Arch Gynecol Obstet. 2010;282:355–61.
31. Smith NM, Chambers SE, Billson VR, Lang I, West CP, Bell JE. Oral teratoma (epignathus) with intracranial extension: a report of two cases. Prenat Diagn. 1993;13:945–52.
32. Clement K, Chamberlain P, Boyd P, Molyneux A. Prenatal diagnosis of an epignathus: a case report and review of the literature. Ultrasound Obstet Gynecol. 2001;18:178–81.
33. Yapar EG, Ekici E, Gokmen O. Sonographic diagnosis of epignathus (oral teratoma), prosencephaly, meromelia and oligohydramnios in a fetus with trisomy 13. Clin Dysmorphol. 1995;4:266–71.
34. Witters I, Moerman P, Louwagie D, Van Assche FA, Migeon BR, Fryns JP. Second trimester prenatal diagnosis of epignathus teratoma in a ring X chromosome mosaicism with inactive ring X chromosome. Ann Genet. 2001;44:179–82.
35. Schwartz S, Raffael LJ, Sun CC, Waters E. An unusual mosaic karyotype detected through prenatal diagnosis with duplication of 1q and 19p and associated teratoma. Teratology. 1992;46:399–404.
36. Staboulidou I, Miller K, Göhring G, Hillemanns P, Wüstemann M. Prenatal diagnosis of an epignathus associated with a 49, XXXXY karyotype: a case report. Fetal Diagn Ther. 2008;24:313–7.
37. Kockling J, Karbasiyan M, Reis A. Spectrum of mutation and genotype-phenotype analysis in Currarino syndrome. Eur J Human Genet. 2001;9:599–605.
38. Ashley DJB. Origin of teratomas. Cancer. 1973;2:390–4.
39. Goldstein I, Drugan A. Congenital cervical teratoma, associated with agenesis of corpus callosum and a subarachnoid cyst. Prenat Diagn. 2005;25:439–41.
40. Vandenhaute B, Leteurtre E, Lecomte-Houcke M, Pellerin P, Nuyts JP, Cuisset JM, Soto-Ares G. Epignathus teratoma: report of three cases with a review of the literature. Cleft Palate Craniofac J. 2000;37:83–91.
41. Thurkow AL, Visser GH, Oosterhuis JW, de Vries JA. Ultrasound observations of a malignant cervical teratoma of the fetus in a case of polyhydramnios: case history and review. Eur J Obstet Gynecol Reprod Biol. 1982;14:375–84.
42. Baumann FR, Nerlich A. Metastasizing cervical teratoma of the fetus. Pediatr Pathol Lab Med. 1995;15:221–2.
43. Shoenfeld A, Ovadia J, Edelstein T, Liban E. Malignant cervical teratoma of the fetus. Acta Obstet Gynecol Scand. 1982;61:7–12.
44. Too S, Ahmad Sarji S, Yik Y, Ramanujam T. Malignant epignathus teratoma. Biomed Imaging Interv J. 2008;4, e18.
45. Ince EZ, Cekmez F, Yıldırım Ş, Demirel A, Bilgic B, Kılıcaslan I, Coban A. Malignant epignathus including a nephroblastoma component and successful management. Ann Diagn Pathol. 2013;17:288–90.
46. Gull I, Wolman I, Har-Toov J, et al. Antenatal sonographic diagnosis of epignathus at 15 weeks gestation. Ultrasound Obstet Gynecol. 1999;13:271–3.
47. Bruhwiler H, Mueller MD, Rabner M. Ultrasound diagnosis of epignathus in the 17th week of pregnancy. Case report and review of the literature. Ultraschall Med. 1995;16:238–40.
48. Ekici E, Soysal M, Kara S, Dogan M, Gokmen O. Prenatal diagnosis of epignathus causing acute polyhydramnios. Acta Obstet Gynecol Scand. 1996;75:498–501.
49. Kang KW, Hissong SL, Langer A. Prenatal ultrasonic diagnosis of epignathus. J Clin Ultrasound. 1978;6:330–1.
50. Teal LN, Angtuaco TL, Jimenez JF, Quirk Jr JG. Fetal teratomas: antenatal diagnosis and clinical management. J Clin Ultrasound. 1988;16:329–36.
51. Martinelli P, Paladini D, Nicotra A, Guerritore T. In utero diagnosis of oropharyngeal teratoma: a case report. Eur J Obstet Gynecol Reprod Biol. 1990;35:291–4.

52. Levine AB, Alvarez M, Wedgwood J, Berkowitz RL, Hozman I. Contemporary management of a potentially lethal fetal anomaly: a successful perinatal approach to epignathus. Obstet Gynecol. 1990; 76:962–6.
53. Gaucherand R, Rudigoz R, Chappuis JP. Epignathus: clinical and sonographic observations in two cases. Ultrasound Obstet Gynecol. 1994;4:241–4.
54. Sağol IIM, Ozsaran A, Oztekin K, Ozbek SS. Prenatal sonographic detection of nasopharyngeal teratoma. J Clin Ultrasound. 1999;27: 469–73.
55. Ozeren S, Yuksel A, Altinok T, Yazgan A, Bilgic R. Prenatal ultrasound diagnosis of a large epignathus. J Obstet Gynecol. 1999;19:660–1.
56. Kuo TN, Sun YH, Hong NS, Tsai HC, Lin CC, Lin MY, Chen SH. Multidisciplinary examination for prenatal diagnosis of posterior cervical teratoma in early second trimester. Taiwan J Obstet Gynecol. 2013;52:270–2.
57. Takagi MM, Bussamra LC, Araujo Júnior E, Drummond CL, Herbst SR, Nardozza LM, Moron AF, Aldrighi JM. Prenatal diagnosis of a large epignathus teratoma using two-dimensional and three-dimensional ultrasound: correlation with pathological findings. Cleft Palate Craniofac J. 2014;51:350–3.
58. Chung JH, Farinelli CK, Porto M, Major CA. Fetal epignathus the case of an early EXIT (Ex Utero Intrapartum Treatment). Obstet Gynecol 2012;119: 466–70.
59. Calda P, Novotna M, Cutka D, Brestak M, Haslik L, Goldova B, et al. A case of an epignathus with intracranial extension appearing as a persistently open mouth at 16 weeks and subsequently diagnosed at 20 weeks of gestation. J Clin Ultrasound. 2011;39: 164–8.
60. Abendstein B, Auer A, Pümpel R, Mark E, Desch B, Tscharf J. Epignathus: prenatal diagnosis by sonography and magnetic resonance imaging. Ultraschall Med. 1999;20:207–11.
61. Werner H, Lopez J, Tonni G, Araujo Júnior E. Plastic reconstruction of fetal anatomy using three-dimensional ultrasound and magnetic resonance imaging scan data in a giant cervical teratoma. Case report. Med Ultrason. 2015;17:252–5.
62. Figueiredo G, Pinto PS, Graham EM, Huisman TA. Congenital giant cervical teratoma: pre- and postnatal imaging. Fetal Diagn Ther. 2010;27:231.
63. Muscatello L, Giudice M, Feltri M. Malignant cervical teratoma: report of a case in a newborn. Eur Arch Otorhinolaryngol. 2005;11:899–904.
64. Rempen A, Feige A. Differential diagnosis of sonographically detected tumours in the fetal cervical region. Eur J Obstet Gynecol Reprod Biol. 1983;14:375–84.
65. Paladini D, Vassallo M, Sglavo G, Lapadula C, Longo M, Nappi C. Cavernous lymphangioma of the face and neck: prenatal diagnosis by three-dimensional ultrasound. Ultrasound Obstet Gynecol. 2005;26:300–2.
66. Tonni G, Centini G, Inaudi P, Rosignoli L, Ginanneschi C, De Felice C. Prenatal Diagnosis of Severe Epignathus in a Twin: Case Report and Review of the Literature. Cleft Palate Craniofac J. 2010;47:421–5.
67. Bergé SJ, von Lindern JJ, Appel T, Braumann B, Niederhagen B. Diagnosis and management of cervical teratomas. Br J Oral Maxillofac Surg. 2004;42: 41–5.
68. Isaacs H. Perinatal (fetal and neonatal) germ cell tumors. J Pediatr Surg. 2004;39:1003–13.
69. Holmgren G, Rydnert J. Male fetus with epignathus originating from the ethmoidal sinus. Eur J Obstet Gynecol Reprod Biol. 1987;24:69–72.
70. Ritwik P, Brannon RB, Musselman RJ. Spontaneous regression of congenital epulis: a case report and review of the literature. J Med Case Reports. 2010;4:331.
71. Fister P, Volavsek M, Novosel Sever M, Jazbec J. A newborn baby with a tumor protruding from the mouth. Acta Dermatoven APA. 2007;16:128–9.
72. Silva GCC, Vieira TC, Vieira JC, Martins CR, Silva EC. Congenital granular cell tumor (congenital epulis): a lesion of multidisciplinary interest. Med Oral Patol Oral Cir Bucal. 2007;12:E428–30.
73. Lapid O, Shaco-Levy R, Krieger Y, Kachko L, Sagi A. Congenital epulis. Pediatrics. 2001;107, E22.
74. Conrad R, Perez MC. Congenital granular cell epulis. Arch Pathol Lab Med. 2014;138:128–31.
75. Kumar B, Sharma SB. Neonatal oral tumors: congenital epulis and epignathus. J Pediatr Surg. 2008;43:e9–11.
76. Rezende KM, Côrrea FN, Côrrea JP, Côrrea MS, Bönecker M. Histogenesis and clinical analysis of 2 cases of congenital gingival granular cell tumour. J Clin Diagn Res. 2015;9:ZD03–5.
77. Damm DD, Cibull ML, Geissler RH, Neville BW, Bowden CM, Lehmann JE. Investigation into the histogenesis of congenital epulis of the newborn. Oral Surg Oral Med Oral Pathol. 1993;76: 205–12.
78. Hasanov A, Musayev J, Onal B, Rahımov C, Farzaliyev I. Gingival granular cell tumor of the newborn: a case report and review of literature. Turk Patoloji Derg. 2011;27:161–3.
79. López de Lacalle JM, Aguirre I, Irizabal JC, Nogues A. Congenital epulis: prenatal diagnosis by ultrasound. Pediatr Radiol. 2001;31:453–4.
80. Pellicano M, Zullo F, Catizone C, et al. Prenatal diagnosis of congenital granular cell epulis. Ultrasound Obstet Gynecol. 1998;11:144.
81. Koch BL, Myer C, Egelhoff JC. Congenital epulis. AJNR Am J Neuroradiol. 1997;18:739.
82. Jiang L, Hu B, Guo Q. Case report prenatal sonographic diagnosis of congenital epulis. J Clin Ultrasound. 2011;39:217–20.
83. Sahu S, Maurya RK, Rao Y, Agarwal A. Multiple congenital epulis in newborn: a rare presentation. J Oral Maxillofac Pathol. 2009;13:78–80.
84. Feller L, Wood NH, Singh AS, Raubenheimer EJ, Meyerov R, Lemmer J. Multiple congenital oral

granular cell tumours in a newborn black female: a case report. Cases J. 2008;1:13.
85. Gokhale UA, Malhotra CJ. Congenital epulis of the newborn. Indian J Pathol Microbiol. 2009;52:436–7.
86. Bornstein E, Boozarjomehri F, Monteagudo A, Santos R, Milla SS, Timor-Tritsch IE. Diagnostic and prognostic aspects in the sonographic evaluation of a fetus with an oral mass. Case report. J Ultrasound Med. 2009;28:689–93.
87. Laje P, Howell LJ, Johnson MP, Hedrick HL, Flake AW, Adzick NS. Perinatal management of congenital oropharyngeal tumors: the ex utero intrapartum treatment (EXIT) approach. J Pediatr Surg. 2013;48:2005–10.
88. Gleizal A, Abouchebel N, Lebreton F, Beziat J-L. Dermoid cyst of the tongue: an association of dermoid cyst with bronchogenic epithelium. J Craniomaxillofac Surg. 2006;34:113–6.
89. Raewyn C, Paul W. Management of congenital lingual dermoid cysts. Int J Pediatr Otorhinolaryngol. 2010;74:567–71.
90. Celik M, Akkaya H, Arda IS, Hiçsönmez A. Congenital teratoma of the tongue: a case report and review of the literature. J Pediatr Surg. 2006;41:e25–8.
91. Kwak EJ, Jung YS, Park HS, Jung HD. Oral foregut cyst in the ventral tongue: a case report. J Korean Assoc Oral Maxillofac Surg. 2014;40:313–5.
92. Donnelly LF, Jones BV, Strife JL. Imaging of pediatric tongue abnormalities. AJR Am J Roentgenol. 2000;75:489–93.
93. Fernandez Moya JM, Cifuentes Sulzberger S, Díaz Recaséns J, Ramos C, Sanz R, Perez Tejerizo G. Antenatal diagnosis and management of a ranula. Ultrasound Obstet Gynecol. 1998;11:147–8.
94. Tamaru S, Kikuchi A, Ono K, Kita M, Horikoshi T, Takagi K. Prenatal ultrasound and magnetic resonance imaging depiction of a small sublingual ranula. J Clin Ultrasound. 2010;38:147–50.
95. Luna MA, Pineda-Daboin KC. Cysts and unknown primary and secondary tumours of the neck, and neck dissection. In: Cardesa A, Slootweg PJ, editors. Pathology of head and neck. New York: Springer; 2006. p. 263–80.
96. Garcia C, Flores P, Arce J, Chuaqu B, Schwartz D. Ultrasonography in the study of salivary gland lesions in children. Pediatr Radiol. 1998;28:418–25.
97. George MM, Mirza O, Solanki K, Goswamy J, Rothera MP. Serious neonatal airway obstruction with massive congenital sublingual ranula and contralateral occurrence. Ann Med Surg (Lond). 2015;4:136–9.
98. Lack EE. Extragonadal germ cell tumors of the head and neck region: review of 16 cases. Hum Pathol. 1985;16:56–64.
99. Hassan S, Sidek DS, Shah Jihan WD, et al. Massive lingual teratoma in a neonate. Singapore Med J. 2007;48:e212–4.
100. Shetty SJ, Bansal S, Kulkarni SR, Desai R, Bablani D, Prasad P. Benign teratoma of the tongue in a neonate: a case report and review of the literature. Pediatr Dent. 2010;32:245–9.
101. Joolay Y, Stewart C. Congenital cystic mass of the tongue. Arch Dis Child Fetal Neonatal Ed. 2011;96(4):F258.
102. Chiang YC, Shih JC, Peng SS, Hsu WC, Lee CN. Tongue teratoma – a rare form of fetal extragonadal teratoma diagnosed at 30 weeks' gestation. Ultrasound Obstet Gynecol. 2006;28:735–41.
103. Hiebert JC, Johnson AB, Tran HH, Yu Z, Glade RS. Congenital tongue mass with concomitant cleft palate and bifid tongue: a case report and review of the literature. Cleft Palate Craniofac J. 2016;53:245–8.
104. Said S, Breathanch F, Fleming A, Ogunlewe F, Malone FD. Prenatal diagnosis of massive fetal tongue teratoma followed by successful, ex-utero intra-partum treatment. J Obstet Gynaecol. 2009;29:55–7.
105. Sauchet IB. Ultrasonography of the fetal neck in the second and third trimesters. Part 3. Anomalies of the anterior and anterolateral nuchal region. Can Assoc Radiol J. 1995;46:426–33.
106. Choi SS, Zalzal GH. Branchial anomalies: a review of 52 cases. Laryngoscope. 1995;105:909–13.
107. Tsai PY, Chang C, Chang FM. Prenatal imaging of the fetal branchial cleft cyst by three-dimensional ultrasound. Prenat Diagn. 2003;23:605–6.
108. Ribichaud J, Papsin BC, Forte V. Third branchial cleft anomaly detected in utero. J Otolaringol. 2000;29:185–7.
109. Bromley B, Frigoletto Jr FD, Cramer D, Osathanondh R, Benacerraf BR. The fetal thyroid: normal and abnormal sonographic measurements. J Ultrasound Med. 1992;11:25–8.
110. Wenstrom KD, Weiner CP, Williamson RA, Grant SS. Prenatal diagnosis of fetal hyperthyroidism using funipuncture. Obstet Gynecol. 1990;762:513–7.
111. Polak M, Leger J, Luton D, Oury JF, Vuillard E, Boissinot C, Czernichow P. Fetal cord blood sampling in the diagnosis and the treatment of fetal hyperthyroidism in the offsprings of a euthyroid mother, producing thyroid stimulating immunoglobulins. Ann Endocrinol (Paris). 1997;58:338–42.
112. Gulraze A, Kurdi W, Tulbah M, Niaz FA. Prenatal diagnosis and treatment perspective of fetal hypothyroidism with goiter. J Coll Physicians Surg Pak. 2013;23:216–8.
113. Corbacioglu Esmer A, Gul A, Dagdeviren H, Turan Bakirci I, Sahin O. Intrauterine diagnosis and treatment of fetal goitrous hypothyroidism. J Obstet Gynaecol Res. 2013;39:720–3.
114. Boon LM, Enjolras O, Mulliken JB. Congenital hemangioma: evidence of accelerated involution. J Pediatr. 1996;128:329–35.
115. Tsukimori K, Hojo S, Kawarabayashi Y, Nakanami N, Masumoto K, Kohashi K, Tsuneyoshi M, Taguchi T, Wake N. Fetal neck capillary hemangioma associated with Kasabach-Merritt syndrome. J Ultrasound Med. 2007;26:397–401.

116. Watzinger F, Gossweiner S, Wagner A, Richling B, Millesi-Schobel G, Hollmann K. Extensive facial vascular malformations and hemangiomas: a review of the literature and case reports. J Craniomaxillofac Surg. 1997;25:335–43.
117. Mulliken JB, Glowacki J. Hemangiomas and vascular malformations in infant and children: a classification based on endothelial characteristics. Plast Reconstr Surg. 1982;69:412–22.
118. Ozcan UA. Rapidly involuting congenital hemangioma: a case of complete prenatal involution. J Clin Ultrasound. 2010;38:85–8.
119. North PE, Waner M, Brodsky MC. Are infantile hemangiomas of placental origin? Ophthalmology. 2002;109:223–4.
120. Bronsthein M, Bar-Hava I, Blumenfeld Z. Early second trimester sonographic appearance of occipital hemangioma simulating encephalocele. Prenat Diagn. 1992;12:695–8.
121. Bell RL. Ultrasound of hemangioma of the neck of a newborn. J Tenn Med Assoc. 1978;71:289.
122. Lasser D, Preis O, Dor N. Antenatal diagnosis of giant cystic cavernous hemangioma by Doppler velocimetry. Obstet Gynecol. 1988;72:476–7.
123. Tseng JJ, Chou MM, Lee YH, Ho ES. In utero diagnosis of cardiac hemangioma. Ultrasound Obstet Gynecol. 1999;13:363–5.
124. Bulas DI, Johnson D, Allen JF, Kapur S. Fetal hemangioma: sonographic and color flow Doppler findings. J Ultrasound Med. 1992;11:499–501.
125. Krol A, MacArthur C. Congenital hemangiomas: rapidly involuting and noninvoluting congenital hemangiomas. Arch Facial Plast Surg. 2005;7:307–11.
126. Mulliken JB, Enjolras O. Congenital hemangiomas and infantile hemangioma: missing links. J Am Acad Dermatol. 2004;50:875–82.
127. Gorincour G, Kokta V, Rypens F, et al. Imaging characteristics of two subtypes of congenital hemangiomas: rapidly involuting congenital hemangiomas and non-involuting congenital hemangiomas. Pediatr Radiol. 2005;35:1178–85.
128. Konez O, Burrows P, Mulliken J, Fishman SJ, Kozakewich HP. Angiographic features of rapidly involuting congenital hemangioma (RICH). Pediatr Radiol. 2003;33:15–9.
129. Kaplan PA, Williams SM. Mucocutaneous and peripheral soft-tissue hemangiomas: MR imaging. Radiology. 1987;163:163–6.
130. Kramer LA, Crino JP, Slopis J, Hankins L, Yeakley J. Capillary hemangioma of the neck: prenatal MR findings. AJNR Am J Neuroradiol. 1997;18:1432–4.
131. Sabbagha RE, Tamura RK, Dal Campo S. Fetal cranial and craniocervical masses: ultrasound characteristics and differential diagnosis. Am J Obstet Gynecol. 1980;138:511–7.
132. Frieden IJ, Reese V, Cohen D. PHACE syndrome. Arch Dermatol. 1996;132:307–11.
133. Pasual-Castroviejo I, Viano J, Moreno F, Palencia R, Martinez Fernandez V, Pascual-Pascual S, Martinez-Bermejo A, Garcia-Penas J, Roche MC. Hemangiomas of the head, neck, and chest with associated vascular and brain anomalies: a complex neurocutaneous syndrome. AJNR Am J Neuroradiol. 1996;17:461–71.
134. Fadell MF, Jones BV, Adams DM. Prenatal diagnosis and postnatal follow-up of rapidly involuting congenital hemangioma (RICH). Pediatr Radiol. 2011;41:1057–60.
135. Baselga E, Cordisco M, Garzon M, Lee MT, Alomar A, Blei F. Rapidly involuting congenital haemangioma associated with transient thrombocytopenia and coagulopathy: a case series. Br J Dermatol. 2008;158:1363–70.
136. Tonni G, Granese R, Martins Santana EF, Parise Filho JP, Bottura I, Borges Peixoto A, Giacobbe A, Azzerboni A, Araujo Júnior E. Prenatally diagnosed fetal tumors of the head and neck: a systematic review with antenatal and postnatal outcomes over the past 20 years. J Perinat Med. 2017;45:149–65.

Micrognathia

7

Edward Araujo Júnior,
Eduardo Felix Martins Santana, Gabriele Tonni,
Amy E. Wong, and Waldo Sepulveda

7.1 Introduction

Micrognathia is a malformation characterized by congenital hypoplasia of the mandible [1]. In severe cases, the mandible can be absent (agnathia), which is associated with abnormal positioning of the lower ears ventromedially toward the front of the neck (melotia or synotia), hypo- or aglossia, and microstomia. The incidence of moderate to severe micrognathia is 1 per 1000 live births [1]. In these cases, this condition can occlude the fetal airway and complicates the establishment of the newborn's airway after birth. Severe micrognathia that is not previously diagnosed or treated prior to birth can lead to death shortly after birth (Fig. 7.1) [2].

E. Araujo Júnior (✉) • E.F.M. Santana
Department of Obstetrics, Paulista School of Medicine – Sao Paulo Federal University of Sao Paulo (EPM-UNIFESP), Sao Paulo, Brazil
e-mail: araujojred@terra.com.br

G. Tonni, MD, PhD
Department of Obstetrics and Gynecology, Prenatal Diagnostic Service, Guastalla Civil Hospital, AUSL Reggio Emilia, Reggio Emilia, Italy

A.E. Wong
Department of Maternal-Fetal Medicine, Palo Alto Medical Foundation, Mountain View, CA, USA

W. Sepulveda
Fetalmed – Maternal-Fetal Diagnostic Center, Santiago, Chile

After the sixth gestational week, mandibular development begins with fusion of ectoderm of the branchial arches and neural crest cells from the dorsal neural tube [3]. This complex process is influenced by both environmental and genetic factors. Micrognathia is the result of hypoplasia of the neural crest cell population and can occur in isolation as in primary mandibular disorders or, more frquently, associated with other conditions such as chromosomal aberrations (particularly triploidy, trisomy 18, and trisomy 9) (Fig. 7.2), genetic syndromes, and other structural anomalies (Fig. 7.3) [4, 5].

Using the technology available in the current era of prenatal diagnosis, three-dimensional (3D) and four-dimensional (4D) ultrasound can visualize the mandible as early as 10 weeks of gestation and permit its detailed evaluation using indices, ratios, and facial angles, as well as mandibular growth charts [6, 7]. However, the diagnosis of a mandibular abnormality and its relationship with multiple malformations when present in complex syndromes remains challenging.

Although ultrasound is the established standard for fetal bone visualization, magnetic resonance imaging (MRI) may be a useful adjunct after 18 weeks of gestation by potentially providing additional details of the mandibular anatomy as well as of other abnormalities that may be present [8]. Despite these tools, assessing the severity of micrognathia is still a challenge for perinatologists. Nevertheless, prenatal evaluation

G. Tonni, W. Sepulveda, and A.E. Wong (eds.), *Prenatal Diagnosis of Orofacial Malformations*,
DOI 10.1007/978-3-319-32516-3_7

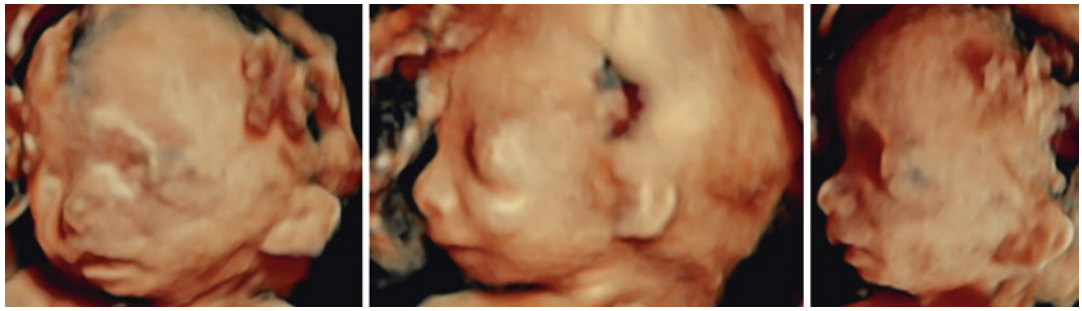

Fig. 7.1 Three-dimensional ultrasound with post-processing rendering using HDLive™ shows a midtrimester fetus with micrognathia and low-set ears (Courtesy of Dr. G. Grisolia)

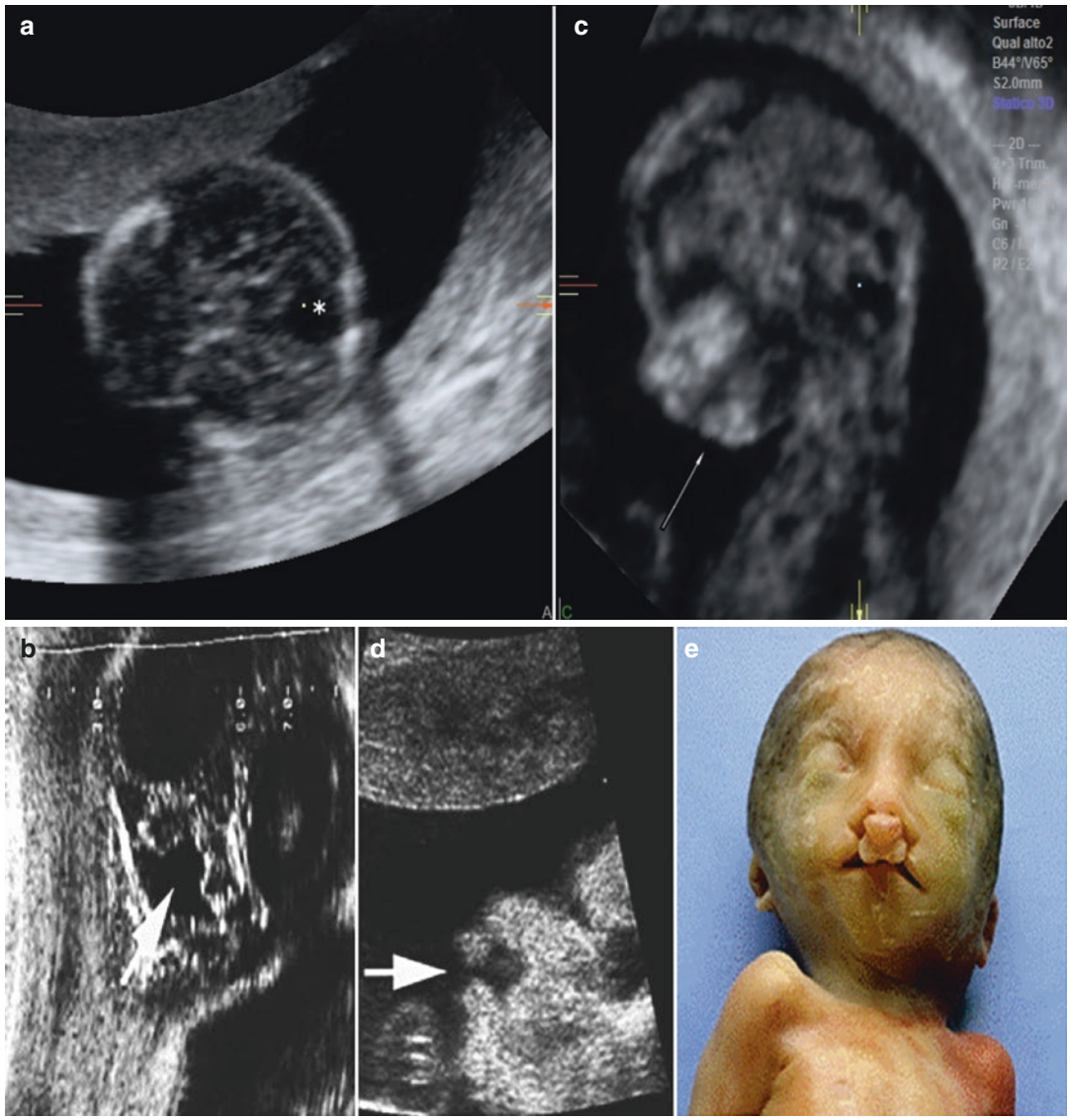

Fig. 7.2 Midtrimester fetus with (**a**, **b**) cerebellar vermian defect (*arrow*), (**c**) micrognathia (*arrow*), and (**d**) cleft lip and palate (*arrow*). (**e**) Postmortem examination confirmed bilateral cleft lip and palate. (**f**) This infant had trisomy 9 (From Tonni et al. [75])

Fig. 7.2 (continued)

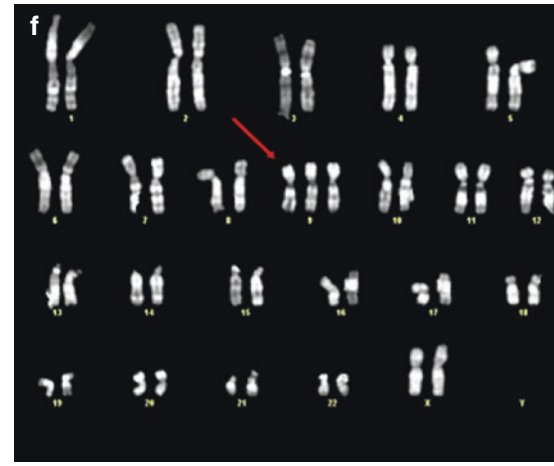

of the fetal facial anatomy is necessary to optimize intrapartum management.

7.2 Genetic Syndromes Associated with Micrognathia

7.2.1 Pierre Robin Syndrome

Pierre Robin Syndrome (PRS, OMIM 261800) is a rare heterogeneous genetic disorder characterized by retro- or micrognathia, glossoptosis, and cleft palate independent of the respiratory and feeding difficulties or the size of the posterior cleft [9]. PRS is an autosomal recessive disorder caused by a mutation on chromosome 17q24.3-q25.1. In a recent study, the visualization of a cleft in the posterior palate in addition to retro- or micrognathia had a positive predictive value of 100 % for PRS [10]. The incidence of PRS has been estimated to occur in 1 of 14,000 live births [11]. PRS can be associated with several genetic disorders including trisomy 21, trisomy 13 [12], 46,XX/XY del(22)(q11), del(4)(q31), del(4)(p-), inv(9)(p11;q12), inv(9)(p11q13), t(X;2) and del(14(qter) [9]. In addition to the classic triad (retro- or micrognathia, glossoptosis, and cleft palate), PRS is also associated with other malformations such as macro- or microglossia, auricular malformations, nasal deformities, dental malformations, and laryngomalacia. Extracranial anomalies are observed in 10–85 % of cases and consist of ocular, cardiovascular, musculoskeletal, neurologic, and genitourinary abnormalities [13].

Prenatal diagnosis of PRS is critical because the tongue may significantly obstruct the airway at the time of birth [2]. Antenatal identification, therefore, allows delivery planning with a multidisciplinary team present at delivery to assist the newborn [12]. The diagnosis is most commonly made in the second trimester of pregnancy when severe retro- or micrognathia is visualized on two-dimensional (2D) ultrasound. Typically, polyhydramnios subsequently develops due to obstruction of oropharynx [13]. 3D ultrasound in the rendering mode allows improved spatial visualization of the fetal face, which is useful for counseling of the parents (Figs. 7.4 and 7.5) [13]. First-trimester diagnosis of PRS has been reported after transvaginal evaluation identified the typical facial dysmorphisms [14, 15]. MRI may also be helpful when the diagnosis is uncertain [8, 16]. However, the detection rate of PRS using 2D ultrasound is low, ranging from 7 to 22 % [17].

After PRS is prenatally identified, the parents should strongly consider genetic amniocentesis because many different genetic disorders may be associated with this syndrome. These include trisomy 13, trisomy 18, cerebrocostomandibular syndrome, CHARGE syndrome (coloboma, heart

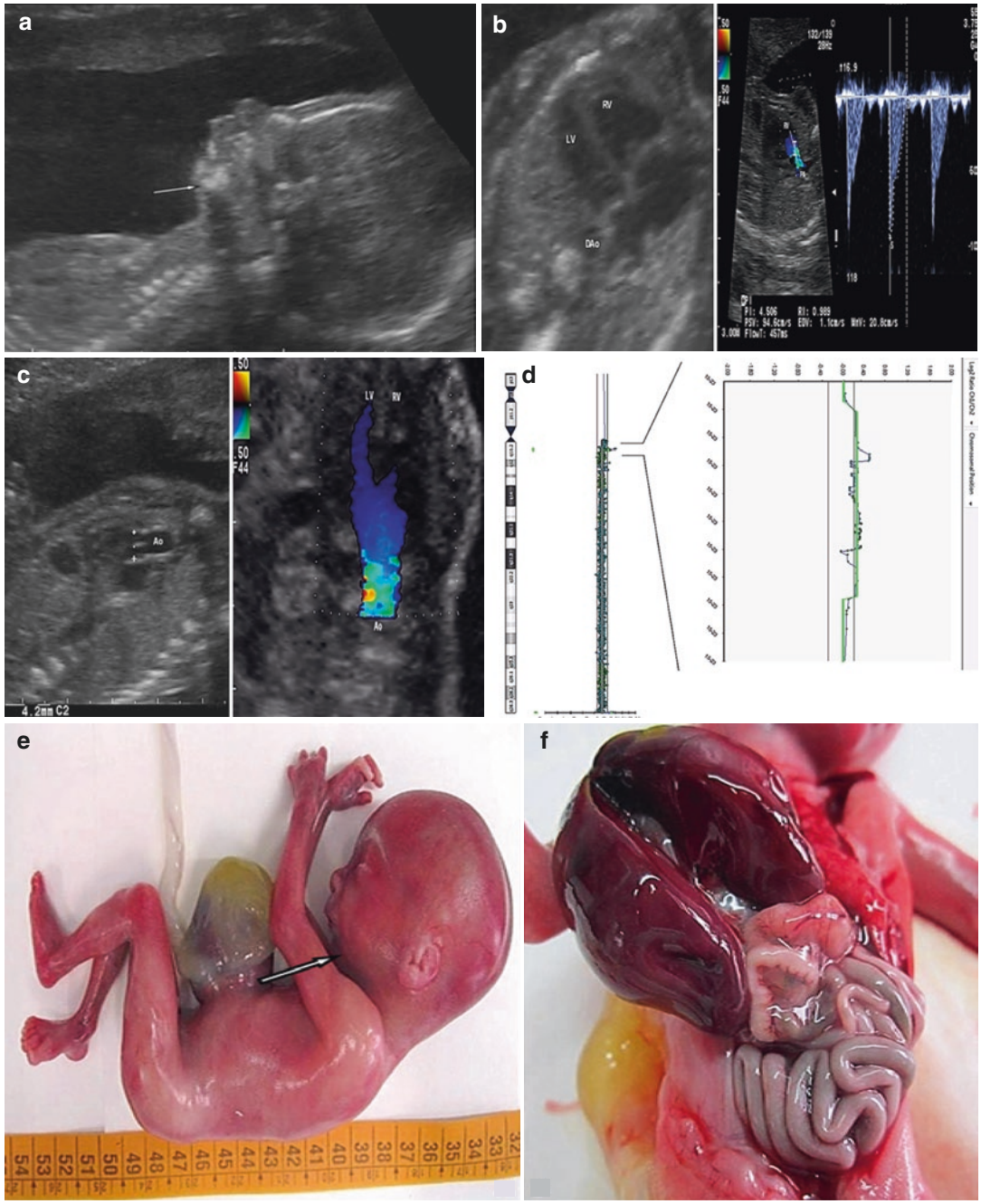

Fig. 7.3 Micrognathia detected by two-dimensional ultrasound in a midtrimester fetus with normal karyotype (**a**) with associated tetralogy of Fallot (**b**, **c**) and exomphalos. Array-CGH demonstrated a 15q.11 microduplication (**d**), with the father as a carrier. Autopsy findings (**e**, **f**) confirm micrognathia (*arrow*) and exomphalos (From Tonni et al. [76])

anomaly, choanal atresia, retardation, genital abnormalities, and ear anomalies), velocardiofacial syndrome, Treacher Collins syndrome, Beckwith–Wiedemann syndrome, Cornelia de Lange syndrome, Smith–Lemli–Opitz syndrome, and Hanhart syndrome [10, 14]. Several cases of PRS have also been reported in the context of Stickler syndrome, which is a rare autosomal

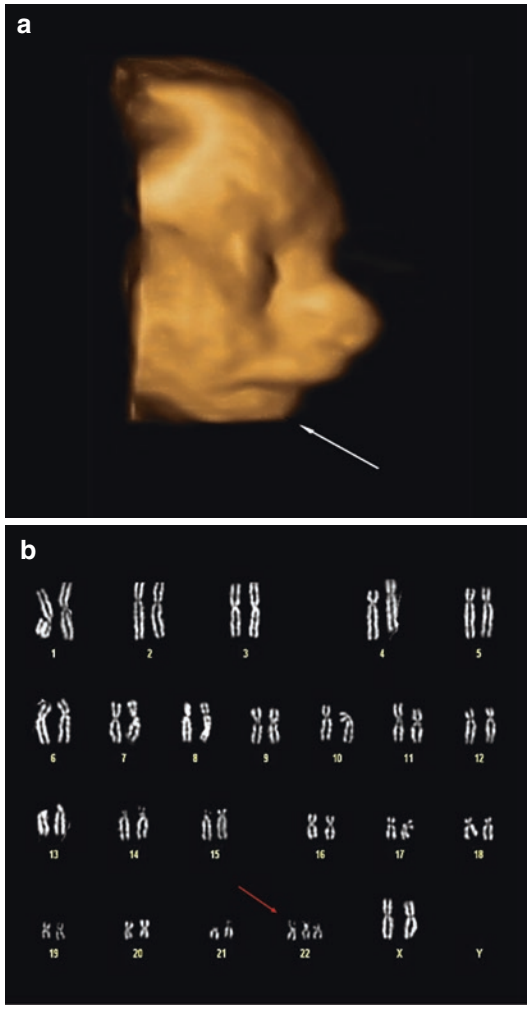

Fig. 7.4 Micrognathia (*arrow*) detected by three-dimensional ultrasound in a second-trimester fetus (**a**) with trisomy 22 (**b**) (From Tonni et al. [77])

dominant connective tissue disorder estimated to affect approximately 1 in 7500 newborns [18]. Stickler syndrome, however, is characterized by ocular manifestations, arthritic changes, orofacial features, and deafness. Ophthalmologic anomalies are the most characteristic and most serious manifestations of the syndrome [19]. The presence of PRS phenotype during prenatal ultrasound in a patient with a family history of Stickler syndrome should raise significant suspicion of recurrence.

The prognosis of PRS usually is very good when it is isolated. After birth, tracheostomy is usually indicated to improve respiratory function. Surgeries to correct the mandibular dysmorphology and the cleft palate are performed between 6 and 18 months of life. Breathing difficulties gradually improve and may resolve completely due to growth of the mandible [13]. The long-term outcome depends on whether the PRS is isolated or associated with other malformations or syndromes. Even when there are associated anomalies, the survival rate of PRS can be as high as 90 %, although mental retardation occurs in 15 % of cases [12].

7.2.2 Neu–Laxova Syndrome

Neu–Laxova syndrome (NLS, OMIM 256520) is a rare, autosomal recessive syndrome that is lethal. NLS is characterized by severe intrauterine growth restriction (IUGR), flexion contractures of the limbs, microcephaly, edema particularly affecting the hands and feet, and ichthyosis [20]. Additional features include micrognathia, exophthalmos, cystic hygroma, cleft lip/palate, lissencephaly, cryptorchidism, and pulmonary hypoplasia [21].

The prenatal diagnosis of NLS by 2D ultrasound is possible in the second and third trimesters of pregnancy. As a lethal condition, the appropriate prenatal diagnosis is important to the parental counseling, particularly for consanguineous parents [22]. The main prenatal ultrasound findings in a series of seven cases are the following: low-set/malformed ears, flat/abnormal nose, micrognathia, microcephaly, rocker-bottom feet, IUGR, short neck, and increased adipose tissue [20]. The absence of breathing movements, suckling, swallowing, or isolated arm and leg movements may also be detected in the third trimester [23]. The association of this syndrome with polyhydramnios is reported in the literature [21, 24]. MRI is important to better assess the central nervous system for abnormalities.

Differential diagnoses include fetal akinesia/hypokinesia syndrome, cerebro-oculo-facioskeletal (COFS) syndrome, lethal multiple pterygium syndrome, Pena–Shokeir phenotype, Cornelia de Lange syndrome, Freeman–Sheldon syndrome, Miller–Dieker syndrome, Seckel syndrome, Smith–Lemli–Opitz syndrome, and intrauterine infections [21, 24]. The karyotype is typically normal [24].

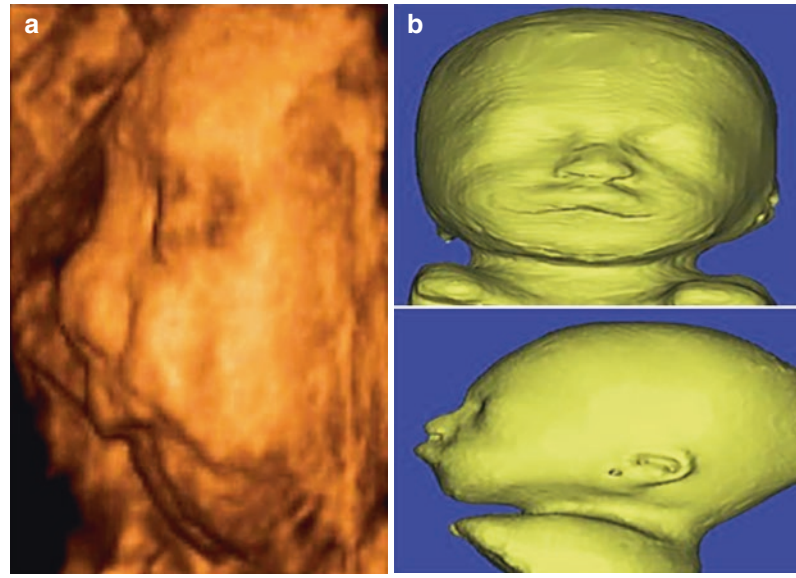

Fig. 7.5 (**a**) Three-dimensional ultrasound in surface rendering mode shows micrognathia in a fetus with Pierre Robin syndrome. (**b**) Three-dimensional virtual physical model printed on photopolymerized resin

7.2.3 Wolf–Hirschhorn Syndrome

Wolf–Hirschhorn syndrome (WHS, OMIM 194190) is a congenital disorder caused by microdeletion of the short arm of chromosome 4 (del 4p16.3), which encodes genes including MSX1, WHSC1, and LETM1 [25]. Most of these deletions occur *de novo*, but 15 % are due to a structural chromosomal rearrangement in one of the parents [26]. The incidence of this rare condition has been estimated to be around 1/50,000 births [27]. WHS is characterized by intrauterine growth restriction (IUGR), mental retardation, characteristic facial dysmorphism, microcephaly, ear lobe anomalies, and closure defects (cleft lip or palate, coloboma of the eye, and cardiac septal defects) [26]. The prenatal diagnosis is possible in the second and third trimesters by 2D and 3D ultrasound when the following malformations are observed: severe IUGR, microcephaly, and a characteristic facies with "Greek warrior helmet" appearance (prominent glabella, high-arched eyebrows, hypertelorism, and a broad high nasal bridge continuing to the forehead), short philtrum, carp-shaped mouth, micrognathia, and low-set ears that frequently have pits and tags (Fig. 7.6) [28, 29]. In a series of 10 cases, the main prenatal ultrasound findings were IUGR, microcephaly, high forehead, micrognathia, prominent glabella, and hypertelorism [30]. Hypospadias in male fetuses is another prominent finding [29].

The microdeletion of the short arm of chromosome 4 is a de novo mutation in most cases; parental testing may demonstrate a balanced translocation in other cases [31]. The main differential diagnoses are the following: Pitt–Rogers–Danks syndrome, Opitz BBB (oculogenitolaryngeal) syndrome, Fryns syndrome, Jacobsen syndrome, triploidy, trisomy 9, and trisomy 18 [25, 32].

The prognosis of WHS depends on its associated malformations. When congenital heart disease is present, there is a 30 % risk of mortality in first 2 years of life. Epilepsy is a primary characteristic; mental retardation is also common. Respiratory infections (including aspiration pneumonia, otitis media, sinusitis, or chronic cough) are very common finding in patients with WHS. Children with WHS also suffer from immunodeficiency. Other complications are the various tooth anomalies, including multiple tooth agenesis and taurodontism [25].

7.2.4 Cornelia de Lange Syndrome

Cornelia de Lange syndrome (CDLS, OMIM 122470), also known as Brachmann–de Lange syndrome [33], has an estimated prevalence of 1 in

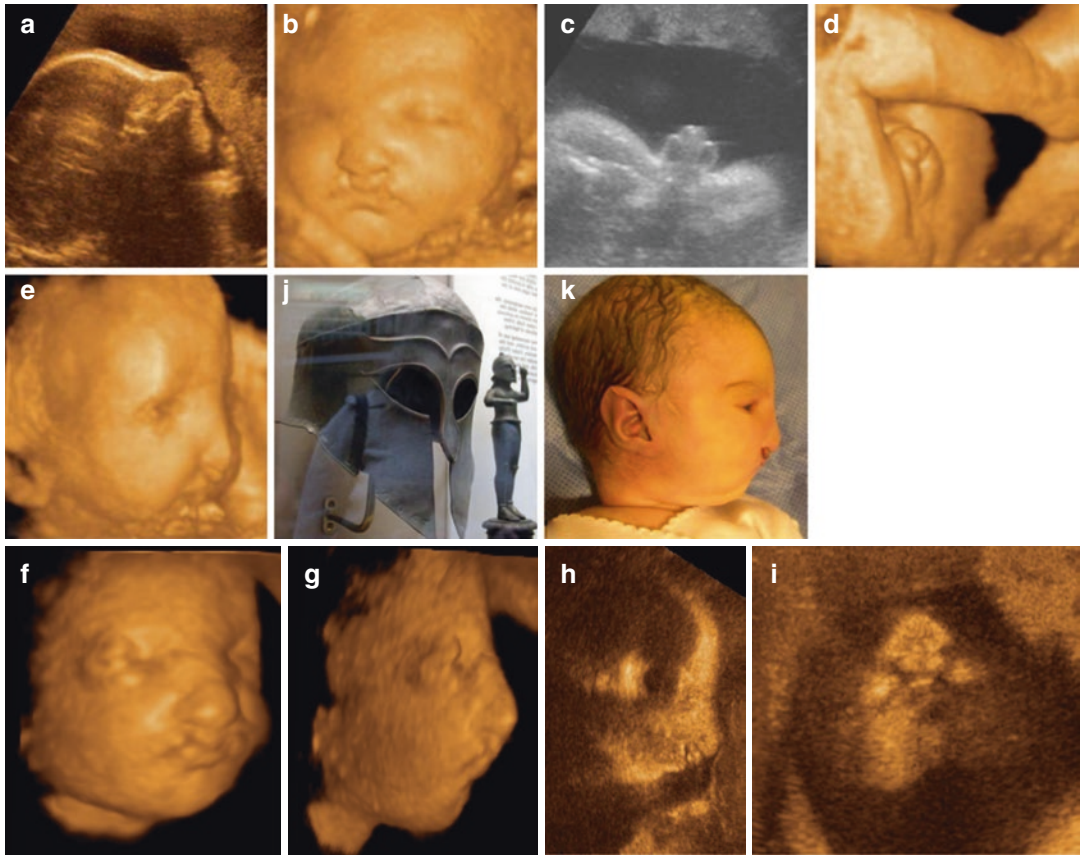

Fig. 7.6 Two- and three-dimensional findings in a male fetus with Wolf-Hirschhorn syndrome (**a-i**). Example of Greek warrior helmet (**j**) and infant with this resemblance (**k**) (From Sepulveda [29])

10,000. Most cases are sporadic resulting from de novo dominant mutations [34]. Mutations of the NIPBL gene, which are typically de novo and associated with an autosomal dominant inheritance, are present in approximately 60% of patients with CDLS [34]. The main characteristics in this syndrome are facial and limb abnormalities that present in combination with intrauterine and postnatal growth restriction [35]. Other frequent findings are cardiac defects, hirsutism, gastrointestinal abnormalities, and severe mental retardation [36].

Prenatal diagnosis of CDLS is possible by 2D and 3D ultrasound in the second and third trimesters of pregnancy, although the accuracy is low [37]. Prenatal ultrasound findings include severe IUGR <5th percentile, long eyelashes, disproportionate shortening of the long bones, depression of the bridge of the nose, and overriding of the upper lip (Fig. 7.7) [38–40]. In a report of seven cases, the main prenatal ultrasound findings were the following: IUGR, radial dysplasia/aplasia, ulnar dysplasia/aplasia, oligodactyly, small nose, prominent upper lip, micrognathia, and skin edema [41].

Although the syndrome is heterogeneous, the overall prognosis is rather poor as 20% of affected children die during the first 2 years of life, while the rest usually face feeding problems, neurodevelopmental delay, and mental retardation similar to autism [42]. Children with CDLS have significant developmental delay and are unable to live without community support; even when phenotypic features are mild, children show poor communication, a delay in the acquisition of verbal skills, and overall significantly impaired cognitive development [43]. Because of this poor prognosis, prenatal diagnosis is very important to provide parental counseling and the option for termination of pregnancy.

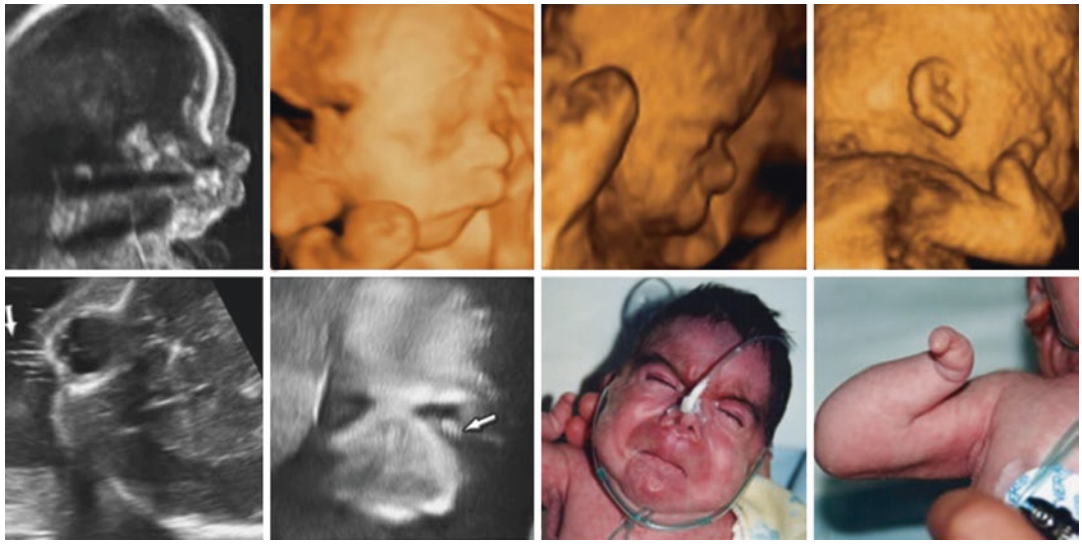

Fig. 7.7 Two- and three-dimensional ultrasound findings in fetus with Cornelia de Lange syndrome. Note frontonasal edema, micrognathia, long philtrum, long eyelashes, and abnormal upper limb (From Sepulveda et al. [39])

7.2.5 Nager Syndrome

Nager syndrome (NS, OMIM 154400), or acrofacial dysostosis, is a heterogeneous syndrome that combines mandibulofacial dysostosis (micrognathia and ear anomalies) with limb defects [44]. The etiology is unknown; both autosomal dominant and recessive inheritance patterns have been hypothesized in some families, and teratogens such as retinoic acid have been linked [44, 45]. Heterozygous mutations in the SF3B4 gene on chromosome 1q12–q21 were found to be responsible for a subset of sporadic and autosomal dominant cases [46]. Depending on the type of limb defect, two major groups have been defined: NS, which has predominant preaxial anomalies, and Genee–Wiedemann or Miller syndrome, which is associated with postaxial malformations [47].

Few cases of NS that have been diagnosed in the prenatal period have been described in the literature. However, the diagnosis is possible in the second and third trimesters based on the following 2D and 3D ultrasound findings: severe micrognathia and limb malformations including the absence of thumbs, the absence of both the fibula and tibia, and shortening of the humerus and femurs (Fig. 7.8). Familiar cases of acrofacial dysostosis may help in the diagnosis. The karyotype is usually normal [44, 45, 47, 48].

The differential diagnosis includes trisomy 18, Treacher Collins syndrome, Richieri–Costa–Pereira syndrome, thrombocytopenia–absent radius (TAR) syndrome, and Roberts syndrome [47]. Recently, SF3B4 mutations have been associated with NS; this suggests that at least some cases of Rodriguez syndrome are either allelic to or represent unusually severe manifestations of NS [49].

Prenatal diagnosis is important because the severe micrognathia can obstruct the upper airways with risk of respiratory insufficiency [48]. The prognosis is poor, and these children undergo several surgeries during childhood to correct the facial and limb dysmorphisms. Genetic counseling, including the option of termination of pregnancy, is important [47].

7.2.6 Femoral–Facial or Femoral Hypoplasia–Unusual Facies Syndrome

Femoral–facial syndrome (FFS, OMIM 134780) or femoral hypoplasia–unusual facies syndrome was first described in 1975 by Daentl et al. and is

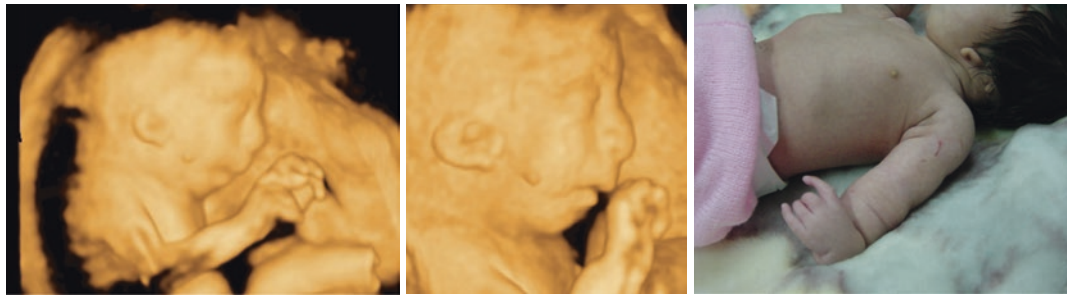

Fig. 7.8 Three-dimensional ultrasound in a fetus with Nager syndrome. Note micrognathia, abnormal ears, skin tag, and abnormal upper limbs

characterized by femoral hypoplasia (or aplasia) and specific facial dysmorphic features. It is usually described in association with other malformations such as renal, neural, skeletal, and genital anomalies [50, 51].

FFS occurs sporadically in females and seems to be associated with maternal diabetes or hyperglycemia, exposure to drugs (thalidomide), viral infections, radiation, focal ischemia or trauma, as well as severe fetal constraint secondary to oligohydramnios [52]. Some studies have suggested an autosomal dominant pattern of inheritance; however, there are no reports of chromosomal abnormalities in their carriers [53].

The facial malformations include micrognathia, low-set or dysplastic ears, cleft lip and palate, upslanting palpebral fissures, short nose with broad tip, long philtrum, and thin upper lip. Skeletal anomalies include sacral dysgenesis, talipes equinovarus, absent or hypomorphic tibia or fibula, humeroradial synostosis, syndactyly, and polydactyly. Renal defects, such as abnormal collecting urinary system, dysplasia or agenesis of kidneys, or multicystic kidneys, may be present. Associated genital anomalies include cryptorchidism, hypoplastic labia, and macrophallus. Central nervous system defects include ventriculomegaly, hydrocephalus, partial agenesis of the corpus callosum, and neuronal migration defects [54]. The subtrochanteric region of the femoral cartilage is also affected and causes shortening of the femoral proximal region. This is typically unilateral, with only 10–15 % of cases involving the legs bilaterally [55].

The prenatal diagnosis of FFS relies on a major defect of the skeletal or craniofacial region in addition to the femoral hypoplasia. The presence of a third malformation, such as unilateral renal agenesis or a spinal or central nervous system abnormality, can lead to the diagnosis [51]. 2D ultrasound can provide a complete evaluation, but 3D ultrasound images may enhance the detection of facial dysmorphisms [51]. MRI may assist in the identification of abnormalities that can lead to the prenatal diagnosis.

7.2.7 Larsen Syndrome

Larsen syndrome (LRS, OMIM 150250) was first described in 1950. The facial features first described were a prominent forehead, a depressed nasal bridge, and widely spaced eyes. Additional reports have presented other characteristics such as hydrocephalus, cleft palate, cardiac malformations, and spinal abnormalities [56]. Autosomal dominant and autosomal recessive patterns of inheritance have been proposed. Different patterns of inheritance could explain the clinical variability that is seen with this syndrome [57].

Larsen-like syndrome, a lethal variant of LRS, was reported by Chen et al. [58]. The characteristic features were tracheomalacia, multiple joint dislocations, pulmonary hypoplasia, collagen abnormalities, and nonimmune hydrops. Other studies have also shown abnormalities of collagen of joint capsules, cartilage matrix, and hyaline cartilage of the trachea [59]. The presence of bifid tongue and severe micrognathia can be

associated and cause respiratory problems at birth. Autosomal recessive inheritance was proposed for this variant [60].

Autosomal dominant LRS is caused by mutations or small frame deletions on the short arm of chromosome 3 involving the FLNB gene, which encode the cytoskeletal protein filamin B. However, the gene involved in the autosomal recessive form of LS is still unknown. The reported patients with Larsen-like syndrome had a mutation in a gene involved in collagen production, which is located either on chromosome 1q or, more likely, on 6p [61]. In these cases, fetal karyotype is normal and the diagnosis is usually made postmortem. Genetic counseling is very important to assess for the recurrence risk of this syndrome. In parents with a previously affected fetus, early sonographic examination should be performed, and DNA mutation analysis by chorionic villous sampling can lead to diagnosis of LRS at an early gestational age [62].

7.2.8 Treacher Collins Syndrome

Treacher Collins syndrome (TCS, OMIM 154500) is an autosomal dominant disorder that is also associated with micrognathia and other findings, such as ear malformations, lower eyelid coloboma, zygomatic hypoplasia, downward-slanting palpebral fissures, hearing loss, cleft lip/palate, and scalp hair extending onto the cheeks. The incidence of TCS is 1 in 50,000 live births, and it is sometimes underestimated because of variable phenotype [63].

Mosaic individuals can be clinically unaffected; even affected individuals usually have adequate intelligence and life span despite the facial malformations. Patients with TCS may have initial respiratory problems at birth requiring airway access with tracheostomy and intubation. Sometimes individuals undergo multiple reconstructive surgeries in early life.

Studies have identified involvement of chromosome locus 5q31-q34 and the disease gene TCOF1 [64]. This specific gene encodes the nuclear phosphoprotein treacle, which is involved in microtubule dynamics, ribosomal biogenesis, rDNA transcription, nucleogenesis, or trafficking of proteins or ribosomal subunits between the nucleolus and cytoplasm [65]. The process of neuroepithelial apoptosis during early embryogenesis is affected, particularly in neural crest cells. At least 130 mutations in the TCOF1 gene (reported in 78–93 % of individuals with TCS) have been reported.

Prenatal sonographic diagnosis for TCS is still a challenge. Abnormal 2D ultrasound findings may be identified on the midsagittal view of the fetal face, although it has been reported that the true midsagittal profile is visualized in only 69 % of attempts. The addition of 3D ultrasound allows greater image detail and identification of minor abnormalities of the jaw [66] (Fig. 7.9).

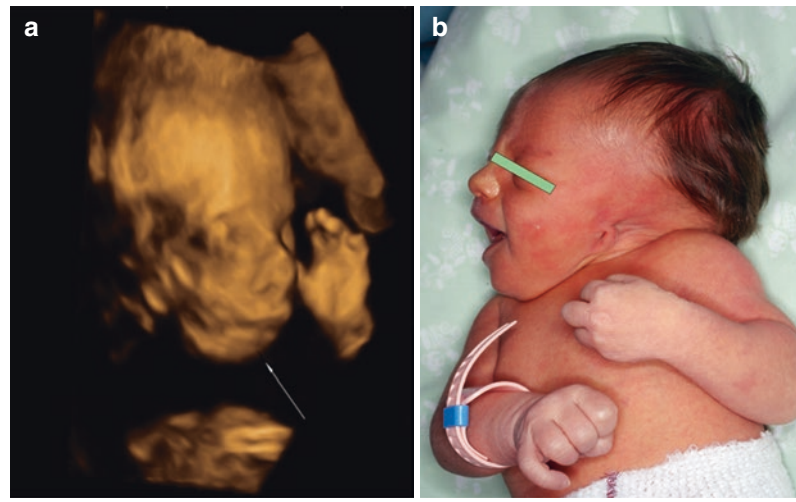

Fig. 7.9 (**a**) Three-dimensional ultrasound (3D) shows micrognathia (*white arrow*) in a fetus with Treacher Collins syndrome. (**b**) Photograph of the newborn infant shows micrognathia and abnormal ear

The differential diagnosis includes Goldenhar syndrome, NS, and PRS. Goldenhar syndrome may be sporadic or be inherited as autosomal dominant in familial cases. The genotype/phenotype shows a wide spectrum from oculoauriculo to vertebral dysplasia. The syndrome usually affects half of the face with micromelia and epibulbar dermoids. Radial defect may be also part of the spectrum. NS involves mandibulofacial dysostosis and preaxial reduction defects of the upper limbs, ranging from radial hypoplasia to aplasia of the thumb with or without involvement of the radius. Finally, the primary finding of PRS sequence is early mandibular hypoplasia and associated anomalies restricted to this area.

7.2.9 Pena–Shokeir Syndrome

Pena-Shokeir syndrome, type 1 (PSS, OMIM 208150), or fetal akinesia deformation sequence, is a rare and lethal syndrome that was first described in 1974 [67]. It is characterized by multiple joint contractures (arthrogryposis), facial anomalies (micrognathia), polyhydramnios, fetal growth restriction, and pulmonary hypoplasia. Its incidence is estimated at 1 in 12,000 births. It is an autosomal recessive disease. There are phenotypic variations that show decreased or even the absence of movement in the uterine environment, with consequent fetal akinesia, which can cause a series of deformities [67]. Limb contractures and muscle atrophy result from lack of adequate movement [68]. Lung development stagnates around the 15th week of pregnancy, during the canalicular phase, leading to pulmonary hypoplasia within the diminished thoracic cavity. This occurs due to the absence of early respiratory movements that allow adequate development of the diaphragm and intercostal muscles. The decreased fetal swallowing results in polyhydramnios, and the underdevelopment of facial muscles explains the craniofacial defects [68].

Even with a considerable number of differential diagnoses, PSS shows similarities to trisomy 18, such as arthrogryposis and micrognathia. If the karyotype is normal and the fetus presents micrognathia, arthrogryposis, and lack of movement, PSS can then be considered as the diagnostic possibility [69]. Although PSS cannot be consistently diagnosed using genetic testing, mutations in the DOK-7 and RASPSN genes have been associated with the syndrome.

The care that should be provided for subsequent pregnancies for couples who have had a fetus with PSS includes serial assessments using ultrasound, with the aim of achieving early detection of abnormalities. However, since the phenotypic condition is derived from heterogeneous causes, the counseling for couples to provide guidance regarding recurrence is imprecise. It has been estimated that the risk in the next pregnancy is around 0–25 % [70].

The addition of 3D ultrasound in rendering mode often permits more detailed evaluation of the suspected fetal abnormality, thereby complementing the 2D ultrasound technique [71]. It also allows improved understanding of the condition by the parents. Ruano et al. [72] reported on the benefit of 3D ultrasound in evaluating fixed postural abnormalities of the extremities and of the limbs of the fetus. In a study from our group, this technique was of unquestionable importance to aid in the understanding the disease [71].

The other imaging modality to diagnose PSS is MRI. Gupta et al. [73] reported a case of a 28-week fetus with kyphoscoliosis and reduced movements. MRI using T1-weighted, T2-weighted half-fourier acquisition single-shot turbo spin echo (HASTE) and true fast imaging with steady-state precession (TrueFISP) sequences was performed to analyze the fetus. 2D ultrasound and MRI demonstrated distorted spine with scoliosis, persistent flexion of the wrists, elbow joints, knee joints, and bilateral club foot; however, retro-or micrognathia and pulmonary hypoplasia were also present and were better depicted on MRI. Although MRI is not essential in the diagnosis of PSS, it should be requested in cases where there is suspicion of fetal central nervous system anomalies.

PSS phenotype is considered a lethal disorder; although some cases reach the age of 1 year, most patients rarely survive to the neonatal period. Therefore, if the diagnosis is made prenatally, termination of pregnancy may be offered [74].

Conclusion

In summary, 2D ultrasound is necessary for early detection of micrognathia and associated fetal defects. 3D ultrasound and MRI are useful adjuncts that allow improved characterization of fetal abnormalities. There are numerous syndromes that involve micrognathia as a feature. Prenatal evaluation must be detailed to develop a differential diagnosis and appropriate genetic counseling must be offered to the parents.

References

1. Sanz-Cortes M, Gomez O, Puerto B. Micrognathia and retrognathia. In: Copel JA, editor. Obstetric imaging. 1st ed. Philadelphia: Elsevier Saunders; 2012;358–65.
2. Morris LM, Lim FY. Severe micrognathia: indications for EXIT-to-Airway. Fetal Diagn Ther. 2009;26:162–6.
3. Paladini D. Fetal micrognathia: almost always an ominous finding. Ultrasound Obstet Gynecol. 2010;35:377–84.
4. Luedders DW, Bohlmann MK, Germer U, Axt-Fliedner R, Gembruch U, Weichert J. Fetal micrognathia: objective assessment and associated anomalies on prenatal sonogram. Prenat Diagn. 2011;31:146–51.
5. Bromley B, Benacerraf BR. Fetal micrognathia: associated anomalies and outcome. J Ultrasound Med. 1994;13:529–33.
6. Otto C, Platt LD. The fetal mandible measurement: an objective determination of fetal jaw size. Ultrasound Obstet Gynecol. 1991;1:12–7.
7. Watson WJ, Katz VL. Sonographic measurement of the fetal mandible: standards for normal pregnancy. Am J Perinatol. 1993;10:226–8.
8. Mirsky DM, Shekdar KV, Bilaniuk LT. Fetal MRI: head and neck. Magn Reson Imaging Clin N Am. 2012;20:605–18.
9. Gorlin RJ, Cohen MM, Hennekam RCM. Syndromes of the head and neck. Oxford/New York: Oxford University Press; 2001.
10. Lind K, Aubry MC, Belarbi N, Chalouhi C, Couly G, Benachi A, Lyonnet S, Abadie V. Prenatal diagnosis of Pierre Robin sequence: accuracy and ability to predict phenotype and functional severity. Prenat Diagn. 2015;35:853–8.
11. Printzlau A, Andersen M. Pierre Robin sequence in Denmark: a retrospective population-based epidemiological study. Cleft Palate Craniofac J. 2004;41:47–52.
12. Hsieh YY, Chang CC, Tsai HD, Yang TC, Lee CC, Tsai CH. The prenatal diagnosis of Pierre Robin sequence. Prenat Diagn. 1999;19:567–9.
13. Chiriac A, Dawson A, Krapp M, Axt-Fliedner R. Pierre Robin syndrome: a case report. Arch Gynecol Obstet. 2008;277:95–8.
14. Teoh M, Meagher S. First-trimester diagnosis of micrognathia as a presentation of Pierre Robin syndrome. Ultrasound Obstet Gynecol. 2003;21:616–8.
15. Bijok J, Massalska D, Michalowska A, Roszkowski T, Ilnicka A, Pawlowska B, Jakiel G. Severe micrognathia in the first trimester in complete trisomy 9 – a case report and literature review. Arch Perinat Med. 2012;18:173–7.
16. Nemec U, Nemec SF, Brugger PC, Weber M, Bartsch B, Bettelheim D, Gruber M, Prayer D. Normal mandibular growth and diagnosis of micrognathia at prenatal MRI: mandibular growth at prenatal MR imaging. Prenat Diagn. 2015;35:108–16.
17. Maarse W, Berge SJ, Pistorius L, van Barneveld T, Kon M, Breugem C, Mink van der Molen AB. Diagnostic accuracy of transabdominal ultrasound in detecting prenatal cleft lip and palate: a systematic review. Ultrasound Obstet Gynecol. 2010;35:495–502.
18. Pacella E, Malvasi A, Tinelli A, Laterza F, Dell'Edera D, Pacella F, Mazzeo F, Ferraresi A, Malarska KG, Cavallotti C. Stickler syndrome in Pierre Robin sequence prenatal ultrasonographic diagnosis and postnatal therapy: two cases report. Eur Rev Med Pharmacol Sci. 2010;14:1051–4.
19. Soulier M, Sigaudy S, Chau C, Philip N. Prenatal diagnosis of Pierre Robin sequence as part of Stickler syndrome. Prenat Diagn. 2002;22:567–8.
20. Rode ME, Mennuti MT, Giardine RM, Zackai EH, Driscoll DA. Early ultrasound diagnosis of Neu-Laxova syndrome. Prenat Diagn. 2001;21:575–80.
21. Durr-e-Sabih, Khan AN, Sabih Z. Prenatal sonographic diagnosis of Neu-Laxova syndrome. J Clin Ultrasound. 2001;29:531–4.
22. Badakali M, Badakali A, Dombale V. Rare manifestations of Neu-Laxova syndrome. Fetal Pathol Pediatr. 2012;31:1–5.
23. Aslan H, Gul A, Polat I, Mutaf C, Agar M, Ceylan Y. Prenatal diagnosis of Neu-Laxova syndrome: a case report. BMC Pregnancy Childbirth. 2002;2:1.
24. Martin A, Eguiluz I, Barber MA, Medina N, Plasencia W, Garcia-Alix A, Garcia-Hernandez JA. A rare cause of polyhydramnios: Neu-Laxova syndrome. J Matern Fetal Neonatal Med. 2006;19:439–42.
25. Paradowska-Stolarz AM. Wolf-Hirschhorn syndrome (WHS) – literature review on the features of the syndrome. Adv Clin Exp Med. 2014;23:485–9.
26. Lurie I, Lazjuk G, Ussova Y, Presman E, Gurevich D. The Wolf–Hirschhorn syndrome I. Genet Clin Genet. 1980;17:375–84.
27. Goodman R, Gorlin R. The malformed infant and child. New York: Oxford University Press; 1983. p. 90.
28. Dietze I, Fritz B, Huhle D, Simoens W, Piecha E, Rehder H. Clinical, cytogenetic and molecular investigation in a fetus with Wolf-Hirschhorn syndrome with paternally derived 4p deletion. Case report and review of the literature. Fetal Diagn Ther. 2004;19:251–60.

29. Sepulveda W. Prenatal 3-dimensional sonographic depiction of the Wolf-Hirschhorn phenotype: the 'Greek warrior helmet' and 'tulip' signs. J Ultrasound Med. 2007;26:407–10.
30. Debost-Legrand A, Goumy C, Laurichesse-Delmas H, Dechelotte P, Beaufrere AM, Lemery D, Francannet C, Gallot D. Prenatal ultrasound findings observed in the Wolf-Hirschhorn syndrome: data from the registry of congenital malformations in Auvergne. Birth Defects Res A Clin Mol Teratol. 2013;97:806–11.
31. Beaujard MP, Jouannic JM, Bessieres B, Borie C, Martin-Luis I, Fallet-Bianco C, Portnoi MF. Prenatal detection of a de novo terminal inverted duplication 4p in a fetus with the Wolf-Hirschhorn syndrome phenotype. Prenat Diagn. 2005;25:451–5.
32. Ikonomou T, Antsaklis P, Daskalakis G, Sindos M, Papantoniou N, Kosmaidou Z, Antsaklis A. Prenatal diagnosis of Wolf-Hirschhorn syndrome: ultrasonography and genetics. J Matern Fetal Neonatal Med. 2013;26:941–2.
33. Opitz JM. The Brachmann-de Lange syndrome. Am J Med Genet. 1985;22:89–102.
34. Gillis LA, McCallum J, Kaur M, DeScipio C, Yaeger D, Mariani A, Kline AD, Li HH, Devoto M, Jackson LG, Krantz ID. NIPBL mutational analysis in 120 individuals with Cornelia de Lange syndrome and evaluation of genotype-phenotype correlations. Am J Hum Genet. 2004;75:610–23.
35. Boog G, Sagot F, Winer N, David A, Nomballais MF. Brachmann-de Lange syndrome: a cause of early symmetric fetal growth delay. Eur J Obstet Gynecol Reprod Biol. 1999;85:173–7.
36. Dave U, Shetty D. Mutational screening and prenatal diagnosis in Cornelia de Lange syndrome. J Obstet Gynaecol India. 2014;61:27–31.
37. Clark DM, Sherer I, Deardorff MA, Byrne JL, Loomes KM, Nowaczyk MJ, Jackson LG, Krantz ID. Identification of a prenatal profile of Cornelia de Lange syndrome (CdLS): a review of 53 CdLS pregnancies. Am J Med Genet A. 2012;158:1848–56.
38. Price N, Bahra M, Griffin D, Hanna G, Stock A. Cornelia de Lange syndrome in association with a balanced reciprocal translocation involving chromosomes 3 and 5. Prenat Diagn. 2005;25:602–3.
39. Sepulveda W, Wong AE, Dezerega V. Brachmann-de Lange syndrome: prenatal diagnosis with 2- and 3-dimensional sonography. J Ultrasound Med. 2009;28:401–4.
40. Spaggiari E, Vuillard E, Khung-Savatovsky S, Muller F, Oury JF, Delezoide AL, Guimiot F. Ultrasound detection of eyelashes: a clue for prenatal diagnosis of Cornelia de Lange syndrome. Ultrasound Obstet Gynecol. 2013;41:341–2.
41. Pajkrt E, Griffin DR, Chitty LS. Brachmann-de Lange syndrome: definition of prenatal sonographic features to facilitate definitive prenatal diagnosis. Prenat Diagn. 2010;30:865–72.
42. Basile E, Villa L, Selicorni A, Molteni M. The behavioural phenotype of Cornelia de Lange syndrome: a study of 56 individuals. J Intellect Disabil Res. 2007;51:671–81.
43. Van Allen MI, Filippi G, Siegel-Bartelt J, Yong SL, McGillivray B, Zuker RM, Smith CR, Magee JF, Ritchie S, Toi A, Reynolds JF. Clinical variability within Brachmann-de Lange syndrome: a proposed classification system. Am J Med Genet. 1993;47:947–58.
44. Verrotti C, Benassi G, Piantelli G, Magnani C, Giordano G, Gramellini D. Acrofacial dysostosis syndromes: a relevant prenatal dilemma. A case report and brief literature review. J Matern Fetal Neonatal Med. 2007;20:487–90.
45. Paladini D, Tartaglione A, Lamberti A, Lapadula C, Martinelli P. Prenatal ultrasound diagnosis of Nager syndrome. Ultrasound Obstet Gynecol. 2003;21:195–7.
46. Bernier FP, Caluseriu O, Ng S, Schwartzentruber J, Buckingham KJ, Innes AM, Jabs EW. Haploinsufficiency of SF3B4, a component of the pre-mRNA spliceosomal complex, causes Nager syndrome. Am J Hum Genet. 2012;90:925–33.
47. Ansart-Franquet H, Houfflin-Debarge V, Ghoumid J, Pasz N, Devisme L, Manouvrier-Hanu S, Andrieux J, Holder-Espinasse M. Prenatal diagnosis of Nager syndrome in a monochorionic-diamniotic twin pregnancy. Prenat Diagn. 2009;29:187–9.
48. Rios LT, Araujo Júnior E, Nardozza LM, Bruns RF, Moron AF, Martins MG. Prenatal diagnosis of Nager syndrome in the third trimester of pregnancy and anatomopathological correlation. J Med Ultrasound. 2012;39:287–9.
49. McPherson E, Zaleski C, Ye Z, Lin S. Rodriguez syndrome with SF3B4 mutation: a severe form of Nager syndrome? Am J Med Genet A. 2014;164:1841–5.
50. Leal E, Macias-Gomez N, Rodriguez L, Mercado FM, Barros-Nunez P. Femoral-facial syndrome with malformations in the central nervous system. Clin Imaging. 2003;27:23–6.
51. Paladini D, Maruotti GM, Sglavo G, Penner I, Leone F, D'Armiento MR, Martinelli P. Diagnosis of femoral hypoplasia-unusual facies syndrome in the fetus. Ultrasound Obstet Gynecol. 2007;30:354–8.
52. Johnson JP, Carey JC, Gooch WM, Petersen J, Beattie JF. Femoral hypoplasia-unusual facies syndrome in infants of diabetic mothers. J Pediatr. 1983;102:866–72.
53. Robinow M, Sonek J, Buttino L, Veghte A. Femoral-facial syndrome–prenatal diagnosis–autosomal dominant inheritance. Am J Med Genet. 1995;57:397–9.
54. Silvas E, Rypens F, Jovanovic M, Delezoide AL, Patey N. Prenatal diagnosis of femoral-facial syndrome: report of two cases. Birth Defects Res A Clin Mol Teratol. 2013;97:770–3.
55. Jeanty P, Kleinman G. Proximal femoral focal deficiency. J Ultrasound Med. 1989;8:639–42.
56. Tonsong T, Wanapirak C, Pongsatha S. Prenatal sonographic diagnosis of Larsen syndrome. J Ultrasound Med. 2000;19:419–21.
57. Knoblauch H, Urban M, Tinschert S. Autosomal recessive versus autosomal dominant inheritance in

Larsen syndrome: report of two affected sisters. Genet Couns. 1999;10:315–20.
58. Chen H, Chang CH, Perrin E, Perrin J. A lethal, Larsen-like multiple joint dislocation syndrome. Am J Med Genet. 1982;13:149–61.
59. Clayton-Smith J, Donnai D. A further patient with the lethal type of Larsen syndrome. J Med Genet. 1988;25:499–500.
60. Caksen H, Kurtoglu S. Larsen syndrome associated with severe congenital hydrocephalus. Genet Couns. 2001;12:369–72.
61. Krakow D, Robertson SP, King LM, Morgan T. Mutations in the gene encoding filamin B disrupt vertebral segmentation, joint formation and skeletogenesis. Nat Genet. 2004;36:405–10.
62. Becker R, Wegner RD, Kunze J, Runkel S, Vogel M, Entezami M. Clinical variability of Larsen syndrome: diagnosis in a father after sonographic detection of a severely affected fetus. Clin Genet. 2000;57:148–50.
63. Hennekam RCM, Krantz ID, Allanson JE. Mandibulofacial dysostosis (Treacher Collins syndrome, Franceschetti-Zwahlen-Klein syndrome). In: Hennekam RC, Krantz ID, Allanson JE, editors. Gorlins' syndromes of the head and neck. 5th ed. New York: Oxford University Press; 2010. p. 889–91.
64. Shoo BA, McPherson E, Jabs EW. Mosaicism of a TCOF1 mutation in an individual clinically unaffected with Treacher Collins syndrome. Am J Med Genet A. 2004;126:84–8.
65. Sakai D, Trainor PA. Treacher Collins syndrome: unmasking the role of TCOF1/treacle. Int J Biochem Cell Biol. 2009;41:1229–32.
66. Cohen J, Ghezzi F, Gongalves L, Fuentes JD, Paulyson KJ, Sherer DM. Prenatal sonographic diagnosis of Treacher Collins syndrome: a case and review of the literature. Am J Perinatol. 1995;12:416–9.
67. Pena SD, Shokeir MH. Syndrome of camptodactyly, multiple ankyloses, facial anomalies and pulmonary hypoplasia. A lethal condition. J Pediatr. 1974;85:373–5.
68. Chen CP. Prenatal diagnosis and genetic analysis of fetal akinesia deformation sequence and multiple pterygium syndrome associated with neuromuscular junction disorders: a review. Taiwan J Obstet Gynecol. 2012;51:12–7.
69. Paladini D, Tartaglione A, Agangi A, Foglia S, Martinelli P, Nappi C. Pena-Shokeir phenotype with variable onset in three consecutive pregnancies. Ultrasound Obstet Gynecol. 2001;17:163–5.
70. Tongsong T, Chanprapaph P, Khunamornpong S. Prenatal ultrasound of regional akinesia with Pena-Shokier phenotype. Prenat Diagn. 2000;20:422–5.
71. Ruano R, Dumez Y, Dommergues M. Three-dimensional ultrasonographic appearance of the fetal akinesia deformation sequence. J Ultrasound Med. 2003;22:593–9.
72. Santana EF, Serni PNO, Rolo LC, Araujo JE. Prenatal diagnosis of arthrogryposis as a phenotype of Pena-Shokeir syndrome using two- and three-dimensional ultrasonography. J Clin Imag Sci. 2014;4:20.
73. Gupta P, Sharma JB, Sharma R, Gadodia A, Kumar S, Roy KK. Antenatal ultrasound and MRI findings of Pena-Shokeir syndrome. Arch Gynecol Obstet. 2011;283:27–9.
74. Katzenstein M, Goodman RM. Pre- and postnatal findings in Pena-Shokeir I syndrome: case report and a review of the literature. J Craniofac Genet Dev Biol. 1988;8:111–26.
75. Tonni G, Lituania M, Chitayat D, Bonasoni MP, Keating S, Thompson M, Shannon P. Complete trisomy 9 with unusual phenotypic associations: Dandy-Walker malformation, cleft lip and cleft palate, cardiovascular abnormalities. Taiwan J Obstet Gynecol. 2014;53:592–7.
76. Tonni G, Bellotti M, Palmisano M, Alesi V, Bertoli M, Bonasoni MP. 408 kb 15q11.2 microduplication by array comparative genomic hybridization in a fetus presenting with exomphalos, micrognathia, tetralogy of Fallot and normal karyotype: a genetic counseling dilemma in paternal carrier status. Congenit Anom (Kyoto). 2015;55:65–70.
77. Tonni G, Ventura A, Pattacini P, Bonasoni M, Ferrari B. Complex cardiac defect, bowing of lower limbs and multiple anomalies in trisomy 22. Ultrasound, postmortem CT findings with necropsy confirmation. Fetal Pediatr Pathol. 2012;31:439–47.

8 Magnetic Resonance Imaging (MRI) in the Evaluation of the Fetal Face

Francisco Sepulveda, Gerlinde M. Gruber, and Daniela Prayer

8.1 Introduction

The use of magnetic resonance imaging (MRI) for the prenatal diagnosis of fetal malformations was first reported in 1983 [1].

However it was only in the 1990s that new technological advances including the development of fast sequences allowed this method to become incorporated into clinical practice. During the last decade, the increased use of this technique has grown exponentially due to the improved resolution and signal/noise ratio, as well as greater accessibility to the pregnant population.

MRI is a safe imaging modality for the detection and characterization of fetal anomalies [2]. It is usually performed after 18 weeks of gestation, because it is from this period onward that this technique can provide useful information for pregnancy management and fetal prognosis [3]. The main indication for fetal MRI is the detection of fetal anomalies on ultrasound, especially if a more detailed evaluation of the fetal anomaly or assessment of other associated malformations is required [3]. In particular, MRI has become a useful adjunct to ultrasound in the assessment of fetal head and neck pathology [4–8].

The study of the fetal face is an important part of the obstetric examination, and interest in its study has grown in the last decade [9]. With ultrasound, it is possible to detect a wide spectrum of facial anomalies and dysmorphisms, of which the absence of the nasal bone, micrognathia, hypertelorism/hypotelorism, and orofacial cleft are among the most important [10–14]. The absence of the nasal bones is a specific marker for trisomy 21, orofacial cleft is the most common midfacial malformation, and hypertelorism/hypotelorism is associated with severe central nervous system (CNS) malformations. With modern ultrasound equipment and proper scanning technique, some of these defects can be detected even in the first trimester of pregnancy [3, 10–12, 15].

Fetal MRI has the potential to add useful information about the facial anatomy, allows a diagnostic confirmation particularly when the ultrasound examination is difficult (e.g., in cases of maternal obesity, previous abdominal surgery,

F. Sepulveda (✉)
Division of Neuroradiology, Department of Radiology, UNC Hospital, University of North Carolina at Chapel Hill, Chapel Hill, NC 27514, USA
e-mail: fransepher@gmail.com

G.M. Gruber
Department of Systematic Anatomy, Center for Anatomy and Cell Biology, Medical University of Vienna, Vienna, Austria

D. Prayer
Division of Neuroradiology and Musculoskeletal Radiology, Department of Radiology, Medical University of Vienna, Vienna, Austria

G. Tonni, W. Sepulveda, and A.E. Wong (eds.), *Prenatal Diagnosis of Orofacial Malformations*,
DOI 10.1007/978-3-319-32516-3_8

suboptimal fetal position, etc.), and allows for the detailed structural evaluation of the fetal brain, which may detect coexisting pathology and assess for any intracranial extension of extracranial disease processes [16]. In addition, MRI may provide additional prognostic information by detecting other malformations that may be present [4].

In this chapter, we review the main indications, techniques, and efficacy of MRI in the evaluation of the fetal face. We also include some pathological conditions affecting primarily the fetal neck that may extend to and affect the facial anatomy. In these cases, MRI is particularly important to assess for the possibility of airway compromise at delivery.

8.2 Technical Aspects

The MRI study should be performed using high-magnetic field equipment; both 1.5 and 3.0 Tesla can be used. However, 1.5 Tesla equipment has less susceptibility to motion artifact due to fetal movement and shorter sequence duration [17]. A surface coil (either cardiac or body coil) can be selected. The surface coil has to be as close as possible to the region of interest with the aim to have a better signal/noise ratio and improve quality images. The patient is positioned in a supine position. In cases in which supine position is not tolerated by the patient, the lateral supine position is an alternative option. Because of the widespread use of ultrafast sequences in clinical practice, nowadays it is not necessary to administer sedatives to obtain good quality images [18].

8.3 Fetal MRI in Congenital Facial Anomalies

8.3.1 Cleft Lip and Palate

Orofacial clefts are congenital malformations that have a profound effect on midfacial development during gestation. It is the most common facial anomaly seen in newborn infants and occurs with a prevalence of about 1 per 600 to 1 per 1000 live births. Orofacial clefts can be divided into clefting of the primary palate, which includes cleft of the upper lip and alveolar ridge, and clefting of the secondary palate, which includes clefts of the hard and soft palates. They can also be classified as cleft lip, if it affects only the lip; cleft lip and palate, if it affects the lip and the palate; and isolated cleft palate, if it only affects the secondary palate including those only including the soft palate (bifid uvula). Regarding their location, they can be classified as unilateral (right or left), bilateral, or medial if they affect the midline. The midline involvement is the most severe form due to its strong association with major brain defects such as holoprosencephaly [4].

The prognosis of orofacial clefts depends on their association with additional malformations, which occurs in 21 % of cases of cleft lip and palate and in 8 % of cases of cleft lip alone [19]. The most common associated chromosomal abnormalities are trisomy 13 and 18 [19, 20].

Ultrasound, as the primary imaging method used in clinical obstetrics, is widely available and inexpensive, and provides real-time examination of the upper lip and alveolus. However, prenatal detection of cleft lip and palate can be difficult because of shadowing from the surrounding bony structures and poor visualization of the fetal face due to suboptimal fetal position [5]. MRI examination is considered a valuable complementary method. Some studies have compared two-dimensional (2D) ultrasound and MRI of the maxillofacial region in the ability of visualizing the location and extent of malformations [4, 5]. These studies have shown better accuracy in the detection of cleft lip and palate on MRI (100 %) versus 2D ultrasound (85 %), as well as better assessment of the extension of the defect (especially if the secondary palate is affected) and in the detection of associated anomalies [6–8]. However, with the incorporation of three-dimensional (3D) ultrasound in the prenatal evaluation of facial clefts, the sonographic diagnostic accuracy has increased, particularly in the assessment of the palate because evaluation of the secondary palate is now feasible [9]. With 3D ultrasound, new techniques have been described and are increasingly incorporated into the routine

ultrasound examination of the fetal face [21]. 3D ultrasound provides a clearer and more precise visualization of the fetal primary and secondary palates, which currently allows the identification of the precise location and extent of the cleft [3, 21–24]. On the other hand, MRI allows the confirmation of the facial defect as early as 18 weeks of gestation and performs better in delineating defects of the secondary palate and associated facial and extrafacial anomalies [22, 23].

8.3.1.1 MRI Examination

T2-weighed imaging (T2WI), echo planar, and steady-state free-precession (SSFP) sequences with 2–4-mm slice thickness must be obtained [4]. As with any study of fetal MRI, ultrafast sequences should be used. The slice numbers have to be carefully selected to include only the region of interest (maxillofacial region), thus avoiding the extra time sequence duration. A recent study demonstrated that fetal brain-targeted MRI sequences are accurate enough to obtain good images for the evaluation of the fetal lip, primary palate, and secondary palate [25]. However, in the case of a suspected orofacial anomaly, the authors suggest a study focused on the fetal craniofacial anatomy.

Axial views should be used to study the lips and alveolar ridge; T2WI and SSFP are the most useful sequences for these purposes (Fig. 8.1). In both sequences, the amniotic fluid is shown as hyperintense liquid that surrounds the fetus. When the amniotic fluid goes through to the oral cavity, it generates a significant contrast with the hypointense structures of the fetal maxillofacial anatomy including the lips and alveolus [4]. These sequences are useful to demonstrate the clefts of the lip and alveolus, where hyperintense amniotic fluid can be clearly seen filling the defects (Fig. 8.2a).

Coronal views are used to assess the palate. T2WI and echo planar are the optimal sequences. The main MRI finding in cleft palate is the loss of focal bone signal loss, which appears as a gap. Because the normal palate is hypointense on T2WI (Fig. 8.1b), in the presence of a cleft palate, a gap will appear with hyperintense signal due to the presence of amniotic fluid filling the bony defect (Fig. 8.2b). Echo planar sequence is useful in these cases because it contrasts the primary palate with hypointense signal with the surrounding hyperintense anatomic structures. When a cleft of the primary palate is present, gradient echo sequence shows a hyperintense signal gap due to lack of bone (Fig. 8.3). The T2WI sequence on sagittal view is used as an adjunct for visualizing the primary and secondary palates, where the normal fetal palate appears as a hypointense structure starting anteriorly at the frenulum of the upper lip and extending posteriorly to the nasal choanae (Fig. 8.1c) [5].

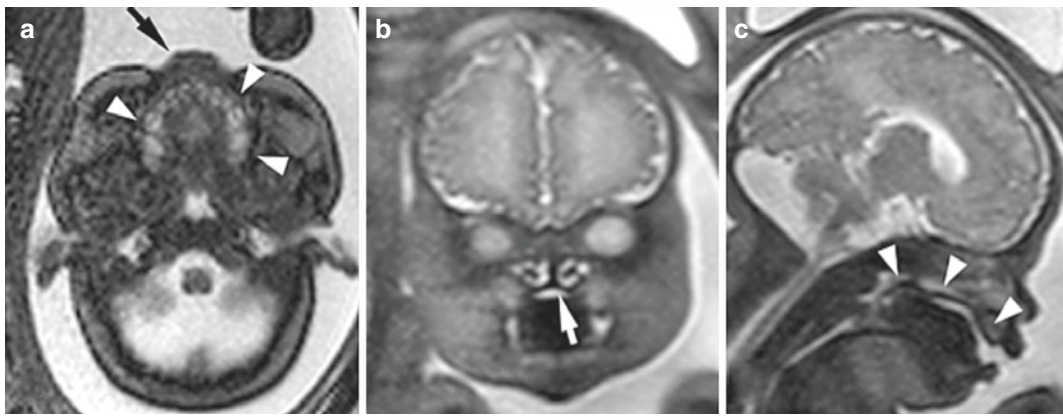

Fig. 8.1 Normal fetus at 32 weeks of gestation. (**a**) Axial SSFP shows upper lip (*arrow*) and alveolus (*arrowheads*) without filling defects. (**b**) Coronal T2WI shows normal palate with hypointense signal (*arrow*). (**c**) Sagittal T2WI demonstrates a normal and continuous palate with hypointense signal (*arrowheads*)

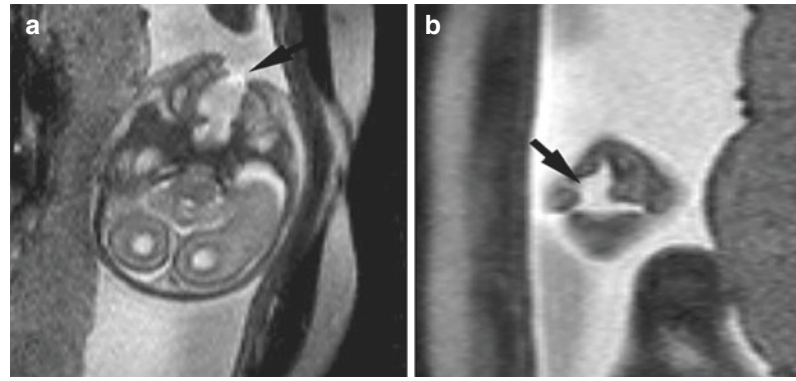

Fig. 8.2 Fetal MRI in a 20-week fetus with unilateral cleft lip and palate. (**a**) Axial T2WI shows disruption of the lip and alveolus ridge (*arrow*). (**b**) Coronal T2WI shows cleft of the lip and palate

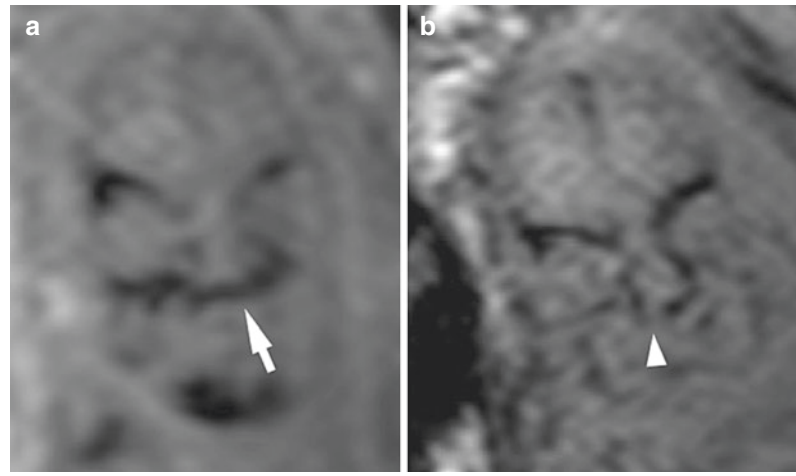

Fig. 8.3 Different fetuses at (**a**) 26 weeks of gestation and (**b**) at 25 weeks of gestation. (**a**) Echo planar sequence shows a normal hypointense signal of the palate (*arrow*). (**b**) Echo planar sequence shows cleft palate with the absence of normal hypointense signal (*arrowhead*)

8.3.2 Abnormal Orbits

The analysis of the fetal face by MRI must include the fetal orbits and eyes. Malformations of these structures are often associated with other congenital abnormalities [26]. Congenital eye and orbit abnormalities that can be found on the MRI examination include anophthalmia, microphthalmia, hypertelorism, hypotelorism, and proptosis and exophthalmos.

8.3.2.1 Anophthalmia

Anophthalmia is a rare condition characterized by the absence of the eyeball. It can be unilateral or bilateral. The affected orbit can be absent or, more frequently, hypoplastic (Fig. 8.4). The cause of anophthalmia is the failure of development of the optic vesicle (primary anophthalmia) or the anterior neural tube (secondary anophthalmia). It is usually associated with trisomy 13, triploidy, Klinefelter syndrome, and severe craniofacial abnormalities [27].

8.3.2.2 Microphthalmia

In microphthalmia, the eyeball has a smaller diameter than expected for gestational age. It can also be unilateral or bilateral and may be associated with many conditions, including triploidy, trisomy 13, Aicardi syndrome, Walker-Warburg syndrome, and CHARGE (coloboma, heart defects, choanal atresia, retarded growth and development, genital anomalies, and ear anomalies) syndrome [16, 27].

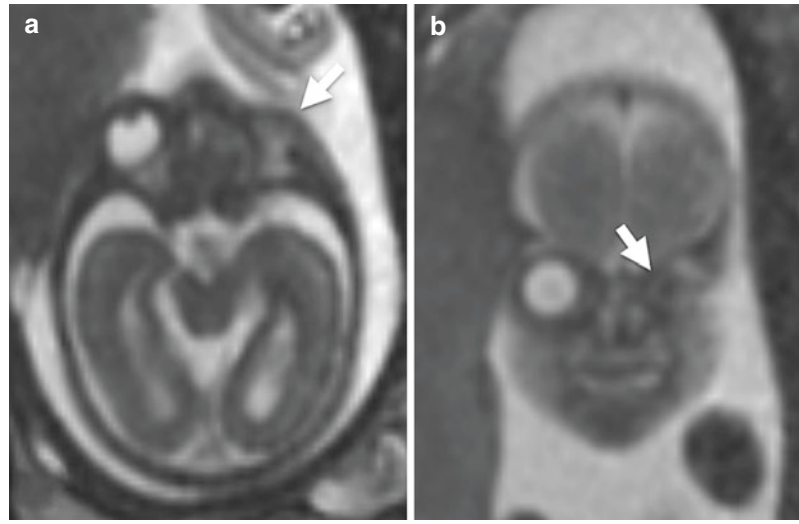

Fig. 8.4 Fetal MRI in a 22-week fetus with left anophthalmia. (**a**) Axial and (**b**) coronal T2WI show absent left eyeball (*arrows*)

8.3.2.3 Hypertelorism

Hypertelorism is the abnormally increased distance between eyes. It can be recognized when the interocular distance is larger than a single orbit width. Isolated primary hypertelorism is rare; hypertelorism is usually associated with other anomalies such as anterior encephalocele, midline facial masses, craniosynostosis, and chromosomal abnormalities.

8.3.2.4 Hypotelorism

Hypotelorism is the abnormally decreased distance between the eyes resulting in a decreased interocular diameter and binocular diameter (Fig. 8.5). A simple approach to assess for hypotelorism is to make sure the interocular distance is not smaller than a single orbit width. Similar to hypertelorism, hypotelorism is rarely seen as an isolated condition and is often associated with severe malformations in the holoprosencephaly spectrum.

8.3.2.5 Proptosis and Exophthalmos

Proptosis is the forward displacement of the eyeball. The forward displacement of both eye globes is called exophthalmos. These entities usually are associated with craniosynostosis, encephalocele, or rarely, with an orbital mass.

MRI Examination

The visualization of orbital abnormalities using MRI primarily depends on the T2WI axial and coronal views, although T2WI sagittal views can also be useful. No specific sequences for the orbit are regularly used, because the sequences utilized in the brain or craniofacial region are adequate for the assessment of the eyeballs. With T2WI technique, the eyeballs are easily recognized because of their water content as two hyperintense spheres. Distinctive findings in anophthalmia are poorly formed shallow orbits with only rudimentary orbital tissue or a congenital cystic eyeball [28].

The qualitative analysis of the eye size and distance between eyeballs is acceptable for trained radiologists, but in the case of any anomaly of the orofacial anatomy or a midline brain defect, a quantitative measure must be performed to detect minor eye abnormalities. Measurements used for the assessment of the eye size are the anteroposterior ocular distance (APD) and latero-lateral ocular distance (LLD). The APD is measured between the anterior and posterior margins of the eyeballs through the lens, and the LLD is measured between the ethmoidal and malar margins of the eyeballs (Fig. 8.6). The APD and LLD are perpendicular. Measurements

used for the detection of hypotelorism and hypertelorism are the interocular distance (IOD) and binocular distance (BOD) (Figs. 8.5 and 8.6). The BOD is measured between the two malar margins of the hyperintense vitreous on the coronal MRI image. Also in coronal T2WI views, the IOD is measured between the two ethmoidal margins of the vitreous. Every measurement obtained must be compared with normative data from fetal MRI according to the gestational age [26]. If the fetus has intrauterine growth restriction, the use of nomogram is not recommended because all eye measurements in these fetuses will be significantly different from normally grown fetuses [26].

8.3.3 Abnormal Mandible

Mandibular development begins after the sixth gestational week. During embryogenesis, interactions between the ectoderm of the branchial arches and neural crest cells from the dorsal neural tube develop into the mandible [29, 30]. This process is susceptible to genetic insult and environmental factors [31, 32]. Among the environmental causes,

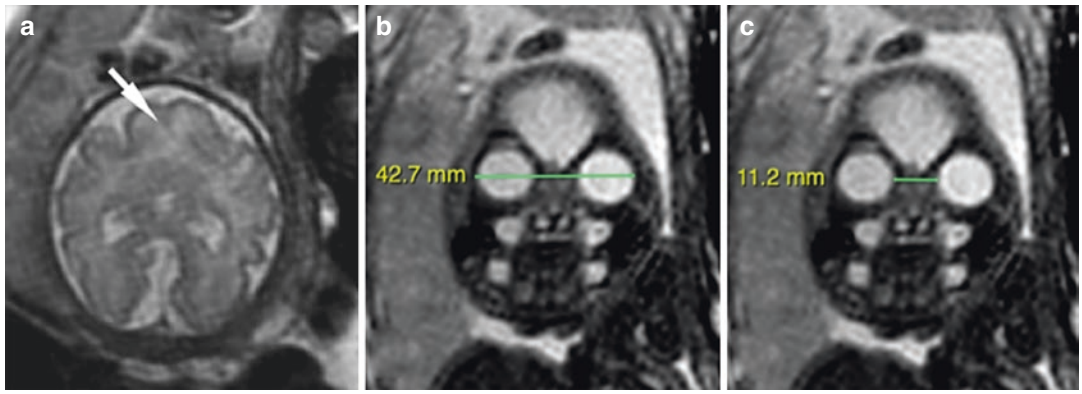

Fig. 8.5 Fetal MRI in a 31-week fetus with semilobar holoprosencephaly and hypotelorism. (**a**) T2WI shows the absence of the anterior interhemispheric fissure and fusion of the frontal lobes (*arrow*). (**b**) The binocular distance measurement (42.7 mm) is below the fifth percentile (44.7 mm). (**c**) The interocular distance measurement (11.2 mm) is below the fifth percentile (15.8 mm)

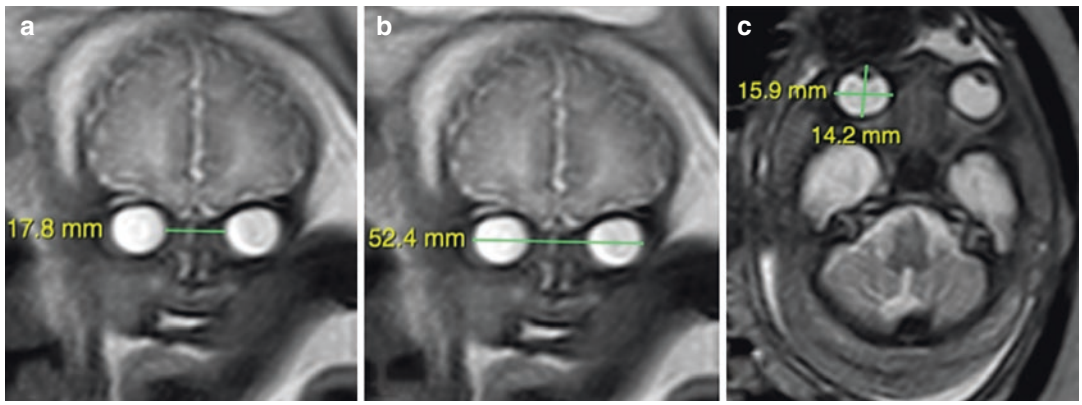

Fig. 8.6 Ocular biometry using T2WI sequence. (**a**) Measurement of interlocular and (**b**) binocular distances on coronal view. (**c**) Measurement of anteroposterior ocular distance (14.2 mm) and latero-lateral ocular distance (15.9 mm) on axial plane

neuromuscular conditions such as fetal akinesia deformation sequence can lead to severe micrognathia [30].

8.3.3.1 Micrognathia and Retrognathia

Micrognathia results from hypoplasia of the neural crest cell population. It is rarely isolated and often associated with other abnormalities, such as hemifacial microsomia, Pierre Robin sequence, and Treacher Collins syndrome (see Chap. 6). It may also be part of a syndrome, skeletal dysplasia, or a fetal akinesia deformation sequence. Chromosomal abnormalities have been reported in 66 % of fetuses with micrognathia, usually triploidy, trisomy 13, and trisomy 18 [31, 32].

The terms micrognathia and retrognathia are usually indistinctive in clinical practice. However, micrognathia refers to a small mandible, and retrognathia to an abnormal mandibular position. Micrognathia is often seen in association with retrognathia (receding chin) [30]. In contrast, true retrognathia is rarely found. Distinguishing between these two conditions based on subjective assessment can be difficult. Therefore, objective measurements (inferior facial angle and jaw index) have been developed to assist in differentiating between micrognathia and retrognathia [33, 34].

2D or 3D ultrasound examination of the fetal mandible is important because mandibular anomalies may lead to the diagnosis of major aneuploidy or genetic syndromes. Fetal MRI has proven to be useful for prenatal diagnosis and postnatal surgical management of craniofacial abnormalities and may be used as a complementary method in the assessment of micrognathia and retrognathia [35, 36].

MRI Examination

Sagittal and axial T2WI views are mandatory to the prenatal assessment of the mandible. The sagittal view, specifically, is required for the subjective as well as the quantitative assessment of the position of the mandible. Fetal MRI of the mandible is usually based on subjective evaluation of the facial profile, and micrognathia may be diagnosed by detecting a receding chin. Although diagnosis of micrognathia is usually based on the subjective finding of a receding chin in the of profile view (Fig. 8.7), a recent study showed that subjective evaluation may lead to undiagnosed mandibular conditions in fetuses in which the mandicular recession is not severe [36].

To quantitatively assess mandibular growth, measurements of the anteroposterior diameter (APD) of the mandible in axial T2WI views are required. Because the APD cannot be directly visualized due to signal superposition of the surrounding anatomic structures, an auxiliary line is draw from the posterior border of the masseter muscle at the mandibular insertion from one side to the other, connecting the presumed mandibular angles. The APD is then measured from the auxiliary line to the symphysis menti (Fig. 8.8). Because in micrognathia the most impaired growth is on the longitudinal plane of the mandibular body, the APD is adequate for assessing the mandibular growth. In addition, transverse growth of the

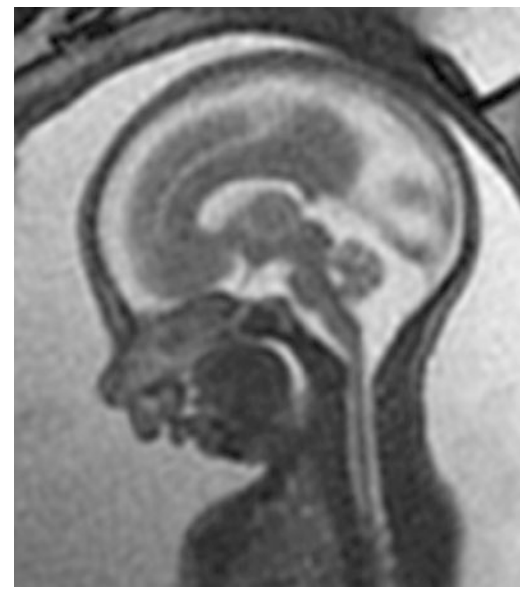

Fig. 8.7 Fetal MRI in a 25-week fetus with severe micrognathia. Sagittal T2WI shows a receding chin easily recognized by subjective assessment. Note associated glossoptosis due to isolated cleft of the soft palate

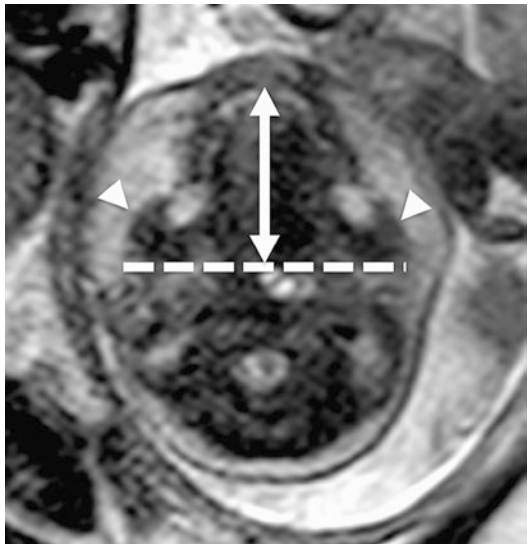

Fig. 8.8 Anteroposterior diameter (APD) on an axial T2WI view. The APD (*long double arrow*) is measured from the symphysis menti to the line (*dotted line*) which connects the posterior borders of the masseter muscles (*arrowheads*)

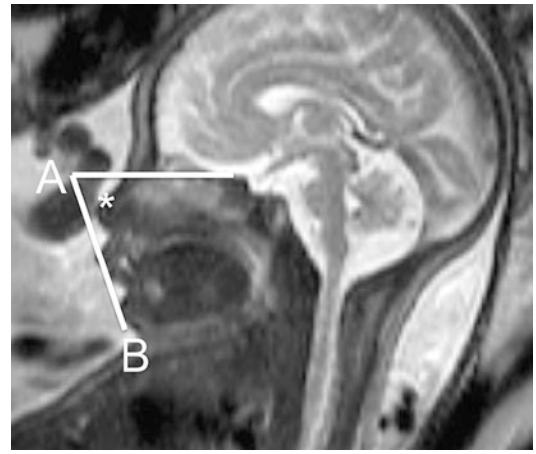

Fig. 8.9 Inferior facial angle (IFA) assessment on sagittal T2WI. IFA (*) is defined as the angle between one line (*A*) at the nasal root and a second line from the mentum tip to the anterior border of the upper lip (*B*)

mandible cannot be clearly measured on T2WI because of similar signal intensity of the adjacent structures [36].

To assess the mandibular position, the inferior facial angle (IFA), T2WI views are required. IFA is defined as the angle formed between the line perpendicular to the vertical part of the forehead at the level of the nasal root and the line tangential to both the tip of the mentum and the anterior border of the upper lip (Fig. 8.9). The IFA must be performed with either a closed or slightly opened mouth (open lips with a slight fluid in the oral cavity). Fetuses with either micrognathia or retrognathia have an IFA <50° [36]. To differentiate micrognathia from retrognathia, the combined assessment of IFA and jaw index is required. Jaw index is calculated as follows: APD/biparietal diameter ×100 [33]. Micrognathia is diagnosed when the IFA is <50° with a jaw index less than the fifth percentile, whereas retrognathia is diagnosed when the IFA is <50° with a normal jaw index. Although micrognathia defined by IFA <50° is the same whether measured on MRI or ultrasound, different jaw indices based on the two modalities have been reported [36]. On the other hand, IFA by MRI has the same threshold of <50° that defines an abnormal profile by ultrasound.

8.4 Tumors of the Fetal Face and Neck

Fetal face and neck tumors are classified according to their content into cystic, solid-cystic, or solid masses. Neck masses may extend to the facial region and can cause significant distortion of the fetal facial anatomy. Moreover, they can impair the swallowing process leading to polyhydramnios in the prenatal period and can compress the upper airway causing obstruction and respiratory failure at birth. Fetal MRI has the capacity of depicting the airway and its relationship with the cervical mass and can also define the tissue composition of the lesion with accuracy. If the facial or neck mass compresses the airway, perinatal asphyxia leading to early neonatal death is expected [37]. This complication can be prevented with the ex utero intrapartum treatment (EXIT) procedure which aims to secure the airway during delivery, while the fetus is still connected to the placental circulation [3]. The most frequent masses of the fetal face and neck are lymphatic malformations, teratomas, and congenital hemangiomas.

8.4.1 Lymphatic Malformation

Lymphatic malformations are cystic, multiseptated masses and are the most common posterior neck mass in the fetus. Lymphatic malformations are caused by the failure of or delayed development of jugular lymphatic connections [37]. These malformations are typically located within the posterior subcutaneous tissues, although they frequently wrap around laterally (Fig. 8.10). Lymphatic malformations can be extensive and may produce pronounced mass effect with postural abnormality and/or with compression of the upper airway. It can also lead to hydrops, which has a very poor prognosis.

8.4.2 Teratomas

Teratomas are germ cell tumors composed of tissue from the three germinal layers. In the fetus, the head and heck are the second most frequently affected location after the sacrococcygeal region. They often contain cystic and solid components, including calcifications and fat. Teratomas show a heterogeneous signal and are usually located in the anterior aspect of the neck. They often produce hyperextension of the neck and can produce airway obstruction. The presence of calcification and fat is characteristic of teratomas, and their presence is the most striking diagnostic clue. Fetal MRI examination is excellent at assessing both the degree of airway compression and the tissue characteristics.

Teratomas arising from the oral/nasal cavity or pharynx (epignathus) most commonly arise from the hard or soft palate. They can be large, fungating oral masses causing the jaw to be held in a fixed open position [16].

Polyhydramnios secondary to obstruction and difficulty in swallowing is common (Figs. 8.11 and 8.12). Hydrops may be present with large masses, especially when they compromise venous or lymphatic circulations.

The orbit is a rare location for teratomas. Orbital teratomas can be primary, when the tumor is arising from an orbit component, or secondary, when the involvement is the result of extension of the tumor from another location, frequently from the intracranial region. Orbital teratomas are often large masses that cause severe facial deformities.

8.4.3 Congenital Hemangiomas

Congenital hemangiomas are rare vascular tumors that can grow rapidly during pregnancy and potentially produce heart failure due to the diversion of blood flow and the "vascular steal" phenomenon. Two subtypes of congenital heman-

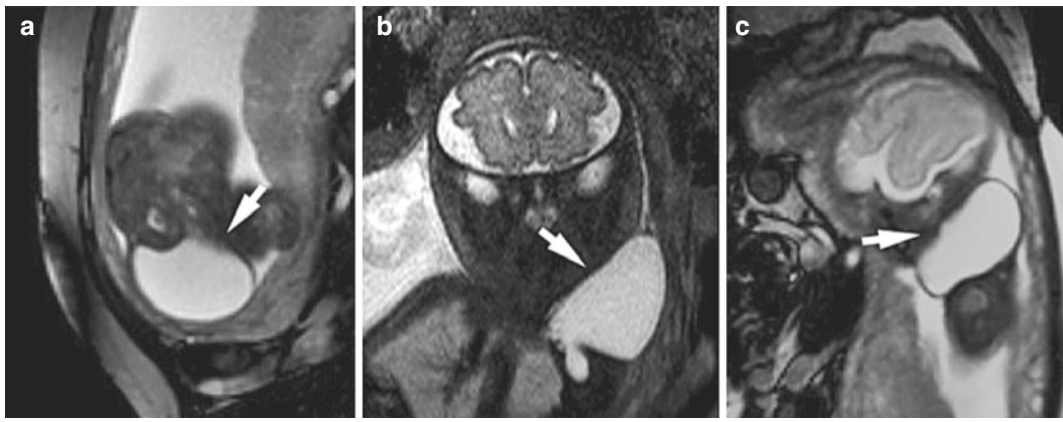

Fig. 8.10 Fetal MRI in a 32-week fetus with cervical lymphangioma in the lateral-posterior region of the neck. Axial (**a**), coronal (**b**), and sagittal (**c**) T2WI views show a thin-walled cystic mass (*arrows*) that produces mass effect and postural abnormality

giomas exist: the rapidly involuting congenital hemangioma, which usually decreases in size and vascularization by 8–14 months of postnatal life, and the non-involuting congenital hemangioma, which may persist into late childhood [38, 39]. With fetal MRI, it is possible to assess the size, location, and internal structure of these types of lesions. A congenital hemangioma appears on fetal MRI as a large, solid, well-circumscribed tumor with the presence of vascular flow void. Congenital hemangiomas can grow rapidly during pregnancy and can occasionally cause heart failure and hydrops.

8.4.3.1 MRI Examination

With face and neck tumors, the most important aims of fetal MRI are to localize the lesion, define the extension of the tumor for presurgical planning purposes, and assess the presence of airway compromise. T2WI sequences must be performed in the three orthogonal planes with 3 mm thickness slices. The airway is easily seen in coronal and axial T2WI views due to the presence of amniotic fluid inside of the upper airway (Fig. 8.12). SSFP imaging is a useful sequence due to its capacity to perform thin slices without loss of quality image.

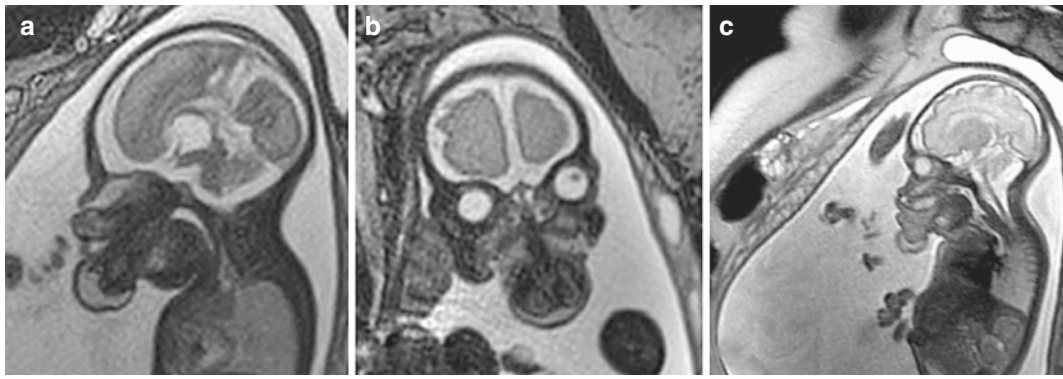

Fig. 8.11 Fetal MRI in a 30-week fetus with orofacial teratoma and hypertelorism. (**a**) Sagittal and (**b**) coronal T2WI views show a heterogeneous mass of the oral cavity that produces severe distortion of the facial anatomy. Note hypertelorism in (**b**). (**c**) Sagittal T2WI shows polyhydramnios due to impaired fetal swallowing

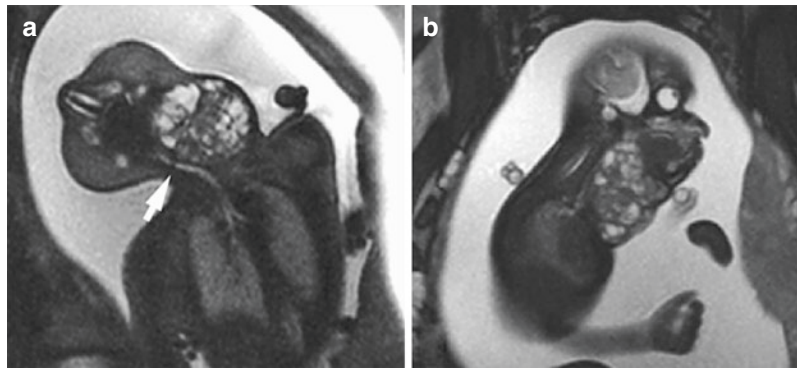

Fig. 8.12 Fetal MRI in a fetus with a cervical teratoma. (**a**) Coronal and (**b**) sagittal T2WI views show a heterogeneous cervical mass and compression of the upper airway (*arrow* in **a**). Note associated polyhydramnios in (**b**) (From Sepulveda et al. [3] with permission from the authors)

The characteristic feature of teratomas is their heterogeneous signal due to their complex composition. T1WI sequence allows the identification of fat within the abnormal mass that is a common finding in this type of tumor. Echo planar imaging is the most sensible sequence for the detection of calcification, which is also a characteristic component of teratomas.

The presence of a multicystic mass in the neck with mass effect is characteristic of lymphatic malformation. These structures show a hyperintense signal on T2WI and SSFP sequences and have a thin cystic wall. In the case of a congenital hemangioma, T2WI sequences show a solid hyperintense mass within which there is a hypointense flow void.

Conclusions

Fetal MRI is an important clinical tool in the prenatal evaluation of some facial abnormalities. This technique can complement the ultrasound findings as well as provide more detailed information regarding associated abnormalities including particularly the central nervous system. Fetuses with facial and neck tumors are also candidates for fetal MRI, especially when patency of the airway should be investigated.

References

1. Smith FW, Adam AH, Phillips WD. NMR imaging in pregnancy. Lancet. 1983;1:61–2.
2. Simon EM, Goldstein RB, Coakley FV, Filly RA, Broderick KC, Musci TJ, et al. Fast MR imaging of fetal CNS anomalies in utero. AJNR Am J Neuroradiol. 2000;21:1688–98.
3. Sepulveda W, Ximenes R, Wong AE, Sepulveda F, Martinez-Ten P. Fetal magnetic resonance imaging and three-dimensional ultrasound in clinical practice: applications in prenatal diagnosis. Best Pract Res Clin Obstet Gynaecol. 2012;26:593–624.
4. Mailath-Pokorny M, Worda C, Krampl-Bettelheim E, Watzinger F, Brugger PC, Prayer D. What does magnetic resonance imaging add to the prenatal ultrasound diagnosis of facial clefts? Ultrasound Obstet Gynecol. 2010;36:445–51.
5. Ghi T, Tani G, Savelli L, Colleoni GG, Pilu G, Bovicelli L. Prenatal imaging of facial clefts by magnetic resonance imaging with emphasis on the posterior palate. Prenat Diagn. 2003;23:970–5.
6. Manganaro L, Tomei A, Fierro F, Di Maurizio M, Sollazzo P, Sergi ME, et al. Fetal MRI as a complement to US in the evaluation of cleft lip and palate. Radiol Med. 2011;116:1134–48.
7. de Milly MN, Alison M, Arthurs O, Vuillard E, Oury JF, Elmaleh-Berges M, et al. Is fetal cerebral MRI worthwhile in antenatally diagnosed isolated cleft lip with or without palate? Prenat Diagn. 2013;33:273–8.
8. Bekiesinska-Figatowska M, Bragoszewska H, Romaniuk-Doroszewska A, Duczkowska A, Jaczynska R, Maciejewski TM. The role of magnetic resonance imaging in the prenatal diagnosis of cleft lip and palate. Dev Period Med. 2014;18:27–32.
9. Wang LM, Leung KY, Tang M. Prenatal evaluation of facial clefts by three-dimensional extended imaging. Prenat Diagn. 2007;27:722–9.
10. Martinez-Ten P, Adiego B, Perez-Pedregosa J, Illescas T, Wong AE, Sepulveda W. First-trimester assessment of the nasal bones using the retronasal triangle view: a 3-dimensional sonographic study. J Ultrasound Med. 2010;29:1555–61.
11. Sepulveda W, Wong AE, Martinez-Ten P, Perez-Pedregosa J. Retronasal triangle: a sonographic landmark for the screening of cleft palate in the first trimester. Ultrasound Obstet Gynecol. 2010;35:7–13.
12. Sepulveda W, Wong AE, Vinals F, Andreeva E, Adzehova N, Martinez-Ten P. Absent mandibular gap in the retronasal triangle view: a clue to the diagnosis of micrognathia in the first trimester. Ultrasound Obstet Gynecol. 2012;39:152–6.
13. Dukhovny S, Wilkins-Haug L, Shipp TD, Benson CB, Kaimal AJ, Reiss R. Absent fetal nasal bone: what does it mean for the euploid fetus? J Ultrasound Med. 2013;32:2131–4.
14. Papasozomenou P, Athanasiadis AP, Zafrakas M, Panteris E, Loufopoulos A, Assimakopoulos E, et al. Three-dimensional versus two-dimensional ultrasound for fetal nasal bone evaluation in the second trimester. J Matern Fetal Neonatal Med. 2015;28:1432–7.
15. Sepulveda W, Wong AE, Sepulveda F, Martinez-Ten P, Ximenes R. Fetal magnetic resonance imaging and three-dimensional ultrasound in clinical practice: general aspects. Best Pract Res Clin Obstet Gynaecol. 2012;26:575–91.
16. Mirsky DM, Shekdar KV, Bilaniuk LT. Fetal MRI: head and neck. Magn Reson Imaging Clin N Am. 2012;20:605–18.
17. Victoria T, Johnson AM, Edgar JC, Zarnow DM, Vossough A, Jaramillo D. Comparison between 1.5-T and 3-T MRI for fetal imaging: is there an advantage to imaging with a higher field strength? AJR Am J Roentgenol. 2016;206:195–201.
18. Prayer D, Brugger PC, Prayer L. Fetal MRI: techniques and protocols. Pediatr Radiol. 2004;34:685–93.
19. Milerad J, Larson O, Ph DD, Hagberg C, Ideberg M. Associated malformations in infants with cleft lip

and palate: a prospective, population-based study. Pediatrics. 1997;100:180–6.
20. Merritt L. Part 1. Understanding the embryology and genetics of cleft lip and palate. Adv Neonatal Care. 2005;5:64–71.
21. Martinez Ten P, Perez Pedregosa J, Santacruz B, Adiego B, Barron E, Sepulveda W. Three-dimensional ultrasound diagnosis of cleft palate: 'reverse face', 'flipped face' or 'oblique face' – which method is best? Ultrasound Obstet Gynecol. 2009;33:399–406.
22. Wang G, Shan R, Zhao L, Zhu X, Zhang X. Fetal cleft lip with and without cleft palate: comparison between MR imaging and US for prenatal diagnosis. Eur J Radiol. 2011;79:437–42.
23. Kazan-Tannus JF, Levine D, McKenzie C, Lim KH, Cohen B, Farrar N, et al. Real-time magnetic resonance imaging aids prenatal diagnosis of isolated cleft palate. J Ultrasound Med. 2005;24:1533–40.
24. Martinez-Ten P, Adiego B, Illescas T, Bermejo C, Wong AE, Sepulveda W. First-trimester diagnosis of cleft lip and palate using three-dimensional ultrasound. Ultrasound Obstet Gynecol. 2012;40:40–6.
25. Moreira NC, Ribeiro V, Teixeira J, Raininko R, Wikstrom J. Visualization of the fetal lip and palate: is brain-targeted MRI reliable? Cleft Palate Craniofac J. 2013;50:513–9.
26. Li XB, Kasprian G, Hodge JC, Jiang XL, Bettelheim D, Brugger PC, et al. Fetal ocular measurements by MRI. Prenat Diagn. 2010;30:1064–71.
27. Verma AS, Fitzpatrick DR. Anophthalmia and microphthalmia. Orphanet J Rare Dis. 2007;2:47.
28. Hopper KD, Sherman JL, Boal DK, Eggli KD. CT and MR imaging of the pediatric orbit. Radiographics. 1992;12:485–503.
29. Smartt Jr JM, Low DW, Bartlett SP. The pediatric mandible: I. A primer on growth and development. Plast Reconstr Surg. 2005;116:14e–23.
30. Paladini D. Fetal micrognathia: almost always an ominous finding. Ultrasound Obstet Gynecol. 2010;35:377–84.
31. Luedders DW, Bohlmann MK, Germer U, Axt-Fliedner R, Gembruch U, Weichert J. Fetal micrognathia: objective assessment and associated anomalies on prenatal sonogram. Prenat Diagn. 2011;31:146–51.
32. Bromley B, Benacerraf BR. Fetal micrognathia: associated anomalies and outcome. J Ultrasound Med. 1994;13:529–33.
33. Paladini D, Morra T, Teodoro A, Lamberti A, Tremolaterra F, Martinelli P. Objective diagnosis of micrognathia in the fetus: the jaw index. Obstet Gynecol. 1999;93:382–6.
34. Rotten D, Levaillant JM, Martinez H, Ducou le Pointe H, Vicaut E. The fetal mandible: a 2D and 3D sonographic approach to the diagnosis of retrognathia and micrognathia. Ultrasound Obstet Gynecol. 2002;19:122–30.
35. Arangio P, Manganaro L, Pacifici A, Basile E, Cascone P. Importance of fetal MRI in evaluation of craniofacial deformities. J Craniofac Surg. 2013;24:773–6.
36. Nemec U, Nemec SF, Brugger PC, Weber M, Bartsch B, Bettelheim D, et al. Normal mandibular growth and diagnosis of micrognathia at prenatal MRI. Prenat Diagn. 2015;35:108–16.
37. von Kaisenberg CS, Nicolaides KH, Brand-Saberi B. Lymphatic vessel hypoplasia in fetuses with Turner syndrome. Hum Reprod. 1999;14:823–6.
38. Boon LM, Enjolras O, Mulliken JB. Congenital hemangioma: evidence of accelerated involution. J Pediatr. 1996;128:329–35.
39. Enjolras O, Mulliken JB, Boon LM, Wassef M, Kozakewich HP, Burrows PE. Noninvoluting congenital hemangioma: a rare cutaneous vascular anomaly. Plast Reconstr Surg. 2001;107:1647–54.

The Fetal Brain in Fetuses with Orofacial Abnormalities

9

Gustavo Malinger

Since the face develops at the same time and in close contact with the brain, it is expected that at least some of the anomalies and defects affecting the face will affect also the brain. Some of them are being diagnosed during fetal life and will be presented in this Chapter. We will describe the possible associations between fetal facial and brain defects at each stage of brain development starting from neurulation and until the first steps of myelination [1].

The development of the median portion of the face and the forebrain are closely related since the prechordal mesoderm forms the median skeleton of the face and is simultaneously involved in the induction of the rostral neural ectoderm, which is the antecessor of prosencephalic development [2]. Anomalies in these mechanisms lead to the protoypical developmental disorder involving the face and brain: holoprosencephaly (HPE). Both neurulation disorders and late developmental events such as proliferation and migration may also be associated with orofacial defects. Almost invariably, these patients present with multiple malformations involving structures in addition to the CNS, head, and face. In these cases, malformation databases and search engines are helpful, such as the Online Mendelian Inheritance in Men (OMIM) and Orphanet Journal of Rare Diseases, as well as the classic textbook "*Smith's Recognizable Patterns of Human Malformations* [3].

9.1 Neurulation Disorders

In general, dorsal induction anomalies due to abnormal neural tube closure do not affect the face. However, when evaluating a fetus with a suspected facial anomaly, the possibility of a neural tube malformation must still be considered since these associations have been reported. Due to the severity of the CNS findings, cases diagnosed during the late first trimester or early second trimester may not be identified as also having a facial malformation (Fig. 9.1).

The association between open neural tube defects and facial anomalies appears to be sporadic and not related to any known syndrome. In a population-based study, Stoll et al. reported on 156 cases of anencephaly/spina bifida diagnosed in Northern France and examined by a clinical dysmorphology geneticist; they found that 3.3 % suffered from facial clefts. Facial cleft was the most common associated anomaly but they were not syndromic [4]. Upon review of current literature, there was only one case that was associated with a de novo -2q deletion [5].

G. Malinger
OB-GYN Ultrasound Unit, Department of OB-GYN, Lis Maternity Hospital, Tel Aviv Medical Center, Tel Aviv, Israel
e-mail: gmalinger@gmail.com

G. Tonni, W. Sepulveda, and A.E. Wong (eds.), *Prenatal Diagnosis of Orofacial Malformations*,
DOI 10.1007/978-3-319-32516-3_9

Anterior cephalocele has been described in fetuses with frontonasal dysplasia (FND), also known as median cleft facial syndrome (http://omim.org/entry/136760) [6, 7] (Table 9.1). This condition is usually sporadic, but autosomal dominant, recessive, and X-linked patterns, as well as 22q11 microdeletion, have been reported. Patients with FND usually present with two or more of the following: pronounced ocular hypertelorism, broadening of the nasal root, median facial cleft affecting the nose and/or upper lip and palate, unilateral or bilateral clefting of the alae nasi, lack of formation of the nasal tip, anterior cranium bifidum occultum, and a V-shaped or widow's peak frontal hairline (Fig. 9.1). The corpus callosum (CC) and other important brain structures may be absent. Severe forms of FND, particularly when involving the brain, may be associated with autosomal recessive mutations in aristaless-like homeobox gene ALX1; ALX1 expression is essential for building oral and nasal cavities as well as proper eye development during early embryogenesis [8].

The Meckel–Gruber syndrome is the most severe form of the autosomal recessive ciliopathies and is characterized by the presence of posterior cephaloceles, polycystic kidneys, and polydactyly; it is also frequently accompanied by facial clefts (25%) and microphthalmia/anophthalmia (20%) [9] (Fig. 9.2). Less severe ciliopathies including Joubert's syndrome and oral–facial–digital syndrome type IV may also be associated to a lesser extent with facial dysmorphism, cleft lip and palate, and facial tumors [10].

9.2 Disorders of Prosencephalic Development

Prosencephalic development starts as the same time as facial development at 5–6 weeks of gestation. At this stage, the brain is composed of three vesicles: the forebrain, the midbrain, and the hindbrain. Failures in the normal development of the forebrain result in a wide range of anomalies ranging from complete failure of formation to abnormal formation of some of the midline brain structures [11]. Failure of formation of the prosencephalon leads to the development of two very rare and severe conditions: aprosencephaly and atelencephaly; failure of cleavage into two separated vesicles results in holoprosencephaly, and anomalous midline development causes commissural and septal anomalies [1] (Tables 9.1 and 9.2).

Although relatively rare in live-born children (prevalence of less than 1/10,000), HPE is the most common fetal malformation, present in as many as

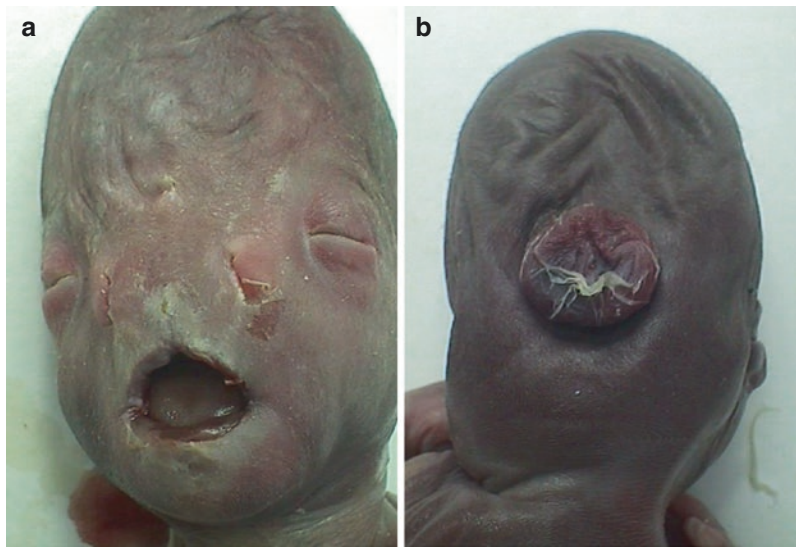

Fig. 9.1 Stillbirth with frontonasal dysplasia. Note the broad nasal cleft and extreme hypertelorism (**a**) and the presence of an occipital cephalocele (**b**)

Table 9.1 Neural tube defects in fetuses with orofacial syndromes and anomalies

Neural tube defect	Facial anomalies	Syndrome	Other CNS findings	Genetics	References
Anencephaly/ spina bifida	Facial clefts		No	Sporadic, de novo deletion 2q	Stoll [4], Goumy [5]
Anterior cephalocele	Median cleft lip, hypertelorism	Frontonasal dysplasia	ACC, lipoma, macrocephaly, HME, cranium bifidum	Sporadic, ALX AR mutations, AD, X-linked patterns, 22q11 microdeletions	Martinelli [6], Esmer [7]
Posterior encephalocele	Microophthalmia/ anophthalmia, orofacial clefts	Meckel–Gruber syndrome, other ciliopathies	Cervical rachischisis, DWM, ACC, hypotelorism, cerebellar hypoplasia, hydrocephalus	MKS1-11 AR sequence variations	Barisic [9], Romani [10]

1 in 250 first-trimester fetuses with the more severe cases resulting in early fetal demise. HPE is associated with chromosomal anomalies, particularly trisomies 13 and 18, triploidy, other known syndromes, as well as single gene disorders.

With the advancements in molecular biology, an increasing number of single gene mutations have been described as causative agents of HPE; these mutations appear to occur with a wide range of different HPE genotypes confirming that HPE apparently represents a continuum of forebrain and craniofacial malformations with no clear-cut distinction among the different subcategories [12]. To date, four major genes responsible for HPE have been described: SHH, ZIC2, SIX3, and TGIF, and a few others seem to play a lesser role in the occurrence of HPE. The "multiple-hit hypothesis" is now the most widely accepted model of HPE. According to this hypothesis, combinations of mutations in major and/or minor HPE genes lead to the occurrence of HPE and may account for variability in terms of severity [13].

In a large European study [14] consisting of 645 probands, of which 51% were fetuses, and 699 relatives systematic molecular analyses showed point mutations or deletions in the four major genes involved in HPE (SHH, ZIC2, SIX3, TGIF) in 25.4% of the subjects. More fetuses than children were found to carry an HPE-associated gene deletion (68% vs. 32%). CGH analysis performed on 260 of the probands demonstrated rearrangements in 22% of cases. Interestingly, HPE spectrum disorders were found in 79 of the 699 relatives (29% in parents and 71% in other relatives). All affected parents were diagnosed with brain microforms, which accounted for 44% of the abnormalities in these 79 relatives. More severe forms were reported in other relatives, such as siblings or cousins: 26% alobar HPE, 13% semilobar HPE, and 7% lobar HPE. Associated brain malformations were observed in 6% of the affected relatives, and neural tube defects were found in 8%.

An association between the severity of facial anomalies and brain anomalies (as in the maxim, "the face predicts the brain") was first reported by DeMyer and colleagues in 1964 [15]. Since then, however, as experience with anomalies has increased, this "face-brain" correlation has become controversial [16]. In a large epidemiologic study, Orioli found that in 10–39% of the cases, there was no such clear correlation between face and brain anomaly subtypes [17]. In contrast, Mercier et al. [14], based on the data for 369 informative probands, found a positive correlation between the severity of type of HPE and severity of facial features for their entires series ($p<0.001$) and also for patients with SHH ($p<0.001$), SIX3 ($p<0.001$), and TGIF ($p<0.001$) subgroups, but not for the ZIC2 subgroup ($p>0.5$).

Prenatal diagnosis of the alobar and semilobar forms of HPE is usually straightforward; the first reported cases in the early 1980s were diagnosed in the second half of pregnancy and represented severe HPE types [18] (Figs. 9.3 and 9.4). In recent years, diagnosis of these severe cases is possible at much early gestational ages, even as

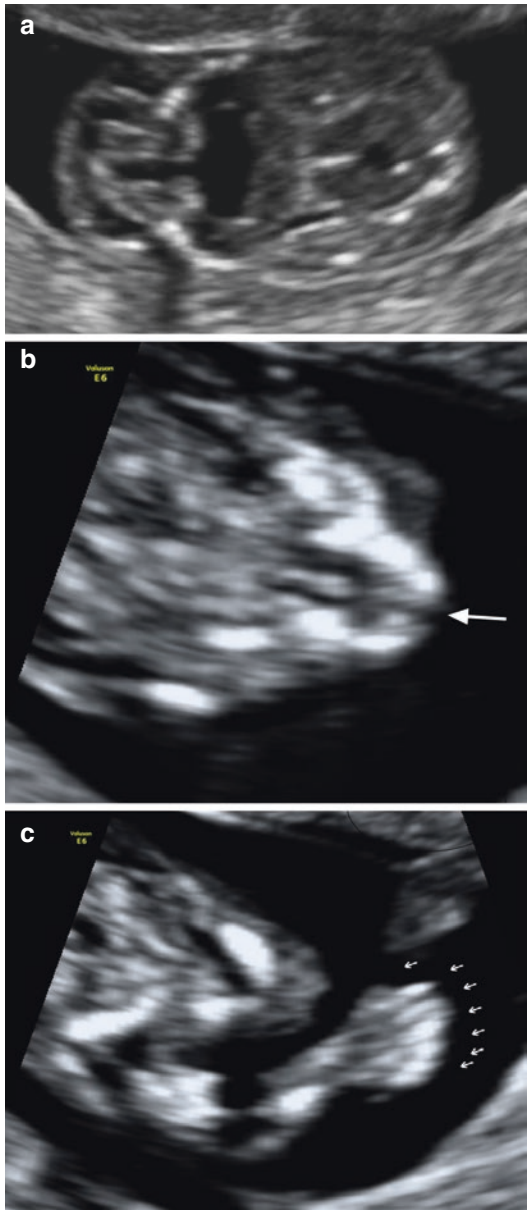

Fig. 9.2 Fetus with Meckel–Gruber syndrome identified at 12 weeks of gestation as demonstrated by TVS. (**a**) Occipital encephalocele; (**b**) note the presence of cleft lip (*arrow*) and (**c**) polydactyly

early as 10–14 weeks [19, 20] (Fig. 9.5). Sepulveda and Wong demonstrated that failure to visualize the choroid plexuses, the "butterfly" sign, during the first trimester is highly predictive of the presence of HPE, and they were able to diagnose 11 cases out of 11,068 fetuses scanned without false-positive or false-negative cases [21]. In alobar and semilobar holoprosencephaly, the first clue for diagnosis may be either the visualization of an abnormal brain or an abnormal face. CNS findings include the presence of a large single ventricle with a thin cerebral mantle, failure to visualize the choroid plexuses, or the visualization of a large noncleaved thalamus (Figs. 9.3, 9.4, 9.5). It may be extremely difficult to differentiate between a fetus with HPE and one with severe hydrocephaly and ruptured septum pellucidum [22]. In these cases, as well as when lobar HPE is suspected, the best way to reach a conclusive diagnosis is by visualization of the most rostral portions of the cerebral hemispheres and frontal horns of the lateral ventricles in a coronal plane; all three classical forms of HPE will have a common frontal ventricle and at least some degree of non-cleavage of the frontal lobe without a normal interhemispheric fissure (Fig. 9.6). Visualization of two separated frontal horns at their foremost anterior position confidenty rules out a classic form of HPE. In these cases, other important findings are the presence of an abnormal anterior cerebral artery trajectory running closer than usual to the anterior subarachnoid space, a single choroid plexus, and the presence of craniofacial anomalies.

Extreme facial malformations as present in the agnathia–otocephaly complex are usually associated with HPE (Fig. 9.7), but can be also isolated [23]. When HPE is not present, a detailed examination may detect less common types of anomalies (Figs. 9.7 and 9.8).

In lobar HPE, the CNS anomalies are usually more subtler, and since most of these fetuses do not have severe facial dysmorphism, many cases may remain undiagnosed during pregnancy. Late diagnosis may be facilitated by the presence of a dysgenetic CC, failure to visualize the septum pellucidum, or following investigation because of suspected microcephaly or mild ventriculomegaly. Atypical forms of HPE may also be hard to diagnose during fetal life, childhood, or even in adulthood. In some cases, the diagnosis is made after the delivery of an affected child with a more severe form of HPE.

Table 9.2 Classification of holoprosencephaly

HPE type	HPE subtype		Eye	Nose	Mouth
Classical forms	Alobar		Range from single orbit/eye to mild hypotelorism	Arrhinia, proboscis, single nostril	Agnathia, cleft lip and palate
	Semilobar		Range from single orbit/eye to mild hypotelorism	Arrhinia, proboscis, single nostril	Agnathia, cleft lip and palate
	Lobar		Small OOD/IOD/normal	Normal	Cleft lip/palate
Atypical forms	Middle interhemispheric variant		Normal	Normal	Normal
	Septopreoptic		Normal	Normal	Single incisor
	Microforms				
		Isolated hypotelorism	Small OOD/IOD	Normal	Normal
		Single incisor	Normal	Normal	Normal

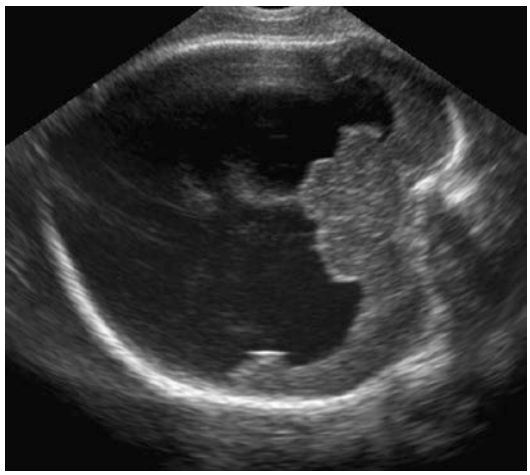

Fig. 9.3 Alobar holoprosencephaly diagnosed at 27 weeks of gestation by the presence of a single ventricle with remnants of brain tissue

9.3 Disorders of Cortical Development

9.3.1 Microcephaly

Microcephaly is frequently found in syndromes affecting the face; in the majority, this condition develops during the postnatal period in children born with normal head circumferences. In these cases, the prenatal diagnosis of microcephaly, particularly during the first and second trimesters, is extremely rare. Although brain proliferation starts during the second month of pregnancy, it cannot be measured or evaluated on imaging until much later in gestation, by which time the associated craniofacial anomalies should be easily identifiable.

Microcephaly syndromes involving the face that have been diagnosed or described in fetuses are few (Table 9.3). When a case of suspected microcephaly is suspected during pregnancy, the fetal face needs to be scrutinized as carefully and comprehensibly as possible.

9.3.2 Macrocephaly

As with microcephaly, macrocephaly is common in children and adults with facial dysmorphism, but this association is rarely reported during the prenatal period.

Kuniba et al. published a case of a severely overgrown fetus with macrocephaly and "coarse" face using 3D ultrasound at 24 weeks diagnosed using whole genomic amplification as Costello syndrome (CS). Although prenatal overgrowth (>+5 SD), macrocephaly (+3 SD)

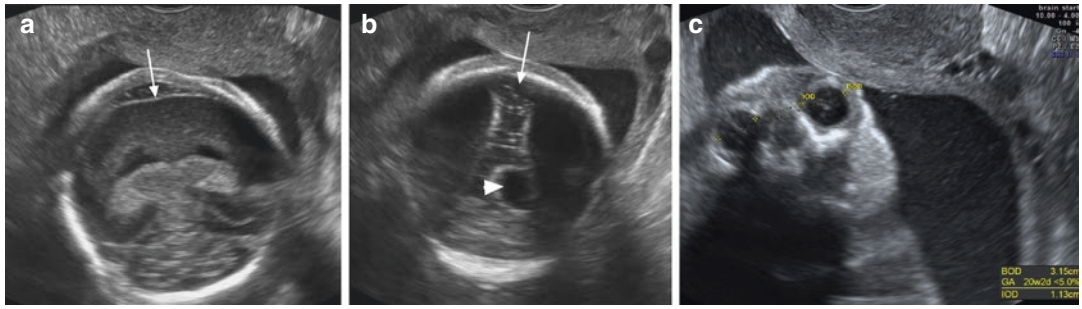

Fig. 9.4 Semilobar holoprosencephaly diagnosed at 23 weeks of gestation. (**a**) Coronal view shows absent cleavage of the brain; note the missing interhemispheric fissure (*arrow*). (**b**) Coronal view shows the occipital lobes separated by the interhemispheric suture (*arrow*); note the presence of a small subarachnoid cyst (*arrowhead*). (**c**) Hypotelorism is observed

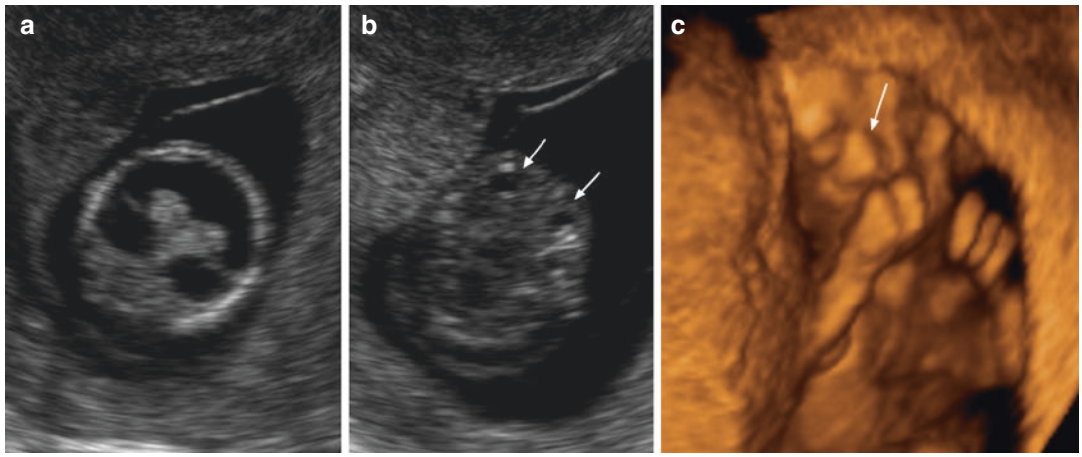

Fig. 9.5 Alobar holoprosencephaly diagnosed at 12 weeks of gestation. (**a**) The thalami are not cleaved and are floating in the large single ventricle; the brain parenchyma is not observed. (**b**) Hypotelorisim is present and one of the eyes is smaller than the other one (*arrows*). (**c**) Three-dimensional reconstruction of the face shows an abnormal bifid nose (*arrow*)

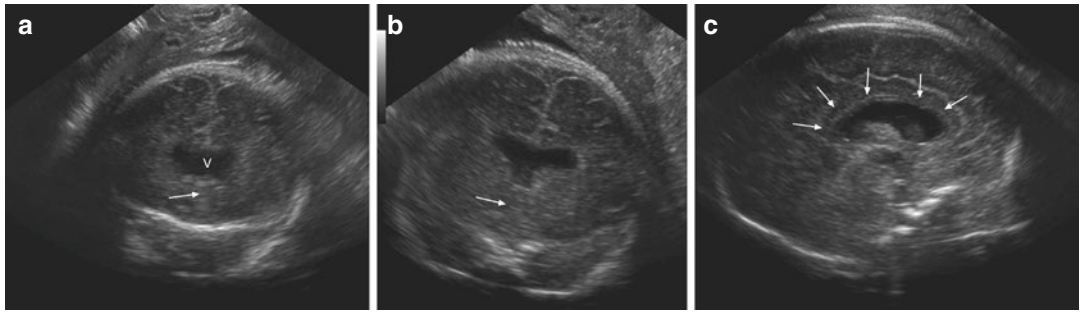

Fig. 9.6 Lobar holoprosencephaly diagnosed at 35 weeks of gestation without facial dysmorphism. (**a**) Coronal view shows fused frontal horns of the lateral ventricle (*V*) and fused hemispheres; the interhemispheric fissure is absent (*arrow*). (**b**) Coronal view shows the absence of the septum pellucideum and fused hemispheres (*arrow*). (**c**) Median view shows dysgenesis of the corpus callosum (*arrows*)

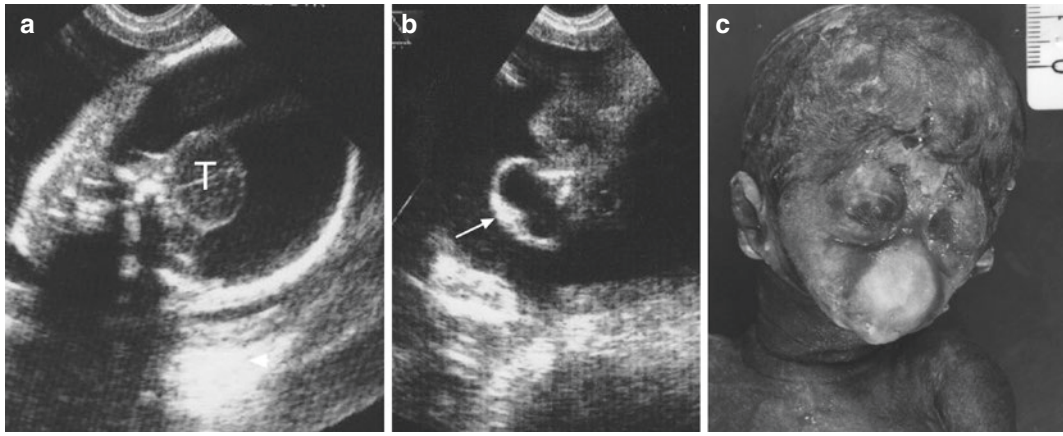

Fig. 9.7 Agnathia–otocephaly complex with lobar HPE at 19 weeks of gestation. (**a**) Lobar HPE; only the thalami are observed (*T*). (**b**) US shows that the mouth is replaced by a cystic structure (*arrow*); note associated hypotelorism. (**c**) Stillborn fetus shows similar findings

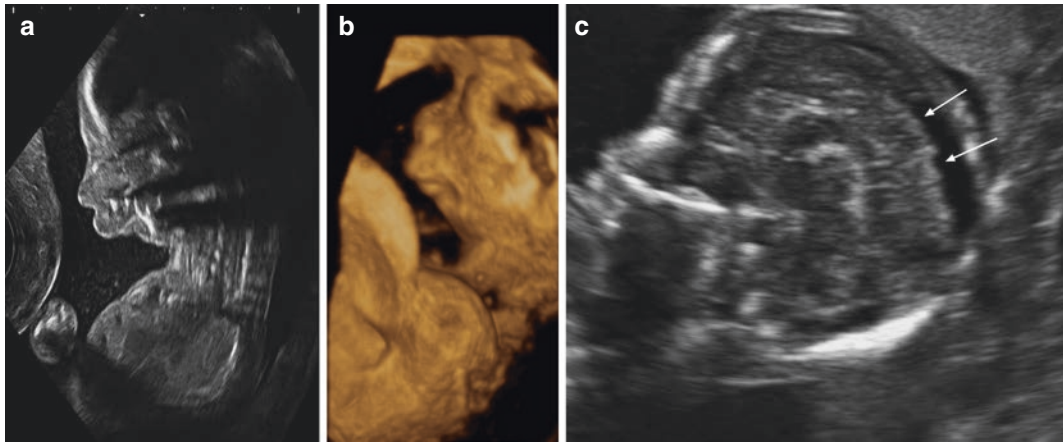

Fig. 9.8 Fetus with agnathia–otocephaly complex. (**a**) and (**b**) 2D and 3D images show severe micrognathia; (**c**) parasagittal view shows irregular cortex consistent with polymicrogyria but without HPE

and polyhydramnios were present at 23 weeks, the facial dysmorphism described by the authors that included "pointed chin, full cheeks, wide nasal bridge, and low-set ears" were difficult to identify in the images provided [24]. Lin et al. found that the association between macrocephaly, polyhydramnios, and atrial tachycardia is prevalent in fetuses with CS; in one of 3 suspected fetuses, macroglossia was diagnosed. In the other two, the facial dysmorphism (hypertelorism and macroglossia) was only diagnosed after delivery [25].

9.3.3 Migration Disorders

According to accepted theories of cortical development, proliferation of neural cells occurs at the periventricular zone; following this step, the cells start to migrate toward the pia mater in six different but orderly waves to form the cortex. Arrest of neuronal migration at its origins produces a condition called periventricular neuronal heterotopia (PNH); when the cells stop in the white matter, the phenomenon is called white matter heterotopia. Failure of neurons to migrate

produces another unwanted effect, the underdevelopment of the zone gray matter called lissencephaly or pachygyria. In cases where the pia mater fails to serve as a barrier for the neurons entering the meninges, a cobblestone pattern, currently considered a form of polymicrogyria, develops.

Cobblestone brain malformation (COB) is characterized by cortical dysplasia and aberrant neuroglial migration through breaches in the pial basal/glial limitans membrane into the subarachnoid space; the result is neuronal ectopia that produces an irregular "lumpy-bumpy" appearance. COB is typically observed in α-dystroglycanopathy types of congenital muscular dystrophies (CMDs), which are associated with various ocular abnormalities, delineating the spectrum of muscle-eye-brain disease [26]. Prenatal diagnosis is possible in cases with a previous affected sibling or when an association between severe ventriculomegaly, cortical and hindbrain malformations, and ocular anomalies are found [27].

Some of these conditions may be found occasionally in fetuses, children, and adults with craniofacial malformations; in other cases, the migration disorder represents the hallmark of the syndrome with craniofacial malformations occasionally present. In some patients with frontonasal dysplasia syndromes, not only PNH but other CNS anomalies, such as encephaloceles, microcephaly, and callosal agenesis, may be present [6]. In Aicardi syndrome [28], a condition defined by the presence of callosal anomalies, chorioretinal lacunae, and infantile spasms and frequently associated with proliferation and migration disorders, craniofacial anomalies involving mainly the eyes and mouth have been described.

9.3.4 Cerebellar Anomalies

Cerebellar anomalies may be associated with facial anomalies, but in most of the cases, other CNS malformations are expected to be found in these fetuses (Tables 9.1, 9.3, and 9.4).

Table 9.3 Malformations of cortical development with facial syndromes and anomalies

MCD anomalies	Facial anomalies	Syndrome	Other CNS findings	Genetics	References
Microcephaly	Mandibular hypoplasia, midline cleft palate, choanal atresia, ear anomalies	Mandibulofacial dysostosis (spliceosomal defects)	None	Mutations in EFTUD2 gene	Lines [29], Lehalle [30]
Microcephaly	Micrognathia, hypertelorism, cataract, microphthalmia, cleft lip and palate	Neu–Laxova	Lissencephaly, ACC, ONTD, Dandy–Walker, cerebellar hypoplasia	Mutations in PHGDH gene	Acuña-Hidalgo [31]
Microcephaly	Micrognathia, prominent upper lip (long philtrum), increased skin thickness forehead	Brachmann–de Lange	None	Mutations in NIPBL and SMC1L1 genes	Pajkrt [32]
Microcephaly	Micrognathia, microphthalmia, prominent upper lip	Cerebro–oculo–facio–skeletal (COFS)	Pachygyria, ACC	Mutation in ERCC genes	Paladini [33]
Macrocephaly	Coarse facies, micrognathia, hypertelorism, thick lips, macroglossia	Costello	Ventriculomegaly, cerebral atrophy, large cerebellum	Mutation in HRAS gene	Kuniba [24] Lin [25]
PNH	Median cleft lip, hypertelorism	Frontonasal dysplasia	Abnormal cerebellum, encephalocele, ACC, microcephaly	Usually sporadic	Recio-Rodriguez [34] Martinelli [6]
Polymicrogyria, heterotopia, pachygyria	Facial asymmetry, microphthalmia, coloboma, retinal detachment, cataract, cleft lip, cleft palate	Aicardi	ACC, abnormal cerebellum, intrahemispheric cysts, large CPC, asymmetric hemispheres, widening of the opercula	X-linked dominant	See text and Fig. 9.8

Table 9.4 Cerebellar malformations with associated facial syndromes and anomalies

Cerebellar anomalies	Facial anomalies	Syndrome	Other CNS findings	Genetics	References
Vermian hypoplasia	Micrognathia, hypertelorism, cleft lip and palate, broad nasal tip	Oral–facial–digital, type VI	Molar tooth sign, hypothalamic hamartoma	Mutation in C5ORF42 gene	Poretti [35]
Pontocerebellar hypoplasia	Microphthalmia, retinal detachment, congenital, cataracts	Cobblestone brain malformation	Ventriculomegaly, macrocephaly, DWM, abnormal cortical lamination	Mutations in POMT1, FKTN, LARGE, and at least other 11 genes	Lacalm [36]
Cerebellar hypoplasia	Cleft lip and palate, micrognathia, microphthalmia	Hydrolethalus	Ventriculomegaly, DWM, ACC, hamartoma, hypoplastic brain stem	Mutations in HYLS1 and KIF7 genes	Paetau [37]

References

1. Volpe JJ. Neural tube formation and prosencephalic development. In: Neurology of the newborn. Philadelphia: Saunders Company; 2008. p. 3–50.
2. Gruss JS, Matthews DN. Median cerebrofacial dysgenesis: the syndrome of median facial defects with hypotelorism. Cleft Palate J. 1978;15:275–81.
3. Jones KL, Smith DW. Smith's recognizable patterns of human malformation. Philadelphia: Elsevier Saunders; 2006.
4. Stoll C, Alembik Y, Dott B. Associated malformations in cases with neural tube defects. Genet Counsel. 2007;18:209–15.
5. Goumy C, Gay-Bellile M, Eymard-Pierre E, Kemeny S, Gouas L, Dechelotte P, Gallot D, Veronese L, Tchirkov A, Pebrel-Richard C, Vago P. De novo 2q36.1q36.3 interstitial deletion involving the PAX3 and EPHA4 genes in a fetus with spina bifida and cleft palate. Birth defects research Part A, Clinical and molecular. Teratology. 2014;100:507–11.
6. Martinelli P, Russo R, Agangi A, Paladini D. Prenatal ultrasound diagnosis of frontonasal dysplasia. Prenat Diagn. 2002;22:375–9.
7. Esmer AC, Kalelioglu I, Kayserili H, Yuksel A, Has R. Prenatal diagnosis of frontonasal dysplasia with anterior encephalocele. J Turk Ger Gynecol Assoc. 2013;14:50–2.
8. Uz E, Alanay Y, Aktas D, Vargel I, Gucer S, Tuncbilek G, von Eggeling F, Yilmaz E, Deren O, Posorski N, Ozdag H, Liehr T, Balci S, Alikasifoglu M, Wollnik B, Akarsu NA. Disruption of ALX1 causes extreme microphthalmia and severe facial clefting: expanding the spectrum of autosomal-recessive ALX-related frontonasal dysplasia. Am J Hum Genet. 2010;86:789–96.
9. Barisic I, Boban L, Loane M, Garne E, Wellesley D, Calzolari E, Dolk H, Addor MC, Bergman JE, Braz P, Draper ES, Haeusler M, Khoshnood B, Klungsoyr K, Pierini A, Queisser-Luft A, Rankin J, Rissmann A, Verellen-Dumoulin C. Meckel-Gruber Syndrome: a population-based study on prevalence, prenatal diagnosis, clinical features, and survival in Europe. Eur J Med Genet. 2015;23:746–52.
10. Romani M, Mancini F, Micalizzi A, Poretti A, Miccinilli E, Accorsi P, Avola E, Bertini E, Borgatti R, Romaniello R, Ceylaner S, Coppola G, D'Arrigo S, Giordano L, Janecke AR, Lituania M, Ludwig K, Martorell L, Mazza T, Odent S, Pinelli L, Poo P, Santucci M, Signorini S, Simonati A, Spiegel R, Stanzial F, Steinlin M, Tabarki B, Wolf NI, Zibordi F, Boltshauser E, Valente EM. Oral-facial-digital syndrome type VI: is C5orf42 really the major gene? Hum Gene. 2015;134:123–6.
11. Jacobson M, Rao MS. Developmental neurobiology. New York: Kluwer Academic/Plenum; 2005.
12. Marcorelles P, Laquerriere A. Neuropathology of holoprosencephaly. Am J Med Genet C Semin Med Genet. 2010;154C:109–19.
13. Ming JE, Muenke M. Multiple hits during early embryonic development: digenic diseases and holoprosencephaly. Am J Hum Genet. 2002;71:1017–32.
14. Mercier S, Dubourg C, Garcelon N, Campillo-Gimenez B, Gicquel I, Belleguic M, Ratie L, Pasquier L, Loget P, Bendavid C, Jaillard S, Rochard L, Quelin C, Dupe V, David V, Odent S. New findings for phenotype-genotype correlations in a large European series of holoprosencephaly cases. J Med Genet. 2011;48:752–60.
15. Demyer W, Zeman W, Palmer CG. The face predicts the brain: diagnostic significance of median facial anomalies for holoprosencephaly (arhinencephaly). Pediatrics. 1964;34:256–63.
16. Cohen MM Jr. Perspectives on holoprosencephaly: part III. Spectra, distinctions, continuities, and discontinuities. Am J Med Genet. 1989;34:271–88.
17. Orioli IM, Castilla EE. Epidemiology of holoprosencephaly: prevalence and risk factors. American journal of medical genetics Part C. Sem Med Genet. 2010;154c:13–21.
18. Hidalgo H, Bowie J, Rosenberg ER, Ram PC, Ford K, Lipsit E. Review. In utero sonographic diagnosis of fetal cerebral anomalies. AJR Am J Roentgenol. 1982;139:143–8.
19. Bronshtein M, Wiener Z. Early transvaginal sonographic diagnosis of alobar holoprosencephaly. Prenat Diagn. 1991;11:459–62.
20. Kagan KO, Staboulidou I, Syngelaki A, Cruz J, Nicolaides KH. The 11-13-week scan: diagnosis and outcome of holoprosencephaly, exomphalos and megacystis. Ultrasound Obstet Gynecol. 2010;36:10–4.
21. Sepulveda W, Wong AE. First trimester screening for holoprosencephaly with choroid plexus morphology ('butterfly' sign) and biparietal diameter. Prenat Diagn. 2013;33:1233–7.
22. Malinger G, Lev D, Kidron D, Heredia F, Hershkovitz R, Lerman-Sagie T. Differential diagnosis in fetuses with absent septum pellucidum. Ultrasound Obstet Gynecol. 2005;25:42–9.
23. Hisaba WJ, Milani HJ, Araujo Junior E, Passos JP, Barreto EQ, Carvalho NS, Helfer TM, Pares DB, Nardozza LM, Moron AF. Agnathia-otocephaly: prenatal diagnosis by two- and three-dimensional ultrasound and magnetic resonance imaging. Case report. Med Ultrasound. 2014;16:377–9.
24. Kuniba H, Pooh RK, Sasaki K, Shimokawa O, Harada N, Kondoh T, Egashira M, Moriuchi H, Yoshiura K, Niikawa N. Prenatal diagnosis of Costello syndrome using 3D ultrasonography amniocentesis confirmation of the rare HRAS mutation G12D. Am J Med Genet A. 2009;149:785–7.
25. Lin AE, O'Brien B, Demmer LA, Almeda KK, Blanco CL, Glasow PF, Berul CI, Hamilton R, Micheil Innes A, Lauzon JL, Sol-Church K, Gripp KW. Prenatal features of Costello syndrome: ultrasonographic findings and atrial tachycardia. Prenat Diagn. 2009;29:682–90.
26. Radmanesh F, Caglayan AO, Silhavy JL, Yilmaz C, Cantagrel V, Omar T, Rosti B, Kaymakcalan H,

Gabriel S, Li M, Sestan N, Bilguvar K, Dobyns WB, Zaki MS, Gunel M, Gleeson JG. Mutations in LAMB1 cause cobblestone brain malformation without muscular or ocular abnormalities. Am J Hum Genet. 2013;92:468–74.
27. Timor-Tritsch IE, Monteagudo A, Pilu G, Malinger G. Ultrasonography of the prenatal brain. New York: McGraw-Hill Professional; 2012.
28. Hergan B, Atar OD, Poretti A, Huisman TA. Serial fetal MRI for the diagnosis of Aicardi syndrome. Neuroradiol J. 2013;26:380–4.
29. Lines M, Hartley T, Boycott K. Mandibulofacial dysostosis with microcephaly. In: Pagon RA, Adam MP, Ardinger HH, Wallace SE, Amemiya A, Bean LJH, Bird TD, Fong CT, Mefford HC, Smith RJH, Stephens K, editors. GeneReviews(R). Seattle: University of Washington; 1993.
30. Lehalle D, Wieczorek D, Zechi-Ceide RM, Passos-Bueno MR, Lyonnet S, Amiel J, Gordon CT. A review of craniofacial disorders caused by spliceosomal defects. Clin Genet. 2015;88:405–15.
31. Acuna-Hidalgo R, Schanze D, Kariminejad A, Nordgren A, Kariminejad MH, Conner P, Grigelioniene G, Nilsson D, Nordenskjold M, Wedell A, Freyer C, Wredenberg A, Wieczorek D, Gillessen-Kaesbach G, Kayserili H, Elcioglu N, Ghaderi-Sohi S, Goodarzi P, Setayesh H, van de Vorst M, Steehouwer M, Pfundt R, Krabichler B, Curry C, MacKenzie MG, Boycott KM, Gilissen C, Janecke AR, Hoischen A, Zenker M. Neu-Laxova syndrome is a heterogeneous metabolic disorder caused by defects in enzymes of the L-serine biosynthesis pathway. Am J Hum Genet. 2014;95:285–93.
32. Pajkrt E, Griffin DR, Chitty LS. Brachmann-de Lange syndrome: definition of prenatal sonographic features to facilitate definitive prenatal diagnosis. Prenat Diagn. 2010;30:865–72.
33. Paladini D, D'Armiento M, Ardovino I, Martinelli P. Prenatal diagnosis of the cerebro-oculo-facio-skeletal (COFS) syndrome. Ultrasound Obstet Gynecol. 2000; 16:91–3.
34. Recio-Rodriguez M, Fernandez-Mayoralas DM, Fernandez-Jaen A, Fernandez-Perrone AL, Cano-Alonso R, Jimenez-de-La-Pena M. Prenatal diagnosis of frontonasal dysplasia associated with bilateral periventricular nodular heterotopia. J Child Neurol. 2014;29:NP122–6.
35. Poretti A, Brehmer U, Scheer I, Bernet V, Boltshauser E. Prenatal and neonatal MR imaging findings in oral-facial-digital syndrome type VI. AJNR Am J Neuroradiol. 2008;29:1090–1.
36. Lacalm A, Nadaud B, Massoud M, Putoux A, Gaucherand P, Guibaud L. Prenatal diagnosis of cobblestone lissencephaly associated with Walker-Warburg syndrome based on a specific sonographic pattern. Ultrasound Obstet Gynecol. 2016;47: 117–22.
37. Paetau A, Honkala H, Salonen R, Ignatius J, Kestila M, Herva R. Hydrolethalus syndrome: neuropathology of 21 cases confirmed by HYLS1 gene mutation analysis. J Neuropathol Exp Neurol. 2008;67: 750–62.

10 Development and Autopsy Assessment of the Fetal Head and Face

J. Ciaran Hutchinson and Neil J. Sebire

10.1 Overview

Embryonic development of the head and face is a complex process occurring during the first trimester, involving interactions between components from all three germ layers, between neural tube formation and associated head and facial development and between multiple branchial/pharyngeal arch components. For these reasons, numerous abnormalities may occur depending on the site, timing and severity of any defects in these processes. However, the general types and mechanisms of such anomalies can be reasonably grouped together, and this chapter aims to provide a brief overview of the major components of facial development in association with clinically significant fetal abnormalities. In addition, the chapter will briefly describe the approach to investigation of such abnormalities at autopsy and major associated features. For those interested, there are excellent and highly detailed accounts available of these processes from an embryological perspective, documenting the mechanisms of cellular interactions during these processes and with experimental evidence for the developmental origins of the various components, which are beyond the scope of this chapter [7, 12, 16, 21].

J.C. Hutchinson • N.J. Sebire (✉)
Department of Paediatric Pathology,
Great Ormond Street Hospital for Children,
London WC1N 3JH, UK
e-mail: neil.sebire@gosh.nhs.uk

10.2 Developmental Aspects of the Head and Face

Development of the head, particularly of the facial structures, represents a cohesive series of events resulting in formation of several anatomical systems including the central nervous system, specialist sense organs, such as the ears, and the first parts of both respiratory and alimentary systems including the nose, pharynx and mouth. In addition, the area demonstrates complex developmental formation of bony structures, muscles and innervation to allow blinking, chewing, swallowing, talking and facial expression.

In order to achieve this final arrangement, embryonic development requires tightly controlled interactions between the numerous systems and developmental elements. The most important overriding concepts in this regard for overall head and face development are:

- Formation of the underlying brain and its impact on development of both the cranium and face
- The pivotal role of the neural crest for all aspects of development at this site
- The important contributions of the branchial/pharyngeal arches to both facial and neck structure development

G. Tonni, W. Sepulveda, and A.E. Wong (eds.), *Prenatal Diagnosis of Orofacial Malformations*,
DOI 10.1007/978-3-319-32516-3_10

10.2.1 Neural Development

Formation of the brain proper will not be covered here; suffice to note that the brain structures proper, peripheral nervous system elements and ectodermal placodes are ultimately derived from the neural plate and neural folds, this tissue forming the brain structures proper, peripheral nervous system elements and ectodermal placodes. Furthermore, as the neural plate forms the neural tube and subsequent central nervous system, non-neuronal neural crest elements play an important contribution to the mesenchymal elements of various head and face structures, as indicated below.

The general brain regions are formed during early conception, even before the neural tube itself has closed. With further differential growth of these regions, a series of folds or flexures occur that divides the brain into segments, each forming distinct components of the mature central nervous system. Concurrently, neural crest cells from these regions are formed, which then contribute to specific regional elements such as trigeminal, facial, vestibuloacoustic and superior petrosal ganglia, in addition to other elements of the sympathetic and parasympathetic nervous system in this region. Similarly, the regional and ordered distribution of the cranial nerves and their nuclei are determined at this time [22].

10.2.2 Skull Development

The skull develops as the cranium proper from local paraxial mesenchyme, which forms the membranous frontal, parietal, squamous and occipital bones that surround the brain. The face and jaw bones are derived from neural crest components.

10.2.3 Overview of Facial Development

The structural complexity of the face is due to its development being related to the growth and folding of the brain, cranial coverings, components formed from the branchial arches (see later) and also the interrelationship with the endodermally derived foregut system [4]. The face essentially forms around the cranial end of the foregut, which is initially closed at the buccopharyngeal membrane, the junction between the endoderm and ectoderm, within a depression, the stomodeum. This area will become the mouth and the other facial elements are hence formed from the surrounding areas. The buccopharyngeal membrane breaks down, and with development of the pharyngeal arches, this part of the foregut forms the mouth and pharynx and its derivatives. Therefore, the majority of the face and neck, including the pharynx and larynx, are derived from a combination of neural fold-derived ectoderm and mesoderm from the pharyngeal arches which surround the developing foregut.

The majority of facial development in terms of formation of structures occurs around weeks 4–8 postconception. Further anatomical changes occur as a consequence of differential growth rather thatn development of new structures.

10.2.4 Branchial/Pharyngeal Apparatus

Given the importance and complexity of the development of the branchial/pharyngeal apparatus to the formation of the head and neck structures, this section will provide further detail. These primitive structures form gills in fish but contribute to many head and neck elements in the human [15]. Around week four of development, neural crest cells migrate into ridges on either side of the future head, which are separated by grooves or clefts, with four major arches (five in total) forming in humans. With subsequent growth these structures become fused and the outer surface of the face and neck is smooth.

The five pharyngeal arches are each composed of a covering of ectoderm (some also contain endoderm), with associated neural crest-derived mesenchymal elements. The arches therefore contribute to epithelial-derived structures, mesenchymal elements such as connective tissue and muscle and mesenchymal-derived vascular structures and nerves. Facial muscles are derived from branchial arch mesenchyme. Each arch is

associated with a corresponding cranial nerve, explaining the innervation of face and neck structures. The overall control of this process in terms of order and regulation appears to be largely controlled by homeobox (Hox) gene expression patterns [4], but a large number of additional factors are now being recognized as potentially important, including BMPs and FGFs [13, 23].

The first arch structures form the lower jaw and midface, including the maxilla and mandible, bones of the middle ear (malleus and incus) and associated muscles and ligaments, and are associated with the trigeminal nerve.

The second arch forms the middle ear stapes and part of the temporal and hyoid bones and is associated with the facial nerve.

The third arch forms part of the hyoid and is associated with the glossopharyngeal nerve.

The fourth to fifth arches form the larynx and are associated with the vagus nerve.

Since the arches are separated by grooves, four well-defined pharyngeal pouches also therefore form, in which the primitive foregut/pharyngeal endoderm is in close proximity to the ectoderm at the base of the grooves.

The first pouch forms the tympanic membrane, cavity and mastoid antrum and Eustachian tube. The second pouch forms the tonsillar fossa, the third pouch forms the inferior parathyroid glands and thymus and the fourth pouch forms the superior parathyroid glands. The first groove therefore persists as the external auditory meatus, whilst all other grooves are obliterated, providing the normal smooth outline of the neck.

Failure of this complex process of endodermal, mesodermal and ectodermal cellular interaction, differential growth and migration may result in a range of associated anomalies, which can be readily predicted based on the knowledge of their normal embryological derivatives. For example, persistence of first groove elements may result in auricular anomalies and congenital auricular sinuses/remnants. Branchial sinuses on the lateral neck are a consequence of persistence of second groove elements. True branchial fistulas result from communications at the site of the base of the pharyngeal grooves, usually between the tonsillar clefts and lateral neck, and remnants of the second branchial groove or cervical sinus may result in branchial cysts.

Similarly, abnormal development of the various branchial arch structures themselves can result in a range of anomalies in relation to their developmental structures described above. Anomalies of the first branchial arch may be associated with abnormal development of the eyes, ears, mandible and palate, presumably a consequence of defective neural crest migration or interaction with surrounding tissues. Examples of such so called "first arch syndromes" include Treacher Collins syndrome and Pierre Robin syndrome, both of which have characteristic facial dysmorphic features. Failure of normal third and fourth arch development leads to DiGeorge syndrome with thymic aplasia and absent parathyroid glands.

10.2.5 Formation of the Central Facial Structures

The face itself is formed from several components, or facial primordia, which develop around the primitive stomodeum. The frontonasal processes develop from the neural fold and significant components, including the paired maxillary and mandibular processes, develop from the first pharyngeal arch, including the paired maxillary and mandibular processes. Neural fold mesenchyme forms around the olfactory placodes forming the medial and lateral nasal swellings, which fuse with the frontonasal prominence to form the nose. The nasal cavities form from underlying nasal sacs, and with degeneration of the oronasal membrane and subsequent formation of the palate, the nasal and oral cavities are separated, but connected by the choanae. Ectodermal epithelium in this region forms the olfactory epithelium. The paranasal sinuses develop only during late fetal life and into childhood, being small and primitive in the fetus.

The maxillary processes of the first arch fuse with the lateral nasal swellings in the midface, the epithelial junction of which (the nasolacrimal groove) develops into the nasolacrimal duct. The maxillary processes also grow medially, via the palatine shelves, to fuse together in the midline and also join with the intermaxillary segment of

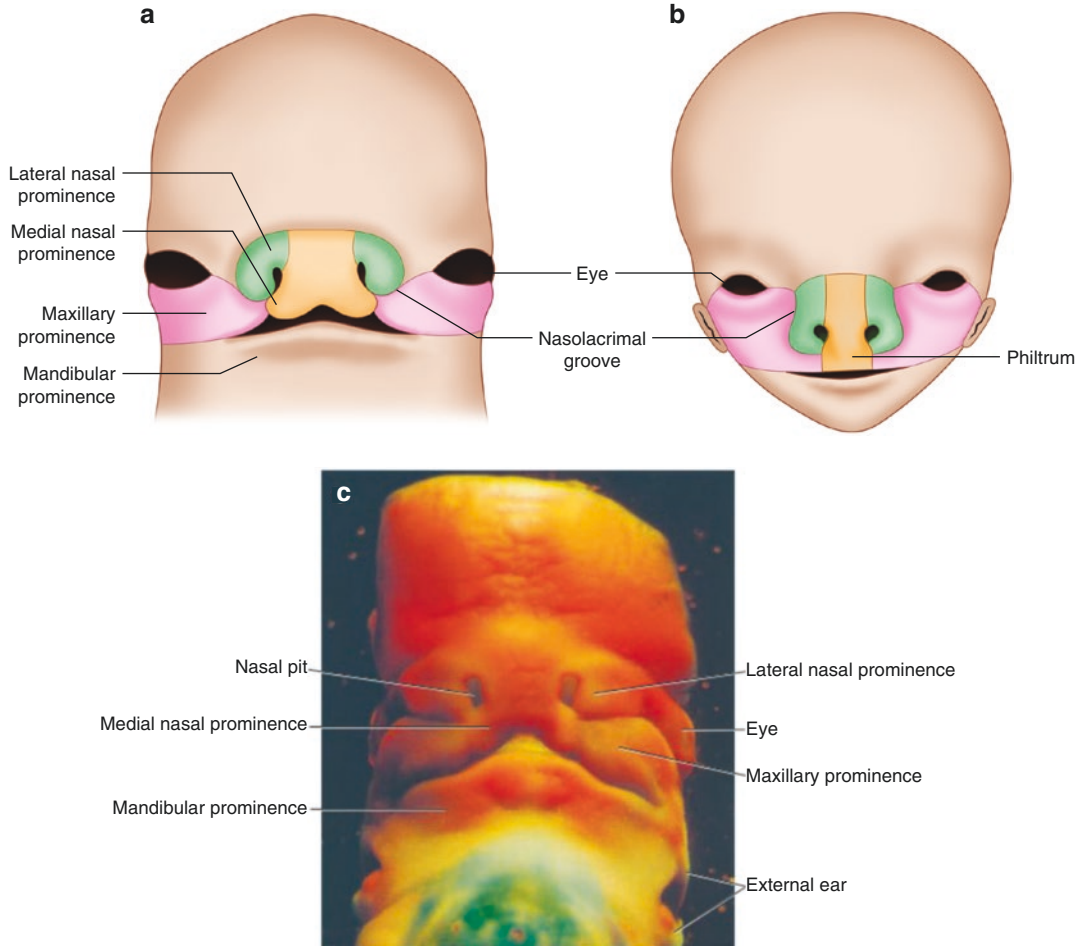

Fig. 10.1 Frontal aspect of the face. (**a**) Seven week embryo. Maxillary prominences have fused with the medial nasal prominences. (**b**) Ten week embryo. (**c**) Photograph of a human embryo at a stage similar to that in (**a**) (From Sadler [16], 12th ed, Fig 17.23 p. 277 and Fig. 17.24 p. 278)

the frontonasal prominence/premaxilla (which also forms the central lip philtrum), to form the normal intact lip and palate (Figs. 10.1 and 10.2).

If such elements fail to fuse normally, facial clefting of various types may result [20]. For example, if mesenchymal fusion between the maxillary process and nasal process is defective, typical anterior asymmetrical cleft lip occurs; the central philtrum area, being formed from the frontonasal process, is often intact although the nasal cavity floor is usually defective. Bilateral cleft lip (Fig. 10.3) occurs when the maxillary processes fail to fuse bilaterally with the medial nasal process. Central cleft palate is due to failure of the midline maxillary processes/palatine shelves to fuse [6]. Less commonly, more extensive fusion failure may result in severe clefts, such as an oblique cleft due to persistence of the nasomaxillary groove, and rarely, other types of facial cleft may occur due to failure of embryological development or fusion at other sites, such as midline cleft.

10.2.6 Tongue

The tongue forms in the floor of the primitive pharynx as the median tongue bud, with lateral tongue buds developing from the mesenchyme of the first branchial arcehes, which fuse to form the anterior part of the tongue. The posterior,

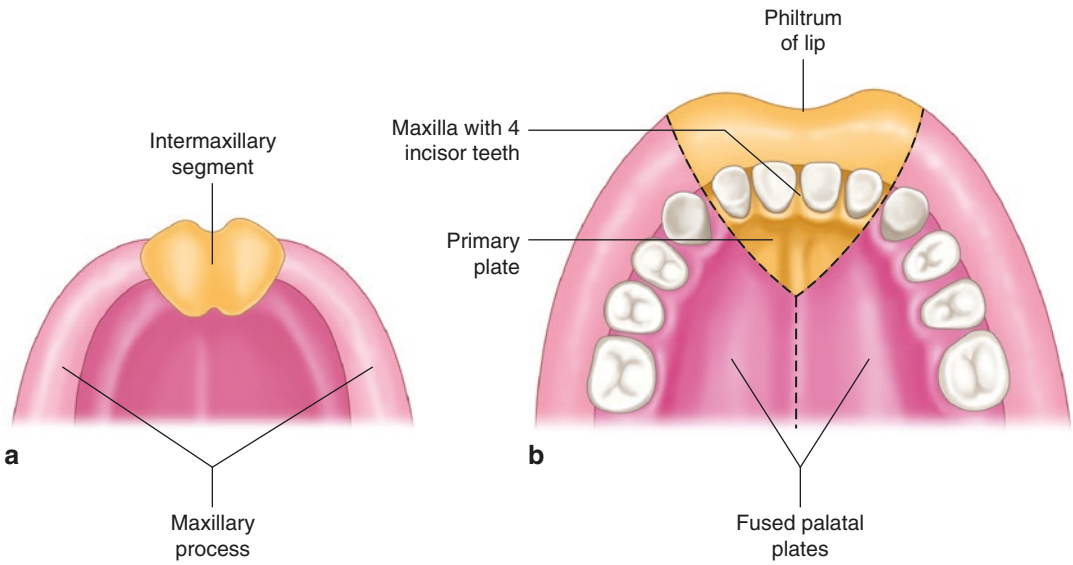

Fig. 10.2 (**a**) Intermaxillary segment and maxillary processes. (**b**) The intermaxillary segment giving rise to the philtrum of the upper lip, the median part of the maxillary bone with its four incisor teeth, and the triangular primary palate (From Sadler [16], 12th ed, Fig 17.23 p. 277 and Fig. 17.24 p. 278)

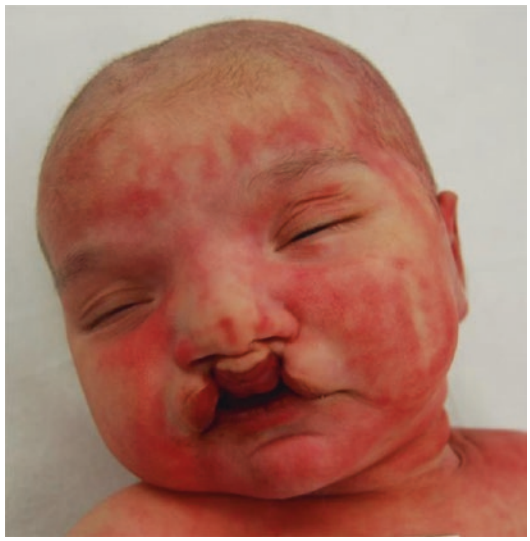

Fig. 10.3 Bilateral cleft lip with hypertelorism and a broad nasal bridge. Bilateral clefting occurs when the maxillary processes fail to fuse bilaterally with the medial nasal process

pharyngeal elements of the tongue are derived from the second, third and fourth branchial arches. Therefore, sensation to the anterior two-thirds is derived from the trigeminal nerve (with taste buds supplied by the facial nerve), whereas the majority of the remainder of the tongue is supplied by the glossopharyngeal nerve. The tongue musculature, which is formed from the occipital somite myocytes, is supplied mainly by the hypoglossal nerve.

Anomalies of tongue development are usually associated with other abnormalities of branchial arch development, but in addition to lingual thyroid and lingual cysts due to thyroglossal duct remnants (see above), isolated abnormalities may occur such as abnormal fusion of the lateral tongue buds resulting in a cleft tongue.

10.2.7 Thyroid Gland

The thyroid gland forms from the pharyngeal endoderm, originating as the thyroid diverticulum which is initially connected to the tongue base by the thyroglossal duct. The duct then normally atrophies with associated thyroid descent. Persistence of elements of the thyroglossal duct may result in a pyramidal thyroid lobe inferiorly, ectopic thyroid gland, such as lingual thyroid, superiorly and thyroglossal duct remnants and cysts anywhere along the course of the tract in the midline of the neck.

10.2.8 Ears

The ears form from the otic placodes, bilateral areas of ectoderm that invaginate into the otic vesicles from which the inner ear structures of the cochlea and semicircular canals develop. The middle ear and Eustachian tube are endodermally derived from the first pharyngeal pouch, with the ossicles formed from the first and second pharyngeal arches (see above). The external auditory meatus and tympanic membrane are formed from the first pharyngeal cleft, whereas the auricle is formed from six auricular nodules (hillocks) from the first and second pharyngeal arches. In this manner, the ears are normally "low set" in the neck region in early embryonic life, but their normal position is attained with development of the other facial structures.

10.2.9 Eyes

Lateral outpouchings of the forebrain form the optic vesicles, which interact with the overlying ectoderm. In conjunction with the surrounding mesenchyme, which contributes to the choroid and sclera, these elements form the globe of the eye and anterior structures such as the lens and cornea. Recent understanding of the molecular interactions involved in eye development has demonstrated a complex communication between the various epithelial/mesenchymal components, with *PAX6* being a major gene involved [2].

10.2.10 Teeth

The teeth are derived from a complex interaction between the ectoderm of the oral region and underlying neural crust mesenchyme. The epithelium initially forms dental buds that then develop into the tooth caps and subsequent outer layers by differentiation to ameloblasts, whereas the neural crest mesenchyme forms the central dental papilla and underlying odontoblasts and cementoblasts.

10.3 Approach to Autopsy Assessment of the Head and Face

Whilst defects of embryogenesis as discussed above are malformations (structural abnormalities arising as a direct result of an abnormal developmental process), facial abnormalities may also be deformations (structural abnormalities arising from localised or generalised mechanical forces acting on a forming anatomical structure) or disruptions (secondary destruction of an organ or structure that was previously normally formed). When assessing such abnormalities, it is therefore important to bear in mind the etiology of the pathology present and distinguish between a sporadic disruption and a malformation with significant recurrence risk. For example, a cleft-like disruption due to amniotic band sequence implies different future implications than orofacial clefting in an autosomal recessive syndrome with a 25 % recurrence risk.

For the majority of prenatally identified facial abnormalities, post-mortem assessment is straightforward, requiring direct visualisation and photographic confirmation only in most cases (Figs. 10.4 and 10.5). However, it should be recognized that changes that occur following death, especially with prolonged intrauterine

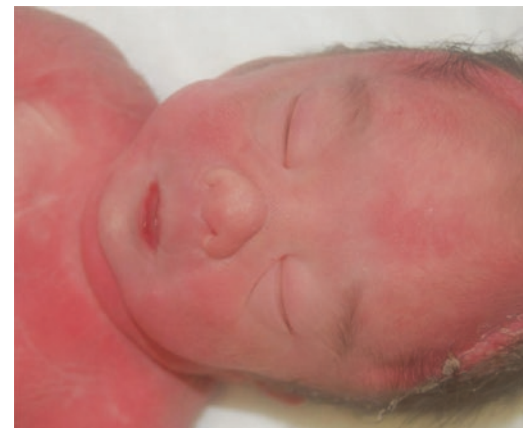

Fig. 10.4 Upslanting palpebral fissures, prominent epicanthal folds, poorly developed nasal bridge, long philtrum and micrognathia in possible Pallister-Hall syndrome. Post-mortem photography enables clinical correlation of findings with antenatal data in difficult cases

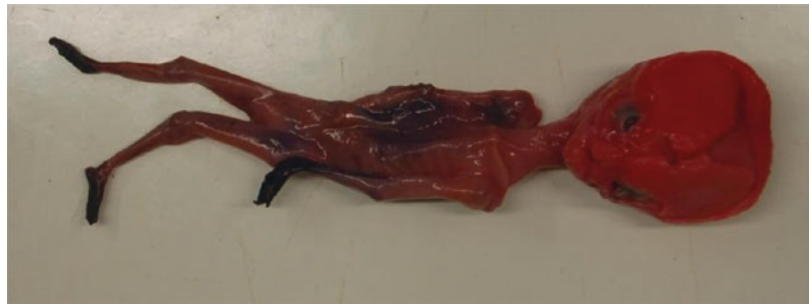

Fig. 10.5 Assessment of the fetus in this case reveals marked hypertelorism with an obvious central cleft lip and palate and minimal nasal development. Karyotyping revealed the presence of triploidy

Fig. 10.6 Maceration following 7 weeks intrauterine retention

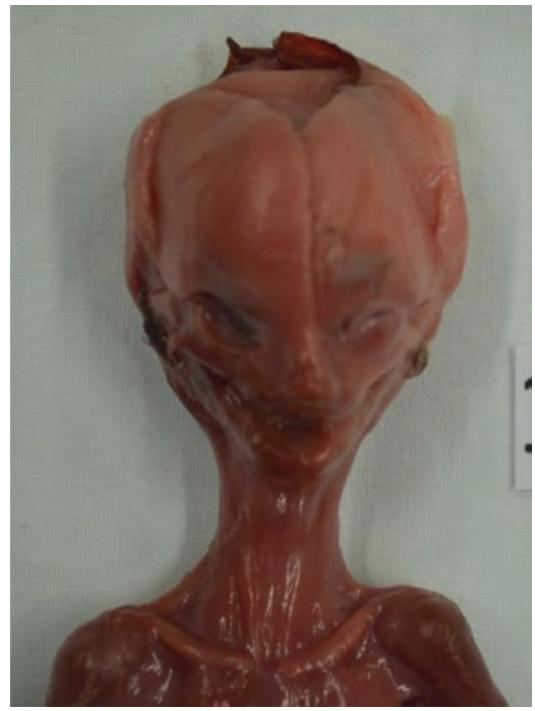

Fig. 10.7 Maceration following 5 weeks intrauterine retention

retention, may lead to secondary alterations to facial appearances making interpretation of subtle dysmorphic features impossible and even making identification of more obvious anomalies more difficult (Figs. 10.6 and 10.7).

Nevertheless, there are two areas in which post-mortem assessment of such cases may provide additional clinically useful information. Firstly, many facial abnormalities, such as facial cleft, are associated with underlying multisystem syndromic disorders (Table 10.1). For some of these conditions, the associated abnormalities in other systems may be subtle and difficult to detect antenatally (such as trachea-esophageal fistula or imperforate anus); therefore, detailed autopsy examination can confirm an isolated facial anomaly or suggest a specific underlying syndromic disorder which may significantly influence recurrence risk and management of future pregnancies. Secondly, facial anomalies may be associated with underlying central nervous system (CNS) malformations, the accurate identification of which may be optimal post-mortem, particularly with the use of ancillary investigations such as post-mortem magnetic resonance imaging (MRI), which can reliably identify CNS anomalies even in cases in which formal neuropathological examination is not possible due to maceration and

Table 10.1 Examples of genetic associations of orofacial abnormalities

Syndrome	Gene	Inheritance pattern	Facial anomalies	Other abnormalities seen at autopsy	Associated neoplasms
Alport	COL4A3, COL4A4, COL4A5	X-linked (AD in 5%, AR rarely)	Misshapen lenses, cataracts, lenticonus, keratoconus, abnormally coloured retina	Leiomyomatosis of esophagus or uterus. Histological renal lesions	Not widely reported
Apert	FGFR2	AD	Craniosynostosis leads to turribrachycephalic skull with midface hypoplasia, proptosis and prognathism. May be cleft palate	"Mitten" syndactyly of 3 fingers/toes, fusion of cervical vertebrae. Occasionally, cardiac, genitourinary and GI anomalies	Case reports of associated dysgerminoma and rhabdomyosarcoma
Beare-Stevenson	FGFR2	AD	Craniosynostosis with midface hypoplasia, proptosis, prognathism, natal teeth, cloverleaf skull and abnormal ear development	Often acanthosis nigricans and cutis gyrata. Also choanal atresia, bifid scrotum, pyloric stenosis, anterior displacement of anus and rugated labia majora. Extremities normal in contrast to Apert	Not widely reported
Beckwith-Wiedemann	Complex, chromosome 11	Complex in 85% AD in 15%	Hemihyperplasia, macroglossia	Omphalocoele, renal anomalies, visceromegaly, hypoglycemia	Wilms' tumor, hepatoblastoma
Carpenter	RAB23/MEGF8	AR	Craniosynostosis with acrocephaly leads to a flat nasal bridge, downslanting palpebral fissures, low-set and abnormally shaped ears	Cryptorchidism, cardiac defects, polydactyly, cutaneous syndactyly and brachydactyly may be present. Also umbilical hernia and obesity	Not widely reported
Cornelia de Lange	NIPBL, SMC1A, HDAC8, RAD21, SMC3	Variable: AD or X-linked dominant Most cases de novo	Wide variation in phenotype. Microcephaly, cleft palate, arched eyebrows with synophrys, long eyelashes, ptosis, low-set ears, small and widely spaced teeth, upturned nose	Growth retardation, hypertrichosis, cardiac defects, gastrointestinal anomalies	Not widely reported
Cri du Chat syndrome	Chromosome 5p	Most cases sporadic	Telecanthus or hypertelorism, low-set ears, microcephaly, micrognathia, rounded face	Cardiac anomalies	Not reported
Crouzon	FGFR2/3	AD	Craniosynostosis leads to significant proptosis, mandibular prognathism	May be seen with (FGFR3) or without (FGFR2) acanthosis nigricans. Hydrocephalus in 30%. Grossly normal extremities	Not widely reported

Down	Trisomy 21 or unbalanced translocation	Only in unbalanced translocation	Small nose, flat nasal bridge, upslanting palpebral fissures, epicanthal folds, macroglossia, microtia, Brushfield spots	"Sandal gap" between the 1st and 2nd toe, single palmar crease, broad hands, cardiac anomalies, umbilical hernia, colonic aganglionosis	Leukemia and testicular cancer
Ectrodactyly, ectodermal dysplasia and cleft lip/palate syndrome	7q11.2-q21.3 TP63	AD	Orofacial clefting with ectodermal dysplasia, dental malformations seen in related syndromes	Ectrodactyly, urogenital abnormalities	Not widely reported
Edwards	Trisomy 18 (5% mosaic)	N/A	Microcephaly, micrognathia, orofacial clefts	Cardiac, esophageal, renal, diaphragmatic, abdominal wall and neural tube defects. Also flexed fingers and rocker bottom feet	Case reports of Wilms' tumor and hepatoblastoma
Freeman-Sheldon	MYH3	Variable: AD, AR	Microstomia with pursed lips, midface hypoplasia, short philtrum, chin dimple, hypertelorism, downslanting palpebral fissures, ptosis, microglossia, micrognathia, high-arched palate	Distal arthrogryposis, scoliosis, ulnar deviation of fifth finger, clubfoot	Not widely reported
Goldenhar (Oculo-auriculo-vertebral)	Unclear	Mostly non-heritable 1–2% AD	A spectrum of abnormalities; facial asymmetry with maxillary and mandibular hypoplasia. Microtia, microphthalmia also seen	Renal, cardiac and vertebral defects	Ocular epibulbar dermoids (choristomas)
Gorlin-Goltz	PTCH1	AD	Multiple basal cell carcinomas and keratocystic odontogenic tumors. Macrocephaly also seen	Depressions in the skin of the hands, axial skeletal abnormalities	Medulloblastoma, basal cell carcinoma cardiac and ovarian fibroma
Hurler	IDUA	AR	Frontal bossing, dolichocephaly due to premature closure of sutures, depressed nasal bridge, anteverted nostrils, macroglossia. Corneal clouding often seen	Cardiac anomalies, inguinal hernia, cardiomyopathy, airway obstruction, dermal melanocytosis, odontoid hypoplasia and subluxation of C1/2	Not reported
Jackson-Weiss	FGFR2	AD	Mandibular prognathism	Abnormal tarsals, medially deviated toes	Not widely reported

(continued)

Table 10.1 (continued)

Syndrome	Gene	Inheritance pattern	Facial anomalies	Other abnormalities seen at autopsy	Associated neoplasms
Klippel-Feil	GDF6, GDF3, MEOX1	GDF6 and GDF3: AD MEOX1: AR	Facial asymmetry, cleft palate, ocular anomalies	Low hairline at the back of the neck, cervical vertebral fusion, genitourinary anomalies, cardiac anomalies	Not widely reported
Lacrimo-auriculo-dento-digital (LADD)	FGF10 FGFR2 FGFR3	AD	Lacrimal duct openings absent or hypoplastic, producing keratoconjunctivitis or epiphora. Low-set ears, xerostomia, small teeth. Orofacial clefts	Absent or duplicated thumbs, syndactyly, triphalangeal thumb, clinodactyly, nephrocalcinosis, hydronephrosis	Not widely reported
Moebius	Unknown	Most cases sporadic	Weakness or paralysis of facial and eye muscles due to neurological pathology. Also seen: micrognathia, microstomia, dental anomalies, cleft palate	Skeletal abnormalities of extremities	Not widely reported
Muenke	FGFR3	AD	Unilateral or bilateral coronal synostosis or megalencephaly without synostosis. Mild midface hypoplasia	Carpal fusion, broad toes	Not widely reported
Nager	Unknown, chromosome 9 implicated	Variable, most sporadic though AD and AR reported	Malar hypoplasia, micrognathia, cleft palate, downslanting palpebral fissures, absent eyelashes, eyelid coloboma, microtia	Malformed or absent thumbs. Also clinodactyly and syndactyly. Less commonly, cardiac, renal and genitourinary anomalies	Not widely reported
Patau	Trisomy 13	Only in translocation	Microphthalmia, orofacial clefts, hypotelorism (may be as severe as cyclopia with proboscis)	Holoprosencephaly, polydactyly, cardiac malformations, renal malformations	Not widely reported
Pfeiffer	FGFR1/2 *(three subtypes)*	AD	Type 1: moderate-severe midface hypoplasia Type 2: cloverleaf skull and severe proptosis Type 3 turribrachycephaly with severe proptosis	Broad, medially deviated thumbs and toes common to all subtypes May also see laryngotracheal anomalies, choanal atresia in types 2 and 3	Not widely reported
Roberts	ESCO2	AR	Orofacial clefts, micrognathia, microcephaly, downslanting palpebral fissures, encephalocoele, small nose, hypoplastic nares	Symmetrical hypomelia or phocomelia; often the arms are more severely affected than the legs. Also digital anomalies, cardiac, renal and genitourinary malformations	Not widely reported

Rubinstein-Taybi	CREBBP	AD	Downslanting palpebral fissures, low columella, high-arched palate, dental anomalies	Broad thumbs and big toes; cardiac defects, cryptorchidism, renal anomalies	Leukemia, oligodendroglioma, medulloblastoma, neuroblastoma, meningioma, pilomatrixoma, choristoma
Saethre-Chotzen	TWIST1	AD	Unilateral or bilateral craniosynostosis, facial asymmetry, ptosis, small pinna and prominent crus. Occasionally cleft palate, maxillary hypoplasia, hypertelorism	Syndactyly, cardiac anomalies, vertebral fusions, duplicated big toe	Not widely reported
Simpson-Golabi-Behmel	GPC3	X-linked	Hypertelorism, macrostomia, macroglossia, palatal anomalies, upturned nose, furrowed tongue	Umbilical and diaphragmatic hernias, diastasis recti, visceromegaly, cardiac defects, genitourinary anomalies	Wilms' tumor Neuroblastoma
Smith-Lemli-Opitz	DHCR7	AR	Microcephaly, bi-temporal narrowing, ptosis, cataracts, broad nasal bridge, anteverted nares, micrognathia, cleft palate/uvula	Syndactyly of 2nd/3rd toes, polydactyly, cardiac anomalies, abnormal lung segmentation, pyloric stenosis, colonic aganglionosis	Not reported
Stickler	COL11A1 COL11A2 COL2A1 COL9A1 COL9A2	AD or AR	Flat facial profile, Pierre Robin sequence, ocular anomalies	Scoliosis, kyphosis, platyspondyly	Not widely reported
Sturge-Weber	Complex	N/A	Nevus flammeus, macrocephaly, ocular manifestations, soft tissue hypertrophy	Choroidal and leptomeningeal angiomas	Leptomeningeal angioma
Treacher Collins	TCOF1 POLR1D POLR1C	TCOF1 and POLR1D: AD POLR1C: AR	Micrognathia, sometimes severe. Microtia, cleft palate, downslanting palpebral fissure, eyelid coloboma, sparse lashes, dental anomalies	Defects of middle ear bones	Not reported
22q11.2 deletion	TBX1 and COMT	Mostly AD. Most cases arise de novo	Orofacial clefts, hypertelorism, microtia, periorbital fullness, everted upper lip, upslanting palpebral fissures	Thymic hypoplasia/absence, cardiac anomalies, kidney abnormalities, spinal abnormalities	Not reported

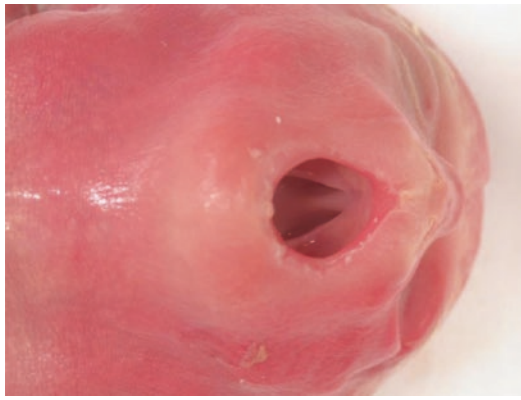

Fig. 10.8 Posterior midline cleft palate may not be easily appreciated on antenatal ultrasound but can be detected with a thorough external examination at autopsy

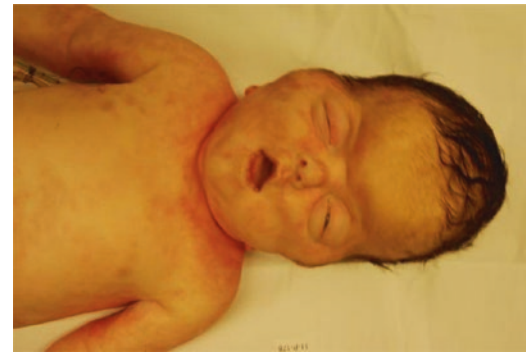

Fig. 10.9 Severe midface hypoplasia in association with Apert syndrome. Post-mortem photography assists with the demonstration of such findings to the clinical team

autolysis or for cases in which the parents do not agree to invasive autopsy [1]. Furthermore, post-mortem imaging with modalities such as computerised tomography (CT) or MRI allows highly accurate 3-D reconstructions of the facial anatomy in a nondestructive manner, allowing morphometric analysis possible. This approach is likely to be of significant future benefit for the objective evaluation of more subtle facial dysmorphic features. Finally, whilst most facial anomalies are readily visible externally, it should be recognized that some malformations, such as isolated posterior cleft palate, may be more difficult to recognize on routine antenatal sonography, and a noninvasive evaluation should be performed where possible even in cases where parents do not agree to invasive autopsy (Fig. 10.8).

Post-mortem assessment of the fetal head and face should be performed in a systematic manner and usually begins with global assessment of the shape of the head and face. For example, frontal "bossing" is a term used to describe unusual prominence or protrusion of the frontal bone; this may be seconary to craniosynostosis but can also arise due to increased extramedullary haematopoiesis. Similarly, a "cloverleaf"-shaped skull may be associated with an underlying skeletal dysplasia or synostosis syndrome; bi-temporal hollowing has been described in association with lissencephaly, particularly in Miller-Dieker and Norman-Roberts syndromes [9].

Midface hypoplasia and maxillary hypoplasia are essentially equivalent terms used to describe underdevelopment of the maxillary area, leading to apparent prominence of the lower jaw and abnormal facial profile. Midface hypoplasia may involve the dentoalveolar area or the whole of the midface and is a feature of craniosynostosis syndromes such as Apert syndrome and Crouzon syndrome (Fig. 10.9).

Examination of the eyes begins by taking into account their size, shape and relationship to each other. These factors can be assessed by measuring the inner and outer canthal distances as well as the interpupillary distance. Telecanthus refers to an increased inner canthal distance in the presence of a normal interpupillary distance. Telecanthus may occur as a result of trauma or arise as part of numerous genetic syndromes, including fetal alcohol and Cri du Chat syndromes. Ocular hypertelorism describes increased inner canthal and interpupillary distance, which may be present in numerous syndromes such as 22q11.2 deletion and Crouzon syndromes. Ocular hypotelorism by contrast indicates decreased inner canthal and interpupillary distances and is associated with syndromes including Meckel-Gruber and holoprosencephaly and can be caused by abnormalities in the sonic hedgehog pathway [10]. The palpebral fissure refers to the elliptical space of the eye itself, the angle of which defined by the positions of the lateral and medial canthi. Slight variation in the angle of

the palpebral fissures can be hereditary or associated with ethnicity; however, several syndromes are associated with marked alterations of this angle. For example, upslanting palpebral fissures are described in Down syndrome and 22q11.2 deletion, whilst downslanting palpebral fissures are associated with Treacher Collins, Nager, Carpenter and Rubinstein-Taybi syndromes. The eyelids and globes should also be closely inspected for notches (coloboma) and abnormalities of the lashes.

The ears should be assessed for their position, rotation and development. Position is difficult to assess in first- and early second-trimester fetuses, and with marked maceration but definite abnormalities of position, development or rotation may be associated with numerous syndromes. The most common abnormality of position is "low-set" ears, relative to the position of the lateral canthus of the eyes, but simplification of the external ear, small ears (microtia) and anteriorly or posteriorly rolated ears have been described.

Assessment of the mouth and oral cavity includes its position and size. The philtrum length may be elongated or shortened, whilst there may be an enlarged mouth and tongue in overgrowth syndromes. Conversely, microstomia may be associated with Freeman-Sheldon and Moebius syndromes. Cleft lip and palate are previously described and may be syndromic or non-syndromic, with both environmental and genetic factors (such as teratogens, chromosomal rearrangements) contributing to the development of this pathology, although no specific gene group has as yet been identified [11].

Dental abnormalities may be associated with anomalies of pharyngeal arch formation, such as Treacher Collins syndrome, but also in a range of conditions such as ectodermal dysplasias. Assessment of the jaw may demonstrate prognathism or micrognathia, though careful assessment of the midface should be made to avoid misinterpreting a normal jaw for prognathism in the context of maxillary hypoplasia. Micrognathia is a component of many syndromes and may vary from a relatively subtle abnormality to complete absence of the jaw (agnathia).

10.3.1 Tumors

Congenital facial tumors are rare but may demonstrate a range of unusual appearances on antenatal imaging, and hence their specific diagnosis often requires post-mortem evaluation. In view of the often complex anatomical changes, post-mortem imaging may be helpful [14]. By far, the most common congenital facial tumor is teratoma, which is thought to be derived from ectopic germ cells [17]. Teratomas usually arise in the midline and at this site may be truly intracranial, displacing the brain within the skull vault or arising from the floor of the mouth (epignathus) or in the neck, usually arising within the thymus. Histological evaluation demonstrates the characteristic mixture of elements derived from all three germ layers, usually containing immature tissues in this context [8]. Facial vascular malformations and hemangioma are also well described, but their diagnosis is often more easily possible sonographically and less commonly associated with poor outcome [3]. A range of other tumors types have been rarely reported, including cutaneous and soft tissue tumors, and even congenital malignancies, such as congenital orbital rhabdomyosarcoma [18, 19], though the commonest malignant ocular tumor in children is retinoblastoma [5].

References

1. Arthurs OJ, Thayyil S, Pauliah SS, Jacques TS, Chong WK, Gunny R, Saunders D, Addison S, Lally P, Cady E, Jones R, Norman W, Scott R, Robertson NJ, Wade A, Chitty L, Taylor AM, Sebire NJ. Diagnostic accuracy and limitations of post-mortem MRI for neurological abnormalities in fetuses and children. Clin Radiol. 2015;70:872–80.
2. Ashery-Padan R, Gruss P. Pax6 lights-up the way for eye development. Curr Opin Cell Biol. 2001;13:706–14.
3. Castillo BVJ, Kaufman L. Pediatric tumors of the eye and orbit. Pediatr Clin North Am. 2003;50:149–72.
4. Couly G, Creuzet S, Bennaceur S, Vincent C, Le Douarin NM. Interactions between Hox-negative cephalic neural crest cells and the foregut endoderm in patterning the facial skeleton in the vertebrate head. Development. 2002;129:1061–73.

5. Dimaras H, Kimani K, Dimba EA, Gronsdahl P, White A, Chan HS, Gallie BL. Retinoblastoma. Lancet. 2012; 379:1436–46.
6. Dudas M, Li WY, Kim J, Yang A, Kaartinen V. Palatal fusion – Where do the midline cells go? A review on cleft palate, a major human birth defect. Acta Histochem. 2007;109:1–14.
7. Gray S, Skandalakis J. Embryology for surgeons. 2nd ed. Baltimore: Lippincott Williams and Wilkins; 1994.
8. Heerema-McKenney A, Harrison MR, Bratton B, Farrell J, Zaloudek C. Congenital teratoma. Am J Surg Pathol. 2005;29:29–38.
9. Levene MI, Chervenak FA. Fetal and neonatal neurology and neurosurgery. 4th ed. New York: Churchill Livingstone; 2009.
10. Maity T, Fuse N, Beachy PA. Molecular mechanisms of Sonic hedgehog mutant effects in holoprosencephaly. Proc Natl Acad Sci U S A. 2005;102:17026–31.
11. Mehrotra D. Genomic expression in non syndromic cleft lip and palate patients: a review. J Oral Biol Craniofacial Res. 2015;5:86–91.
12. Moore KL, Persaud T, Torchia M. The developing human: clinically oriented embryology. 9th ed. Philadelphia: Saunders; 2012.
13. Nie X, Luukko K, Kettunen P. BMP signalling in craniofacial development. Int J Dev Biol. 2006;50: 511–21.
14. Papadopoulou I, Sebire NJ, Shelmerdine SC, Bower S, Arthurs OJ. Postmortem image-guided biopsy for less-invasive diagnosis of congenital intracranial teratoma. Ultrasound Obstet Gynecol. 2015;46:741–3.
15. Piotrowski T, Schilling TF, Brand M, Jiang YJ, Heisenberg CP, Beuchle D, Grandel H, van Eeden FJ, Furutani-Seiki M, Granato M, Haffter P, Hammerschmidt M, Kane DA, Kelsh RN, Mullins MC, Odenthal J, Warga RM, Nüsslein-Volhard C. Jaw and branchial arch mutants in zebrafish II: anterior arches and cartilage differentiation. Development. 1996;123:345–56.
16. Sadler TW. Langman's medical embryology. 13th ed. Philadelphia: Lippincott Williams and Wilkins; 2014.
17. Sebire NJ, Malone M, Ashworth MT, Jacques TS. Paediatric surgical pathology. 1st ed. London: Churchill Livingstone; 2010.
18. Shields JA, Shields CL, Scartozzi R. Survey of 1264 patients with orbital tumors and simulating lesions: the 2002 Montgomery Lecture, part 1. Ophthalmology. 2004;111:997–1008.
19. Shields JA, Shields CL. Eyelid, conjunctival, and orbital tumors: an atlas and text. 2nd ed. Philadelphia: Lippincott Williams and Wilkins; 2007.
20. Som PM, Naidich TP. Illustrated review of the embryology and development of the facial region, part 1: early face and lateral nasal cavities. Am J Neuroradiol. 2013;34:2233–40.
21. Sperber G, Sperber S, Guttmann G. Craniofacial embryogenetics and development. 2nd ed. Shelton: PMPH; 2010.
22. ten Donkelaar HJ, Lammens M, Hori A. Clinical neuroembryology: development and developmental disorders of the human central nervous system. 2nd ed. Berlin Springer; 2014.
23. Wang Y, Song L, Zhou CJ. The canonical Wnt/ß--catenin signaling pathway regulates FGF signalling for early facial development. Dev Biol. 2011;349: 250–60.

Postnatal Management of Cleft Lip and Palate

11

Fabio Xerfan Nahas, Natasha Sallum, and Lydia Masako Ferreira

11.1 Introduction

Cleft lip and palate are the most common causes of facial malformation, with an approximate incidence of 1 in 1250 live births [1, 2]. The high incidence of this malformation is due to the sensitivity of the cells of the face to teratogenic events.

The birth of a child with facial cleft results in a strong emotional reaction by the parents. Very early correction of the defect, even during the same hospital stay as the birth, may be desired by the parents. This treatment is adopted by some surgeons and is seen as a strategy to improve the family's experience when a child is affected with a facial congenital deformity.

However, most surgeons prefer to delay correction of these defects until the child is at least 3-6 months of age when the structures are larger and more readily identifiable [3].

11.2 Embryology

Understanding of the development of the cleft lip and palate can be obtained from the knowledge of the embryological structures from which the facial bones and soft tissues originate (Table 11.1 and Fig. 11.1).

11.3 Diagnosis

Except for some posterior palate clefts hidden by a mucosal union between the left and right sides, facial clefts may be diagnosed by prenatal ultrasound. The upper lip and palate can be visualized, and an eventual loss of continuity of the tissues can be detected [4].

11.4 Classification

There are many classifications of face and palate clefts in the literature. One of the most used is the one described by Kernahan [5] that classifies the labial palate clefts using the shape of the letter "Y." The center of the "Y" is represented by the incisive foramen. A simple classification of the labial palate clefts can be seen as follows (Table 11.2).

The ideal timing for surgical correction of cleft lip and palate is at the following ages:

- Primary cleft lip correction: from 3 to 6 months
- Primary palatoplasty: from 18 to 24 months, before the development of the speech
- Alveolar bone graft: around 12 years old
- Rhinoseptoplasty: after 16 years old
- Orthognathic surgery: after 16 years old

F.X. Nahas, MD, PhD (✉) • N. Sallum, MD
L.M. Ferreira, MD, PhD
Division of Plastic Surgery, Federal University of São Paulo/UNIFESP, São Paulo, Brazil

G. Tonni, W. Sepulveda, and A.E. Wong (eds.), *Prenatal Diagnosis of Orofacial Malformations*,
DOI 10.1007/978-3-319-32516-3_11

Table 11.1 Embryological origin of facial bones and soft tissues

Embryological structure	Anatomical area	Anatomical structures
Nasal prominence	Primary palate	Premaxilla
		Anterior septum
		Upper lip
Maxillary prominence	Secondary palate	Hard palate (posterior to the incisive foramen[a])
		Soft palate
		Uvula

[a]The incisive foramen separates the primary and the secondary palates

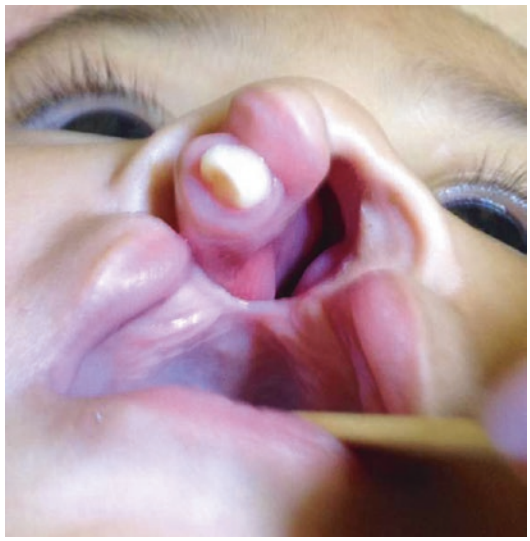

Fig. 11.1 Bilateral cleft lip (preforamen cleft). The photograph shows the embryological differentiation of the structures formed by the primary and secondary palates

Table 11.2 Classification of the labial palate clefts

Cleft	Lip	Complete	Right
	Palate	Incomplete	Left
	Lip and palate		Bilateral

11.5 Clinical Aspect - Breast Feeding

Most children with cleft lip and/or cleft palate can breastfeed normally, although some may experience difficulties. When the nasal cavity communicates with the oral cavity, there is less negative pressure that is able to be created within the mouth during the infant's suck and therefore the suction that is necessary for breastfeeding may not be adequate. Nevertheless, allowing these children to attempt breastfeeding seems to be the best strategy [6]. Because breast tissue is more flexible compared to bottles, allowing some sealing of the communication between cavities, breastfeeding may be possible.

However, breastfeeding should be avoided in syndromic patients, those with associated malformations or other severe conditions, and also patients with neurologic complications. Infants with a soft prolabium may experience a prolabium fracture during breastfeeding. These children are candidates to alternative feeding techniques such as the use of bottles and cups.

11.6 Surgical Treatment

Surgical technique depends on whether (1) the cleft is unilateral or bilateral, (2) the cleft is restricted to the lips or if the palate is also involved, and (3) any associated malformations are present. It may be possible for surgical correction to be performed concurrently with other necessary surgeries.

11.6.1 Cleft Lip Correction

A well-performed surgery closes and aligns the tissue and also allows future facial growth. There are some anatomical parameters to be considered: the orbicularis oris muscle, the dry and wet vermilions, nasal alae, and the nasal floor. In the first operation, modern patient management includes the repositioning of the ipsilateral nasal alar cartilage and the use of a vomer flap for nasal floor closure (Fig. 11.2).

11.6.2 Lip Adhesion

This operation is indicated in cases of bilateral cleft lip when alignment of the orbicularis oris

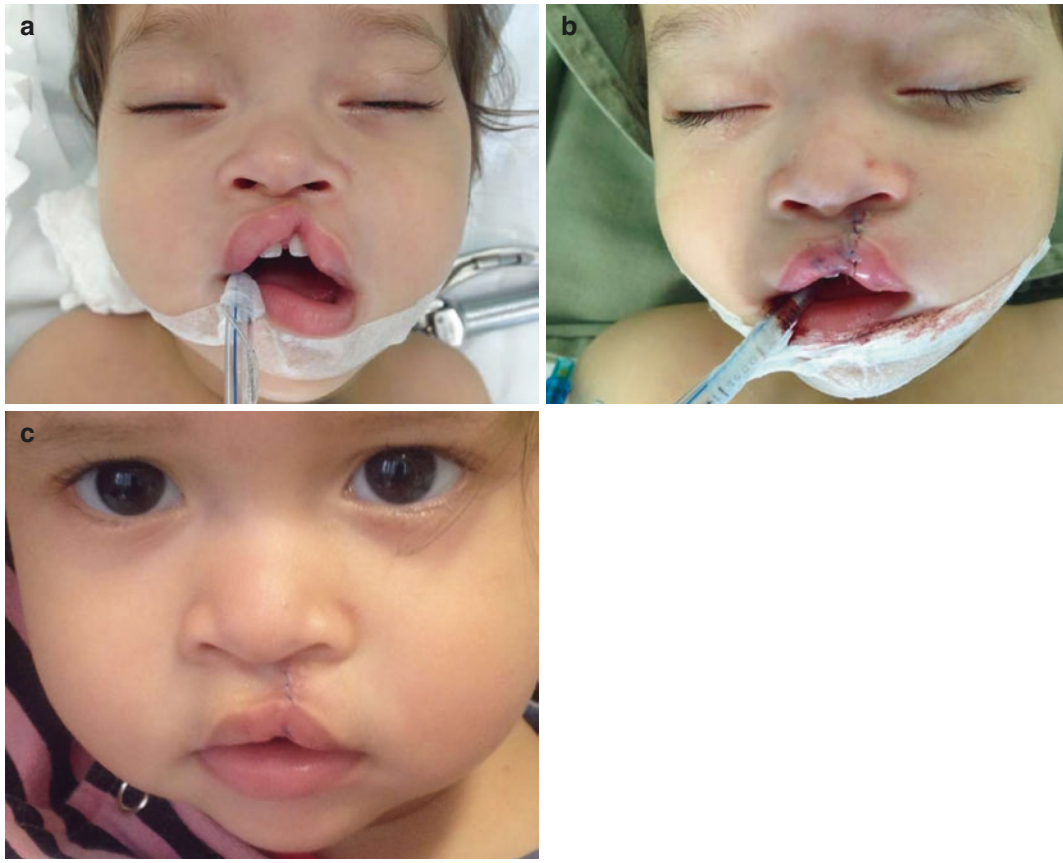

Fig. 11.2 (**a**) Preoperative and (**b**, **c**) postoperative photographs of a cheiloplasty on a patient with an incomplete cleft lip. As this patient presented with an incomplete defect, no nasal floor was needed

muscle is not also performed. When the child is older, the muscle alignment is done in another procedure [7].

11.6.3 Palatoplasty

In a conventional palatoplasty, a closure in two layers should be performed to close the defect: on the nasal floor and the oral mucosa. The velar muscles are located between the nasal floor and the oral mucosa. These muscles are typically dystopic and not correctly inserted in patients with cleft. Correct velar muscle alignment (intravelar veloplasty) is mandatory on primary palatoplasties (Fig. 11.3).

11.6.4 Alveolar Bone Graft

Cleft lip and cleft palate patients may present with a gap in the maxillary bone. Most surgeons harvest iliac crest bone grafts to reestablish the maxillary contour to allow a secondary orthodontic treatment.

11.6.5 Rhinoseptoplasty

This operation corrects septal deviation and the nasal asymmetry secondary to unilateral cleft lip and palate. Surgery includes columellar elongation on bilateral defects [8].

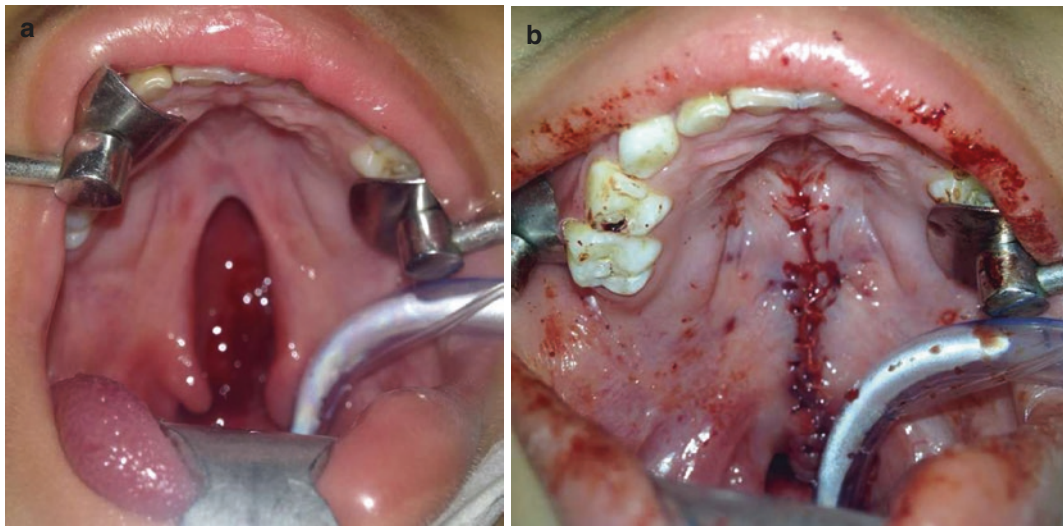

Fig. 11.3 (**a**) Preoperative and (**b**) immediate postoperative photograph of a posterior palatopathy. Surgery includes closure of the nasal and oral layers and repositioning of the velar muscles

11.6.6 Orthognathic Surgery

Cleft palate patients commonly present with maxillary hypoplasia. Surgery includes lateral expansion of the maxilla, maxillary advancement, or both. To reestablish normal dental occlusion, a mandibular surgery may be necessary (combined with orthognathic surgery).

11.7 Complications

11.7.1 Palate Dehiscence

Dehiscence of the palate occurs for two main reasons: (1) as a consequence of poor surgical technique, when sutures are placed under tension or when a single layer closure is used; and (2) due to inadequate postoperative care, such as when solid food is offered in the immediate postoperative days or when pacifiers or baby bottles are used. Dehiscence also occurs due to tissue ischemia and devascularization of the palate, which may be caused by injury of the vascular pedicle of the palate or occur due to individual systemic factors, such as malnutrition and anemia (Fig. 11.4).

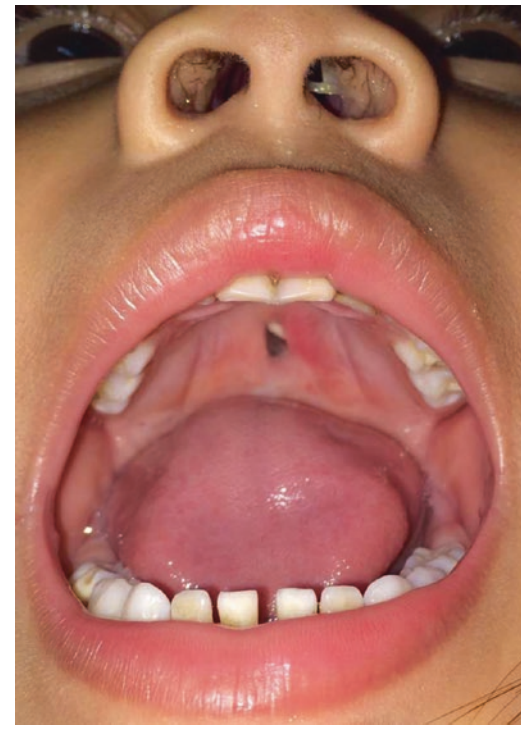

Fig. 11.4 Photograph of a patient with a prior posterior palatoplasty who presented with a dehiscence posterior to the velar muscles on the soft palate

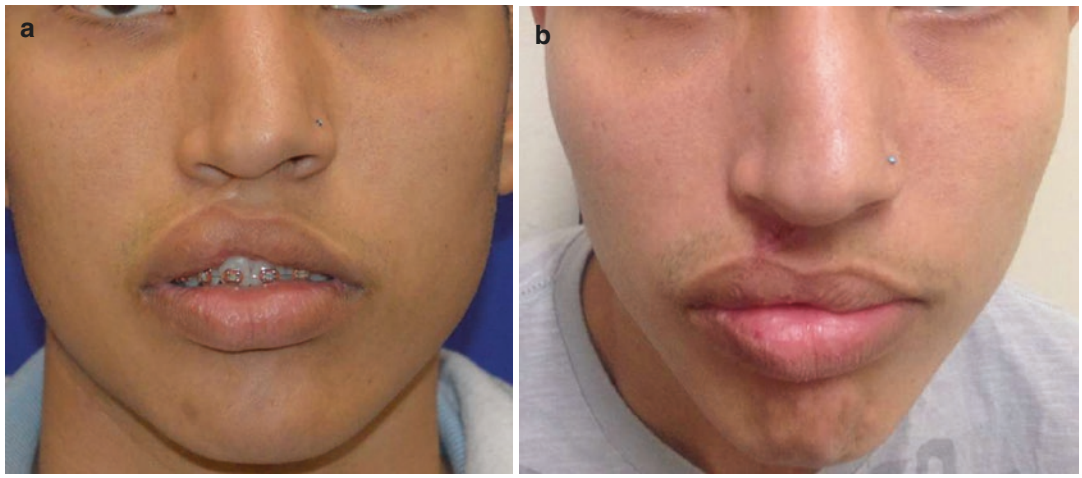

Fig. 11.5 (**a**) Preoperative and (**b**) postoperative photographs of a patient who underwent a unilateral secondary cheiloplasty. An improved orbicular alignment is seen postoperatively

11.7.2 Loss of Alignment of the Cheiloplasty

When this complication occurs, a second cheiloplasty can be performed when the child is older with the goals of obtaining a better aesthetic result and improving function of the upper lip (Fig. 11.5).

11.7.3 Velopharyngeal Insufficiency

Velopharyngeal insufficiency is a complication of palatoplasties. It may occur for two reasons: lack of alignment of the velopharyngeal sphincter or malfunctioning of the same sphincter. On clinical exam, hypernasal speech is noted and the diagnosis can be confirmed by nasolaryngoscopy. A secondary surgery to improve speech, such as pharyngoplasty, may be necessary.

11.8 Multidisciplinary Care

A multidisciplinary team that includes a nurse, pediatrician, geneticist, ENT (ear, nose and throat) specialist, odontologist, and speech therapist is necessary to provide comprehensive medical care for these patients. Some of these providers will follow the children as they grow.

11.8.1 Nurse

At the hospital after birth, nurses, or possibly lactation consultants, should provide information regarding breastfeeding including techniques to be applied to a newborn with a cleft. Frequently, the nurse will be the first educator before a specialized cleft team is introduced to the family.

11.8.2 Pediatrician

Pediatricians are essential to follow these children over time to assess growth and for the development of other issues that may require referral to other professionals.

11.8.3 Geneticist

All family members should be evaluated for abnormalities that may be a part of syndromes associated with cleft lip/palate. In counseling the family, it is important to emphasize that clefts can

be an isolated event but may appear as a part of syndromes or genetic conditions.

11.8.4 ENT

When the child with a cleft does not have his/her anatomy surgically corrected, he/she is more prone to develop upper respiratory tract infections. Tonsillectomy may be necessary in some cases. Tonsillectomy can be performed with palatoplasty with the goal of reducing the escape of air.

11.8.5 Odontologist

Odontologists are very important members of the team because tooth decays occur more frequently in patients with buccal respiration, which is very commonly seen in cleft patients. Dental extraction is sometimes necessary in patients undergoing palatoplasty and alveoloplasty. These patients also require frequent adjustments in the dental arch.

11.8.6 Speech Therapist

An anomalous insertion of the velopharyngeal sphincter may lead to escape of air and hypernasal speech. Even after sphincter correction (intravelar veloplasty), the sphincter may not work adequately for a period of time. In these cases, the child's speech may have a transition period and follow up with a speech therapist is necessary.

References

1. Tanaka SA, Mahabir RC, Jupiter DC, Menezes JM. Updating the epidemiology of cleft lip with or without cleft palate. Plast Reconstr Surg. 2012;129:511e–8e.
2. Nagase Y, Natsume N, Kato T, Hayakawa T. Epidemiological analysis of cleft lip and/or palate by cleft pattern. J Maxillofac Oral Surg. 2010;9:389–95.
3. Shkoukani MA, Chen M, Vong A. Cleft lip – a comprehensive review. Front Pediatr. 2013;1:53.
4. Shaikh D, Mercer NS, Sohan K, Kyle P, Soothill P. Prenatal diagnosis of cleft lip and palate. Br J Plast Surg. 2001;54:288–9.
5. Kernahan DA. The Striped Y – a systematic classification for cleft lip and palate. Cleft Palate J. 1973;10:247.
6. Reilly S, Reid J, Skeat J, Cahir P, Mei C, Bunik M. ABM clinical protocol #18: guidelines for breastfeeding infants with cleft lip, cleft palate, or cleft lip and palate, revised 2013. Breastfeed Med. 2013;8:349–53.
7. Nagy K, Mommaerts MY. Lip adhesion revisited: a technical note with review of literature. Indian J Plast Surg. 2009;42:204–12.
8. Mulliken JB. Primary repair of bilateral cleft lip and nasal deformity. Plast Reconstr Surg. 2001;108:181–94.

Part II

Interesting Cases and Rare Syndromes

12 Binder Syndrome: Prenatal Diagnosis, Management, and Prognosis

Edward Araujo Júnior, Gabriele Tonni, and Waldo Sepulveda

12.1 Introduction

Binder syndrome, also called naso-maxillary dysplasia or maxillo-nasal dysostosis, is a congenital malformation characterized by a "dish-face" deformity and retruded flat nose [1]. The first characterization of this syndrome was performed by Zuckerkandl in 1882 who described an anomaly of the anterior nasal floor in which the normal crest that separates the nasal floor from the anterior surface of the maxilla was absent [2]. In 1939, Noyes described a patient with a flat nasal tip sitting on a retruded naso-maxillary base [3]. In 1962, Binder described the syndrome in three cases that were characterized by a short nose with flat bridge, a short columella, an acute nasolabial angle, perialar flatness, a convex upper lip, and "reverse overbite" (or class III malocclusion) [4].

E. Araujo Júnior (✉)
Department of Obstetrics, Paulista School of Medicine – Sao Paulo Federal University of Sao Paulo (EPM-UNIFESP), Sao Paulo, Brazil
e-mail: araujojred@terra.com.br

G. Tonni, MD, PhD
Department of Obstetrics and Gynecology, Prenatal Diagnostic Service, Guastalla Civil Hospital, AUSL Reggio Emilia, Reggio Emilia, Italy
e-mail: Tonni.Gabriele@ausl.re.it

W. Sepulveda
Fetalmed – Maternal-Fetal Diagnostic Center, Santiago, Chile

Binder syndrome is a congenital malformation that is likely multifactorial in origin, although the true etiology is unknown. It can occur as an isolated syndrome; however, most cases are associated with genetic conditions such as the Xp22.3 deletion [5] and cholesterol disorders [6]. This syndrome also is associated with deficiency of vitamin K [6], alloimmune maternal diseases such as systemic lupus erythematosus [7], and maternal exposure to warfarin and alcohol in the first trimester of pregnancy [8, 9]. Malformations of the cervical spine can occur in 50 % of the patients, typically involving a defective posterior or anterior wall of the atlas or axis, fused vertebrae, and persistence of the chorda dorsalis [10]. A separate odontoid process, spina bifida occulta, and mild scoliosis and/or kyphosis also have been described.

The incidence of Binder syndrome is unknown, largely because it is usually misdiagnosed as X-linked chondrodysplasia punctata due to the similarity in facial abnormalities. X-linked chondrodysplasia punctata is a congenital disorder of bone and cartilage development caused by a deficiency of the Golgi enzyme, ARSE, the gene of which is located in Xp22.3 [11]. It is a disorder that includes pulmonary disorders, cervical spine compression, mental retardation, strabismus, and ichthyosis [12]. Because it is controversial whether Binder syndrome is a true syndrome or a phenotype of abnormalities involving the nasomaxillary regions [13], when

G. Tonni, W. Sepulveda, and A.E. Wong (eds.), *Prenatal Diagnosis of Orofacial Malformations*,
DOI 10.1007/978-3-319-32516-3_12

prenatal ultrasound findings consistent with Binder syndrome are seen, chondrodysplasia punctata must be considered [14].

In this report, the clinical and facial ultrasound features, as demonstrated by two-dimensional (2D) and three-dimensional (3D) ultrasound, in a case of Binder syndrome are presented. The main prenatal ultrasound findings, differential diagnoses, prognosis, and management of this rare condition are also reviewed.

12.2 Case Description

A 35-year-old primigravida was referred to one of the authors (W.S.) at 27 weeks of gestation after the detection of abnormal ultrasound findings at the second-trimester anatomy scan. Her medical and obstetric histories were unremarkable and the current pregnancy was otherwise normal. Of note, the first-trimester nuchal scan and an office ultrasound at 20 weeks were reported as normal. However, a formal, detailed second-trimester anatomy scan at 23 weeks revealed several abnormal findings including a small-for-gestational age fetus, reduced thoraco-abdominal size, scoliosis with hemivertebrae, premature calcification of the vertebral bodies, moderate short long bones, and multiple epiphyseal calcifications of long bones. Focused examination of the face revealed a depressed nasal bridge and a small nose with absent nasal bone. Borderline ventriculomegaly was also noted. The tentative diagnosis of chondrodysplasia punctata was made. Chromosomal analysis performed by amniocentesis revealed a normal 46,XX karyotype. At 26 weeks, polyhydramnios with a deepest pocket of 10 cm was detected. At referral, the abovementioned findings were confirmed. The placenta was posterior in location and the amniotic fluid was increased with a single deepest pocket of 9.2 cm consistent with moderate polyhydramnios. The fetal face was assessed with 2D and 3D ultrasound, demonstrating nasal hypoplasia and severe depression of the midface (Figs. 12.1 and 12.2). Fetal magnetic resonance imaging at 30 weeks did not reveal any additional clinical information. Subsequent antenatal course was complicated by severe polyhydramnios requiring three amnioreductions. However, during the last procedure performed at 32 weeks, the fetus developed severe bradycardia requiring an emergency cesarean section and a female infant with low Apgar scores weighing 1115 and measuring 33 cm was delivered. The newborn infant depicted the classical facial features of Binder syndrome (Fig. 12.3). Despite intensive neonatal care, the infant died in the first hours of life. Postnatal studies were not performed. However, the mother was tested for seven mutations of chondrodysplasia punctata (AGPS, ARSE, EBP, GNPAT, IMPAD1, LBR, and PEX7) by massive parallel sequencing and the results were reported as normal.

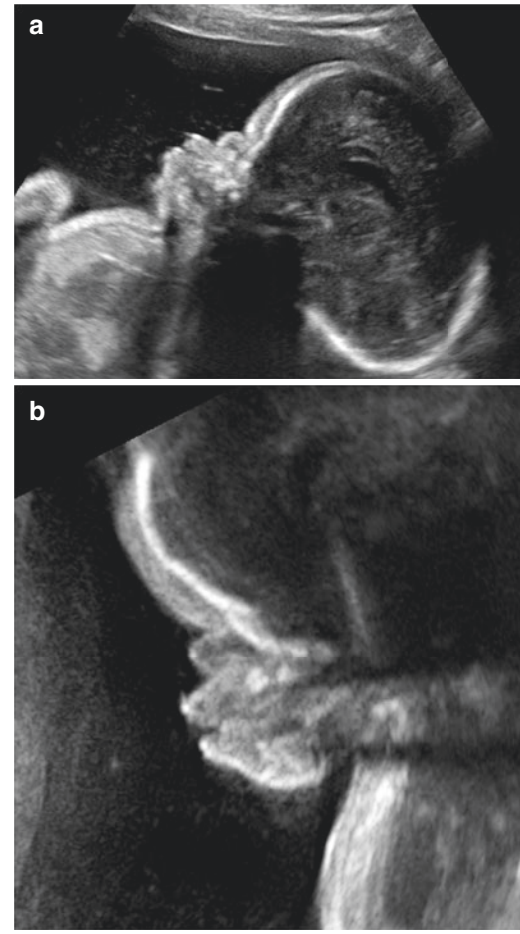

Fig. 12.1 (**a**, **b**) Sagittal 2D ultrasound views of the fetal profile show severe midfacial hypoplasia. Note the almost absent nose and severe depression of the midface. Moderate polyhydramnios was also present

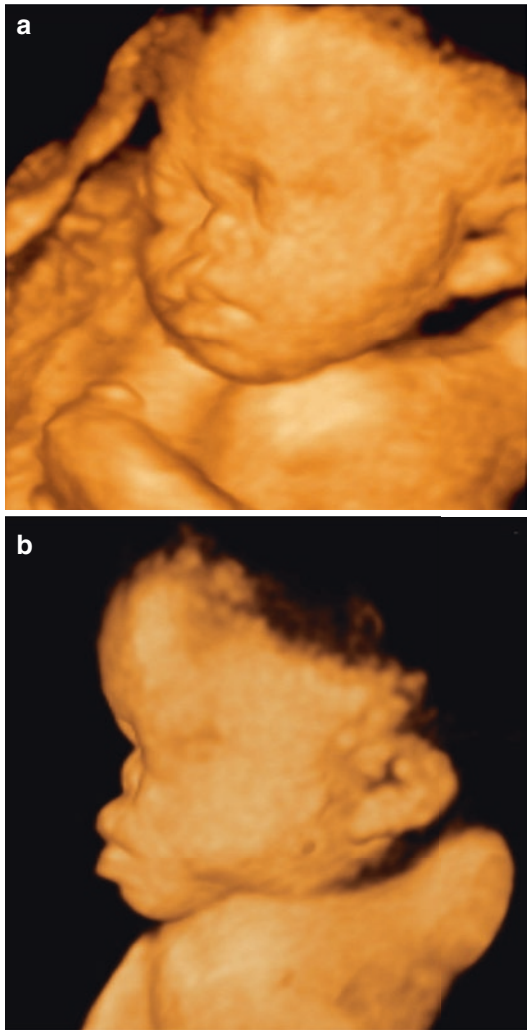

Fig. 12.2 (**a**, **b**) Three-dimensional surface-rendering ultrasound view of the fetal face show the characteristic features associated with the Binder phenotype

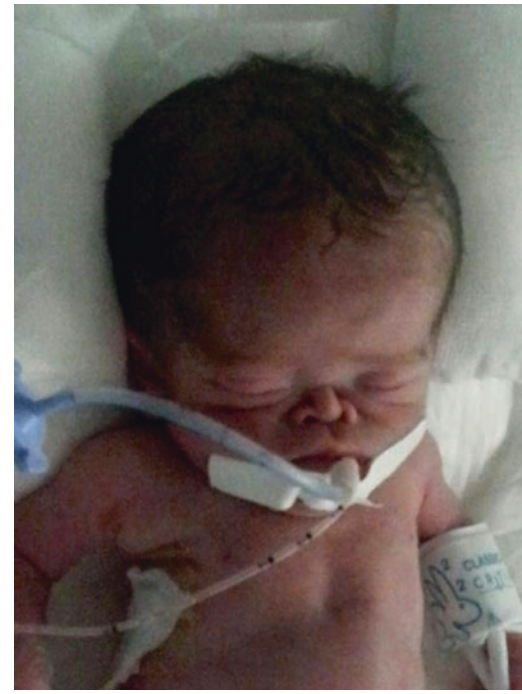

Fig. 12.3 Photograph of the neonate (with permission from the parents)

12.3 Prenatal Diagnosis

Binder syndrome has rarely been diagnosed during the prenatal period. Cook et al. [15] described a case diagnosed at 21 weeks of gestation during the routine second-trimester scan. 2D ultrasound identified nasal hypoplasia with reduced nasofrontal angle and mild hypertelorism. The karyotype was normal (46,XY). After discussion with geneticists, the leading differential diagnosis was Binder syndrome. After counseling, the parents decided to terminate the pregnancy and postmortem examination confirmed the facial dysmorphism, flat midface, mild hypertelorism, atresia of the right choanus, and stenosis of the left choanus. In this case, the suspicion of Binder syndrome was based on the flat nose as the primary abnormality, in contrast to other syndromes that usually are associated with multiple other malformations.

Cuillier et al. [16] described a case of Binder syndrome at 24 weeks of gestation. The routine second-trimester ultrasound demonstrated nasal hypoplasia with reduced naso-frontal angle. 3D ultrasound in rendering mode enhanced visualization of the abnormal facies. The karyotype was normal (46,XX). After discussion with geneticists and neonatologists, the main diagnostic hypothesis was Binder syndrome. The parents decided to continue the pregnancy and delivery occurred at 37 weeks of gestation. The neonatal exam confirmed the prenatal ultrasound findings.

In the largest case series of prenatal diagnosis of Binder syndrome, Levaillant et al. [11] described eight fetuses with Binder syndrome characteristics using both 2D and 3D ultrasound. The gestational age at diagnosis ranged from 22 to 31 weeks. All fetuses presented with verticalized nasal bones and abnormal convexity of the maxilla, consistent with the Binder profile appearance. Association with chondrodysplasia punctata was noted in five cases and one case was associated with exposure to warfarin in the first trimester of pregnancy.

As mentioned above, some authors consider Binder syndrome as a phenotype of chondrodysplasia punctata. Benaicha et al. [17] described a case of the prenatal diagnosis of chondrodysplasia punctata at 30 weeks of gestation that presented with flat nasal bridge and polyhydramnios with Binder profile. The karyotype was normal (46,XY). Furthermore, the ultrasound exam showed stippling of the vertebrae, coccyx, proximal femora, and tarsal and carpal bones with triangular hypoplastic tufts suggestive of brachytelephalangic type. The postnatal radiographic exams confirmed the prenatal diagnosis. Brachytelephalangic chondrodysplasia punctata is an X-linked inherited form and is caused by mutations in the arylsulfatase E gene and usually has a more favorable prognosis because psychomotor development is normal.

Boulet et al. [14] described another case of prenatal diagnosis of brachytelephalangic chondrodysplasia punctata performed at 23 weeks of gestation after the ultrasound exam revealed fetal midface abnormalities compatible with Binder phenotype and punctation of the upper femoral epiphyses. 3D computed tomography performed at 30 weeks of gestation confirmed the ultrasound diagnosis suspicion. Screening for Xp22 deletion and for maternal lupus was negative. Delivery occurred at 35 weeks and the postnatal radiology exam confirmed the Binder phenotype. On follow-up at 6 months, the psychomotor development was normal.

In another case of prenatally diagnosed brachytelephalangic chondrodysplasia punctata, ultrasound examination at 32 weeks of gestation showed polyhydramnios associated with Binder phenotype and low-set ears, thoracic hypoplasia, finger contracture, and cervicothoracic kyphosis. The karyotype was normal (46,XY). Magnetic resonance imaging demonstrated spinal canal stenosis with cord compression at the upper cervical level as well as a kyphotic deformity at the cervicothoracic junction. Delivery occurred at 34 weeks of gestation and the radiological exam confirmed brachytelephalangy of the hands. Computed tomography and magnetic resonance imaging confirmed the atlanto-axial subluxation with spinal cord compression [18].

12.4 Differential Diagnosis

The differential diagnosis of Binder syndrome includes other facial disorders, most of which are usually associated with genetic disorders (Table 12.1). Binder syndrome should be suspected when prenatal ultrasound identifies a low flat nasal bridge. Chondrodysplasia punctata is also associated with scoliosis and asymmetrical shortening of the limbs. Robinow syndrome is associated with short forearms, clinodactyly, and macrocephaly. Aarskog syndrome is associated with brachycephaly and clinodactyly of the 5th finger. Crouzon syndrome is associated with craniosynostosis and short occipital-frontal diameter. Apert syndrome is characterized by irregular craniosynostosis, short occipital-frontal diameter, flat occiput, ventriculomegaly, and syndactyly. Rudiger syndrome presents with short digits and talipes [19, 20]. Keutel syndrome is characterized by calcification and/or ossification of the cartilage in the external ears, nose, larynx, epiglottis, thyroid, trachea, ala nasi, and ribs; this syndrome also presents with peripheral pulmonary stenosis, sensory hearing loss, and borderline-to-mild mental retardation [21].

12.5 Management and Prognosis

When a prenatally diagnosed abnormality prompts fetal magnetic resonance imaging on which cervical spinal canal stenosis is identified in utero, delivery planning can be performed that

Table 12.1 Differential diagnosis in fetuses with sever midfacial hypoplasia

Syndrome	Facial Features	Other Features	Inheritance
Binder	Flat midface Nasal hypoplasia		AR/AD
Robinow	Flat face Hypertelorism	Short forearms Clinodactyly Macrocephaly	AD
Aarskog	Flat nose Hypertelorism	Brachy-/clinodactyly of the 5th finger	X-linked recessive
Rudiger	Flat nasal bridge	Short digits	AR
Stickler	Facial cleft Flat face Micrognathia	Osteo-chondrodysplasia Talipes	AD
CDP	Nasal hypoplasia	Scoliosis Asymmetrical shortening of limbs	X-linked dominant
Apert	Flat nose Maxillary hypoplasia	Craniosynostosis Flat occiput Syndactyly	AD

CDP chondrodysplasia punctata, *AR* autosomal recessive, *AD* autosomal dominant

may prevent adverse perinatal outcomes such as lower Apgar scores, respiratory distress with acidosis, and temperature dysregulation during the neonatal period [12, 18]. However, the diagnosis of Binder syndrome is typically made in the neonatal period by the neonatology exam identifying the following characteristic facial features: midface hypoplasia, convex upper lip, broad philtrum, crescent-shaped nostrils, and a deep fold or fossa between nose and upper lip. Radiologic exams are essential to confirm the facial anomalies. In adolescence or adulthood, the typical facial features can become less prominent or disappear, and the diagnosis of this syndrome may not be able to be performed. Older patients may sometimes show terminal phalangeal hypoplasia of the hand, though only in some digits [16].

The management of Binder syndrome differs with the degree of facial bone abnormalities. The prognosis of a fetus diagnosed with Binder syndrome by prenatal ultrasound is generally good. The face can be structurally modified by plastic surgeries and orthodontic treatment. The nose can be significantly lengthened and enlarged through a frontal craniotomy incision connected with an upper buccal sulcus incision, without any incision on the face [22]. The nose may also be modified with only costal cartilage grafts using a combined oral vestibular and external rhinoplasty approach [23]. The use of serial silicone implants to expand the nasal soft tissue before definitive costochondral reconstruction has also been described [24]. Le Fort II osteotomy may correct the midface deficiency and the class III occlusion which is observed in 15% of patients with Binder syndrome [25]. With growth of the child, the face will develop into a normal profile [23]. Although mental retardation has been described [12], intelligence is most often normal in Binder syndrome.

Conclusions

Binder syndrome is a rare congenital anomaly of heterogeneous etiology. It is characterized by a short nose with flat bridge, a short columella, an acute nasolabial angle, perialar flatness, a convex upper lip, and a tendency to angle class III malocclusion. The prenatal diagnosis is possible when the Binder phenotype, usually in association with polyhydramnios, is identified in the second or third trimester of pregnancy. The prognosis is usually good; mental retardation is rare. The face can be surgically corrected by plastic and orthodontic surgeries during childhood. Nevertheless, as demonstrated by the case presented here, the prognosis can be poor if increasing polyhydramnios leads to severe preterm delivery.

References

1. Chummun S, McLean NR, Nugent M, Anderson PJ, David DJ. Binder syndrome. J Craniofac Surg. 2012;23:986–90.
2. Zuckerkandl E. Fossae praenasales: normale und pathologische. Anat Nasenhohle. 1882;1:48.
3. Noyes FB. Case report. Angle Orthod. 1939;9:160.
4. Binder KH. Dysostosis maxillo-nasalis, ein arhinencephaler Missbildungskomplex. Deutsh Zahnaerztl DZZ. 1962;17:438–44.
5. Petit C, Melki J, Levilliers J, Serville F, Weissenbach J, Maroteaux P. An interstitial deletion in Xp22.3 in a family with X-linked recessive chondrodysplasia punctata and short stature. Hum Genet. 1990;85:247–50.
6. Jaillet J, Robert-Gnansia E, Till M, Vinciguerra C, Edery P. Biliary lithiasis in early pregnancy and abnormal development of facial and distal limb bones (Binder syndrome): a possible role for vitamin K deficiency. Birth Defects Res A Clin Mol Teratol. 2005;73:188–93.
7. Austin-Ward E, Castillo S, Cuchacovich M, Espinoza A, Cofré-Beca J, González S, Solivelles X, Bloomfield J. Neonatal lupus syndrome: a case with chondrodysplasia punctata and other unusual manifestations. J Med Genet. 1998;35:695–7.
8. Leicher-Duber A, Schumacher R, Spranger J. Stippled epiphyses in fetal alcohol syndrome. Pediatr Radiol. 1990;20:369–70.
9. Howe AM, Hawkins JK, Webster WS. The growth of the nasal septum in the 6-9 week period of foetal development–Warfarin embryopathy offers a new insight into prenatal facial development. Aust Dent J. 2004;49:171–6.
10. Olow-Nordenram MAK, Radberg CT. Maxillonasal dysplasia (Binder syndrome) and associated malformations of the cervical spine. Acta Radiol. 1984;25:353–60.
11. Levaillant JM, Moeglin D, Zouiten K, Bucourt M, Burglen L, Soupre V, Baumann C, Jaquemont ML, Touraine R, Picard A, Vuillard E, Belarbi N, Oury JF, Verloes A, Vazquez MP, Labrune P, Delezoide AL, Gérard-Blanluet M. Binder phenotype: clinical and etiological heterogeneity of the so-called Binder maxillonasal dysplasia in prenatally diagnosed cases, and review of the literature. Prenat Diagn. 2009;29:140–50.
12. Garnier A, Dauger S, Eurin D, Parisi I, Parenti G, Garel C, Delbecque K, Baumann C. Brachytelephalangic chondrodysplasia punctata with severe spinal cord compression: report of four new cases. Eur J Pediatr. 2007;166:327–31.
13. Nino M, Matos-Miranda C, Maeda M, Chen L, Allanson J, Armour C, Greene C, Kamaluddeen M, Rita D, Medne L, Zackai E, Mansour S, Superti-Furga A, Lewanda A, Bober M, Rosenbaum K, Braverman N. Clinical and molecular analysis of arylsulfatase E in patients with brachytelephalangic chondrodysplasia punctata. Am J Med Genet A. 2008;146A:997–1008.
14. Boulet S, Dieterich K, Althuser M, Nugues F, Durand C, Charra C, Schaal JP, Jouk PS. Brachytelephalangic chondrodysplasia punctata: prenatal diagnosis and postnatal outcome. Fetal Diagn Ther. 2010;28:186–90.
15. Cook K, Prefumo F, Presti F, Homfray T, Campbell S. The prenatal diagnosis of Binder syndrome before 24 weeks of gestation: case report. Ultrasound Obstet Gynecol. 2000;16:578–81.
16. Cuillier F, Cartault F, Lemaire P, Alessandri JL. Maxillo-nasal dysplasia (Binder syndrome): antenatal discovery and implications. Fetal Diagn Ther. 2005;20:301–5.
17. Benaicha A, Dommergues M, Jouannic JM, Jacquette A, Alexandre M, Le Merrer M, Ducou Le Pointe H, Garel C. Prenatal diagnosis of brachytelephalangic chondrodysplasia punctata: case report. Ultrasound Obstet Gynecol. 2009;34:724–6.
18. Ochiai D, Takamura K, Nishimura G, Ikeda T, Yakubo K, Fukuiya T. Prenatal diagnosis of cervical spinal cord compression in chondrodysplasia punctata brachytelephalangic type: a case report and literature review. Congenit Anom. 2013;53:160–3.
19. Romero R, Pilu G, Jeanty P, Ghidini A, Hobbins J. Prenatal diagnosis of congenital anomalies. New York: Appleton & Lange; 1987.
20. Bronshtein M, Blumenfeld I, Zimmer EZ, Ben-Ami M, Blumenfeld Z. Prenatal sonographic diagnosis of nasal malformations. Prenat Diagn. 1998;18:447–54.
21. Keutel J, Jorgensen G, Gabriel P. A new autosomal recessive syndrome: peripheral pulmonary stenoses, brachytelephalangism, neural hearing loss and abnormal cartilage calcifications-ossification. Birth Defects Orig Artic Ser. 1972;VIII:60–8.
22. McCollum AG, Wolford LM. Binder syndrome: literature review and long-term follow-up on two cases. Int J Adult Orthodon Orthognath Surg. 1998;13:45–58.
23. Munro IR, Sinclair WJ, Rudd NL. Maxillonasal dysplasia (Binder's syndrome). Plast Reconstr Surg. 1997;63:657–63.
24. Holmes AD, Lee SJ, Greensmith A, Heggie A, Meara JG. Nasal reconstruction for maxillonasal dysplasia. J Craniofac Surg. 2010;21:543–51.
25. Jain U, Thakur G, Kallury A. Binder's syndrome. BMJ Case Rep. 2011. doi:10.1136/bcr.08.2011.4665.

13 Atypical Facial Cleft Detected by Prenatal Scan and Confirmed by Postmortem Reconstructive Computed Tomography (CT REC)

Inbal Dona Amar, Yaakov Melcer, Rebecca Cohn, and Ron Maymon

13.1 Introduction

Fetal facial clefts are among the most common congenital anomalies. They develop as a result of both genetic and environmental influences and have a prevalence of about 1:500 to 1:1000 live births [1–4]. The common forms of cleft lip (CL), cleft palate (CP), and cleft lip and palate (CLP) involve disruption of tissue planes above the lip going through the nares and/or the palate.

Two distinct embryological pathways underlie the pathogenesis of facial clefts. First, CL is most commonly unilateral and may be associated with a cleft of the ipsilateral alveolus. Any cleft anterior to the incisive foramen, which may involve only the lip or both the lip and the alveolus, is considered a cleft (complete or incomplete) of the primary palate. This terminology is useful when detecting forms of cleft seen antenatally, since differentiating between the types of clefts has implications on fetal prognosis. Second, a CL can be associated with a cleft of the secondary palate when the defect continues posterior to the incisive foramen.

I.D. Amar • Y. Melcer • R. Cohn • R. Maymon (✉)
Ultrasound Unit, Department of Obstetrics and Gynecology, Assaf Harofeh Medical Center, Zerifin, Israel

Sackler School of Medicine, Tel Aviv University, Tel Aviv, Israel
e-mail: maymonrb@bezeqint.net

Accordingly, a cleft is defined by both its location and its laterality (unilateral, bilateral, or midline). CL alone occurs in 25 % of cases of cleft, CLP in 51 % of cases, and isolated CP in 24 % of cases [5]. Tessier [6] published an anatomic classification of facial clefts involving the mouth, maxilla, eyes, nose, and forehead. This classification may also extend to the viscerocranium and the neurocranium and may be labeled as an oro-occular cleft and fronto-nasal dysplasia. They are numbered from 0 to 14 based on the extension of the cleft and are divided into 4 groups: median, para-median, orbital, and lateral.

About 70 % of cases of CLP appear as unique entities without other obvious cognitive or structural anomalies and are termed "isolated, non-syndromic CLP". The other cases are composed of a large variety of malformation syndromes, including chromosomal abnormalities, syndromes secondary to teratogen exposure, and over 500 Mendelian syndromes. Therefore, it is preferred to describe the etiology of CLP as multifactorial, involving both genetic and environmental factors. In terms of environmental exposure, maternal smoking is known to be an important risk factor associated with CLP [7]. Moreover, certain teratogens such as valproate [8] are associated with CP. Furthermore, stress, ionizing radiation, maternal obesity, and infection have been studied as contributing factors to the development of CLP [9].

G. Tonni, W. Sepulveda, and A.E. Wong (eds.), *Prenatal Diagnosis of Orofacial Malformations*,
DOI 10.1007/978-3-319-32516-3_13

While isolated clefts demonstrate low perinatal mortality and morbidity and primarily pose functional and esthetic problems postnatally, complicated clefts that involve the alveolus or the palate are associated with a much worse prognosis [10]. Children born with complicated facial clefting face unique challenges including difficulties related to feeding, speech and language development, and social integration [1]. Therefore, they require a larger number of surgical corrective procedures in comparison with those having cleft lip alone, and their follow-up more often involves additional orthodontic and orthophonic treatment [11, 12]. Thus, CLP is a source of considerable morbidity and poses a substantial financial burden for families, in addition to having societal consequences [13].

13.2 Case Description

We report a case of a 36-year-old primigravida with an unremarkable medical history and no parental consanguinity. Nuchal translucency and first-trimester fetal anomaly scans were reported to be normal as well. She was referred to our ultrasound unit at 24 weeks of gestation after a CLP was diagnosed during the mid-trimester anomaly scan using two-dimensional (2D) ultrasound. No other fetal anomalies or abnormal findings were seen on the prenatal scan.

We performed a three-dimensional (3D) ultrasound study, which allowed for visualization of the facial structures demonstrating a unilateral left CL involving the skin and the subcutaneous tissue (Fig. 13.1a). The 3D ultrasound skeletal

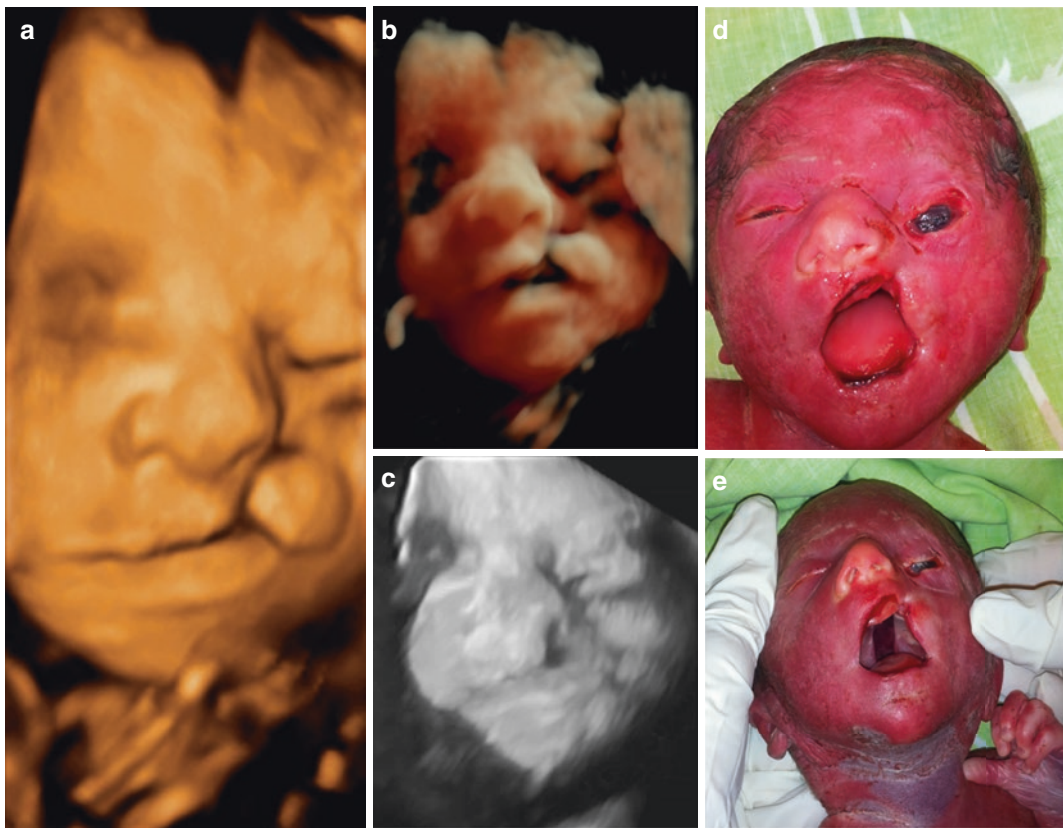

Fig. 13.1 Representative images of the fetus and the postmortem findings. Prenatal 3D ultrasound in surface-rendering mode of the fetal face shows a wide, left-sided cleft lip with malformation of the ipsilateral eye (**a**). Same case using HDLive™ mode (**b**) and (**c**) skeletal mode. Postmortem findings show cleft lip and cleft palate (**d**, **e**). CT scan in 3D skeletal mode (**f**). Same modality showing cleft palate and the deformation of the maxillary bone (**g**). Volume reconstruction using 3D CT scan shows the bony defect of the palate (**h**)

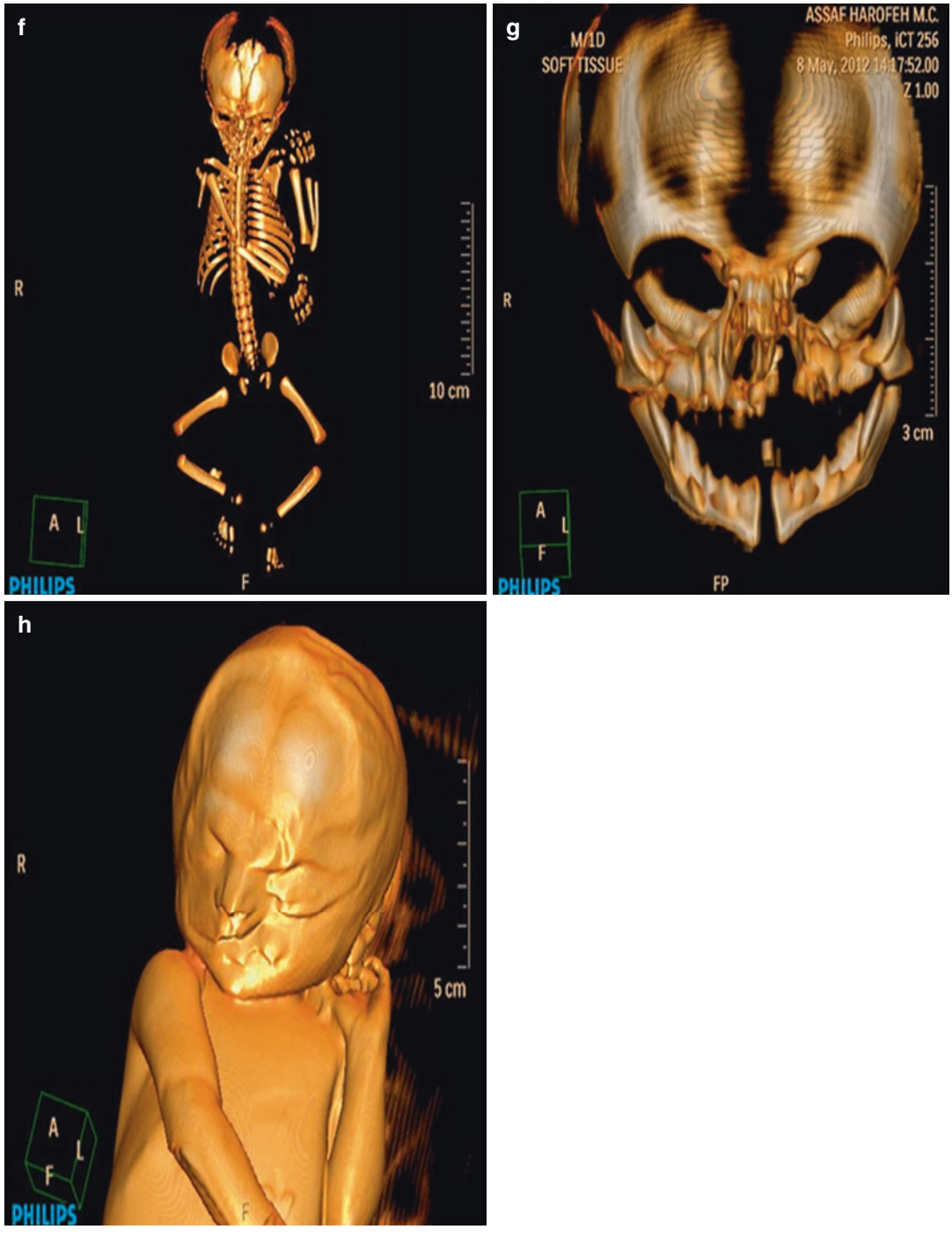

Fig. 13.1 (continued)

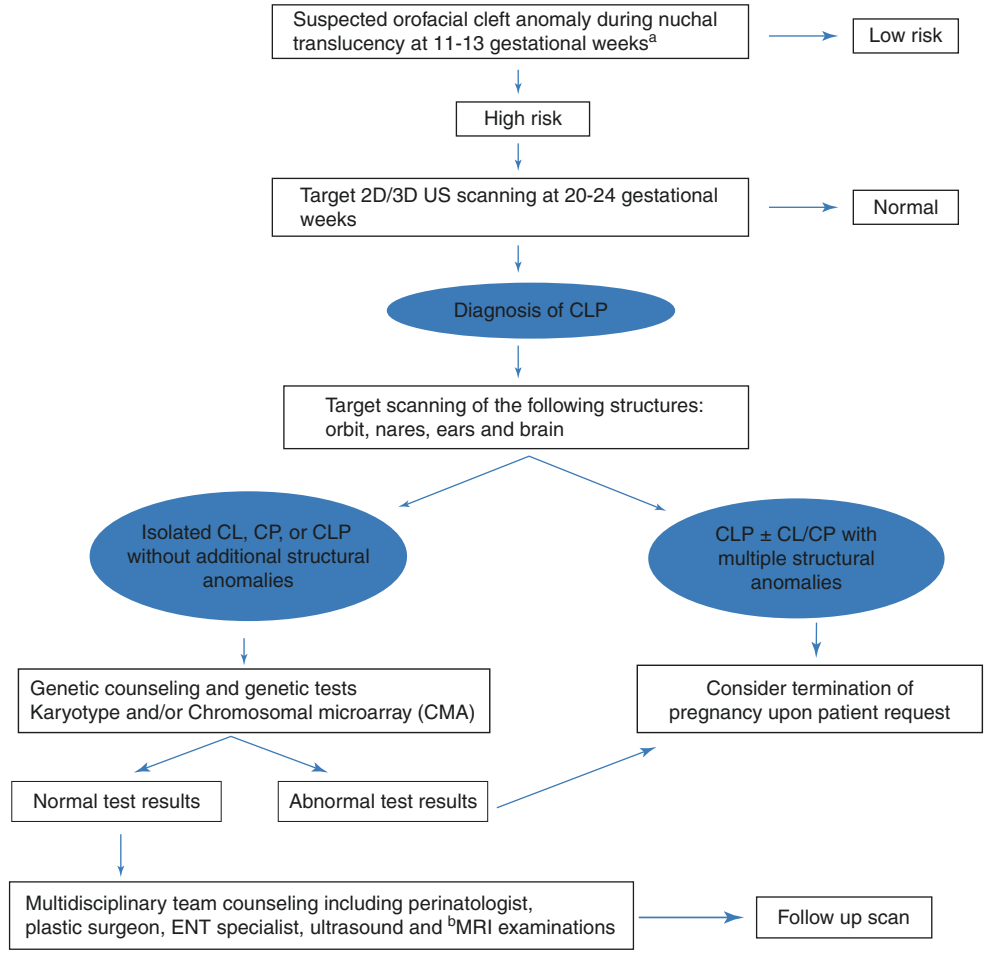

Fig. 13.2 Diagnostic flowchart to be used in obstetrics practice in case a fetus with suspected orofacial clefting is detected by prenatal ultrasound. [a]According to Martinez-Ten et al. 2012 [17] and Tonni et al. 2013 [15]. [b]In selected cases

mode and the HDLive™ mode demonstrated that the cleft involved the maxillary bone and the base of the orbit, resulting in distortion of a significant portion of the left hemiface (Fig. 13.1b, c). In the current case, the prenatal diagnosis corresponded to Tessier number 4 [6]. A multidisciplinary team including geneticists, a perinatologist, ear, nose and throat (ENT) specialists, and plastic surgeons were gathered in order to discuss the patient's options and advise the couple about postnatal complications. The team concluded that major surgical and rehabilitative interventions would be required in the postnatal period (Fig. 13.2).

The patient requested legal termination of the pregnancy, which was approved by a special committee in accordance with our national law. Termination of pregnancy was conducted at 26 weeks of gestation and postpartum findings confirmed the prenatal diagnosis (Fig. 13.1d, e). The couple signed a consent form for postmortem pathological examination. A postmortem skeletal CT scan demonstrated a missing part of the maxillary bone on the left side causing a deformation of the left orbit base (Fig. 13.1f, g). A reconstructive computed tomography (CT REC) was also conducted, which demonstrated a left unilateral CLP extending to the level of the left orbit, but without involving it (Fig. 13.1h). This correlated well with the macroscopic evaluation of the abortus.

13.3 Discussion

The embryological pathways underlying facial clefting are well characterized. CL always begins at the lip and extends dorsally to various degrees (alveolus, hard palate, soft palate). CP is characterized as a cleft in the alveolar ridge or primary palate. CP always begins at the uvula and extends anteriorly through the midline, involving either the soft palate only or both the soft and hard palates. The lip usually fuses by 8 weeks of gestation and the palate by 12 weeks of gestation. On prenatal scan, CL is best visualized in the coronal plane and the alveolus is best viewed in the transverse plane. Sagittal views of the fetal head may show abnormalities, especially if the CLP is bilateral or midline and not unilateral.

A large Italian study [3] suggested that the best period for detecting facial defects is between 18 and 23 weeks of gestation, the same optimal period for the detection of major malformations in general as recommended by international ultrasound societies. However, early detection at 13–14 weeks of gestation by transvaginal sonography has been reported by Bronshtein et al. [14]. Recently, Tonni et al. [15] have evaluated facial clefting at 11–14 weeks of gestation using a novel 3D ultrasound technique, which reformats the retronasal triangle (RNT) [16]. Using the virtual navigation of the fetal palate with 3D ultrasound seems to be an accurate modality for diagnosis of clefting in the first trimester of pregnancy [17].

The success of ultrasound screening for CLP differs extensively among series. A Dutch study [18] found that screening for orofacial clefts in a low-risk population by transabdominal 2D ultrasound has a moderately low detection rate but low false-positive diagnosis with a substantial improvement in detection rate over time. Stoll et al. [19] showed that a systematic method improved the discovery rate of facial clefts from 5.3 % between the years 1979 and 1988 to 26.5 % between the years 1989 and 1998. Despite this, the rate of prenatal diagnosis of isolated CP is particularly low since a palatal defect will not be visualized on the standard oblique view of the face that is commonly used to assess the upper lip and alveolar ridge. Shadowing of the palate by the dense bony ridge makes the above visualization difficult [20]. A novel marker for the diagnosis of isolated cleft palate is the “equals sign” [21]. Due to the dome-shaped structure of the palate, it cannot be visualized in its entirety by 2D ultrasound. Because CP always begins at the uvula (uvula bifida as the mildest form) and continues anteriorly along the midline, the intact uvula is used as an indicator for an intact palate.

Two different techniques are described to identify the uvula. The first method is by obtaining a coronal section through the neck and the pharyngeal space, in which the uvula can be visualized cranial to the epiglottis. The normal uvula has a characteristic ultrasound appearance that highly resembles an “equals sign” (two hyperechoic lines with a hypoechoic intermediate space). Another method, which yields a higher success rate, is to take a transverse section through the head at the level of the thalamus. The transducer is moved parallel to this plane caudally until the nasopharynx is viewed centrally. By moving the transducer further in the caudal direction, the soft palate and the uvula are seen.

As a complementary tool to the conventional 2D ultrasound, 3D ultrasound has been introduced in order to perform a more accurate evaluation of orofacial malformations. The conventional 3D ultrasound display consists of the orthogonal display mode and the surface-rendering mode. The former mode permits the concurrent analysis of the three reference planes: sagittal, axial, and coronal. The primary palate is identified in the axial plane by visualizing the two front tooth buds and by rotating the volume for symmetric viewing of the anterior alveolar ridge. Surface-rendering mode allows imaging of the soft tissues of the face; this technique provides images that are very useful in counseling parents about the nature of the malformation. In addition, the maximum mode permits improved imaging of the bony structures.

Viewing the hard and soft palates involves manipulation of the orthogonal planes in the 3D volume obtained on routine surface rendering of the fetal face. A routine 3D sweep of the fetal face in the surface-rendering mode allows visualization of the skin and soft tissues of the face,

including the lips. In the orthogonal planes within the multiplanar display, the lips and the anterior part of the palate may be evaluated. Further manipulation of the 3D volume to obtain oblique, axial, and sagittal planes permits evaluation of the uvula, which serves as a good landmark for guiding the examination of the soft and hard palates [22].

In 2003, an ultrasound technique called the 3D reverse face (3D RF) view was described by Campbell and Lees [23], which aimed to overcome problems of shadowing when evaluating the fetal palate. This technique proved to be simple, rapid, and quite effective at visualizing the palate and palatal defects. The fetal face is viewed by obtaining a 2D ultrasound of the profile (or near profile) and the volume box is adjusted to include the entire facial outline and cranium. The view bar is adjusted to deliver an optimized surface-rendered image of the face. After the lips are inspected, the view bar is scrolled until a view of the alveolar ridge is achieved. In order to achieve an unobstructed view of the retro-facial area, a return to the frontal view of the face and a 180-degree rotation is made to obtain a coronal plane. In this plane, the intact palate will usually be seen as a distinct line separating the nasal and oral cavity. The 3D RF technique is rapid and highly effective from 20 weeks of gestation onward. Attention should be paid to cases of tongue protrusion through the defect that can obscure the edges of the cleft. In addition, the "flipped face" technique allows for evaluation of the hard palate by obtaining a volume in the sagittal plane, visualizing the profile, and then flipping that profile on its head. After placing the marker dot in the region of the palate, the palate can be rendered with a narrow box. This yields an axial image of the primary and secondary palates [24].

Although ultrasound is the preferred diagnostic modality of facial cleft diagnosis, its accuracy may be limited by pathological conditions of the fetus such as oligohydramnios, complex malformation syndromes, or maternal obesity. The technique is also highly operator dependent. Fetal magnetic resonance imaging (MRI) is progressively becoming a powerful additional technique in the diagnosis of facial anomalies, particularly since the introduction of ultrafast sequences that minimize motion artifacts and offer excellent spatial resolution [25]. MRI is capable of directly visualizing the cleft and defining involvement of the primary and/or secondary palate. In T2-weighted sequences, the signal intensity of the amniotic fluid swallowed by the fetus provides excellent visualization of the oropharynx, therefore demonstrating involvement of the secondary palate in cases where the tongue would otherwise impair evaluation. Moreover, MRI is able to identify the direct communication between the oral and the nasal cavities [26].

In summary, despite the different imaging techniques available for prenatal diagnosis of CL, CP, and CLP, this abnormality still remains a diagnostic challenge. We propose a flowchart (Fig. 13.2) for the evaluation of fetuses with facial cleft. This is based on our experience and reflects our common practice. As research about this issue continues to be performed and new diagnostic techniques are suggested, the ability to properly diagnose and evaluate orofacial clefting malformations will continue to improve.

References

1. Hawkes N. £5m Pound UK study aims to discover what causes cleft lip and palate. BMJ. 2012;344:e2372.
2. Cash C, Set P, Coleman N. The accuracy of antenatal ultrasound in the detection of facial clefts in a lowrisk screening population. Ultrasound Obstet Gynecol. 2001;18:432–6.
3. Tonni G, Centini G, Rosignoli L. Prenatal screening for fetal face and clefting in a prospective study on low-risk population: Can 3- and 4-dimensional ultrasound enhance visualization and detection rate? Oral Surg Oral Med Oral Pathol Oral Radiol Endod. 2005;100:420–6.
4. Dixon MJ, Marazita ML, Beaty TH. Cleft lip and palate: synthesizing genetic and environmental influences. Nat Rev Genet. 2011;12:167–78.
5. Offerdal K, Jebens N, Syvertsen T, Blaas H-GK, Johannsen OJ. Prenatal ultrasound detection of facial clefts: a prospective study of 49 314 deliveries in a non-selected population in Norway. Ultrasound Obstet Gynaecol. 2008;31:639–46.
6. Tessier P. Anatomical classification facial, craniofacial and laterofacial clefts. J Maxillofac Surg. 1976;4:69–92.

7. Little J, Cardy A, Munger RG. Tobacco smoking and oral clefts: a meta-analysis. Bull World Health Organ. 2002;82:213–8.
8. Jentink J, Loane MA, Dolk H, Barisic I, Garne E, Morris JK, de Jong-van den Berg LT. EUROCAT. Antiepileptic Study Working Group. Valproic acid monotherapy in pregnancy and major congenital malformations. N Engl J Med. 2010;362:2185–93.
9. Wehby GL, Murray JC. Folic acid and orofacial clefts: a review of the evidence. Oral Dis. 2010;16:11–9.
10. To WW. Prenatal diagnosis and assessment of facial clefts: where are we now? Kong Med J. 2012;18:146–52.
11. Heinrich A, Proff P, Michel T, Ruhland F, Kirbschus A, Gedrange T. Prenatal diagnostics of cleft deformities and its significance for parental and infant care. J Craniomaxillofac Surg. 2006;34 Suppl 2:14S–6.
12. Oosterkamp BC, Dijkstra PU, Remmelink HJ, van Oort RP, Goorhuis-Brouwer SM, Sandham A, de Bont LG. Satisfaction with treatment outcome in bilateral cleft lip and palate patients. Int J Oral Maxillofac Surg. 2007;36:890–5.
13. Wehby G, Cassell CH. The impact of orofacial clefts on quality of life and healthcare use and costs. Oral Dis. 2010;16:3–10.
14. Bronshtein M, Blumenfeld I, Kohn J, Blumenfeld Z. Detection of cleft lip by early second transvaginal sonography. Obstet Gynecol. 1994;84:73–6.
15. Tonni G, Grisolia G, Sepulveda W. Early prenatal diagnosis of orofacial clefts: evaluation of the retronasal triangle using a new three-dimensional reslicing technique. Fetal Diagn Ther. 2013;34:31–7.
16. Sepulveda W, Wong AE, Martinez-Ten P, Perez-Pedregosa J. Retronasal triangle: a sonographic landmark for the screening of cleft palate en the first trimester. Ultrasound Obstet Gynecol. 2010;35:7–13.
17. Martinez-Ten P, Adiego B, Illescas T, Bermejo C, Wong AE, Sepulveda W. First-trimester diagnosis of cleft lip and palate using three-dimensional ultrasound. Ultrasound Obstet Gynecol. 2012;40:40–6.
18. Maarse W, Berge SJ, Pistorius L. T Diagnostic accuracy of transabdominal ultrasound in detecting prenatal cleft lip and palate: a systematic review. Ultrasound Obstet Gynecol. 2010;35:495–502.
19. Stoll C, Dott B, Alembic Y, Roth MP. Evaluation of prenatal diagnosis of cleft lip/palate by foetal ultrasonographic examination. Ann Genet. 2000;43:11–4.
20. Campbell S, Lees C, Moscoso G, Hall P. Ultrasound antenatal diagnosis of cleft palate by a new technique: the 3D 'reverse face' view. Ultrasound Obstet Gynecol. 2005;25:12–8.
21. Wilhelm L, Borgers H. The 'equals sign': a novel marker in the diagnosis of fetal isolated cleft palate. Ultrasound Obstet Gynecol. 2010;36:439–44.
22. Wong HS, Tait J, Pringle KC. Viewing of the soft and the hard palate on routine 3-D ultrasound sweep of the fetal face--a feasibility study. Fetal Diagn Ther. 2008;24:146–54.
23. Campbell S, Lees CC. The three-dimensional reverse face (3D RF) view for the diagnosis of cleft palate. Ultrasound Obstet Gynecol. 2003;22:552–4.
24. Platt L, Devore G, Pretorius D. Improving cleft palate/cleft lip antenatal diagnosis by 3-dimensional sonography: the "flipped face" view. J Ultrasound Med. 2006;25:1423–30.
25. Manganaro L, Tomei A, Fierro F. Fetal MRI as a complement to US in the evaluation of cleft lip and palate. Radiol Med. 2011;116:1134–48.
26. Wang G, Shan R, Zhao L, Zhu X, Zhang X. Fetal cleft lip with and without cleft palate: comparison between MR imaging and US for prenatal diagnosis. Eur J Radiol. 2011;79:437–42.

14 Congenital Subcutaneous Mixed Venous-Lymphatic Orofacial Malformation Associated with Macroglossia: Prenatal Diagnosis with Ultrasound and Fetal MRI

Marcello Napolitano, Alice Munari, Anna Ravelli, and Anna Venegoni

14.1 Introduction

Subcutaneous mixed venous-lymphatic malformations may be proliferative tumors or nonproliferative heterogeneous congenital malformations involving the capillary, lymphatic, venous, or arterial system or be seen as mixed lesions. These lesions may appear as partly solid and cystic (macro- or microcystic) and the prenatal diagnosis relies upon ultrasound and fetal magnetic resonance imaging (MRI) [1].

Macroglossia can be seen as an isolated finding or associated to genetic syndromes, commonly in Beckwith-Wiedemann syndrome where macroglossia is detected in 78.6 % of cases [2]. Recently, Poreau et al. [3] have reported a female fetus with macrocephaly and macroglossia harboring 13q31.1 microdeletion encompassing three genes: SPRY2, NDFIP2, and RBM26. NDFIP2 protein is involved in ubiquitination and in Ras/mitogen-activated protein kinase (MAPK) signaling pathways. While SPRY2 protein inhibits the Ras/MAPK pathways, Ras/MAPK pathway plays important role in complex cellular programs including cell differentiation and proliferation.

14.2 Case Description

A 30-year-old woman, gravida 2, para 0, was referred to our prenatal unit at 35 weeks' gestation with suspected oropharyngeal teratoma seen on level 2 ultrasound performed the prior week. The parents were non-consanguineous, with a noncontributory family history. The pregnancy was uncomplicated, with first-trimester screening for Down syndrome showing low risk. Normal fetal biometry and interval growth were observed. Ultrasound examination showed a female fetus with normal amniotic fluid and anterior placenta. Ultrasound evaluation of the fetal face revealed a mixed, solid and cystic mass of 5 × 30 mm infiltrating the soft tissue of the right orofacial region, from the temporal area to the chin, with invasion into the entire tongue. Several small foci of decreased echogenicity were present, suggestive of vacuolated cavities, and no evidence of significant intralesional vascularity was observed.

No calcification was identified. The mass extended into the inferior labrum region while the superior labrum appeared normal. No other significant abnormalities were found and an oral

M. Napolitano (✉) • A. Munari • A. Ravelli
A. Venegoni
Pediatric Radiology and Neuroradiology Department, Children's Hospital "V. Buzzi", Milan, Italy
e-mail: marcello.napolitano@asst-fbf-sacco.it

G. Tonni, W. Sepulveda, and A.E. Wong (eds.), *Prenatal Diagnosis of Orofacial Malformations*,
DOI 10.1007/978-3-319-32516-3_14

teratoma tumor was suspected. A fetal MRI was planned to better define the tissue characteristics of the mass and its relationship with the upper airway. The family was counseled regarding the clinical implications of these findings, anticipated delivery complications, prognosis, and impact on quality of life. Following discussion with the family, consent was obtained for fetal MRI. Prenatal MRI, using single-shot-fast-spin echo (SSFSE) T2-weighted single-slice images and T1-weighted 3D turbo field-echo sequences, obtained in the three orthogonal planes, characterized the voluminous mass as a soft tissue lesion infiltrating the right cervico-facial region from the temporal area to the chin, with invasion of the entire tongue, the floor of the mouth, the right masticator space, and the cheek. MRI also showed a large, lobulated, homogeneous hyperintense lesion on T2-weighted images with corresponding hypointense signal on T1-weighted sequences, without fat signal or hemorrhagic areas. No macrocysts were identified and no area of flow void was observed. The lesion infiltrated the tongue (protruding out of the mouth consistent with macroglossia), the floor of the mouth, the right masticator space, and the cheek. Although the macroglossia resulted in a partial obstruction of the oral cavity, the trachea, larynx, and anterior neck were noted to be patent. No other additional abnormal findings were found.

A subcutaneous mixed venous-lymphatic orofacial malformation was suspected. The lesion determines a partial compression of the rhino-oropharynx, imprinting the soft palate. The lesion partially compressed the rhino-oropharynx including the soft palate, but the larynx and trachea remained patent (Fig. 14.1). As recommended by the multispecialty team, cesarean delivery with an EXIT (ex utero intrapartum treatment) procedure was planned at 38 weeks' gestation. Intratracheal intubation was performed to secure the fetal airway. Postnatal MRI at 6 days of life confirmed the prenatal findings and confirmed an extended subcutaneous venous-lymphatic orofacial malformation (Fig. 14.2).

A protective tracheostomy was performed at 4 months of age followed by a subtotal glossectomy and multiple laser treatment and foam sclerotherapy.

14.3 Discussion

Subcutaneous mixed venous-lymphatic malformations are usually seen as proliferative tumors such as hemangiomas and/or lymphangioma [1]. Isolated macroglossia is rarely detected prenatally, and even when associated with Beckwith-Wiedemann syndrome, the diagnosis is typically

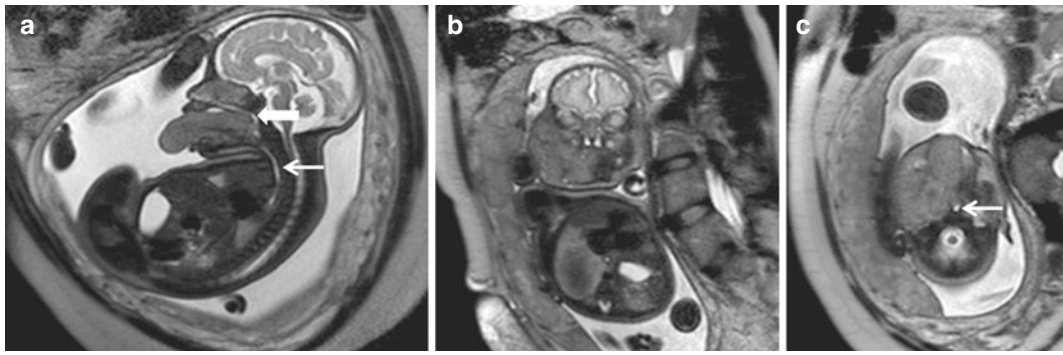

Fig. 14.1 Fetal T2-weighted MRI at 34.6 weeks' gestation in the three planes (sagittal plane (**a**), coronal plane (**b**), axial plane (**c**)) demonstrates the partial exophytic hyperintense soft tissue mass infiltrating the right orofacial region from the temporaral area to the chin, with invasion of the entire tongue, the floor of the mouth, the right masticator space, and the cheek. Note, in (**a**), the macroglossia, with the tongue protruding out of the mouth, and partial obstruction of the oral cavity. Note the mass effect of the lesion on the soft palate and compression of rhino-oropharynx (*thick arrow*) with visualization of a patent and nondistended cervical trachea and larynx (*thin arrow* in **a** and **c**)

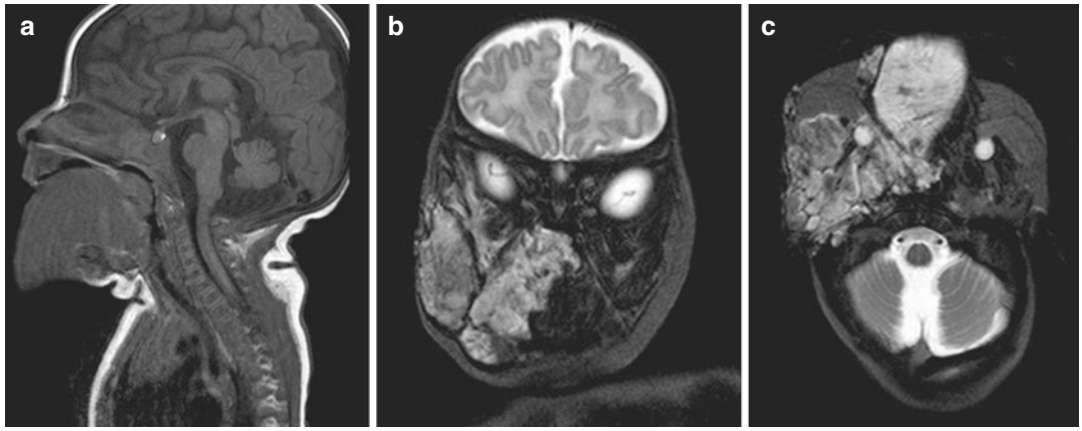

Fig. 14.2 Postnatal MRI at 45 days of life confirmed the voluminous, subcutaneous venous-lymphatic orofacial malformation. T1-weighted sagittal image (**a**) shows the homogeneous hypointense lesion with corresponding heterogeneous hyperintense signal on T2-weighted images (**b**, coronal image; **c** axial image)

made after birth [4]. In the case reported here, accurate prenatal diagnosis, by means of ultrasound and fetal MRI, of a subcutaneous mixed venous-lymphatic malformation associated with macroglossia aided the genetic counseling and the parents' decision-making process and allowed appropriate antenatal and post-natal care management [5]. In addition, adding fetal MRI to ultrasound and Doppler study of the fetal vascular anomalies enhances the characterization of these lesions and the accuracy of the antenatal diagnosis and assists with patient selection for an EXIT procedure [6, 7].

References

1. Odibo IN, Linam LE, Richter GE, Jackson RJ, Dajani NK. Extensive fetal congenital subcutaneous mixed venous lymphatic lesion: prenatal diagnosis and postnatal management. AJP Rep. 2015;5:e37–42.
2. Le Vaillant C, Beneteau C, Chan-Leconte N, David A, Riteau AS. Beckwith-Wiedemann syndrome: what do you search in prenatal diagnosis? About 14 cases. Gynecol Obstet Fertil. 2015;43:705–11.
3. Poreau B, Lin S, Bosson C, Dieterich K, Satre V, Devillard F, Guigue V, Ronin C, Brouillet S, Barbier C, Jouk PS, Coutton C. 13q31.1 microdeletion: a prenatal case report with macrocephaly and macroglossia. Eur J Med Genet. 2015;58:526–30.
4. Williams DH, Gauthier DW, Maizels M. Prenatal diagnosis of Beckwith-Wiedemann syndrome. Prenat Diagn. 2005;25:879–84.
5. Laje P, Peranteau WH, Hedrick HL, Flake AW, Johnson MP, Moldenhauer JS, Adzick NS. Ex utero intrapartum treatment (EXIT) in the management of cervical lymphatic malformation. J Pediatr Surg. 2015;50:311–4.
6. Shih JC, Hsu WC, Chou HC. Prenatal three-dimensional ultrasound and magnetic resonance imaging evaluation of a fetal oral tumor in preparation for the ex-utero intrapartum treatment (EXIT) procedure. Ultrasound Obstet Gynecol. 2005;25:76–9.
7. Calvo-Garcia MA, Kline-Fath BM, Adams DM, Gupta A, Koch BL, Lim FY, Laor T. Imaging evaluation of fetal vascular anomalies. Pediatr Radiol. 2015;45:1218–29.

Acromelic Frontonasal Dysplasia (Median Cleft Face Syndrome)

15

Mario Lituania and Gabriele Tonni

15.1 Introduction

Frontonasal dysplasia (FND) is characterized by multiple anomalies including hypertelorism, broadening of the nasal root, median facial cleft lip/palate associated with clefting of the alae nasi, absent formation of the nasal tip, cranium bifidum occultum and a "V-shaped" frontal hairline [1, 2]. FND exhibits a wide genotype to phenotype correlation that may encompasses from acromelic frontonasal dysplasia, acrofrontofacionasal dysostosis syndromes to oculoauriculofrontonasal syndrome and prenatal diagnosis is always very challenging. FND may be associated with multiple central nervous system anomalies including callosal dysgenesis, encephalocele, occipital meningocele, Dandy-Walker malformations, limb defects and post-axial polydactyly [3, 4]. Guion-Almeida et al. [5] studying 21 patients with FND suggested that this congenital anomaly may not be a single developmental defect that may be inherited as autosomal dominant sequence or recessive as Shanske syndrome.

M. Lituania
Periconceptional and Prenatal Diagnostic Service, IRCCS Galliera Hospital, Genoa, Italy

G. Tonni, MD, PhD (✉)
Department of Obstetrics and Gynecology, Prenatal Diagnostic Service, Guastalla Civil Hospital, AUSL Reggio Emilia, Reggio Emilia, Italy
e-mail: Tonni.Gabriele@ausl.re.it

15.2 Case Description

A 39-year-old woman, gravida 3, para 1, was referred for level II ultrasound at 16 weeks 5 days of gestation due to a suspected midline facial anatomy that was detected at her routine obstetric scan. The parents were non-consanguineous and their medical and family histories were unremarkable. First-trimester screening for Down syndrome yielded normal fetal biometry and anatomy and a low risk for common trisomies.

Upon referral, the ultrasound examination showed a fetus with biparietal diameter (BPD) and a BPD/FOD (fronto-occipital diameter) <5th percentile and a BPD/FL (femur length) <3rd percentiel for expected gestational age. Evaluation of the fetal anatomy performed with conventional two-dimensional ultrasound revealed a heterogeneous mixed solid and cystic mass measuring 5 × 30 mm occupying the midline of the fetal face. The parenchyma of the mass had an echogenicity resembling that of cerebral tissue (Fig. 15.1a, b). Doppler ultrasound showed a blood supply to the lesion coming directly from the circle of Willis circle. In addition, the anterior cerebral artery was seen to have an anomalous course. Neither the cavum septi pellucidum nor the corpus callosum could be observed. Severe hypertelorism was seen. Three-dimensional ultrasound using surface-rendering mode enhanced spatial reconstruction and enabled the detection of a tumor

G. Tonni, W. Sepulveda, and A.E. Wong (eds.), *Prenatal Diagnosis of Orofacial Malformations*,
DOI 10.1007/978-3-319-32516-3_15

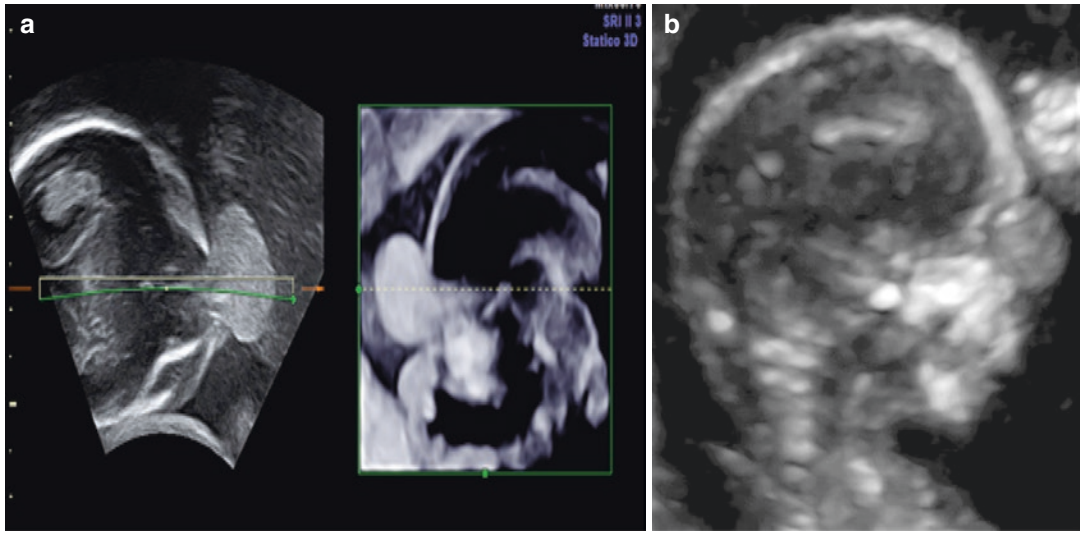

Fig. 15.1 Three-dimensional ultrasound at 16 weeks 5 days of gestation in the axial plane (**a**) and surface rendering mode (**b**) demonstrating an exophytic midline lesion originating from the brain and protruding through the nasal cavity

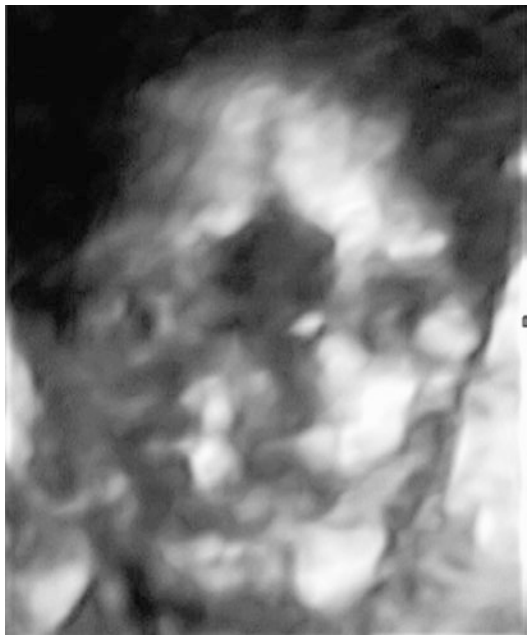

Fig. 15.2 Three-dimensional (3D) ultrasound in the coronal plane using "skeleton" mode: a midline fronto-ethmoid bony defect was clearly detected and rendered

projecting through the nasal cavity. Moreover, a fronto-ethmoid bony defect was detected and clearly rendered using "skeleton" mode (Fig. 15.2). Tomographic ultrasound imaging (TUI) was also applied with thin 1 mm slices (Fig. 15.3). Dedicated transvaginal ultrasound demonstrated normal posterior fossa anatomy and normal brainstem. No other associated anomalies, such as cleft lip/palate, were identified.

A presumptive diagnosis of frontonasal dysplasia (FND) with anterior cephalocele was entertained. Differential diagnosis included nasal glioma (central nervous system (CNS) heterotypia) and/or oral teratoma (epignathus). The parents received extensive genetic counseling concerning in utero evolution, delivery complications, prognosis, and impact on quality of life. Following discussion with the family, consent was obtained for fetal karyotyping with QF-PCR (normal 46,XX), amniotic fluid acetylcholinesterase determination and fetal magnetic resonance imaging (MRI). Fetal MRI was performed using single-shot-fast-spin echo (SSSE) T2-weighted single-slice images and T1-weighted 3D turbo field echo obtained in the three planes confirmed the mass to be regarded as anterior, fronto-ethmoid cephalocele. MRI showed a large, lobulated, homogeneous hyperintense lesion on T2-weighted images with corresponding hypointense signal on T1-weighted sequences, without fat signal or hemorrhagic areas (Fig. 15.4). No macrocysts were identified and no areas of flow void were

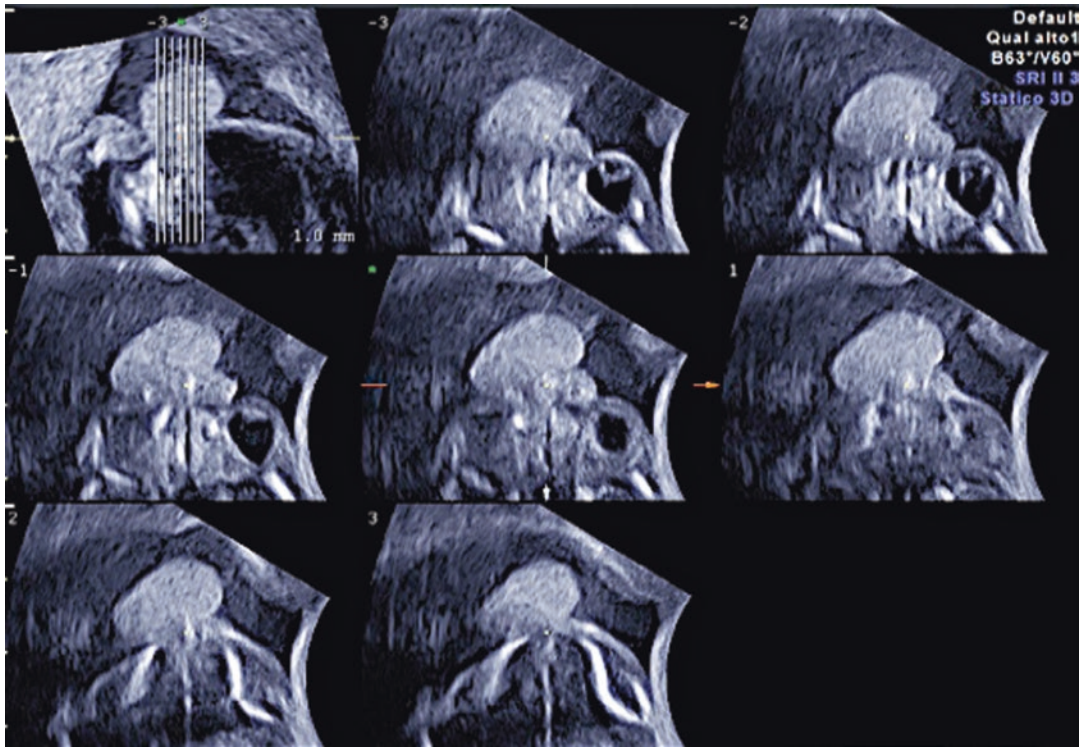

Fig. 15.3 Three-dimensional ultrasound using tomographic ultrasound imaging (TUI) in the coronal plane with slice thickness of 1 mm: a hyperechogenic tumor with undefined contour is seen projecting anteriorly through the nasal cavity. Severe hypertelorism was an associated finding

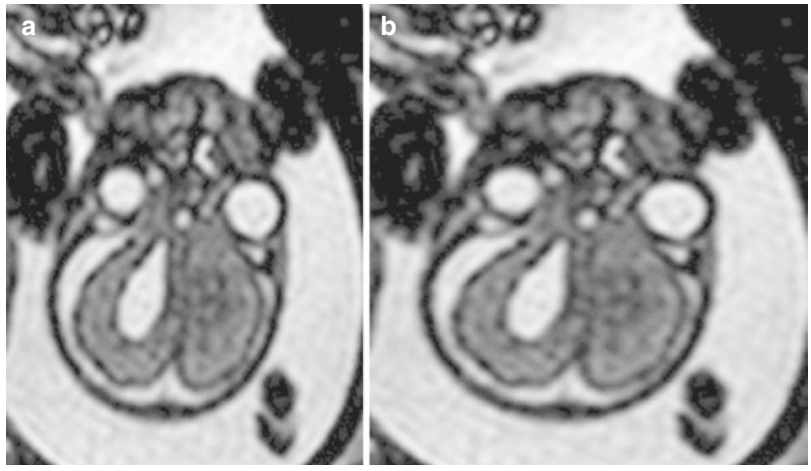

Fig. 15.4 (**a**, **b**). Fetal T2-weighted MRI at 19 weeks 5 days of gestation showed the homogeneous hyperintense lesion with corresponding heterogeneous hyperintense signal on T2-weighted images

observed. The lesion was seen in continuity with the brain, projecting anteriorly between the fetal orbits and extending from the upper aspects of the forehead to the nasal bridge. The floor of the mouth, trachea, larynx, and anterior neck were not infiltrated by the tumor and no other additional

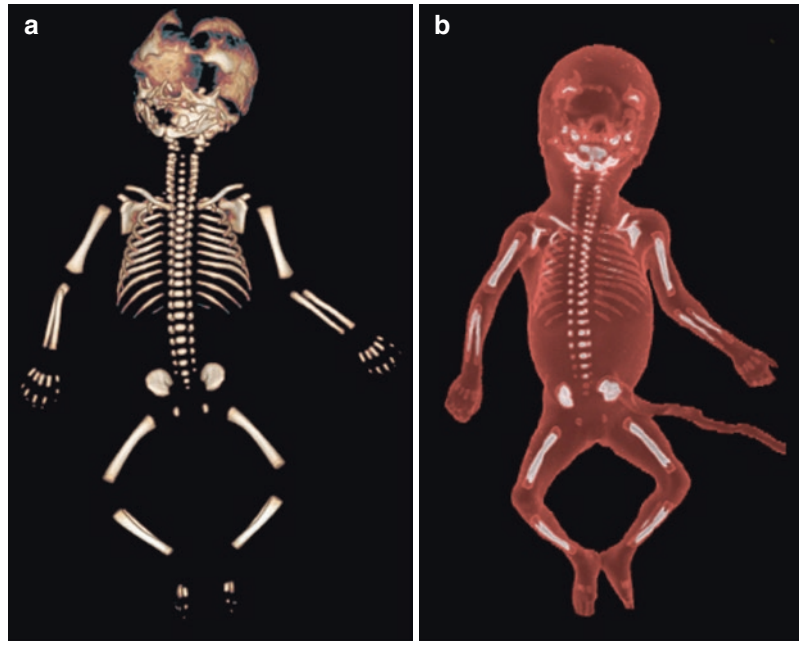

Fig. 15.5 (**a**) Postmortem CT scan with (**b**) 3D rendering confirming the prenatal US findings of fronto-ethmoid bony defect

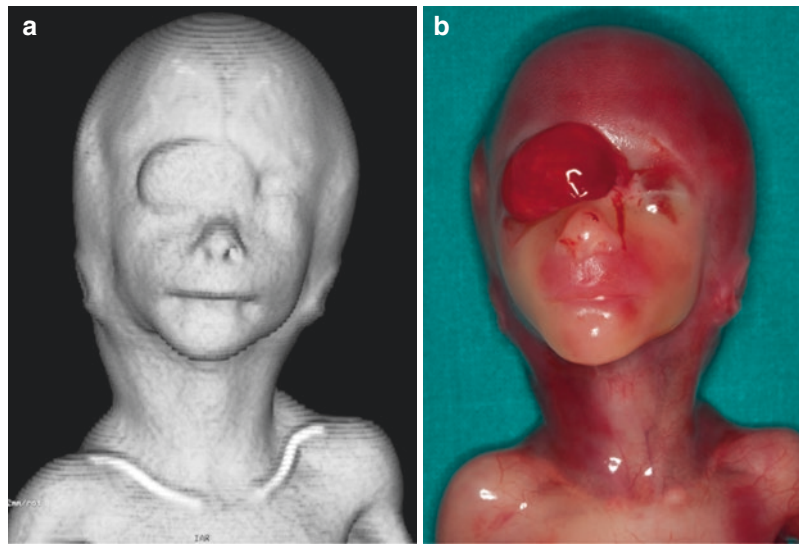

Fig. 15.6 (**a**) Postmortem CT scan with 3D rendering and (**b**) gross pathology

findings were noted. However, due to major congenital malformations affecting the CNS, the parents opted for pregnancy termination with postmortem diagnostic investigation (computerized tomography (CT) scan, digital scan, digital pictures, and autopsy) (Figs. 15.5a, b and 15.6a, b). Neuropathology confirmed the presence of neural tissue within the tumor (Fig. 15.7).

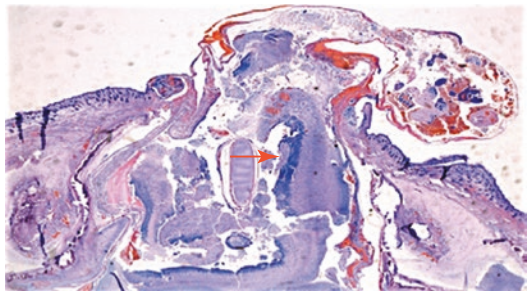

Fig. 15.7 Neuropathology confirmed the presence of neural tissue within the tumor (*arrow*)

15.3 Discussion

Isolated anterior fronto-ethmoid cephalocele has been rarely reported in the medical literature. Usually, it has been documented in fetuses with FND. FND refers to midline facial anomalies caused by abnormal development of the facial primordia and is split into three types in relation to different gene encoding for the disease. FND-1 (OMIM136760), also designated frontorhiny, is caused by homozygous mutation in the aristaless-like homeobox-3 gene (ALX3; 606014) on chromosome 1p13. The disease is characterized by autosomal recessive inheritance. FND-2 (OMOM 613451) is caused by a mutation in the ALX4 gene (OMIM 605420) on chromosome 11p11.2, while FND-3 (OMIM 613456) is caused by a mutation in the ALX1 gene (OMIM 601527) on chromosome 12q21. In addition, nasal glioma or central nervous system heterotypia should be considered in the differential diagnosis [6] as well as oral teratoma or epignathus [7, 8]. In a zebrafish model, it has been demonstrated that ALX1 plays a crucial role in regulating the migration of cranial neural crest (NC) cells into the frontonasal primordia [9]).

Corbacioglu et al. [10] reported a case of prenatal diagnosis of FND with anterior encephalocele detected at 27 weeks' gestation. Abnormal facial phenotype was characterized by prominent hypertelorism and two facial clefts and the nostrils were extremely separated. Interestingly, fetal karyotype was normal and no mutation in the ALX1 gene was found, excluding ALX1-related FND in the differential diagnosis.

References

1. Sedano HO, Cohen MM Jr, Jirasek J, Gorlin RJ. Frontonasal dysplasia. J Pediat 1976:906–13.
2. Sedano HO, Gorlin RJ. Frontonasal malformation as a field defect and in syndromic associations. Oral Sur Oral Med Oral Path 1988;65:704–10.
3. Verloes A, Gillerot Y, Walczak E, Van Maldergem L, Koulischer L. Acromelic frontonasal "dysplasia": further delineation of a subtype with brain malformation and polydactyly (Toriello syndrome). Am J Med Genet 1992;42:180–3.
4. Toriello HV, Radecki LL, Sharda J, Looyenga D, Mann R. Frontonasal "dysplasia," cerebral anomalies, and polydactyly: report of a new syndrome and discussion from a developmental field perspective. Am J Med Genet Suppl 1986;2:89–96.
5. Guion-Almeida ML, Richieri-Costa A, Saavedra D, Cohen MM Jr. Frontonasal dysplasia: analysis of 21 cases and literature review. Int J Oral Maxillofac Surg 1996;25:91–7.
6. Tonni G, Lituania M, Bonasoni MP, De Felice C. Prenatal ultrasound and histological diagnosis of fetal nasal glioma (heterotopic central nervous system tissue): report of a new case and review of the literature. Arch Gynecol Obstet. 2011;283 Suppl 1:55–9.
7. Tonni G, Centini G, Inaudi P, Rosignoli L, Ginanneschi C, De Felice C. Prenatal diagnosis of severe epignathus in a twin: case report and review of the literature. Cleft Palate Craniofac J. 2010;47:421–5.
8. Tonni G, De Felice C, Centini G, Ginanneschi C. Cervical and oral teratoma in the fetus: a systematic review of etiology, pathology, diagnosis, treatment and prognosis. Arch Gynecol Obstet. 2010;282:355–66.
9. Dee CT, Szymoniuk CR, Mills PE. Defective neural crest migration revealed by a Zebrafish model of Alx1-related frontonasal dysplasia. Hum Mol Genet. 2013;22:239–51.
10. Corbacioglu A, Kalelioglu I, Kayserili H, Yuksel A, Has R. Prenatal diagnosis of frontonasal dysplasia with anterior encephalocele. J Turkish-German Gynecol Assoc. 2013;14:50–2.

16 Prenatal Diagnosis of Severe Midfacial Hypoplasia Using 3D Ultrasound

Gabriele Tonni, Jurandir Piassi Passos, and Mario Lituania

16.1 Introduction

Interactions at cellular level regulate both the brain and the craniofacial morphogenesis during early gastrulation stages of embryo development *via* ectodermal cells [1–3]. In the animal model, it has been demonstrated that prenatal ethanol exposure is associated with central nervous system dysfunction, growth retardation, and craniofacial abnormalities as severe end of the spectrum of fetal alcohol syndrome (FAS) [4, 5]. Specifically, activation of the *Shh* (sonic hedgehog) signaling in the brain is responsible for an altered pattern in the ectoderm cells covering the upper jaw; these changes cause facial dysmorphologies [3]. The maxilla-mandible-nasion (MMN) angle, obtained in the midsagittal plane, is a newly developed and promising ultrasound marker to assess the degree of midfacial hypoplasia during the second and third trimesters of pregnancy and has proved to be useful in the ultrasonographic evaluation of the common trisomies [6, 7]. Morever, the MNM angle is independent of gestational age, is significantly smaller in trisomy 21 fetuses compared with controls [7], and may be added to the fetal profile (FP) line to enhance prenatal diagnostic accuracy [7].

16.2 Case Description

A 32-year-old woman, gravida 2 para 1, was referred for a thorough ultrasound examination at 21.5 weeks of gestation with a suspected facial anomaly that was seen on a routine second-trimester ultrasound examination. The parents were non-consanguineous, with unremarkable medical and family histories. First-trimester screening for Down syndrome showed a low risk for common trisomies with normal fetal biometry and anatomy.

At referral, an ultrasound examination using a Voluson E8 (GE, Milwaukee, WI) apparatus equipped with multifrequency transabdominal and transvaginal volumetric probes was performed. Using three-dimensional (3D) ultrasound in multiplanar mode with volume rendering, a wide median cleft was visualized (Fig. 16.1). Tomographic ultrasound imaging (TUI) using thin slices of 1 mm was applied and confirmed the diagnosis and clearly demonstrated extension of the median cleft to involve the nose, lips, and hard and soft palates (Fig. 16.2). 3D ultrasound in surface-rendering mode clearly illustrated the lesion (Figs. 16.3 and 16.4). Using color Doppler, bidirectional

G. Tonni, MD, PhD (✉)
Department of Obstetrics and Gynecology, Prenatal Diagnostic Service, Guastalla Civil Hospital, AUSL Reggio Emilia, Reggio Emilia, Italy
e-mail: Tonni.Gabriele@ausl.re.it

J.P. Passos
Department of Obstetrics and Gynecology, Paulista School of Medicine, Federal University of Sap Paulo (UNIFESP), Sao Paulo, Brazil

M. Lituania
Periconceptional and Prenatal Diagnostic Service, IRCCS Galliera Hospital, Genoa, Italy

G. Tonni, W. Sepulveda, and A.E. Wong (eds.), *Prenatal Diagnosis of Orofacial Malformations*,
DOI 10.1007/978-3-319-32516-3_16

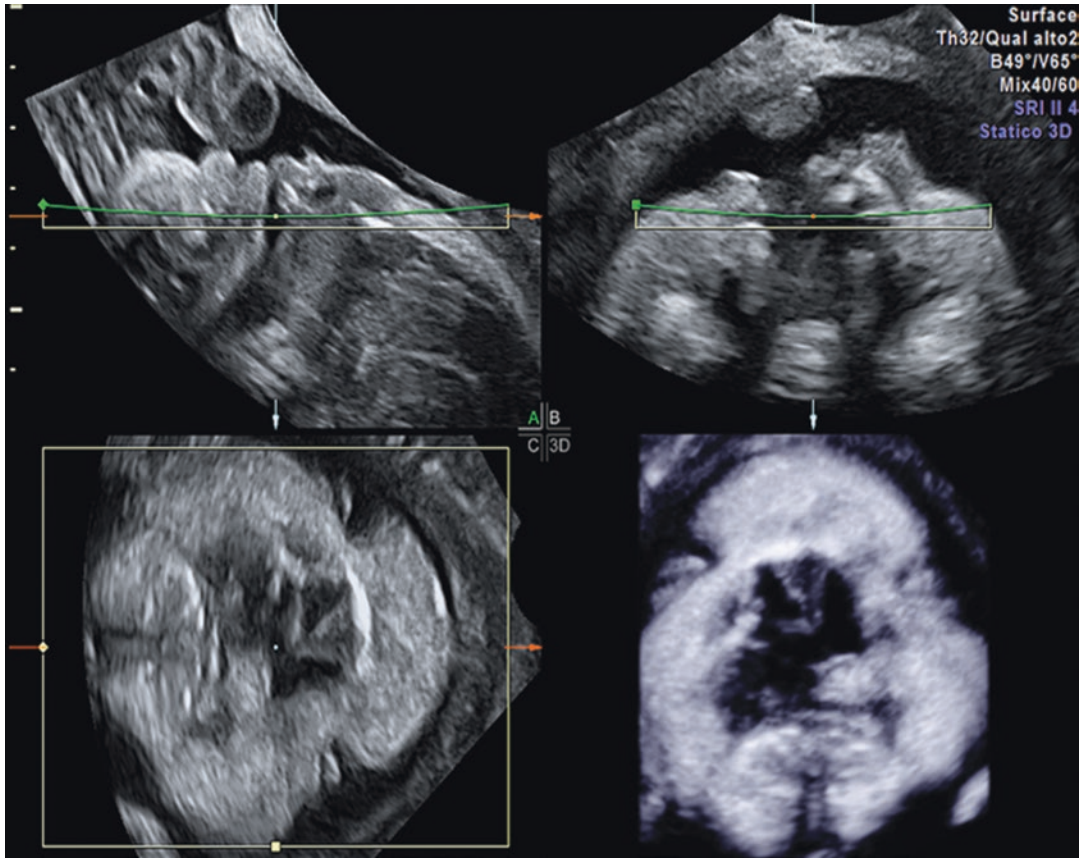

Fig. 16.1 Three-dimensional ultrasound at 21.5 weeks of gestation in multiplanar mode and with volume reconstruction. The green toolbar was placed at the level of the midportion of the fetal face and showed a wide, midfacial cleft involving the nasal bone and the palate

flow through the cleft was visualized. The parents received extensive counseling by the multispecialty team regarding the potential genetic associations and anticipated in utero development, delivery complications, prognosis, and impact on quality of life. After this counseling, rapid fetal karyotyping with QF-PCR was performed with an uncomplicated amniocentesis that resulted in a normal 46,XX karyotype. The parents desired to continue the pregnancy. Monthly serial ultrasounds were scheduled. No polyhydramnios developed. A newborn weighing 3250 g was delivered vaginally at term (Fig. 16.5). In order to prevent respiratory and feeding complications, the newborn was immediately intubated. Postnatal reconstruction surgery by Le Fort III osteotomy was planned at 10 days postnatally with *restitutio ad integrum* following development of a 3D model.

16.3 Discussion

Failure or delay in midfacial development as well as any abnormal fusion of the medial and lateral nasal and maxillary prominences will result in developmental defects of the midface with varying degrees of severity, including cleft and hypoplasia. The midportion of the face, defined as the nose, upper lip, maxilla, primary palate, and zygomatic bones, starts to develop from the fifth week post-fertilization and is

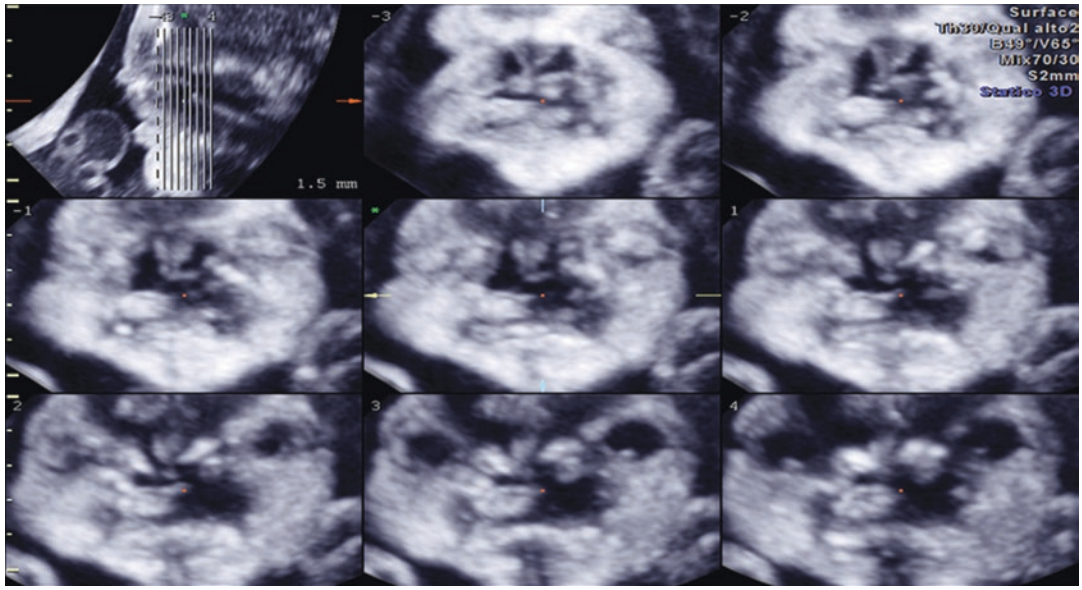

Fig. 16.2 Three-dimensional ultrasound using tomographic ultrasound imaging with thin 1 mm slices. Note the green dot (reference point) set at the level of the midportion of the hard palate

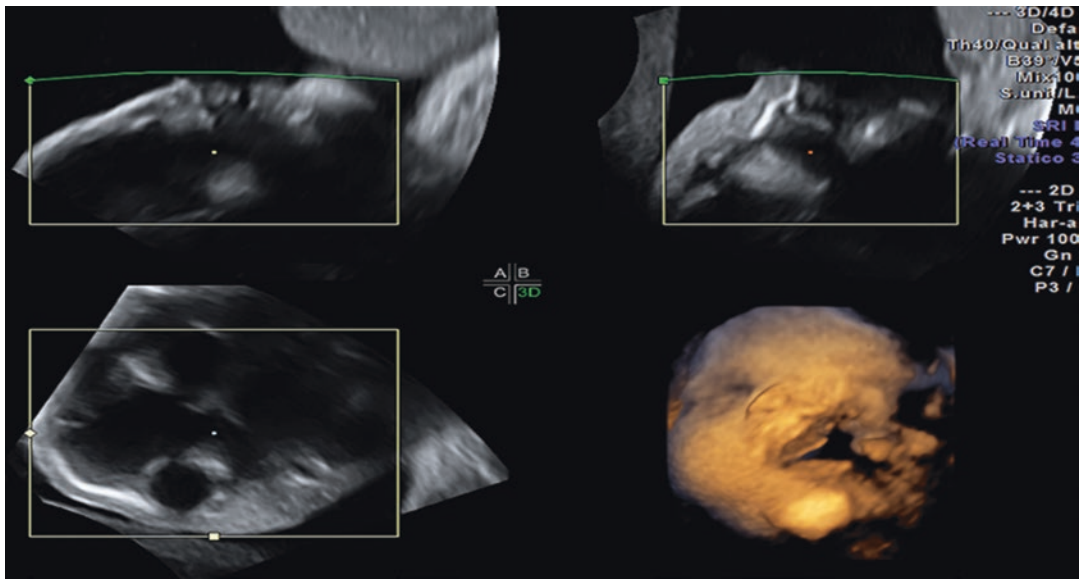

Fig. 16.3 Three-dimensional ultrasound using surface mode: a wide, median cleft was clearly rendered by volume reconstruction

completed by week seven. This process involves the development and fusion of seven processes (the frontonasal process the paired lateral and medial nasal processes, and the paired maxillary processes) [9], and requires the coordination of both mesenchymal cells derived from the cranial neural crest which are covered by ectoderm [10, 13]. Mutations in signaling pathways genes

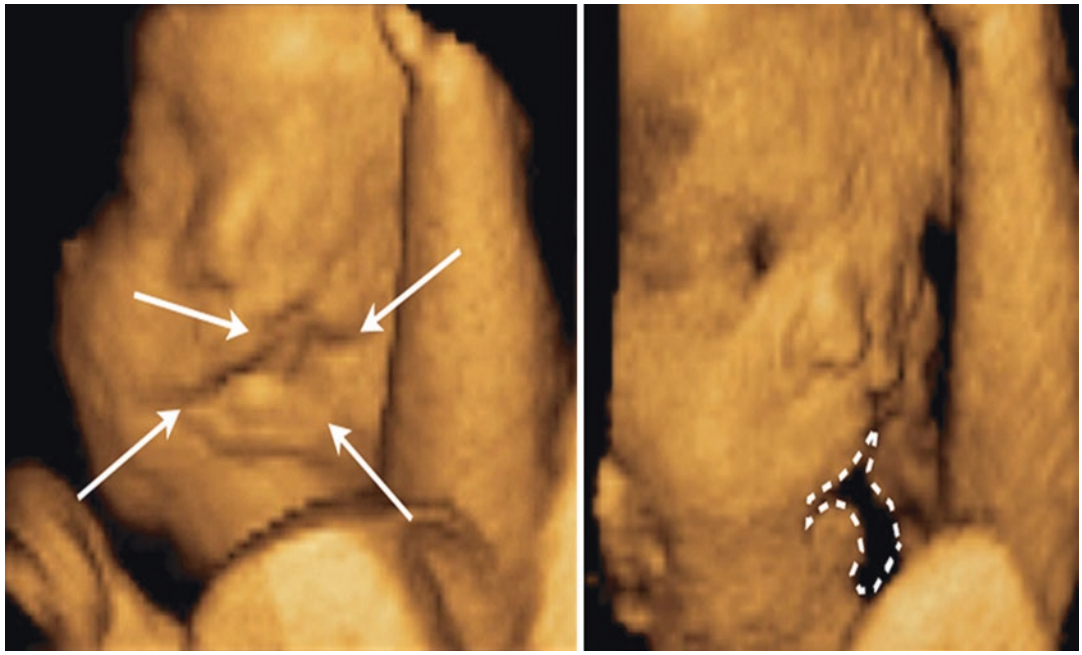

Fig. 16.4 Three-dimensional ultrasound in surface mode: detail of the wide, midfacial cleft lip and palate. Note the abnormal nose

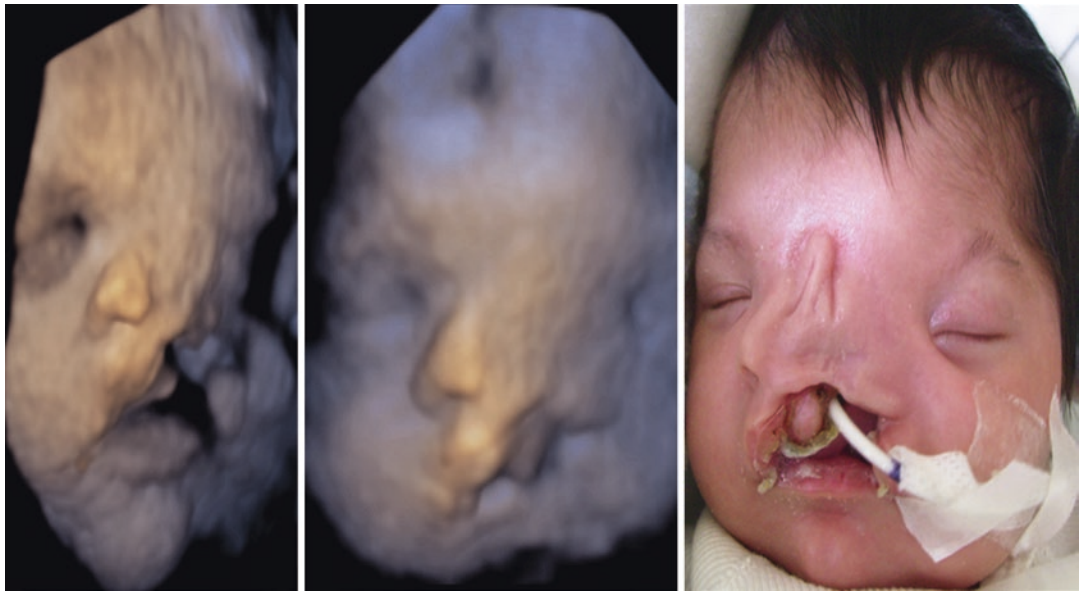

Fig. 16.5 Three-dimensional ultrasound using "glass body" rendering and newborn baby at delivery for comparison

such as fibroblast growth factor receptor (FGFR), WNT, transforming growth factor-beta (TGFβ), and bone morphogenetic protein (BMP) have been hypothesized. During morphogenesis, FGF regulates neural crest patterning [12] and FGFR 1 and FGFR 2 are widely expressed in facial mesenchyme and ectoderm [8]. In craniofacial development, WNT signaling plays critical roles in the generation, migration, and proliferation of cranial neural crest (CNC) cells in the facial processes in mice [11]. Perturbation of BMP, a member of the TGFβ superfamily, results in orofacial clefting because BMP acts by regulating cell proliferation, extracellular matrix synthesis, and cellular differentiation [13].

The use of 3D ultrasound was of value in the detection and characterization of the extension of the bony defect and closely correlated with postnatal findings. The technique allowed improved understanding of the abnormality and more thorough counseling to assist the parents in the decision-making process and antenatal management. In addition, 3D ultrasound enabled appropriate perinatal care by the multispecialty team by delivering the gold standard of care, avoiding neonatal complications, and providing accurate anatomic information for surgical plastic reconstruction.

References

1. Lipinski RJ, Hammond P, O'Leary-Moore SK, Ament JJ, Pecevich SJ, Jiang Y, Budin F, et al. Ethanol-induced face-brain dysmorphology patterns are correlative and exposure-stage dependent. PLoS One. 2012;7:e43067.
2. Marcucio RS, Cordero DR, Hu D, Helms JA. Molecular interactions coordinating the development of the forebrain and face. Dev Biol. 2005;284:48–61.
3. Hu D, Marcucio RS. A SHH-responsive signaling center in the forebrain regulates craniofacial morphogenesis via the facial ectoderm. Development. 2009;136:107–16.
4. Riley EP, Infante MA, Warren KR. Fetal alcohol spectrum disorders: an overview. Neuropsychol Rev. 2011;21:73–80.
5. Sulik KK, Johnston MC, Webb MA. Fetal alcohol syndrome: embryogenesis in a mouse model. Science. 1981;214:936–8.
6. Weichert J, Gembicki M, Ribbat-Idel J, Hartge DR. Assessment of midfacial hypoplasia in down syndrome fetuses – validity of a two-line approach and introduction of a novel angle (maxilla-mandible-nasion angle). Ultrasound Int Open. 2016;2:E58–62.
7. Vos FI, de Jong-Pleij EA, Bakker M, Tromp E, Kagan KO, Bilardo CM. Fetal facial profile markers of Down syndrome in the second and third trimesters of pregnancy. Ultrasound Obstet Gynecol. 2015;46:168–73.
8. Britto JA, Evans RD, Hayward RD, Jones BM. From genotype to phenotype: the differential expression of FGF, FGFR, and TGFbeta genes characterizes human cranio skeletal development and reflects clinical presentation in FGFR. Plast Reconstr Surg. 2001;108:2026–39.
9. Cox TC. Taking it to the max: the genetic and developmental mechanisms coordinating midfacial morphogenesis and dysmorphology. Clin Genet. 2004;65:163–76.
10. Helms JA, Cordero D, Tapadia MD. New insights into craniofacial morphogenesis. Development. 2005;132:851–61.
11. Mani P, Jarrell A, Myers J, Atit R. Visualizing canonical Wnt signaling during mouse craniofacial development. Dev Dyn. 2010;239:354–63.
12. Nie X, Luukko K, Kettunen P. FGF signalling in craniofacial development and developmental disorders. Oral Dis. 2006;12:102–11.
13. Suzuki A, Sangani DR, Ansari A, Iwata J. Molecular mechanisms of midfacial developmental defects. Dev Dyn. 2016; 245:276–93.

17 3D Virtual Model Reconstruction by 3D Ultrasound Volume Data Sets in a Case of Prenatally Diagnosed Agnathia/Otocephaly Complex Associated with Multiple Congenital Anomalies

Heron Werner, Gabriele Tonni, Gláucia Aparecida Menezes, and Edward Araujo Júnior

17.1 Introduction

Agnathia/otocephaly complex (OMIM 202650) is a rare congenital malformation characterized by multiple malformations involving anatomic structures originating from the first pharyngeal arch as a consequence of failed mesenchymal migration of the maxillary prominence and atrophy of the development of the mandibular prominences [1]. Features of agnathia/otocephaly complex are absence or hypoplasia of the mandible, microstomia, hypoglossia/aglossia, and variable anterior midline fusion of the ears (melotia, synotia) [2]. An incidence of less than 1 in 70,000 births has been estimated [3]. The complex has been linked with a heterozygous mutation of the PRRX1 gene on chromosome 1q24. Genotype/phenotype heterogeneity is possible, and the disease may be inherited in either autosomal recessive or autosomal dominant patterns. In addition, association with environmental teratogens have been described [2, 4]. Recently, it has been demonstrated that perturbations in the PRRX1 and OTX2 genes may alter DNA signaling pathways, suggesting a role in palatal development [2, 5, 6].

17.2 Case Description

A 39-year-old nulliparous woman was referred for level II ultrasound examination for an unspecified complex facial anomaly detected on a routine third-trimester scan. The ultrasound examination was performed using transabdominal and transvaginal two-dimensional (2D) and three- and four-dimensional (3D/4D) volumetric probes. Digital 2D ultrasound imaging and 3D/4D volume datasets were stored onto an optical disk for offline analysis. Ultrasound

H. Werner (✉)
Department of Radiology, Clínica de Diagnóstico por Imagem (CDPI), Rio de Janeiro, Brazil
e-mail: heronwerner@hotmail.com

G. Tonni, MD, PhD
Department of Obstetrics and Gynecology, Prenatal Diagnostic Service, Guastalla Civil Hospital, AUSL Reggio Emilia, Reggio Emilia, Italy

G.A. Menezes
Department of Gynecology and Obstetrics, Federal University of Latin American Integration (UNILA), Foz do Iguacu, Brazil

E.Araujo Júnior
Department of Obstetrics, Paulista School of Medicine – Federal University of Sao Paulo (EPM-UNIFESP), Sao Paulo, Brazil

G. Tonni, W. Sepulveda, and A.E. Wong (eds.), *Prenatal Diagnosis of Orofacial Malformations*,
DOI 10.1007/978-3-319-32516-3_17

examination showed findings consistent with congenital agenesis of the mandible (agnathia), proboscis, and hypotelorism (Fig. 17.1). Multiple skeletal anomalies were visualized, consisting of the absence of the right ulna and right fibula associated with shortening of the contralateral long bones, syndactyly of 5th finger of right hand, and bilateral clubfoot. A multicystic right dysplastic kidney, single umbilical artery, and polyhydramnios were additionally seen. 3D ultrasound volume datasets were transmitted to an expert at remote site (HW) and a physical model reconstruction on photopolymerized resin was constructed using postprocessing software. Specifically, Mimics v. 12, Materialise (Leuven, Belgium), was used for 3D virtual model reconstruction, and the model was exported into a standard triangular language (STL) format and converted into an "OBJ" extension for adjustment using 3D modeling polygonal software (Autodesk Mudbox, San Francisco, CA, USA).

A presumptive diagnosis of agnathia/otocephaly complex associated with multiple congenital anomalies was entertained (Fig. 17.2). Although prognosis of the disease was poor and the parents declined fetal magnetic resonance imaging (MRI) investigation, the 3D virtual model improved the parents' understanding of the fetal anomalies and aided counseling. Termination of pregnancy was not performed due to legal limitations. Intrauterine fetal demise occurred shortly after ultrasound examination and gross pathology confirmed the antenatal diagnosis (Fig. 17.3). Interestingly, the anatomic details of the 3D virtual model substantially overlapped with the characteristic features of the agnathia/otocephaly complex.

17.3 Discussion

Agnathia/otocephaly complex may be isolated [7] or associated with other anomalies. Anencephaly and meningomyelocele [8], skeletal, genitourinary, and cardiovascular anomalies, and situs inversus have been reported [3]. However, the most common associated congenital anomaly is holoprosencephaly [9, 10].

The antenatal diagnosis of agnathia/otocephaly complex is challenging. Although it has most commonly been detected in the third trimester [4, 11, 12], detection at 12 weeks has also been reported [13]. 3D ultrasound ultrasound may aid the prenatal diagnosis of agnathia/otocephaly complex [4, 10–13] and a systematic look at the "CHIN" is advocated ("CHIN": *c*hin, *h*eadbone outline, *i*nner head, *n*uchal translucency) [13]. 3D ultrasound has also proven to be of clinical value in the characterization of the disease and in planning neonatal treatment by the multispecialty team [14], although outcome is generally poor and newborns requires ventilatory support [1].

In addition to 3D virtual modeling of the anomaly that improves parents' understanding and enhances prenatal counseling, 3D computed tomography (CT) scan has been used postmortem in a case of agnathia/otocephaly complex associated with organomegaly to obtain detailed anatomic information about this lethal disease [15].

This work was based on a previously published report [4].

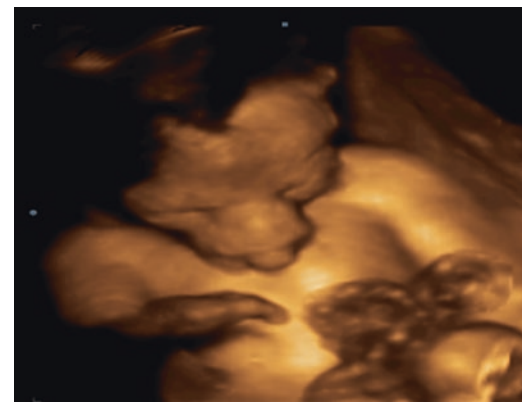

Fig. 17.1 Three-dimensional ultrasound in surface-rendering mode showing proboscis and severe hypotelorism

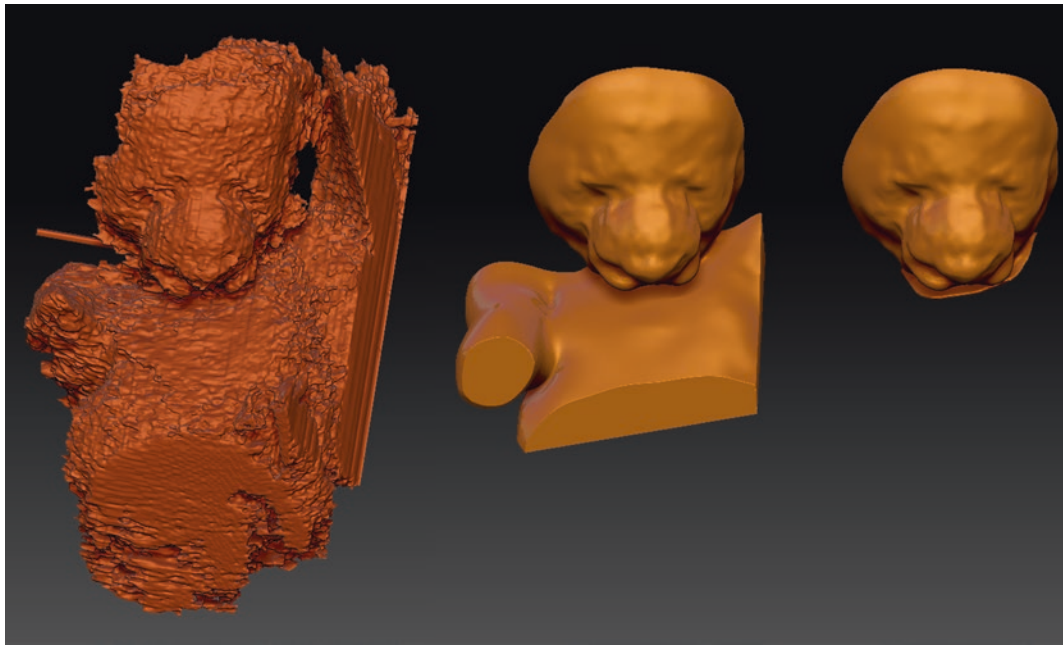

Fig. 17.2 3D virtual physical model showing the typical features of the congenital malformation

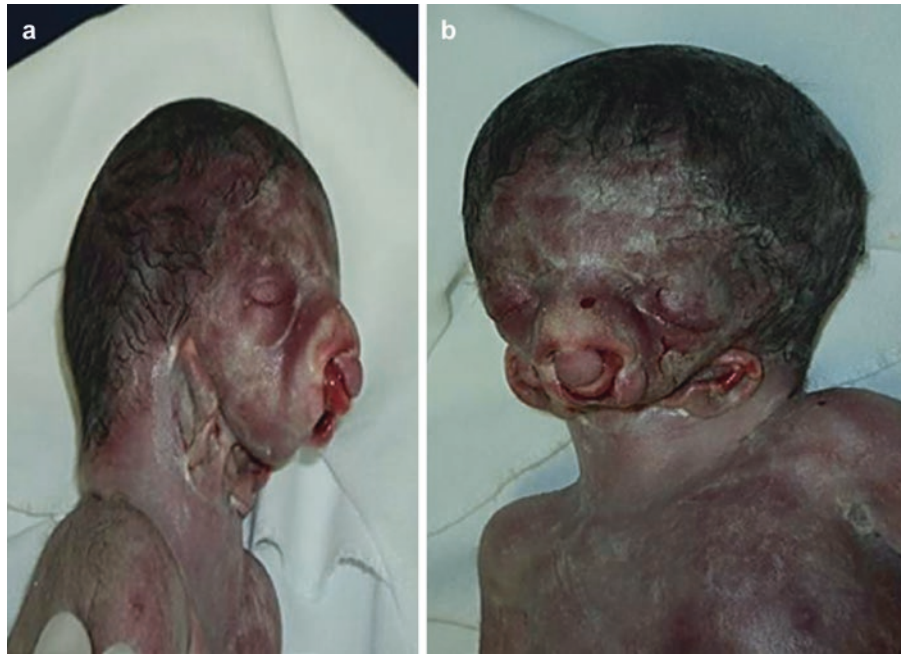

Fig. 17.3 Postmortem photographs showing the agnathia/otocephaly complex in lateral (**a**) and frontal (**b**) views confirming the accuracy of the prenatal ultrasound diagnosis

References

1. Gekas J, Li B, Kamnasaran D. Current perspectives on the etiology of agnathia-otocephaly. Eur J Med Genet. 2010;53:358–66.
2. Herman S, Delio M, Morrow B, Samanich J. Agnathia-otocephaly complex: a case report and examination of the OTX2 and PRRX1 genes. Gene. 2012;494:124–9.
3. Faye-Petersen O, David E, Rangwala N, Seaman JP, Hua Z, Heller DS. Otocephaly: report of five new cases and a literature review. Fetal Pediatr Pathol. 2006;25:277–96.
4. Menezes GA, Araujo Junior E, Lopes J, Belmonte S, Tonni G, Werner H. Prenatal diagnosis and physical model reconstruction of agnathia-otocephaly with limb deformities (absent ulna, fibula and digits) following maternal exposure to oxymetazoline in the first trimester. J Obstet Gynecol Research. 2016;42:1016–20.
5. Sergouniotis PI, Urquhart JE, Williams SG, Bhaskar SS, Black GC, Lovell SC, Whitby DJ, Newman WG, Clayton-Smith J. Agnathia-otocephaly complex and asymmetric velopharyngeal insufficiency due to an in-frame duplication in OTX2. J Hum Genet. 2015;60:199–202.
6. Chassaing N, Sorrentino S, Davis EE, Martin-Coignard D, Iacovelli A, Paznekas W, Webb BD, Faye-Petersen O, Encha-Razavi F, Lequeux L, Vigouroux A, Yesilyurt A, Boyadjiev SA, Kayserili H, Loget P, Carles D, Sergi C, Puvabanditsin S, Chen CP, Etchevers HC, Katsanis N, Mercer CL, Calvas P, Jabs EW. OTX2 mutations contribute to the otocephaly-dysgnathia complex. J Med Genet. 2012;49:373–9.
7. Yang SH, Seo YS, Lee YS, Choi SJ, Kim YA, Kim JH. Prenatal sonographic diagnosis of isolated agnathia: a case report. Ultrasound Obstet Gynecol. 2003;22:190–3.
8. Tos T, Ceylaner S, Senel S, Aktas S, Alp Y. A case of otocephaly with anencephaly and meningomyelocele. Genet Couns. 2010;21:325–8.
9. Rolland M, Sarramon MF, Bloom MC. Astomia-agnathia-holoprosencephaly association. Prenatal diagnosis of a new case. Prenat Diagn. 1991;11:199–203.
10. Chaoui R, Heling KS, Thiel G, Karl K. Agnathia-otocephaly with holoprosencephaly on prenatal three-dimensional ultrasound. Ultrasound Obstet Gynecol. 2011;37:745–8.
11. Hisaba WJ, Milani HJ, Araujo Júnior E, Passos JP, Barreto EQ, Carvalho NS, Helfer TM, Pares DB, Nardozza LM, Moron AF. Agnathia-otocephaly: prenatal diagnosis by two- and three-dimensional ultrasound and magnetic resonance imaging. Case report. Med Ultrason. 2014;16:377–9.
12. Tantbirojn P, Taweevisit M, Sritippayawan S, Tanawattanacharoen S, Uerpairojkit B. Prenatal three-dimensional ultrasonography in a case of agnathia-otocephaly. J Obstet Gynaecol Res. 2008;34:663–5.
13. Huissoud C, La Mela Jumel A, Bisch C, Dijoud F, Pages O, Rudigoz RC. Take a look at the CHIN! --early diagnosis of isolated agnathia using two- and three-dimensional sonography. Fetal Diagn Ther. 2008;24:246–9.
14. Umekawa T, Sugiyama T, Yokochi A, Suga S, Uchida K, Sagawa N. A case of agnathia-otocephaly complex assessed prenatally for ex utero intrapartum treatment (EXIT) by three-dimensional ultrasonography. Prenat Diagn. 2007;27:679–81.
15. Rajan PV, Wing DA, Bocian M, McKeown A. Computed tomographic reconstruction of a fetus with the dysgnathia complex (agnathia-otocephaly). Prenat Diagn. 2007;27:130–2.

18 Unilateral Agenesis of the Mandible (Agnathia) in a Fetus with 4p-/10q Duplication Associated with Balanced Paternal Cryptic 4p/10q Translocation: Multidisciplinary Management of a Complex Case

Lucia Rosignoli, Gabriele Tonni, Elisabetta Pelo, and Marco di Maurizio

18.1 Introduction

Agenesis of the ramus of the mandible (agnathia) is a rare disease that can be part of more than 100 genetic syndromes. From an embryological point of view, agenesis of the mandible is linked to defects in migration of neural crest cells that determine a developmental anomaly of the first arch, or mandibular arch, during the 4th week of embryogenesis [1]. Agnathia can be isolated or associated with other malformations, of which the most frequent is holoprosencephaly. Indeed, evidence from humans and animal models suggests that agnathia-holoprosencephaly represents a causally heterogeneous single developmental field defect [2]. Agnathia may be usually recognized by ultrasound during the second trimester of pregnancy and may be misinterpreted as micrognathia [3–5]. If micrognathia is the only ultrasound finding identified, parents should be aware of possible respiratory complications at birth, presence of facial clefting, and/or developmental delay [6]. Chromosomal abnormalities have been detected in 66 % of fetuses with micrognathia, in 77 % with macroglossia, in 48 % with cleft lip and palate, in 45 % with severe hypotelorism or cyclops, and in 32 % with nasal hypoplasia, proboscis, or single nostril [4, 7]. Teoh and Meagher [8] reported a first-trimester (13 weeks) diagnosis of micrognathia and receding chin by using transvaginal ultrasound, with later diagnostic confirmation at 19 weeks' gestation. These findings were associated with complex cardiac defect and unilateral talipes equinovarus in a fetus with normal karyotype and with a definitive diagnosis of Pierre Robin syndrome. Sepulveda et al. [9] have demonstrated the value of the retronasal triangle view for

L. Rosignoli
Prenatal Diagnostic Unit, University Hospital Meyer, Florence, Italy

G. Tonni, MD, PhD (✉)
Department of Obstetrics and Gynecology, Prenatal Diagnostic Service, Guastalla Civil Hospital, AUSL Reggio Emilia, Reggio Emilia, Italy
e-mail: Tonni.Gabriele@ausl.re.it

E. Pelo
Medical Genetics, University Hospital Careggi, Florence, Italy

M. di Maurizio
Diagnostic Imaging, University Hospital Meyer, Florence, Italy

G. Tonni, W. Sepulveda, and A.E. Wong (eds.), *Prenatal Diagnosis of Orofacial Malformations*,
DOI 10.1007/978-3-319-32516-3_18

detecting micrognathia in the first trimester. Absent visualization of the mandibular gap or failure to identify the mandible in coronal view is highly suggestive of micrognathia and should prompt a targeted ultrasound scan to assess for other anomalies. The role of the retronasal triangle view in the early prenatal diagnosis of orofacial clefts has been subsequently confirmed byTonni et al. [10].

18.2 Case Description

A 25-year-old primigravida underwent first-trimester combined screening for common trisomies at 12 weeks 2 days of gestation. Although the test resulted as low risk, the fetus had premaxillary protrusion and micrognathia at the ultrasound evaluation of the sagittal plane of the face (Fig. 18.1). Chorionic villus sampling was performed the same day. Quantitative fluorescence polymerase chain reaction (QF-PCR) for chromosomes 21, 18, 13 and sex chromosomes resulted as normal. Fetal karyotype in cultured villi was 46,XY. A thorough ultrasound examination, which included three-dimensional (3D) ultrasound of the fetal face and skull, was performed at 20 weeks of gestation. Application of 3D ultrasound reverse face techinque in surface maximum mode enabled clear detection of unilateral, left mandibular agenesis, micrognathia, and cleft lip (Fig. 18.2).

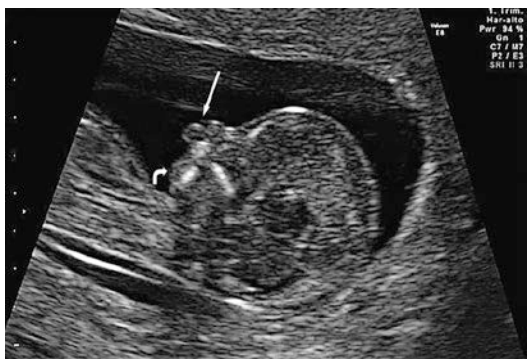

Fig. 18.1 Two-dimensional ultrasound performed at 12 weeks and 2 days of gestation. Note premaxillary protrusion (*arrow*) and micrognathia (*curved arrow*) in midsagittal plane

The nose was abnormal in shape resembling a proboscis. The diagnostic clue was failure to identify the ossifying mandible in the sagittal and coronal planes from the temporo-mandibular joint to the symphysis of the chin. No other congenital malformatiosn were detected on ultrasound. Fetal magnetic resonance imaging (MRI) examination was arranged as complementary diagnostic investigation and confirmed the ultrasound diagnosis in both sagittal (Fig. 18.3) and coronal (Fig. 18.4) planes.

Full genetic consultation was then performed. Family history was remarkable for a first-degree cousin on the maternal side that had surgery for macroglossia due to Beckwith-Wiedemann syndrome. In addition, the father had an older brother with congenital clubfoot, a brother who died in the neonatal period due to multiple congenital malformations including cleft palate, clubfoot, and renal anomalies, and his mother had a miscarriage at 20 weeks of gestation after the ultrasound diagnosis of multiple congenital malformations in the fetus (Fig. 18.5).

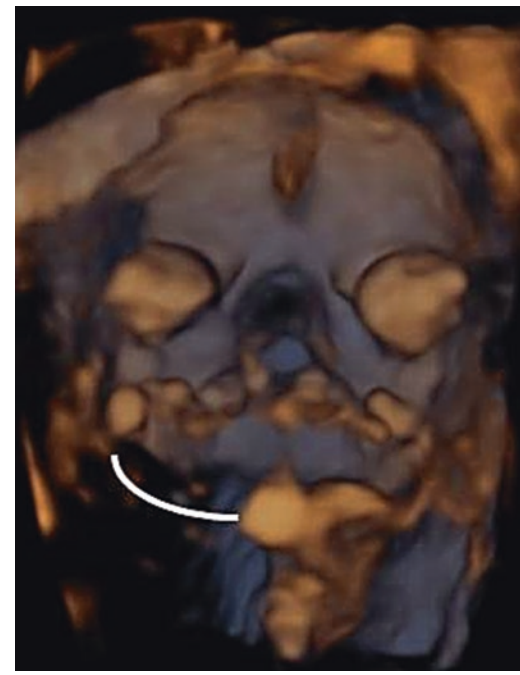

Fig. 18.2 Three-dimensional ultrasound performed at 20 weeks' gestation using reverse face in surface maximum mode in coronal plane: unilateral, left mandibular agenesis was detected (*curved line*)

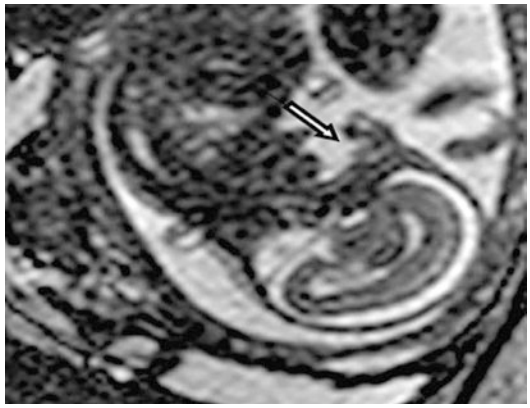

Fig. 18.3 Fetal MRI in BTFE sequence: an abnormal fetal profile is confirmed. Abnormal anatomy of the hard palate is also visible in sagittal plane (*arrow*)

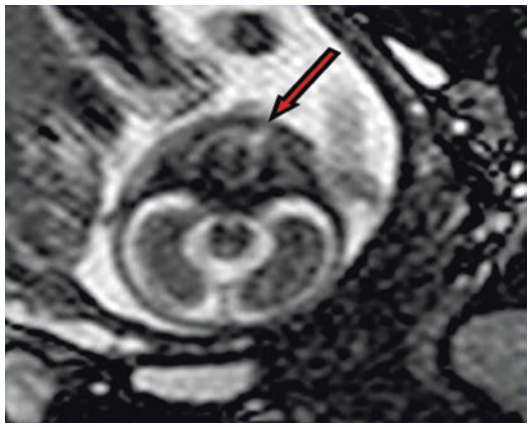

Fig. 18.4 Fetal MRI in BTFE sequence showing left-sided cleft lip (*red arrow*)

Multiplex ligation-dependent probe amplification (MLPA) was performed in a frozen sample of chorionic villi revealing a subtelomeric deletion of the short arm of chromosome 4 and a subtelomeric duplication of the long arm of chromosome 10 (Fig. 18.6). Subsequent paternal fluorescence in situ hybridization (FISH) was performed showing a balanced, cryptic translocation in the subtelomeric 4p/10q region (Fig. 18.7). The rearrangement in the father was inherited from his mother. In this case, the detected anomalies were attributed to a segregated, unbalanced, familial, cryptic translocation. Genetic counseling was conducted and the wide spectrum of ocular-auricular-vertebral anomalies involving the first and second pharyngeal arch such as Gorlin-Goldenhar, Treacher Collins and auriculo-condylar syndromes were discussed. The pathogenesis of Gorlin-Goldenhar syndrome may be associated with *in utero* exposure to teratogenic agents, chromosomal abnormalities (chromosomes 5, 18, 22, and X), while Treacher Collins is caused by haploinsufficiency of TOCF1 gene, the auriculocondylar syndromes (ARCND) are caused by gene mutations at different loci on chromosome 1p13 (ARCND1, GNAI3 gene), chromosome 20p12 (ARCND2, PLCB4 gene) and chromosome 6p24 (ARCND3, EDN1 gene). Beckwith-Wiedemann syndrome, characterized by macroglossia, macrosomia, abdominal wall defect, and hemi-hyperplasia, and Silver-Russell syndrome (Pierre Robin sequence, cleft palate, renal anomalies, and fetal growth restriction) were also considered. The parents opted for second-trimester termination of pregnancy according to Italian legislation.

18.3 Discussion

Prenatal ultrasound examination of the fetal face and maxillo-facial region is possible from the first trimester onward although 2D and 3D ultrasound may be challenging early in gestation. Maxillo-facial abnormalities can be seen in isolation or associated with other congenital abnormalities or genetic syndromes. Attempts have been made to standardize the ultrasound evaluation of the fetal face and diverse techniques have been proposed and validated. With conventional 2D ultrasound, the examination of the lip and palate is performed using the three spatial planes: sagittal, coronal, and axial or transverse/cross sections. The profile is obtained by scanning the face in sagittal plane, while the nose and the lips are obtained by scanning the face in coronal plane.

Finally, to confirm integrity of the upper lip, as well as the surrounding alveolus, or primary palate, an axial plane or cross section must be performed. Attempts have been made to standardize the ultrasound evaluation of the fetal face by 3D ultrasound and diverse techniques have been proposed and validated. The most used are the

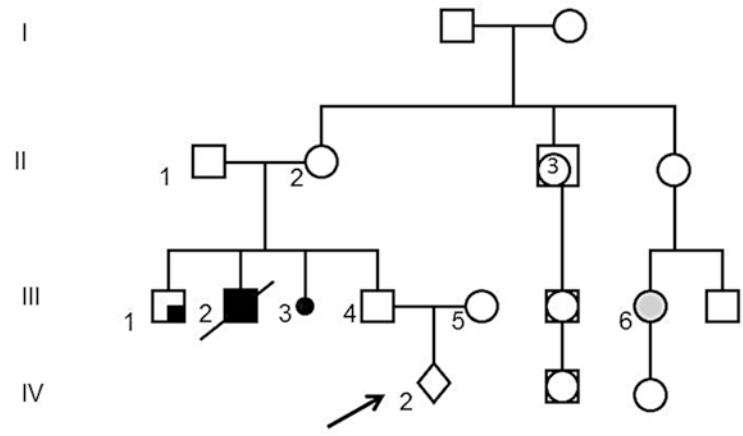

Fig. 18.5 Family pedigree. Arrow shows the index case

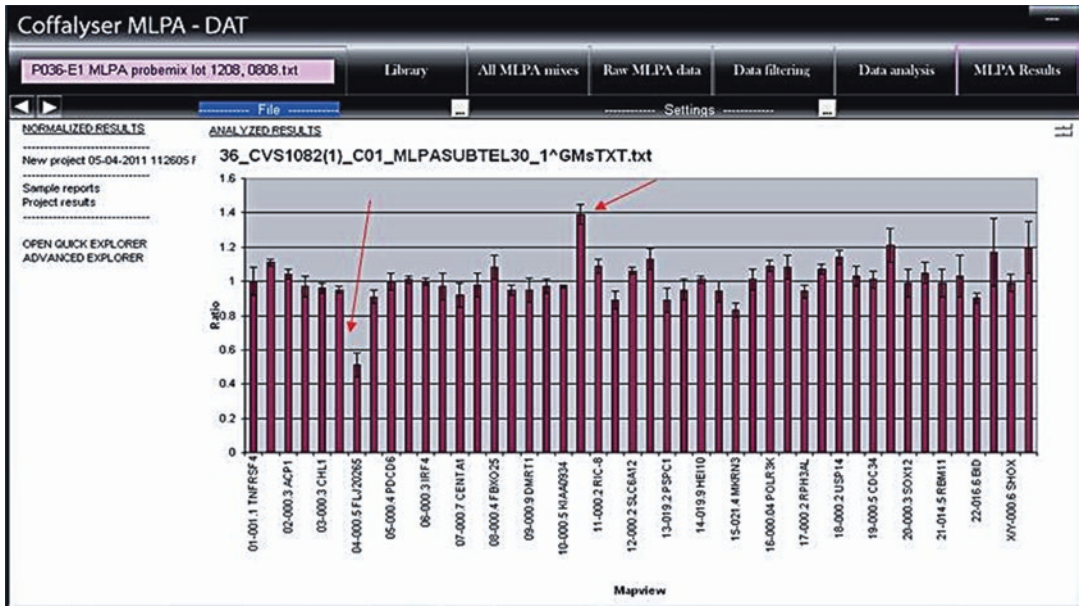

Fig. 18.6 Genetic investigation using multiplex ligation-dependent probe amplification (MLPA) revealed a 4p-/10q duplication in the fetus

"reverse face" [11], the "flipped face" [12], variations of both techniques [13–16], and "oblique face" [17]. Tonni et al. [18] have reconstructed from volume proposed the use of the OmnView tool in the study of both hard and soft palates. OmniView technique is a 3D ultrasound application that enables selection of non-conventional planes (oblique or curved) to be reconstructed from volumes.

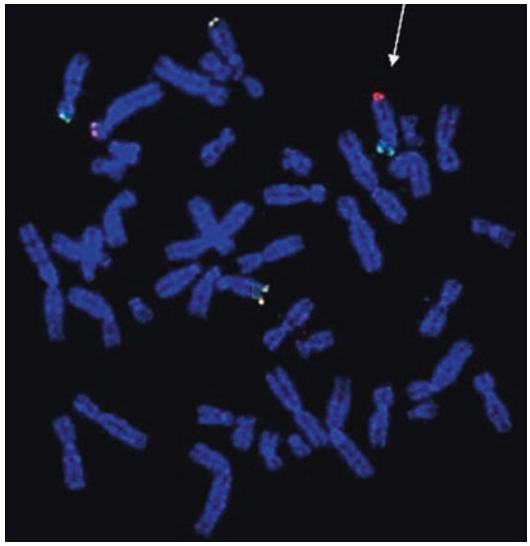

Fig. 18.7 Paternal fluorescence in situ hybridization revealed a balanced, cryptic translocation in subtelomeric 4p-/10q region

In addition, Tonni et al. [19] have also demonstrated the usefulness of the HDLive 3D algorithm to study the soft palate and the uvula. When a prenatal ultrasound diagnosis of facial cleft is made, a thorough ultrasound examination is mandatory. If micrognathia is the only sonographic finding identified, physicians and families should be prepared for possible respiratory difficulty at delivery, the presence of a cleft palate, and/or developmental delay.

Alongside detection of facial clefting, identification of dysmorphic features may lead to the suspicion of genetic syndromes, thus eliciting targeted molecular investigation. Prenatal ultrasound examination by 3D ultrasound and fetal MRI may provide useful data concerning facial abnormalities; in addition, 3D ultrasound and fetal MRI datasets can be integrated to produce physical models of the congenital anomalies -that may have great impact when counseling the parents-to-be and planning intrapartum and/or postnatal surgical management, where indicated. Moreover, when normal fetal karyotype is detected on conventional cytogenetic testing, molecular studies such as MLPA or array-comparative genomic hybridization (a-CGH) should be performed. Molecular testing may comprise a wide panel of genes and genetic counseling is mandatory to discuss clinical prognosis and calculate recurrence risk.

References

1. Jones KL. Smith's recognizable patterns of human malformation. 5th ed. London: WB Saunders; 1997.
2. Pauli RM, Petterson JC, Arya S, Gilbert EF. Familial agnathia-holoprosencephaly. Am J Med Genet. 1983;14:677–98.
3. Turner GM, Twining P. The facial profile in the diagnosis of fetal abnormalities. Clin Radiol. 1993;47:389–95.
4. Nicolaides KH, Salvesen DR, Snijders RJM, Gosden CM. Fetal facial defects: associated malformations and chromosomal abnormalities. Fetal Diagn Ther. 1993;8:1–9.
5. Bromley B, Benacerraf BR. Fetal micrognathia: associated anomalies and outcome. J Ultrasound Med. 1994;13:529–33.
6. Vettraino I, Lee W, Bronsteen RA, Harper CE, Aughton D, Comstock CH. Clinical outcome of fetuses with sonographic diagnosis of isolated micrognathia. Obstet Gynecol. 2003;102:801–5.
7. Brizot ML, Schultz R, Patroni LT, Lopes LM, Ambruster-Moraes E, Zugaib M. Trisomy 10: ultrasound fetures and natural history after first trimester diagnosis. Prenat Diagn. 2001;21:672–5.
8. Teoh M, Meagher S. First-trimester diagnosis of micrognathia as a presentation of Pierre Robin syndrome. Ultrasound Obstet Gynecol. 2003;21:616–8.
9. Sepulveda W, Wong AE, Vinals F, Andreeva E, Adzehova N, Martinez-Ten P. Absent mandibular gap in the retronasal triangle view: a clue to the diagnosis of micrognathia in the first trimester. Ultrasound Obstet Gynecol. 2012;39:152–6.
10. Tonni G, Grisolia G, Sepulveda W. Early prenatal diagnosis of orofacial clefts: evaluation of the retronasal triangle using a new three-dimensional reslicing technique. Fetal Diagn Ther. 2013;34:31–7.
11. Campbell S, Lees C, Moscoso G, Halls P. Ultrasound antenatal diagnosis of cleft palate by a new technique: the 3D 'reverse face' view. Ultrasound Obstet Gynecol. 2005;25:12–8.
12. Platt LD, Devore GR, Pretorius DH. Improving cleft palate/cleft lip antenatal diagnosis by 3-dimensional sonography: the "flipped face" view. J Ultrasound Med. 2006;25:1423–30.
13. Tonni G, Ventura A, Centini G, Rosignoli L. Sonographic imaging of the fetal hard palate during the second-trimester pregnancy scan setting the standard for 3D sonography in a training program. J Diagn Med Sonography. 2009;25:179–84.
14. Wilhelm I, Borgers H. The "equals sign": a novel marker in the diagnosis of fetal isolated cleft palate. Ultrasound Obstet Gynecol. 2010;36:439–44.

15. Faure JM, Captier G, Bäumler M, Boulot P. Sonographic assessment of normal fetal palate using three-dimensional imaging: a new technique. Ultrasound Obstet Gynecol. 2007;29:159–65.
16. Wang LM, Leung KY, Tang M. Prenatal evaluation of facial clefts by three-dimensional extended imaging. Prenat Diagn. 2007;27:722–9.
17. Martinez-Ten P, Perez Pedregosa J, Santacruz B, Adiego B, Barron E, Sepulveda W. Three-dimensional ultrasound diagnosis of cleft palate: 'reverse face', 'flipped face' or 'oblique face'-which method is best? Ultrasound Obstet Gynecol. 2009;33:399–406.
18. Tonni G, Lituania M. A novel 3-Dimensional sonographic technique in the study of the fetal hard and soft palates using OmniView algorithm. J Ultrasound Med. 2012;31:313–8.
19. Tonni G, Grisolia G. Fetal uvula: navigating and lightening the soft palate using HDlive. Arch Gynecol Obstet. 2013;288:239–44.

19 Prenatal Diagnosis of Beckwith-Wiedemann Syndrome Using 3D Ultrasound and Fetal MRI

Heron Werner and Gabriele Tonni

19.1 Introduction

Beckwith-Wiedemann syndrome (BWS) (OMIM 130650) is an autosomal dominant disease, inherited with variable expression, characterized by somatic overgrowth and a predisposition to embryonal tumors. It was first described by Beckwith in 1963 and by Wiedemann in 1964 [1, 2]. The incidence is estimated to be 1 in 14,000 births, evenly distributed between males and females [3].

19.2 Case Description

A 35-year-old Caucasian primigravida with no significant past medical surgical, or family history was referred at 35 weeks of gestation due to polyhydramnios, renal dysplasia, and protruding tongue. The first-trimester combined screening test showed low risk for Down syndrome. Ultrasound evaluation was conducted using Voluson 730 Pro apparatus (GE, Milwaukee, WI) equipped with two-dimensional (2D) and three- and four-dimensional (3D/4D) ultrasound probes. Fetal magnetic resonance imaging (MRI) was performed for complementary diagnostic investigation. MRI was acquired using a 1.5-T scanner (Magnetom Avanto, Siemens, Erlangen, Germany), with body coil. The MRI protocol was a T2-weighted sequence in three planes of the fetal body (HASTE; TR shortest, TE 140 ms, field of view 300–200 mm, matrix 256 × 256, slice thickness 4 mm, acquisition time 21 s, 40 slices). In addition, we applied a 3D, T2-weighted TrueFISP sequence in the sagittal plane (TRUFI; TR/TE = 3.02/1.34; voxel size 1.6 × 1.6 × 1.6 mm^3; flip angle = 70°; acquisition time, 26 s). The entire examination time took less than 30 minutes.

Ultrasound and fetal MRI detected macroglossia (Figs. 19.1, 19.2, and 19.3), exomphalos (Figs. 19.4, 19.5, and 19.6), severely enlarged kidneys (Figs. 19.6 and 19.7), associated polyhydramnios, and increased placental thickness (Fig. 19.8). Estimated fetal weight was 3795 g.

A presumptive prenatal diagnosis of BWS was posed. Planned cesarean delivery at 37 weeks of gestation was performed and a male infant weighing 4125 g (>97th percentile) with normal Apgar scores at 1 and 5 minutes was delivered.

H. Werner (✉)
Prenatal Diagnostic Service, Clínica ALTA Excelência Diagnóstica, Rio de Janeiro, Brazil
e-mail: heronwerner@hotmail.com

G. Tonni, MD, PhD
Department of Obstetrics and Gynecology, Prenatal Diagnostic Service, Guastalla Civil Hospital, AUSL Reggio Emilia, Reggio Emilia, Italy
e-mail: Tonni.Gabriele@ausl.re.it

G. Tonni, W. Sepulveda, and A.E. Wong (eds.), *Prenatal Diagnosis of Orofacial Malformations*,
DOI 10.1007/978-3-319-32516-3_19

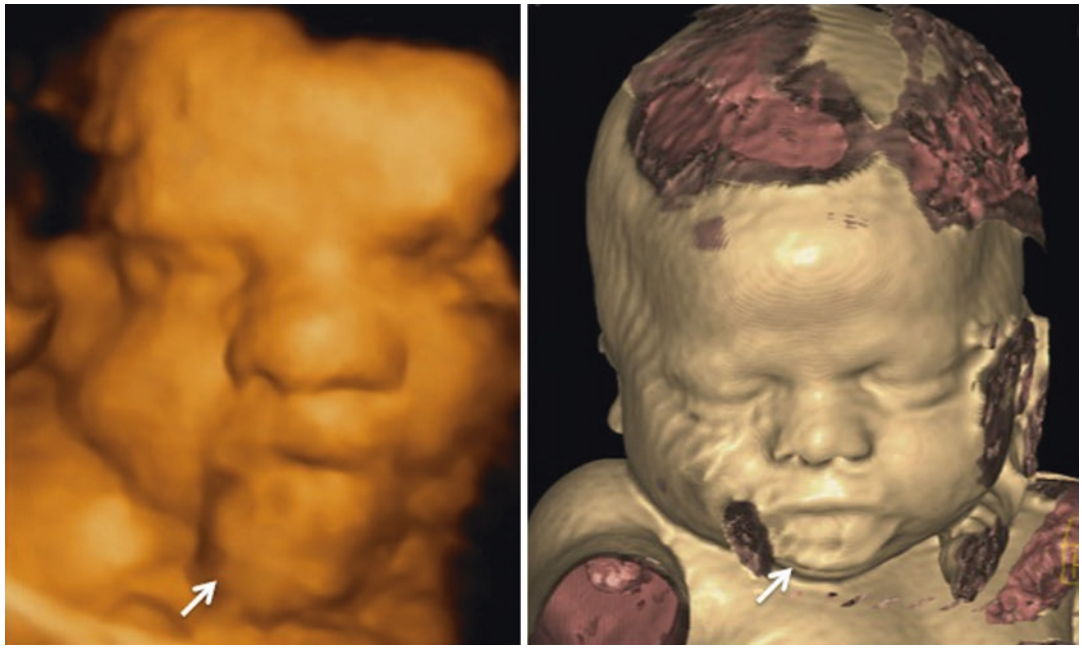

Fig. 19.1 Three-dimensional ultrasound and three-dimensional MRI demonstrated macroglossia (*arrow*)

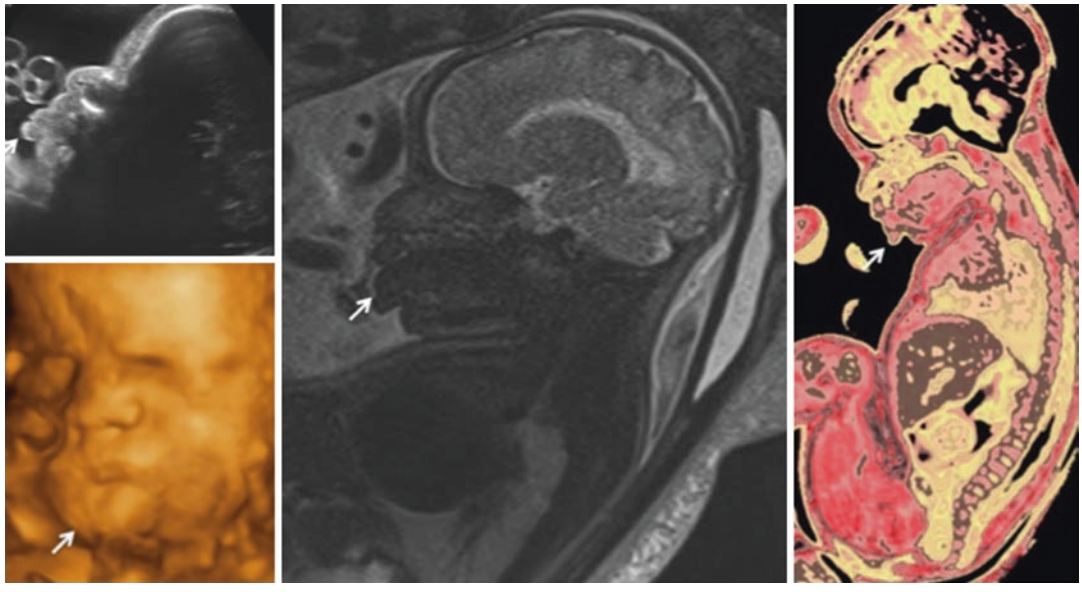

Fig. 19.2 Two-dimensional ultrasound, three-dimensional ultrasound, and fetal MRI demonstrated macroglossia (*arrow*)

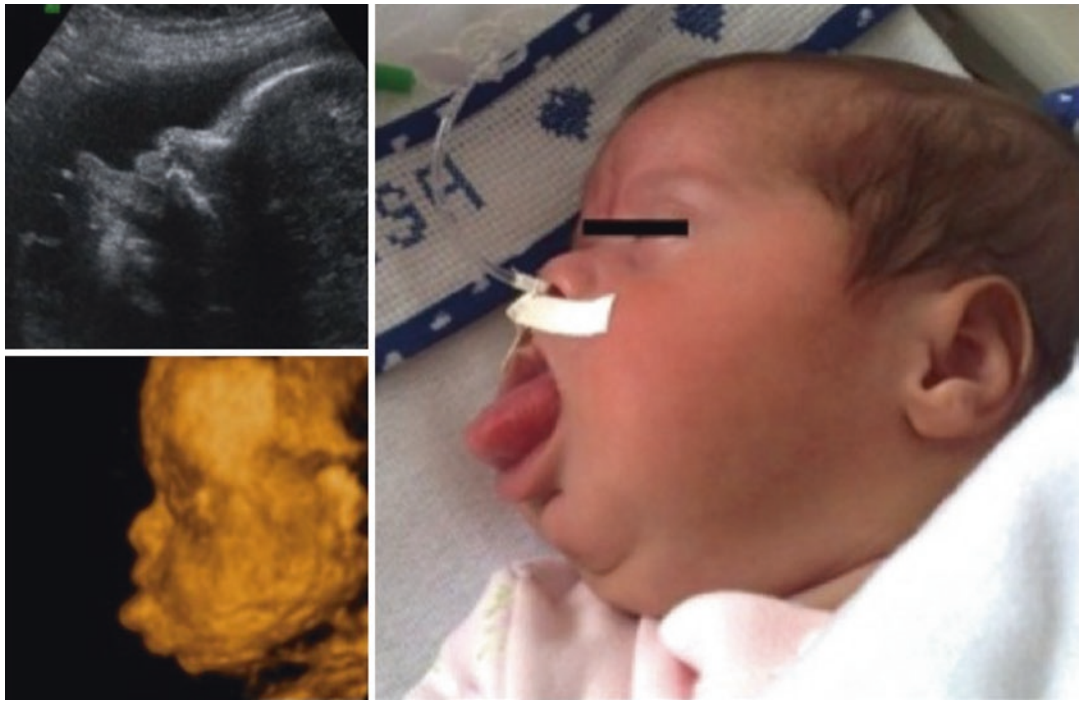

Fig. 19.3 Two-dimensional ultrasound, three-dimensional ultrasound, and postnatal photograph showed macroglossia

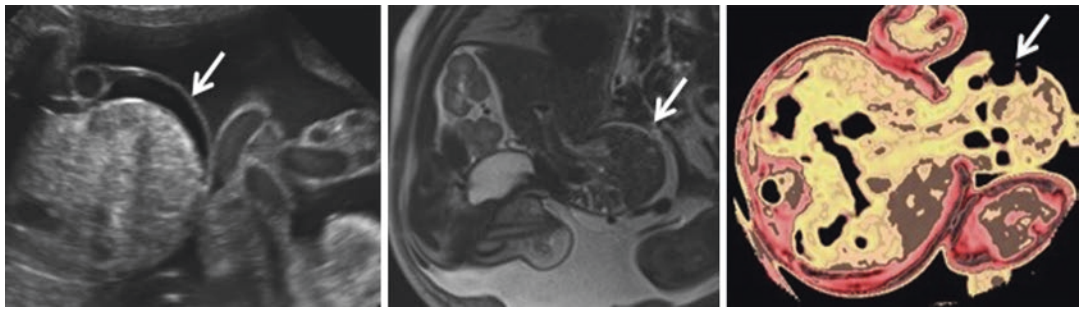

Fig. 19.4 Two-dimensional ultrasound and fetal MRI detected a large (*arrow*)

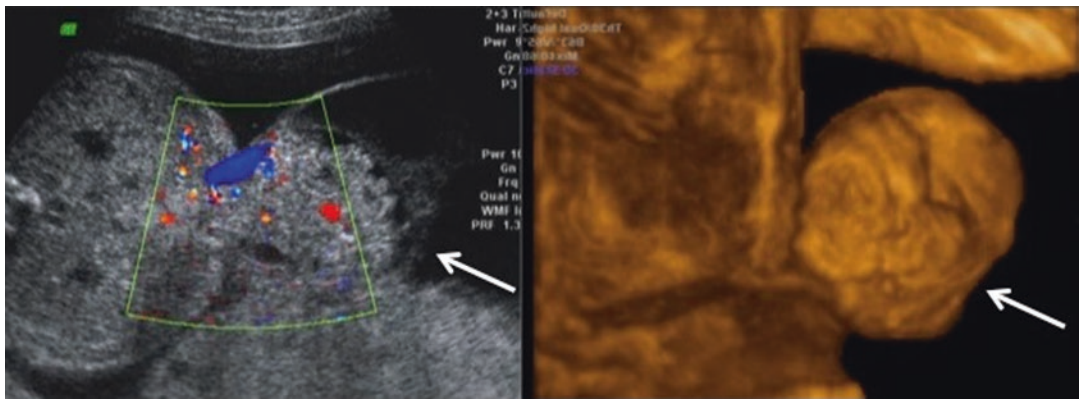

Fig. 19.5 Doppler ultrasound confirmed a left-sided fetal abdominal wall defect and three-dimensional ultrasound clearly rendered the omphalocele (*arrows*)

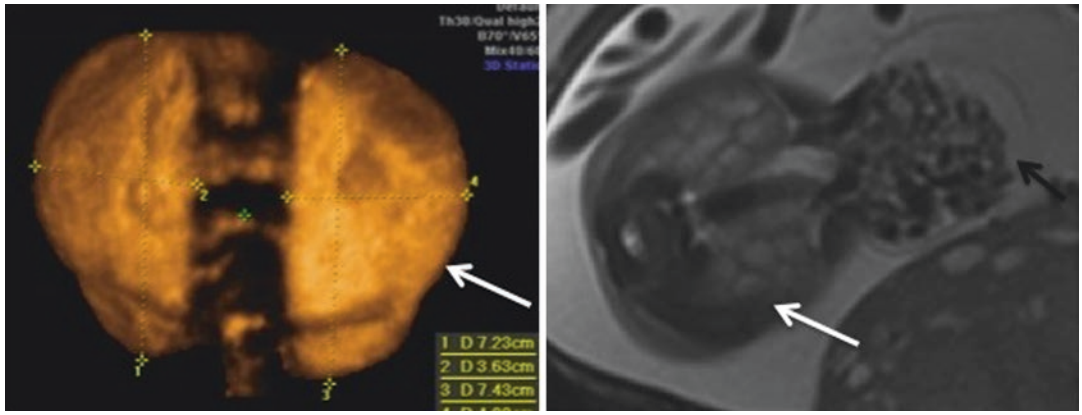

Fig. 19.6 Three-dimensional ultrasound and fetal MRI detected markedly enlarged kidneys (*arrows*). Note exomphalos on fetal MRI image (*black arrow*)

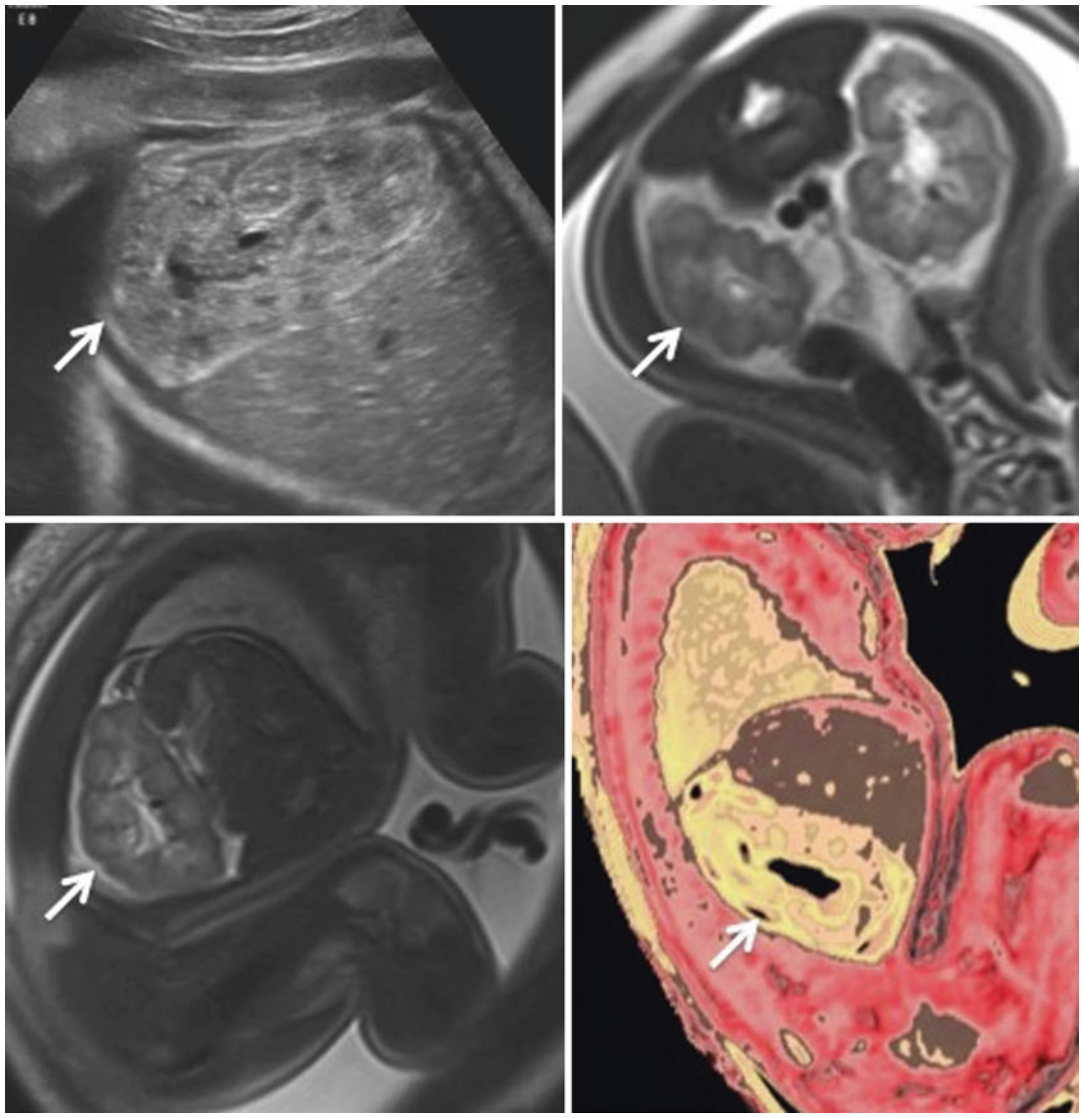

Fig. 19.7 Two-dimensional ultrasound and fetal MRI detected markedly enlarged kidneys (*arrows*)

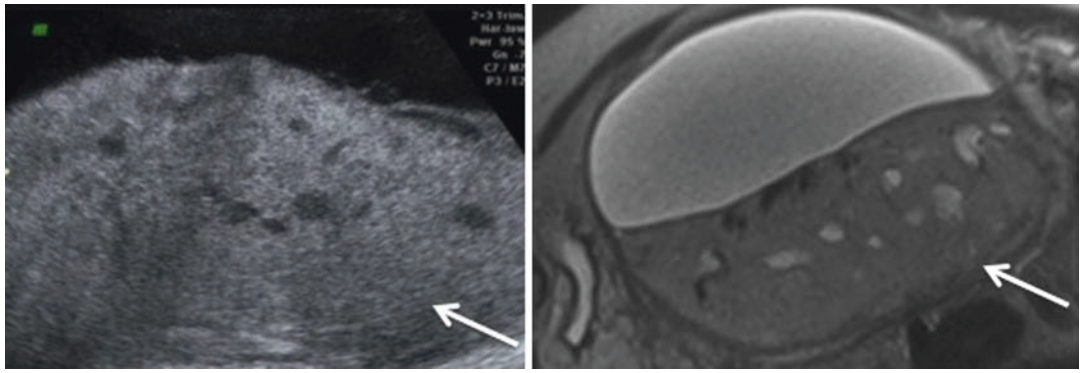

Fig. 19.8 Two-dimensional ultrasound and fetal MRI documented a large placenta with cystic components (*arrows*)

19.3 Discussion

BWS is caused by mutation or deletion of imprinted genes within chromosome 11p15.5. Specific genes involved include p57(KIP2), H19, and LIT1. Hypermethylation and variation in the H19/IGF2-imprinting control region (ICR1; 616186) on chromosome 11p15.5, which regulates imprinted expression of H19 and IGF2, are also associated with BWS. Advanced paternal age may be a clinical risk factor. Recurrence risk for other offspring is 50 % [3, 4]. The diagnosis is typically made after birth, but previous reports have suggested that prenatal diagnosis can be made in the third trimester [4, 5]. The main features include large size for gestational age (overgrowth may be limited to a portion of the body, such as the legs); protruding tongue (macroglossia); large abdominal organs such as the kidneys, liver, and pancreas; increased abdominal circumference; exomphalos; large placenta; and polyhydramnios. In childhood, Wilms' tumors, hepatoblastoma, adrenal tumors, neuroblastoma, and facial nevi may be observed [1, 2, 6, 7].

References

1. Wiedemann HR. Complexe malformatif familial avec hernie ombilicale et macroglossie: un "syndrome nouveau"? J Genet Hum. 1964;13:223–32.
2. Beckwith JB. Macroglossia, omphalocele, adrenal cytomegaly, gigantism, and hyperplastic visceromegaly. Birth Def Orig Art Ser. 1969;V:188–96.
3. Araujo Jr E, Simion C, Marcondes L, Nardozza M, Moron AF. Prenatal diagnosis of Beckwith-Wiedemann syndrome by two- and three-dimensional ultrasonography. Radiol Bras. 2014;46:379–81.
4. Eckmann-Scholz C, Jonat W. 3-D ultrasound imaging of a prenatally diagnosed Beckwith-Wiedemann syndrome. Arch Gynecol Obstet. 2011;284:1051–2.
5. Williams DH, Gauthier DW, Maizels M. Prenatal diagnosis of Beckwith-Wiedemann syndrome. Prenat Diagn. 2005;25:879–84.
6. Chitayat D, Friedman JM, Dimmick JE. Neuroblastoma in a child with Wiedemann-Beckwith syndrome. Am J Med Genet. 1990;35:433–6.
7. Beckwith JB. Children at increased risk for Wilms tumor: monitoring issues. J Pediat. 1998;132:377–9.

20 Prenatal Diagnosis of Tessier 7 Cleft in a Case of Femoral Hypoplasia-Unusual Facies Syndrome with Associated Absent Fibula and Digit Abnormalities

Gianpaolo Grisolia and Gabriele Tonni

20.1 Introduction

A homozygous mutation in the PVRL1 gene (nectin 1) on chromosome 11q23 is responsible for lateral orofacial clefting (macrostomia), classified as Tessier 7 cleft [1, 2]. This mutation is responsible for non-syndromic cleft lip, with or without cleft palate (CL/CLP), and for ectodermal dysplasia syndrome [3, 4]. The disease is inherited as an autosomal recessive condition and may be considered one of the most common types of atypical orofacial cleft, with an estimated incidence of 2 in 10,000 live births [5]. Tessier 7 cleft may be found in association with Dandy-Walker syndrome [6], Goldenhar syndrome (oculo-auriculo-vertebral spectrum with radial defect) [7], or micrognathia [8]. Interestingly, a potential role in the pathogenesis of orofacial clefts may involve vascular abnormalities, resulting in hypoperfusion of the left side of the face thus causing a Tessier 7 cleft [9], or be the result of compression by an amniotic band [10]. Although the central part of the fetal face can be better imaged by two-dimensional (2D) ultrasound, three- and four-dimensional (3D/4D) ultrasound facilitate the antenatal visualization of the lateral aspect of the face and is of clinical value in cases of atypical orofacial clefts [11]. Although unilateral Tessier 7 cleft is six times more common than bilateral cases [2], prenatal detection of a bilateral case at 26 weeks of gestation by 2D ultrasound in the coronal plane has been reported [12].

20.2 Case Description

A 32-year-old woman, gravida 1, underwent fetal karyotyping due to increased nuchal transluency (NT) >99th percentile. Chorionic villus sampling (CVS) demonstrated an 46,XY karyotype. A thorough ultrasound examination and fetal echocardiography was performed at 19 weeks and 5 days. Ultrasound evaluation was conducted using Voluson 8 apparatus (GE, Milwaukee, WI) equipped with 2D and 3D/4D ultrasound probes. 3D ultrasound was carried out using surface-rendering and skeleton mode. Ultrasound examination showed an increased nuchal fold (7 mm), prenasal edema, and a lateral cleft extending from the left commissure of the mouth to the chin, with

G. Grisolia
Prenatal Diagnostic Service, Department of Obstetrics & Gynecology, “Carlo Poma” Hospital, Mantua, Italy

G. Tonni, MD, PhD (✉)
Department of Obstetrics and Gynecology, Prenatal Diagnostic Service, Guastalla Civil Hospital, AUSL Reggio Emilia, Reggio Emilia, Italy
e-mail: Tonni.Gabriele@ausl.re.it

G. Tonni, W. Sepulveda, and A.E. Wong (eds.), *Prenatal Diagnosis of Orofacial Malformations*,
DOI 10.1007/978-3-319-32516-3_20

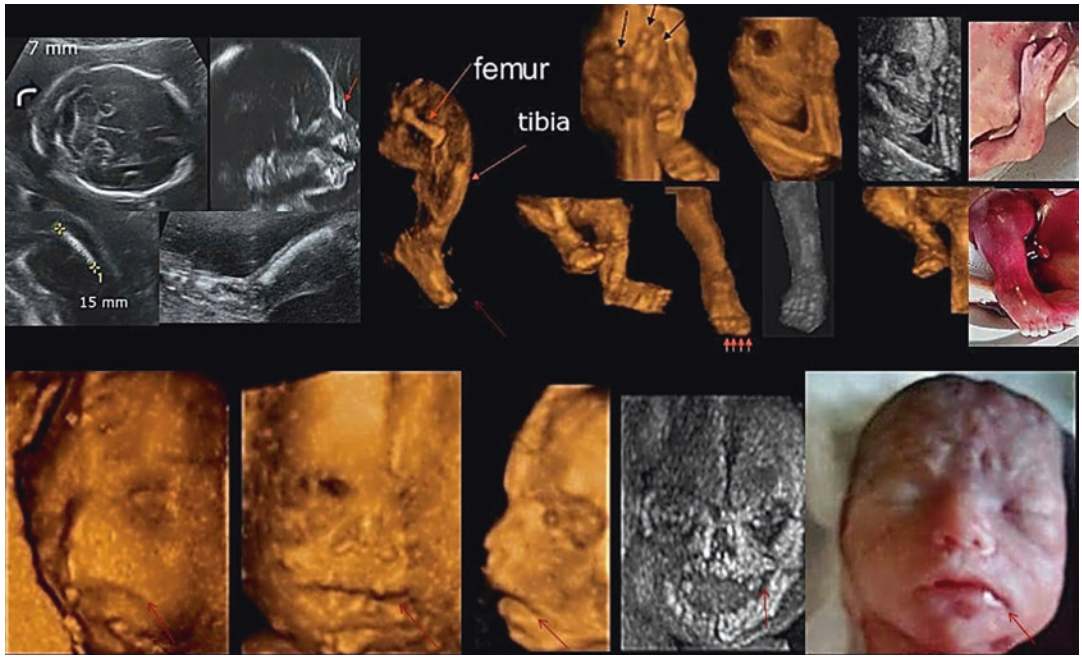

Fig. 20.1 Two- and three-dimensional ultrasound using surface-rendering and "skeleton" mode showing increased nuchal fold, prenasal edema, femoral hypoplasia, curved tibia and absent fibula, and oligodactyly of hands and feet associated with syndactyly of the right hand (*arrows*). The fetal face was characterized by a Tessier type 7 cleft (macrostomia) extending from the left commissure of the mouth and pointing to the chin with sunken appearance of the cheek (see autopsy finding for comparison) (*arrow*)

sunken appearance of the cheek. Multiple sonographic markers of skeletal dysplasia were characterized by bilateral femoral hypoplasia (femur length <3rd percentile for expected gestational age), curved tibia, and absent fibula. In addition, oligodactyly of the hands and feet and syndactyly of the right hand were identified (Fig. 20.1).

A presumptive prenatal diagnosis of Tessier number 7 cleft (macrostomia) associated with femoral hypoplasia-unusual facies syndrome (FH-UFS) was considered. Due to multiple severe congenital malformations, termination of pregnancy was performed using vaginal administration of PGE. Postmortem examination confirmed the antenatal diagnosis.

20.3 Discussion

FH-UFS (OMIM 134780) is a rare and sporadic skeletal disorder that was first described by Daentl in 1975 [13]. Nowaczyk et al. [14] emphasized the role of 3D ultrasound in the early prenatal diagnosis of femoral facies syndrome detected at 12, 15, and 19 weeks of gestation, respectively.

Tessier [2] classified facial clefts below the orbit and numbered them from 0 to 7, where number 7 represents a lateral cleft. Lateral facial clefting or macrostomia is an atypical cleft that represents about 3.1 % of all clefts. It may arise due to failed penetration of ectomesenchyme between the developing maxillary and mandibular prominences. It can be seen as an isolated defect or associated with features consistent with skeletal dysplasia [12]. The incidence is estimated as 1 in 50,000–175,000 live births [2]. The unilateral type is six times more frequently observed than the bilateral type [2]. Lampert [15] and Robinow et al. [6] demonstrated an autosomal dominance inheritance. Presti et al. [12] and Pilu et al. [11] reported the prenatal ultrasound detection of bilateral and unilateral Tessier number 7 cleft at 26 and 22 weeks of gestation, respectively. Lateral facial

clefting may be part of an overlapping genetic syndrome such as mandibulofacial dysostosis and oculo-auriculo-vertebral spectrum [17, 18].

References

1. Sozen MA, Suzuki K, Tolarova MM, Bustos T, Fernandez Iglesias JE, Spritz RA. Mutation of PVRL1 is associated with sporadic, non-syndromic cleft lip/palate in northern Venezuela. Nat Genet. 2001; 29:141–2.
2. Tessier P. Anatomical classification of facial craniofacial and lateral-facial clefts. J Maxillofac Surg. 1976;4:69–92.
3. Suzuki K, Hu D, Bustos T, Zlotogora J, Richieri-Costa A, Helms JA, Spritz RA. Mutations of PVRL1, encoding a cell-cell adhesion molecule/herpesvirus receptor, in cleft lip/palate-ectodermal dysplasia. Nat Genet. 2000;25:427–30.
4. Zlotogora J. Syndactyly, ectodermal dysplasia, and cleft lip/palate. J Med Genet. 1994;31:957–9.
5. Butow KW, Botha A. A classification and construction of congenital lateral facial clefts. J Craniomaxillofac Surg. 2010;38:477–84.
6. Dhupar V, Kumar P, Akkara F, Kumar A. Dandy Walker syndrome with Tessier 7 cleft – a rare case report and a surgical note on the use of vermilion flap and lazy W-plasty. J Maxillofac Oral Surg. 2012; 11:368–70.
7. Chauhan DS, Guruprasad Y. Goldenhar syndrome with Tessier's 7 cleft: report of a case. J Maxillofac Oral Surg. 2015;14:42–6.
8. Asai S, Tanaka M, Miyakoshi K, Kim SH, Minegishi K, Matsuzaki Y, Kosaki K, Ogata H, Yoshimura Y. A case of Tessier number 7 cleft with severe micrognathia: prenatal sonographic and three-dimensional helical computed tomographic images. Prenat Diagn. 2010;30:159–61.
9. Bajaj A, Dyke P, Zaleski C, Cava J, McPherson E. Mild Tessier No. 7 cleft with PHACE syndrome: the case for pulmonary vascular steal. Am J Med Genet. 2011;155A:2298–301.
10. Stelnicki EJ, Hoffman W, Foster R, Lopoo J, Longaker M. The in utero repair of Tessier number 7 lateral facial clefts created by amniotic band-like compression. J Craniofac Surg. 1998;9:557–62.
11. Pilu G, Visentin A, Ambrosini G, D'Antona D, Andrisani A. Three-dimensional sonography of unilateral Tessier number 7 cleft in a mid-trimester fetus. Ultrasound Obstet Gynecol. 2005;26:98–9.
12. Presti F, Celentano C, Marcazzo L, Dolcetta G, Prefumo F. Ultrasound prenatal diagnosis of a lateral facial cleft (Tessier number 7). Ultrasound Obstet Gynecol. 2004;23:606–8.
13. Daentl DL, Smith DW, Scot CI, Hal BD, Gooding CA. Femoral hypoplasia-unusual facies syndrome. J Pediatr. 1975;86:107–11.
14. Nowaczyk MJ, Huggins MJ, Fleming A, Mohide PT. Femoral-facial syndrome: prenatal diagnosis and clinical features. Report of three cases. Am J Med Genet. 2010;152A:2029–33.
15. Lampert R. Dominant inheritance of femoral hypoplasia-unusual facies syndrome. Clin Genet. 1980;17:255–8.
16. Robinow M, Sonek J, Buttino L, Veghte A. Femoral facial syndrome-prenatal diagnosis-autosomal dominant inheritance. Am J Med Genet. 1995;57:397–9.
17. de Die-Smulders CE, Moog U, Engelen JJ, Peters JJ, Damen A, Vos W, Frins JP. Lateral facial clefts: a case report. Genet Couns. 2001;12:163–5.
18. Gorlin RJ, Cohen MM, Stefan Levin L. Orofacial clefting syndromes. In: Syndrome of the head and neck, Oxford monographs on medical genetic no. 19. 3rd ed. New York: Oxford University Press; 1990.

21 Median Cleft Lip and Palate, Cutaneous Nasal Polyps, and Corpus Callosum Lipoma: A Case of Pai Syndrome Associated with Ventricular Septal Defects

Jose H. Ochoa, Rolando P. Vildoza, Adriana Echegaray, and Alejandra Colubriale

21.1 Introduction

Pai syndrome is a rare facial anomaly characterized by median cleft lip and cleft palate of variable complexity in association with single or multiple pedunculated polyps of the skin and nasal mucosa that may be sessile or pedunculated [1]. Affected individuals often have mild hypertelorism and an interhemispheric lipoma with or without corpus callosum agenesis/dysgenesis. Neuropsychologic development is normal. The syndrome is also rarely associated with ocular abnormalities, such as iris coloboma [2]. Other findings that have been rarely reported include temporal triangular alopecia, posterior lenticonus, bilateral palatal pits, bifid uvula, hypospadias, sacral dimple, true tracheal bronchus, and epilepsy [3].

We describe a case of Pai syndrome that was diagnosed prenatally by ultrasound at 34 weeks of gestation. Although the main prenatal finding was the presence of cleft lip and palate, a thorough anatomic examination with two-dimensional (2D) and three-dimensional (3D) surface-rendering ultrasound also revealed other distinctive features of the syndrome.

21.2 Case Description

An 18-year-old primigravida, with no history of consanguinity or physical or genetic abnormalities in either side of the family, was referred to our center at 34 weeks of gestation for ultrasound evaluation after the detection of several abnormal findings at her third-trimester growth scan. At referral, ultrasound examination revealed a normally grown fetus with normal amniotic fluid volume. Detailed ultrasound anatomic examination demonstrated a female fetus with a median cleft lip and palate. In addition, a large polypoid structure protruding from the right nostril, several polypoid appendages of the nasal dorsum, and a skin tag on the left cheek were detected and confirmed with 3D/4D ultrasound (Fig. 21.1). Examination of the brain also revealed an interhemispheric hyperechoic mass with mild corpus callosum dysgenesis, which was consistent with corpus callosum lipoma (Fig. 21.2). Examination of the heart also revealed two small ventricular septal defects, one muscular and the other perimembranous (Fig. 21.3).

J.H. Ochoa (✉) • R.P. Vildoza
Diagnus – Prenatal Diagnosis and Teaching Center, Cordoba, Argentina

Department of Fetal Diagnosis, Cordoba University Hospital, Cordoba, Argentina
e-mail: josehochoa.cba@gmail.com

A. Echegaray • A. Colubriale
Diagnus – Prenatal Diagnosis and Teaching Center, Cordoba, Argentina

G. Tonni, W. Sepulveda, and A.E. Wong (eds.), *Prenatal Diagnosis of Orofacial Malformations*,
DOI 10.1007/978-3-319-32516-3_21

Given the fetal phenotypic features, the diagnosis of Pai syndrome was made and confirmed after birth (Fig. 21.4a). The newborn infant had no major neonatal complications. Initial feeding problems were managed with a palatal obturator. Postnatal karyotype was reported as normal. Repair of the cleft lip and excision of the polyp were performed during the neonatal period. In a subsequent operation, the palate was surgically reconstructed. The small ventricular septal defects spontaneously closed during the first year of age. Figure 21.4b shows the postoperative results at the age of 3 years. The infant is currently

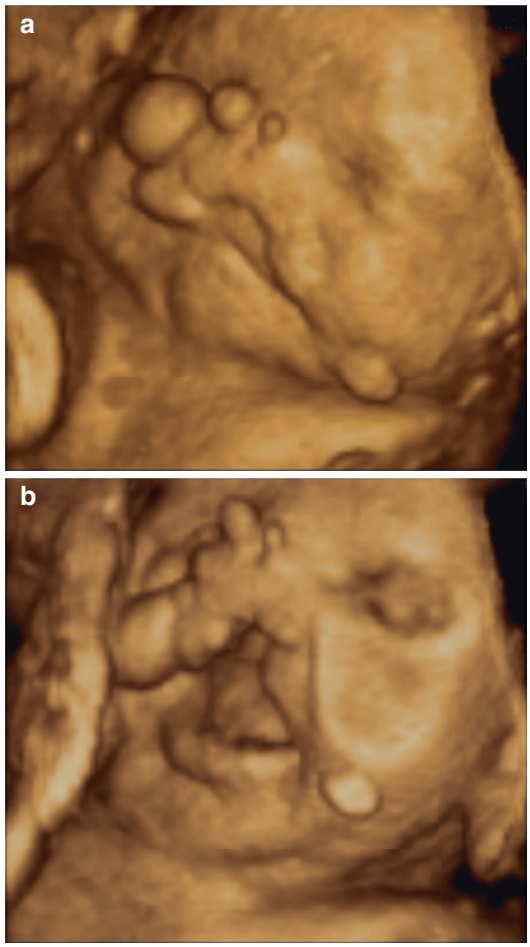

Fig. 21.1 (**a**) Three-dimensional surface-rendering ultrasound of the fetal face shows cleft lip, a large polyp protruding through the right nostril, two nasal dorsal polyps, and a left cheek skin tag. (**b**) Same view as in (**a**) with open mouth for a better depiction of the median upper lip cleft

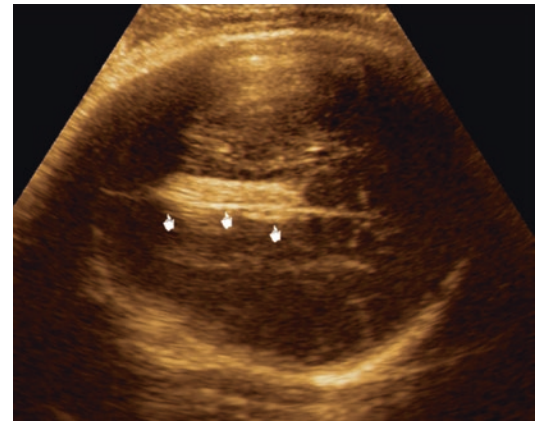

Fig. 21.2 Axial two-dimensional ultrasound image of the fetal head shows an echogenic mass in the interhemispheric fissure representing a lipoma

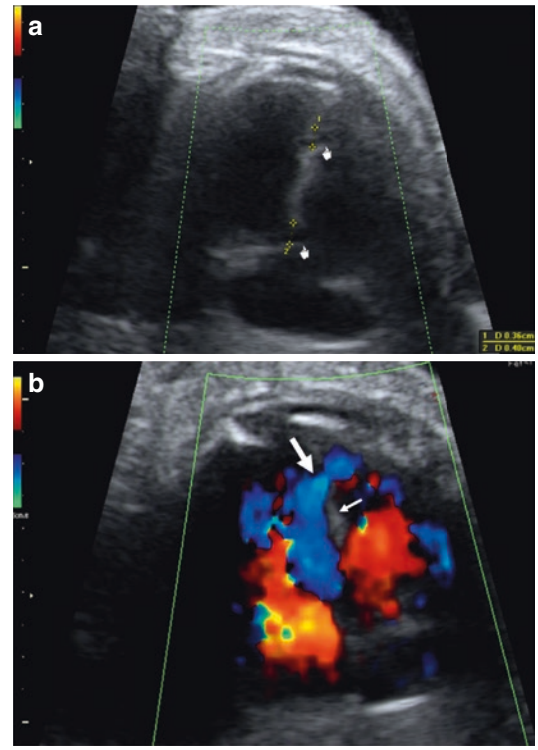

Fig. 21.3 (**a**) Four-chamber view in B-mode depicts two small ventricular septal defects (denoted by *calipers*). (**b**) Color Doppler ultrasound shows flow through the muscular ventricular septal defect (*arrow*). *Small arrow* denotes the septum

5 years of age and her neurodevelopmental assessment has been reported as normal.

21.3 Discussion

Pai syndrome is a rare disorder first described by Pai et al. in 1987 in a female newborn that presented with clefting of the upper lip, nasal skin polyps, and midline lipoma of the brain [1]. As an isolated finding, median clefting of the upper lip is rare. However, this condition may be related to several syndromes [4]. The nasal polyps are considered the hallmark of Pai syndrome and the most common site of presentation is the nasal septum that gives rise to polyps arising through the nostrils. The columella is the second most common site; rare locations are the dorsum/bridge and tip of the nose [5]. Usually, these polyps are hamartomas (lipomas and myolipomas) [5, 6].

After the original description of this syndrome, several cases characterized by median facial cleft without cleft palate, nasal or facial polyps, or brain interhemispheric lipomas have been reported. Therefore, minimum diagnostic criteria for Pai syndrome have been established: one or more hamartomatous nasal polyps plus a median cleft lip (with or without cleft alveolus or palate) and/or mid-anterior alveolar process congenital polyp [5]. As pericallosal lipoma was reported in 85% of the cases that underwent brain imaging, this feature has also been proposed as an additional criterion [3].

Interhemispheric/pericallosal lipomas have typical ultrasound features that make them very easy to identify during prenatal ultrasound in the majority of cases [7]. As there is no adipose tissue in the brain, lipomas of the central nervous system are presumed to arise from the primitive meninx descending into the interhemispheric fissure during cleavage of the prosencephalic vesicle [8]. At this location, the lipoma may interfere with corpus callosum development [7]; therefore, complete/partial agenesis or hypoplasia of the corpus callosum is a frequently associated finding [5, 7, 9]. Other developmental anomalies of the craniofacial region that are included in the clinical spectrum of Pai syndrome are bifid nose, bifid uvula, double frenulum, midline sinus, median alveolar cleft, and ocular hypertelorism. Occasionally, ophthalmic abnormalities of the iris and cornea, like coloboma, microcornea, or lenti-

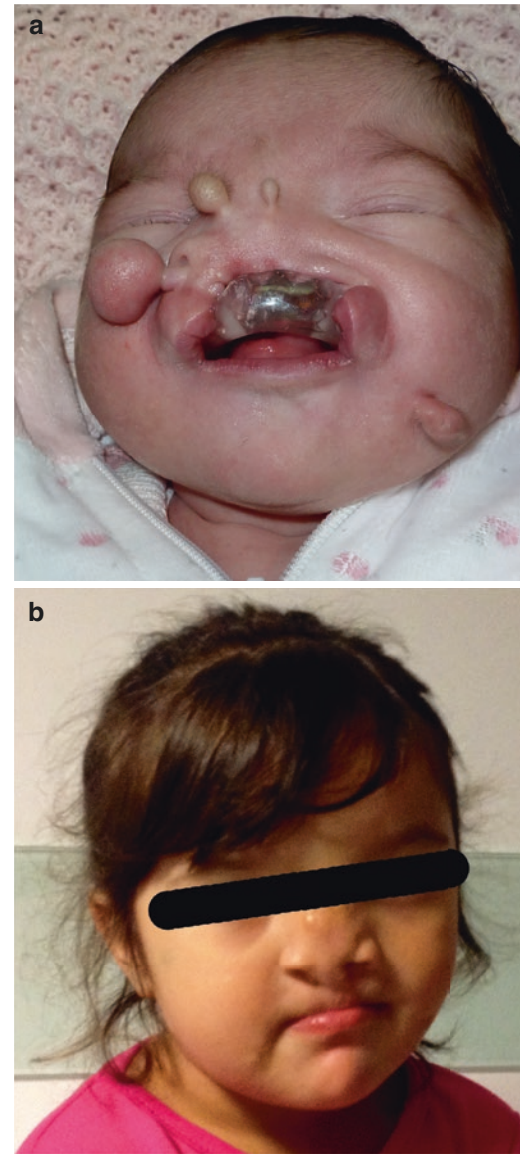

Fig. 21.4 (**a**) Photograph of the newborn infant shows the facial features of Pai syndrome. The nasal polyp protruding from the right nostril and the skin tags are clearly seen. The palate obturator, used for feeding purposes, prevents full view of the cleft lip and palate. (**b**) Follow-up at 3 years of age shows the postoperative results (**a**, **b** published with permission from the parents)

conus, have been also reported [2, 3, 8]. DeMyer [10] stated that median cleft of the upper lip is associated with orbital hypertelorism and five other facial defects: V-shaped frontal hairline, cranium bifidum occultum, primary telecanthus, median cleft of the premaxilla, and median cleft palate.

A ventricular septal defect has been described in one previously published case [5]. In our case, two small ventricular septal defects (one muscular and another perimembranous) were detected in the third trimester of pregnancy, and both underwent spontaneous closure on postnatal follow-up. It is still unclear if this is an associated feature of Pai syndrome that is rare or, more likely, a coincidental finding unrelated to the syndrome.

It has been hypothesized that a genetic defect in mesodermal differentiation and penetration would result in the particular type of anomalies associated with Pai syndrome. The pathogenesis of median facial clefts has two main theories [8]. According to the classical or "fusion" theory of His, the median cleft lip is the result of defective fusion between the maxillary process and the two peninsulas of the frontal process during embryogenesis and fetal growth [8]. The second theory, proposed by Veau, hypothesizes that median clefting of the upper lip is due to absent or deficient mesodermal penetration into the epithelial wall of the primary palate at about the sixth week of embryological development [8]. Consequently, the cutaneous polyps may be the result of an excess of mesodermal tissue proliferation in the oral cavity at the same embryonic stage.

Currently, the cause of Pai syndrome is unknown, although autosomal dominant inheritance [2] and a balanced X;16 translocation [11] have been reported. Pai et al. [1] and Guion-Almeida et al. [12] suggested it could be a particular expression of frontonasal dysplasia, while others postulate a multifactorial origin [13]. Chromosomal analysis is still recommended for these patients, but the result is usually normal in those with the typical phenotype [5]. Exome sequencing may shed more light on the etiology of Pai syndrome and will probably replace conventional karyotype in the near future [3, 13].

Regarding the long-term outcome, most authors report an excellent prognosis in these patients, with normal neurologic and psychomotor development despite the presence of interhemispheric lipomas [8, 14, 15]. Nevertheless, special attention should be paid to the aesthetic, dental, phonetic, and psychological sequelae of the clefting.

References

1. Pai GS, Levkoff AH, Leithiser RE, Reynolds JF. Median cleft of the upper lip associated with lipomas of the central nervous system and cutaneous polyps. Am J Med Genet. 1987;26:921–4.
2. Rudnik-Schoneborn S, Zerres K. A further patient with Pai syndrome with autosomal dominant inheritance? J Med Genet. 1994;31:497–8.
3. Lederer D, Wilson B, Lefesvre P, van der Poorten V, Kirkham N, Mitra D, Verellen-Dumoulin C, Devriendt K. Atypical findings in three patients with Pai syndrome and literature review. Am J Med Genet A. 2012;158:2899–904.
4. Reardon W, Jones B, Baraitser M. Median clefting of the upper lip associated with cutaneous polyps. J Med Genet. 1990;27:337–8.
5. Castori M, Rinaldi R, Bianchi A, Caponetti A, Assumma M, Grammatico P. Pai syndrome: first patient with agenesis of the corpus callosum and literature review. Birth Defects Res (Part A): Clin Mol Teratol. 2007;79:673–9.
6. Zanetta A, Cuestas G, Oviedo M, Tiscornia C. Unilateral nasal obstruction in children: Pai syndrome. Arch Argent Pediatr. 2011;109:e100/e3.
7. Ickowitz V, Eurin D, Rypens F, Sonigo P, Simon I, David P, Brunelle F, Avni FE. Prenatal diagnosis and postnatal follow-up of pericallosal lipoma: report of seven new cases. Am J Neuroradiol. 2001;22:767–72.
8. Szeto C, Tewfik TL, Tewfika TL, Jewer D, Rideout A. Pai syndrome (median cleft palate, cutaneous nasal polyp, and midline lipoma of the corpus callosum): a case report and literature review. Int J Pediatr Otorhinolaryngol. 2005;69:1247–52.
9. Savasta S, Chiapedi S, Perrini S, Tognato E, Corsano L, Chiara A. Pai syndrome: a further report of a case with bifid nose, lipoma, and agenesis of the corpus callosum. Childs Nerv Syst. 2008;24:773–6.
10. DeMyer W. The median cleft face syndrome: differential diagnosis of cranium bifidum occultum, hypertelorism, and median cleft nose, lip and palate. Neurology. 1967;17:961–71.
11. Masuno M, Imaizumi K, Fukushima Y, Tanaka Y, Ishii T, Nakamura M, Kuroki Y. Median cleft of upper lip and pedunculated skin masses associated with de

novo reciprocal translocation 46, X, t(X; 16) (q28;ql 1.2). J Med Genet. 1997;34:952–4.
12. Guion-Almeida ML, Mellado C, Beltran C, Richieri-Costa A. Pai syndrome: report of seven South American patients. Am J Med Genet. 2007;143A: 3273–9.
13. Al-Mazrou KA, Al-Rekabi A, Alorainy IA, Al-Kharfi T, Al-Serhani AM. Pai syndrome: a report of a case and review of the literature. Int J Pediatr Otorhinolaryngol. 2001;61:149–53.
14. Abdelmaaboud M, Nimeri N. Pai syndrome: first reported case in Qatar and review of literature of previously published cases. BMJ Case Rep. 2012. doi:10.1136/bcr-02-2012-5940.
15. Chousta A, Ville D, James I, Foray P, Bisch C, Depardon P, Rudigoz RC, Guibaud L. Pericallosal lipoma associated with Pai syndrome: prenatal imaging findings. Ultrasound Obstet Gynecol. 2008;32:708–10.